INSIGHTS IN CARDIAC RHYTHMOLOGY: 2021

EDITED BY: Gaetano M. De Ferrari and Matteo Anselmino
PUBLISHED IN: Frontiers in Cardiovascular Medicine

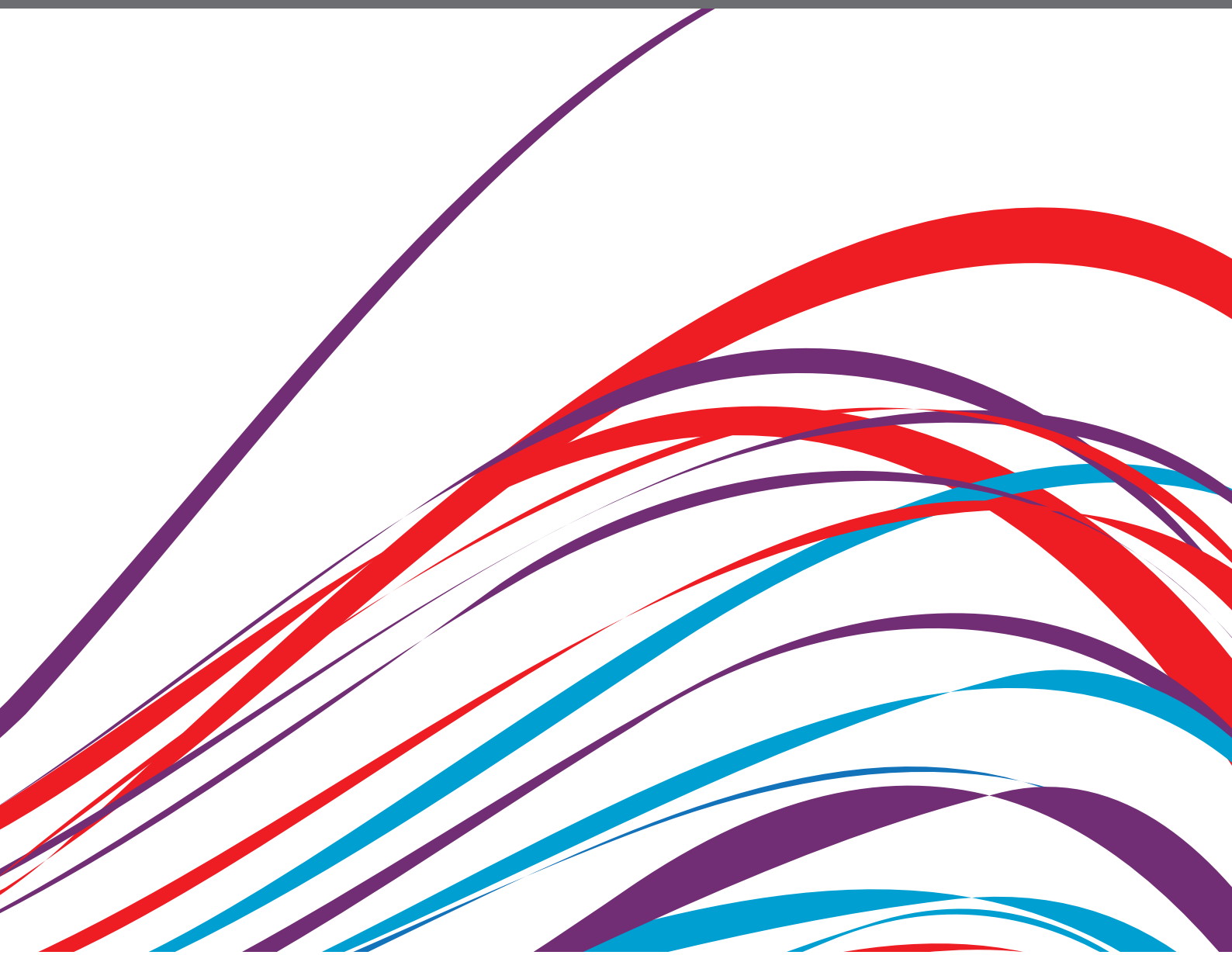

frontiers Research Topics

ISSN 1664-8714
ISBN 978-2-83250-079-8
DOI 10.3389/978-2-83250-079-8

About Frontiers

Frontiers is more than just an open-access publisher of scholarly articles: it is a pioneering approach to the world of academia, radically improving the way scholarly research is managed. The grand vision of Frontiers is a world where all people have an equal opportunity to seek, share and generate knowledge. Frontiers provides immediate and permanent online open access to all its publications, but this alone is not enough to realize our grand goals.

Frontiers Journal Series

The Frontiers Journal Series is a multi-tier and interdisciplinary set of open-access, online journals, promising a paradigm shift from the current review, selection and dissemination processes in academic publishing. All Frontiers journals are driven by researchers for researchers; therefore, they constitute a service to the scholarly community. At the same time, the Frontiers Journal Series operates on a revolutionary invention, the tiered publishing system, initially addressing specific communities of scholars, and gradually climbing up to broader public understanding, thus serving the interests of the lay society, too.

Dedication to Quality

Each Frontiers article is a landmark of the highest quality, thanks to genuinely collaborative interactions between authors and review editors, who include some of the world's best academicians. Research must be certified by peers before entering a stream of knowledge that may eventually reach the public - and shape society; therefore, Frontiers only applies the most rigorous and unbiased reviews.
Frontiers revolutionizes research publishing by freely delivering the most outstanding research, evaluated with no bias from both the academic and social point of view. By applying the most advanced information technologies, Frontiers is catapulting scholarly publishing into a new generation.

What are Frontiers Research Topics?

Frontiers Research Topics are very popular trademarks of the Frontiers Journals Series: they are collections of at least ten articles, all centered on a particular subject. With their unique mix of varied contributions from Original Research to Review Articles, Frontiers Research Topics unify the most influential researchers, the latest key findings and historical advances in a hot research area! Find out more on how to host your own Frontiers Research Topic or contribute to one as an author by contacting the Frontiers Editorial Office: frontiersin.org/about/contact

INSIGHTS IN CARDIAC RHYTHMOLOGY: 2021

Topic Editors:
Gaetano M. De Ferrari, University of Turin, Italy
Matteo Anselmino, University of Turin, Italy

Citation: De Ferrari, G. M., Anselmino, M., eds. (2022). Insights in Cardiac Rhythmology: 2021. Lausanne: Frontiers Media SA.
doi: 10.3389/978-2-83250-079-8

Table of Contents

frontiers | Frontiers in Cardiovascular Medicine

TYPE Editorial
PUBLISHED 16 August 2022
DOI 10.3389/fcvm.2022.1003843

OPEN ACCESS

EDITED AND REVIEWED BY
Antonio Sorgente,
EpiCURA, Belgium

*CORRESPONDENCE
Gaetano Maria De Ferrari
gaetanomaria.deferrari@unito.it

SPECIALTY SECTION
This article was submitted to Cardiac Rhythmology, a section of the journal Frontiers in Cardiovascular Medicine

RECEIVED 26 July 2022
ACCEPTED 01 August 2022
PUBLISHED 16 August 2022

CITATION
Ballatore A, De Ferrari GM and Anselmino M (2022) Editorial: Insights in cardiac rhythmology 2021. *Front. Cardiovasc. Med.* 9:1003843. doi: 10.3389/fcvm.2022.1003843

Editorial: Insights in cardiac rhythmology 2021

Andrea Ballatore, Gaetano Maria De Ferrari* and Matteo Anselmino

Division of Cardiology, Department of Medical Sciences, "Città della Salute e della Scienza di Torino" Hospital, University of Turin, Turin, Italy

KEYWORDS

arrhythmias, electrophysiology, innovation, cardiac, atrial fibrillation

Editorial on the Research Topic
Insights in cardiac rhythmology: 2021

2021 has been a year of transition and, again, of great change. Old but never quiescent challenges have risen anew after the pandemic, being the effects of climate change and international political crisis blatant these days. The scientific community has proven an unprecedented sense of cooperation and showed its strength by providing a safe and effective solution to one of the greatest health and social crises of the last century. The widespread availability of vaccines for COVID-19 allowed a gradual relaxation of restraint measures and a progressive return to normality.

Indeed, 2021 scientific production has been characterized by this sense of international corporate effort, being the scientific community aware of its crucial role in providing effective solutions; cardiac rhythmology included (Figure 1).

A great consideration has been given to atrial fibrillation (AF) and its therapeutic strategies. Out of the classic questions, attention to the metabolic relationships of the arrhythmia has emerged. New evidence shows how epicardial adipose tissue is linked to perioperative AF following cardiac surgery (Petraglia et al.); this relation is mediated by an increased level of inflammation pointing toward the importance of immunology and metabolic interplay in the development of the arrhythmia. Moreover, Kim, Shim et al. demonstrated that malnutrition, which is associated with an increased risk of AF occurrence, is also linked to a greater risk of complications after AF catheter ablation. Similarly, a low BMI and female gender was associated to a greater risk of non-transient phrenic nerve palsy (Pott et al.); in this case, it is probably due to an increased proximity of the right phrenic nerve to the ablation target in these patients, however, as suggested by the authors, the increased levels of epicardial adipose tissue in men and in those with higher BMI may play a relevant role in thermal insulation. Therefore, bearing in mind the recent experience with gliflozines, widening their effects from diabetes mellitus treatment to cardiovascular prevention in heart failure patients, greater attention should be raised to metabolic aspects when approaching AF patients.

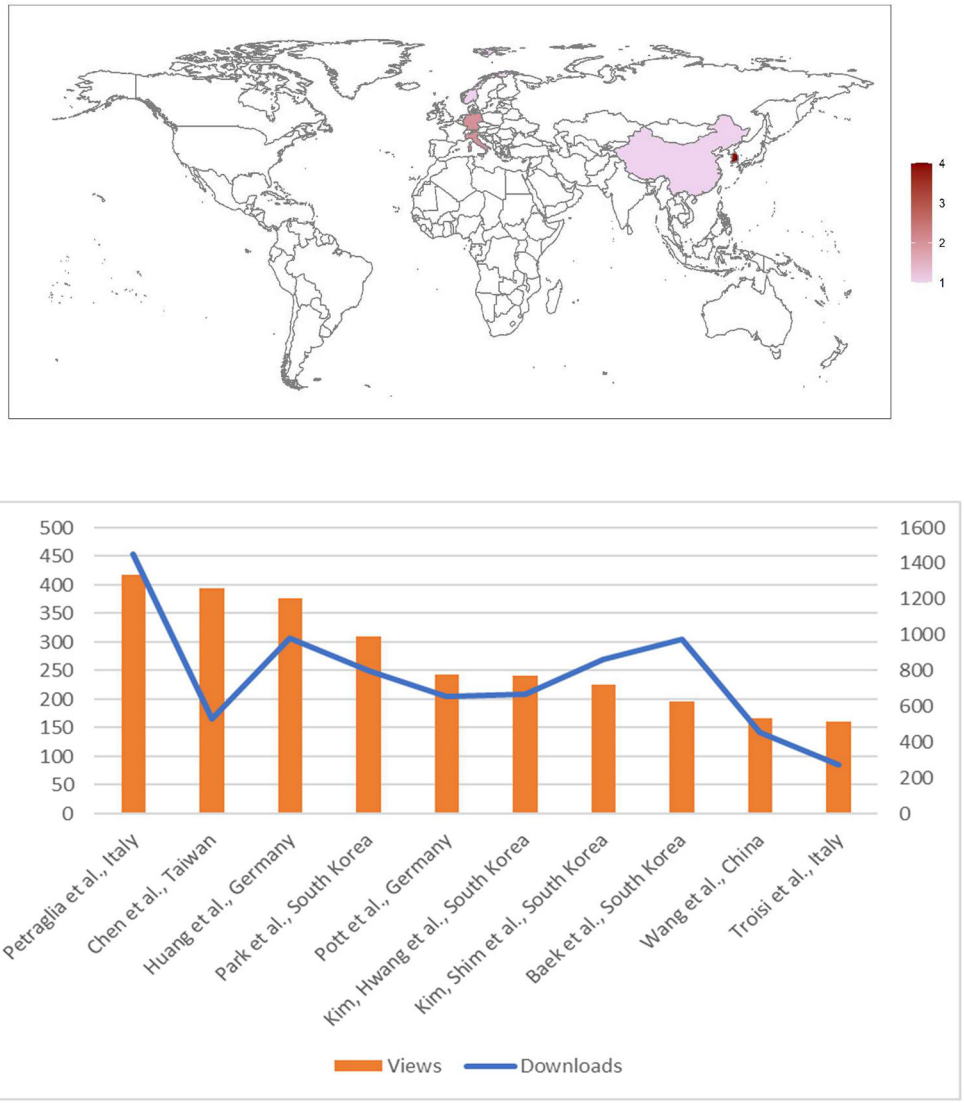

FIGURE 1
Metrics (lower panel; update on July 18th, 2022) and number of articles per Country of Authors' origin (upper panel) of papers published in Frontiers in Cardiovascular Medicine: Insights in cardiac rhythmology 2021.

Technological improvement is constant and new tools are available on almost a daily basis in cardiac electrophysiology, allowing, for instance, the development of new ablation strategies and a deeper knowledge of AF pathophysiology (Kim, Huang et al.). In this respect, pulmonary vein isolation as the sole ablation target in persistent AF is currently questioned and a more comprehensive approach may be advocated (1). The development of new mapping technologies will lead to a further reduction of fluoroscopy use and greater diffusion of "zero X-rays" procedures (Baek et al.; Troisi et al.; Wang et al.) also for complex and extensive-substrate transcatheter procedures.

The attention to new treatment strategies for AF management is rooted in the results of the EAST-AFNET 4 trial, which showed the benefit of rhythm control strategies in the early phases of the disease (2). The publication of the exciting 1 year follow-up results of pulse-field ablation trials suggests that this technology will soon have an increasingly relevant role in the invasive management of arrhythmias (3). Growing evidence point toward catheter ablation as first line

treatment (4); however National Health services could struggle to cope with this high demand of ablation procedures, and efforts should be aimed to increase their availability.

In addition, the approach to the treatment of ventricular tachycardia is undergoing a complete change with catheter ablation assuming a major role. The increasing knowledge of arrhythmogenesis and improved substrate definition pave the way for a more effective management for this dire arrhythmia (Huang et al.). Eventually, artificial intelligence will play a progressively central role in medicine, with the use of large database allowing to develop new algorithms in order to better stratify patients and predict response to therapy and disease progression (Chen et al.; Park et al.).

However, many questions still lay unsolved. A clear definition of the relationship between AF and stroke and firm evidence on need and timing of anticoagulation for subclinical AF episodes are still lacking. The solution of these conundrums is at quest of several studies. Given these premises, we foresee that future years will be at least as scientifically exciting as 2021, and we eagerly await apprises that will soon arrive; so, keep in touch!

Author contributions

MA and AB conceived the editorial. MA and GD revised the text. All authors contributed to the article and approved the submitted version.

Conflict of interest

MA has received educational grants from Abbott, is consultant for Biosense Webster and proctor for Medtronic.

The remaining authors declare that the research was conducted in the absence of any commercial or financial relationships that could be construed as a potential conflict of interest.

Publisher's note

References

1. Saglietto A, Ballatore A, Gaita F, Scaglione M, Ponti R De, Ferrari GM De, et al. Comparative efficacy and safety of different catheter ablation strategies for persistent atrial fibrillation: a network meta-analysis of randomized clinical trials. *Eur Heart J Qual Care Clin Outcomes.* (2021) 2021:qcab066. doi: 10.1093/ehjqcco/qcab066

2. Kirchhof P, Camm AJ, Goette A, Brandes A, Eckardt L, Elvan A, et al. Early rhythm-control therapy in patients with atrial fibrillation. *N Engl J Med.* (2020) 383:1305–16. doi: 10.1056/NEJMoa2019422

3. Reddy VY, Dukkipati SR, Neuzil P, Anic A, Petru J, Funasako M, et al. Pulsed field ablation of paroxysmal atrial fibrillation: 1-year outcomes of IMPULSE, PEFCAT, and PEFCAT II. *Clin Electrophysiol.* (2021) 7:614–27. doi: 10.1016/j.jacep.2021.02.014

4. Saglietto A, Gaita F, De Ponti R, De Ferrari GM, Anselmino M. Catheter ablation vs. anti-arrhythmic drugs as first-line treatment in symptomatic paroxysmal atrial fibrillation: a systematic review and meta-analysis of randomized clinical trials. *Front Cardiovasc Med.* (2021) 8:664647. doi: 10.3389/fcvm.2021.664647

frontiers in Cardiovascular Medicine

ORIGINAL RESEARCH
published: 06 October 2021
doi: 10.3389/fcvm.2021.746225

HATCH Score and Left Atrial Size Predict Atrial High-Rate Episodes in Patients With Cardiac Implantable Electronic Devices

Ju-Yi Chen, Tse-Wei Chen and Wei-Da Lu*

Department of Internal Medicine, National Cheng Kung University Hospital, College of Medicine, National Cheng Kung University, Tainan, Taiwan

Background: Patients with sustained atrial high-rate episodes (AHRE) have a high risk of major adverse cardio/cerebrovascular events (MACCE). However, the prediction model and factors for the occurrence of AHRE are unknown. We aimed to identify independent factors and various risk models for predicting MACCE and AHRE.

Methods: We retrospectively enrolled 314 consecutive patients who had cardiac implantable electronic devices (CIEDs). The primary endpoint was MACCE after AHRE ≥3, 6 min, and 6 h. Atrial high-rate episodes was defined as >175 bpm (Medtronic®) lasting ≥30 s. Multivariate Cox and logistic regression analysis with time-dependent covariates were used to determine variables associated with independent risk of MACCE and occurrence of AHRE ≥3 min, respectively.

Results: One hundred twenty-five patients (39.8%) developed AHRE ≥3 min, 103 (32.8%) ≥6 min, and 55 (17.5%) ≥6 h. During follow-up (median 32 months), 77 MACCE occurred (incidence 9.20/100 patient years, 95% CI 5.66–18.39). The optimal AHRE cutoff value was 3 min for MACCE, with highest Youden index 1.350 (AUC, 0.716; 95% CI, 0.638–0.793; $p < 0.001$). Atrial high-rate episodes ≥3 min−6 h were independently associated with MACCE. HATCH score and left atrial diameter were independently associated with AHRE ≥3 min. The optimal cutoff for HATCH score was 3 and for left atrial diameter was 4 cm for AHRE ≥3 min.

Conclusion: Patients with CIEDs who develop AHRE ≥3 min have an independently increased risk of MACCE. Comprehensive assessment using HATCH score and echocardiography of patients with CIEDs is warranted.

Keywords: atrial high-rate episodes, cardiac implantable electronic device, major adverse cardio/cerebrovascular events, left atrial enlargement, atrial fibrillation, HATCH score, C_2HEST score

OPEN ACCESS

Edited by:
Daniele Pastori,
Sapienza University of Rome, Italy

Reviewed by:
Yan-Guang Li,
Peking University Third Hospital, China
Hygriv B. Rao,
KIMS Hospitals, India

****Correspondence:***
Ju-Yi Chen
juyi@mail.ncku.edu.tw
orcid.org/0000-0003-2760-9978

Specialty section:
This article was submitted to Cardiac Rhythmology, a section of the journal Frontiers in Cardiovascular Medicine

Received: *23 July 2021*
Accepted: *13 September 2021*
Published: *06 October 2021*

Citation:
Chen J-Y, Chen T-W and Lu W-D (2021) HATCH Score and Left Atrial Size Predict Atrial High-Rate Episodes in Patients With Cardiac Implantable Electronic Devices. Front. Cardiovasc. Med. 8:746225. doi: 10.3389/fcvm.2021.746225

INTRODUCTION

All cardiac implantable electronic devices (CIEDs), including dual-chamber pacemakers; dual-chamber implantable cardioverter defibrillators; cardiac resynchronization therapy; and resynchronization-defibrillator, if an atrial lead is present, may record atrial tachyarrhythmias. Pacemaker-detected atrial high-rate episodes (AHRE), are predictors for atrial fibrillation (AF)

TABLE 1 | Baseline characteristics of the overall study group and with/without primary endpoints.

Variables	All patients (n = 314)	Primary endpoints MACCE[a]		Univariate P-value
		Yes (N = 77)	No (N = 237)	
Age (years)	73 (62–81)	77 (68–84)	71 (60–79)	<0.001
Gender				0.023
Male	194 (61.8%)	56 (72.7%)	138 (58.2%)	
Female	120 (38.2%)	21 (27.3%)	99 (41.8%)	
BMI[b] (kg/m^2)	24.6 (22.5–26.3)	24.3 (21.6–26.2)	24.7 (22.6–26.5)	0.240
Device type				0.103
Dual chamber PM[c]	220 (70.1%)	62 (80.5%)	158 (66.7%)	
Dual chamber ICD[d]	66 (21.0%)	12 (15.6%)	54 (22.8%)	
CRTP[e]	23 (7.3%)	2 (2.6%)	21 (8.9%)	
CRTD[f]	5 (1.6%)	1 (1.3%)	4 (1.7%)	
Primary indication				0.106
Sick sinus syndrome	141 (44.9%)	41 (53.2%)	100 (42.2%)	
Atrioventricular block	79 (25.2%)	21 (27.3%)	58 (24.5%)	
Heart failure/VT[g]/VF[h]	94 (29.9%)	15 (19.5%)	79 (33.4%)	
Atrial pacing (%)	25.0 (5.8–71.4)	28.3 (6.3–82.5)	24.3 (5.3–70.7)	0.726
Ventricular pacing (%)	1.9 (0.2–98.3)	4.9 (0.2–94.5)	1.5 (0.2–98.4)	0.263
CHA_2DS_2-VASc score[i]	3 (2–4)	4 (3–4)	3 (1–4)	<0.001
HAS-BLED score[j]	2 (1–3)	3 (2–3)	2 (1–2)	<0.001
C_2HEST score[k]	3 (1–3)	3 (2.5–4)	3 (1–3)	<0.001
HATCH score[l]	2 (1–3)	3 (2–4)	2 (1–2)	<0.001
Hypertension	253 (80.6%)	70 (90.9%)	183 (77.2%)	0.008
Diabetes mellitus	142 (45.2%)	53 (68.8%)	89 (37.6%)	<0.001
Hyperlipidemia	241 (76.8%)	72 (93.5%)	169 (71.3%)	<0.001
Chronic obstructive pulmonary disease	14 (4.5%)	5 (6.5%)	9 (3.8%)	0.319
Prior stroke	19 (6.1%)	7 (9.1%)	12 (5.1%)	0.198
Prior myocardial infarction	57 (18.2%)	25 (32.5%)	32 (13.5%)	<0.001
Heart failure				0.004
Preserved LVEF[m]	44 (14.0%)	13 (16.9%)	31 (13.1%)	
Reduced LVEF[m]	68 (21.7%)	26 (33.8%)	42 (17.7%)	
None	202 (64.3%)	38 (49.4%)	164 (69.2%)	
Chronic kidney disease	108 (34.4%)	44 (57.1%)	64 (27.0%)	<0.001
Chronic liver disease	15 (4.8%)	6 (7.8%)	9 (3.8%)	0.153
Echo parameters				
LVEF[m] (%)	66 (53.8–73.0)	60.0 (40.0–72.0)	67.0 (58.0–73.0)	0.063
Mitral E/e'	11.0 (8.0–13.6)	12.0 (10.0–15.0)	10.6 (8.0–13.0)	<0.001
LA[n] diameter (cm)	3.8 (3.2–4.1)	3.9 (3.5–4.3)	3.6 (3.1–4.1)	0.003
RV[o] systolic function (s', m/s)	12.0 (11.0–13.6)	12.0 (10.1–12.2)	12.0 (11.0–14.0)	0.016
Drug prescribed at baseline				
Antiplatelets	121 (38.5%)	49 (63.6%)	72 (30.4%)	<0.001
Anticoagulants	30 (9.6%)	5 (6.5%)	25 (10.5%)	0.293
Beta blockers	122 (38.9%)	33 (42.9%)	89 (37.6%)	0.407
Ivabradine	25 (8.0%)	8 (10.4%)	17 (7.2%)	0.365
Amiodarone	58 (18.5%)	17 (22.1%)	41 (17.3%)	0.348
Dronedarone	4 (1.3%)	2 (2.6%)	2 (0.8%)	0.253
Flecainide	1 (0.3%)	0 (0.0%)	1 (0.4%)	1.000
Propafenone	13 (4.1%)	3 (3.9%)	10 (4.2%)	1.000
Digoxin	5 (1.6%)	3 (3.9%)	2 (0.8%)	0.097
Non-DHP CCBs[p]	12 (3.8%)	2 (2.6%)	10 (4.2%)	0.737
RAAS[q] inhibitors	141 (45.0%)	41 (53.2%)	100 (42.4%)	0.096

(Continued)

TABLE 1 | Continued

Variables	All patients ($n = 314$)	Primary endpoints MACCE[a]		Univariate *P*-value
		Yes ($N = 77$)	No ($N = 237$)	
Diuretics	47 (15.0%)	19 (24.7%)	28 (11.8%)	0.006
Statins	121 (38.5%)	31 (40.3%)	90 (38.0%)	0.720
Metformin	50 (15.9%)	15 (19.5%)	35 (14.8%)	0.326
SGLT2[r] inhibitors	13 (4.1%)	6 (7.8%)	7 (3.0%)	0.064
Follow-up duration (months)	32 (16–52)	26.0 (13.0–48.0)	34.0 (16.0–53.5)	0.077
AHRE[s] duration ≥3 min	125 (39.8%)	51 (66.2%)	74 (31.2%)	<0.001
AHRE[s] duration ≥6 min	103 (32.8%)	44 (57.1%)	59 (24.9%)	<0.001
AHRE[s] duration ≥6 h	55 (17.5%)	29 (37.7%)	26 (11.0%)	<0.001

Data are presented as medians (interquartile interval) or n (%). Non–parametric continuous variables, as assessed using the Kolmogorov–Smirnov method, were analyzed using the Mann–Whitney U-test. Statistical significance is set at $p < 0.05$.

[a] *MACCE, major cardio/cerebrovascular events.*

[b] *BMI, body mass index.*

[c] *PM, pacemaker.*

[d] *ICD, implantable cardioverter defibrillator.*

[e] *CRTP, cardiac resynchronization therapy pacemaker.*

[f] *CRTD, cardiac resynchronization therapy defibrillator.*

[g] *VT, ventricular tachycardia.*

[h] *VF, ventricular fibrillation.*

[i] *CHA_2DS_2-Vasc score: Range 0–9. History of heart failure, hypertension, diabetes, vascular disease, age 65–74 years, and female sex each is calculated as 1 point; 75 years or older and prior stroke, TIA, or thromboembolism each is calculated as 2 points.*

[j] *HASBLED score: Range from 0 to 9. Point score is calculated as 1 point each for hypertension, abnormal kidney function, abnormal liver function, prior stroke, prior bleeding, or bleeding predisposition, labile international normalized ratio (INR), older than 65 years, medication usage predisposing to bleeding, and alcohol use.*

[k] *C_2HEST score: Range from 0 to 8. C_2: CAD/COPD (1 point each); H: hypertension (1 point); E: elderly (age ≥75 years, 2 points); S: systolic HF (2 points); and T: thyroid disease (hyperthyroidism, 1 point).*

[l] *HATCH score: Range from 0 to 7. Hypertension, 1 point; age >75 years, 1 point; stroke or transient ischemic attack, 2 points; chronic obstructive pulmonary disease, 1 point; heart failure, 2 points.*

[m] *LVEF, left ventricular ejection fraction.*

[n] *LA, left atrium.*

[o] *RV, right ventricle.*

[p] *Non-DHP CCBs, non-dihydropyridine calcium channel blockers.*

[q] *RAAS, renin-angiotensin-aldosterone system.*

[r] *SGLT2, sodium glucose co-transporters 2.*

[s] *AHRE, atrial high-rate episodes.*

(1) and major cardiovascular events (MACCE), including myocardial infarction, coronary revascularization, ventricular tachyarrhythmia, cardiovascular or heart failure hospitalization, and cardiovascular death (2–7). Therefore, the latest guidelines (8) recommend that AHRE be closely monitored and treated. However, the prediction of CIED-detected AHRE for MACCE has not been sufficiently assessed.

The cutoff value for AHRE duration that is associated with increased risk of MACCE remains controversial. The European Society of Cardiology guidelines state that non-valvular AF (8) with AHRE >5–6 min and >180 bpm increase the risk for ischemic stroke, but the risk for MACCE is unknown. Atrial high-rate episodes lasting ≥30 s (2) also has been shown associated with increased risk of stroke. These differences in cutoff values suggest that patients with implanted CIEDs should undergo regular assessment for detection of AHRE (8), and those with AHRE should undergo further rhythm assessment (including long-term electrocardiographic monitoring) for MACCE risk factors.

Several risk scoring systems for predicting AF, including CHA_2DS_2-VASc score (9), C_2HEST score (10), and HATCH (11, 12) have been evaluated, but only C_2HEST score has been evaluated for sustained AHRE >24 h (13). Independent predictors for AHRE in patients with dual-chamber pacemakers include sick sinus syndrome (14), increased left atrial diameter (14, 15), paced QRS duration (15), prior AF and inflammatory markers (16), and C_2HEST score (13). However, a meta-analysis of 28 studies with 24,984 patients revealed that patients' baseline characteristics of advanced age, lower resting heart rate, diabetes, hypertension, coronary artery disease, stroke and thromboembolic events, congestive heart failure, increased left atrial diameter, and even $CHADS_2$ scores were not associated with device-detected AHRE (17). These results suggest that predictors of AHRE are not well-established, and additional study is needed to identify independent predictors.

The present study investigated the optimal cutoff durations of AHRE for MACCE in patients who had CIEDs but no history of AF, and assessed independent predictive factors and

Abbreviations: AF, atrial fibrillation; AHRE, atrial high-rate episodes; CIEDs, cardiac implantable electronic devices; MACCE, major adverse cardio/cerebrovascular events; TIA, transient ischemic attacks.

validation of risk-prediction scoring systems (CHA_2DS_2-VASc score, HASBLED score, C_2HEST score, and HATCH score) for AHRE in such patients.

METHODS

Consecutive patients aged 18 years or older who had CIEDs implanted (Medtronic® dual chamber pacemaker, dual chamber implantable cardioverter defibrillator, cardiac resynchronization therapy-pacing, or cardiac resynchronization therapy-defibrillator) in the Cardiology Department of National Cheng Kung University Hospital from January 2015 to April 2021 were included. Every time of interrogation data of CIEDs of each enrolled patients were saved in a chart-record system in our hospital.

Ethical Considerations

The protocol for this cohort study was reviewed and approved by the ethics committee of National Cheng Kung University Hospital and was conducted according to guidelines of the

TABLE 2 | Types and incidences of major adverse cardio/cerebrovascular events in patients with or without AHRE.

Types of MACCE[a]	Number	AHRE[b](+) 209	Incidence rate (100 patient-years)	CI[c] 95%	AHRE[b](–) 105	Incidence rate (100 patient-years)	CI[c] 95%
TIA[d]	11	11	1.80	1.21–3.72	0	0	0
Ischemic stroke	7	6	0.98	0.66–2.03	1	0.38	0.24–0.79
Embolic event	2	2	0.33	0.22–0.68	0	0	0
ACS[e]	34	28	4.59	3.09–9.46	6	2.29	1.43–4.73
Sustained VT[f]/VF[g]	6	4	0.66	0.44–1.35	2	0.76	0.48–1.58
All-cause mortality	17	16	2.62	1.77–5.40	1	0.38	0.24–0.79
Total events	77	67	10.99	7.40–22.63	10	3.81	2.38–7.88

[a] *MACCE, major adverse cardio/cerebrovascular events.*
[b] *AHRE, atrial high rate episode.*
[c] *CI, confidence intervals.*
[d] *TIA, transient ischemic attack.*
[e] *ACS, acute coronary syndrome: including ST elevation myocardial infarction, non-ST elevation myocardial infarction, and unstable angina.*
[f] *VT, ventricular tachycardia.*
[g] *VF, ventricular fibrillation.*

TABLE 3 | Multivariate Cox regression analysis for major adverse cardio/cerebrovascular events.

Variables	Model A-1			Model A-2			Model A-3		
	HR	95%CI	*p*	HR	95%CI	*p*	HR	95%CI	*p*
Age (y/o)	1.016	0.990–1.042	0.229	1.020	0.994–1.046	0.128	1.021	0.994–1.048	0.126
Gender (male)	0.870	0.498–1.521	0.625	0.939	0.536–1.645	0.825	0.879	0.503–1.535	0.650
Hypertension (yes)	1.386	0.000–4.240	0.965	1.943	0.000–4.236	0.964	1.337	0.000–2.233	0.963
Diabetes mellitus (yes)	1.754	0.945–3.256	0.075	1.764	0.948–3.283	0.073	1.713	0.913–3.212	0.094
Hyperlipidemia (yes)	0.713	0.163–3.119	0.654	0.465	0.103–2.098	0.319	0.622	0.141–2.744	0.531
Prior MI (yes)	0.860	0.429–1.726	0.672	0.990	0.490–2.002	0.979	0.806	0.389–1.669	0.561
CKD (yes)	1.592	0.885–2.863	0.121	1.505	0.837–2.706	0.172	1.296	0.702–2.392	0.406
Heart failure reduced ejection fraction (yes)	3.001	1.366–6.594	0.006	2.895	1.274–6.580	0.011	3.599	1.605–8.070	0.002
AHRE duration ≥3 min	3.216	1.745–5.927	<0.001						
AHRE duration ≥6 min				2.800	1.591–4.931	<0.001			
AHRE duration ≥6 h							2.220	1.254–3.927	0.006

Variables	Model B-1			Model B-2			Model B-3			Model B-4		
	HR	95%CI	*p*	HR	95%CI	*p*	HR	95%CI	*p*	HR	95%CI	*p*
CHA_2DS_2-VASc score	1.584	1.292–1.940	<0.001									
HAS-BLED score				2.040	1.586–2.623	<0.001						
C_2HEST score							1.354	1.179–1.555	<0.001			
HATCH score										1.789	1.500–2.135	<0.001
AHRE duration ≥3min	3.675	2.051–6.586	<0.001	3.323	1.851–5.964	<0.001	2.391	1.477–3.869	<0.001	2.680	1.463–4.907	0.001

International Conference on Harmonization for Good Clinical Practice (B-ER-108-278). All included patients provided signed informed consent at the time of their implantation procedures for data to be recorded for later publication.

Data Collection and Definitions

Patients' medical history and data of co-morbidities and echocardiographic criteria were collected from chart records for retrospective evaluation. Diabetes mellitus was defined by the presence of symptoms and casual plasma glucose concentration ≥200 mg/dl, fasting plasma glucose concentration ≥126 mg/dl, 2-h plasma glucose concentration ≥200 mg/dl from a 75-g oral glucose tolerance test, or taking medication for diabetes mellitus. Hypertension was defined as in-office systolic blood pressure values ≥140 mm Hg and/or diastolic blood pressure values ≥90 mm Hg or taking antihypertensive medication. Dyslipidemia was defined as low-density lipoprotein ≥140 mg/dl, high-density lipoprotein <40 mg/dl, triglycerides ≥150 mg/dl, or taking medication for dyslipidemia. Chronic kidney disease was defined as an estimated glomerular filtration rate (eGFR) <60 ml/min/1.73 m^2 for at least 3 months. The primary endpoint for this study was the occurrence of MACCE after the date of CIED implantation, including ST-elevation myocardial infarction, non-ST-elevation myocardial infarction, unstable angina, systemic thromboembolism, sustained ventricular tachycardia/fibrillation, all-cause mortality, and cerebrovascular events, including stroke or transient ischemic attack (TIA) diagnosed by experienced neurologists. For each outcome, only the first event of that outcome in a subject was included. For the composite outcome, only the first event was included.

Atrial high-rate episodes were extracted from the devices via telemetry at each office visit (3–6 months). Atrial high-rate episodes electrograms were reviewed by at least one experienced electrophysiologist, who excluded lead noise or artifacts, far-field R-waves, paroxysmal supraventricular tachycardia, and visually confirmed AF that had been recorded as AHRE. Atrial sensitivity was programmed to 0.3 mV with bipolar sensing of Medtronic devices. Atrial high-rate episodes was defined as heart rate >175

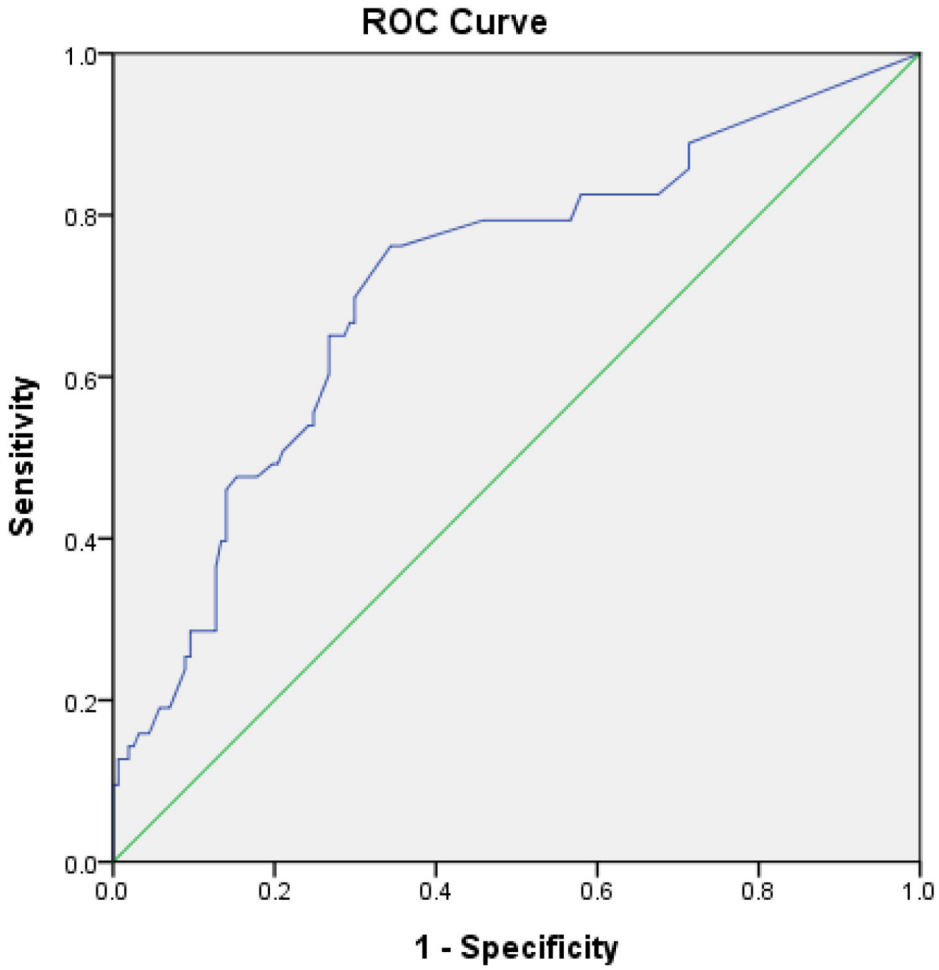

FIGURE 1 | Receiver-operating characteristic curve analysis of atrial high-rate episodes (min) in patients with CIEDs with subsequent systemic embolic events. Atrial high-rate episodes (min): optimal cutoff value with the highest Youden index, 3 min; sensitivity, 76.2%; specificity, 70.0%; AUC, 0.716; 95% CI, 0.638–0.793; $p < 0.001$.

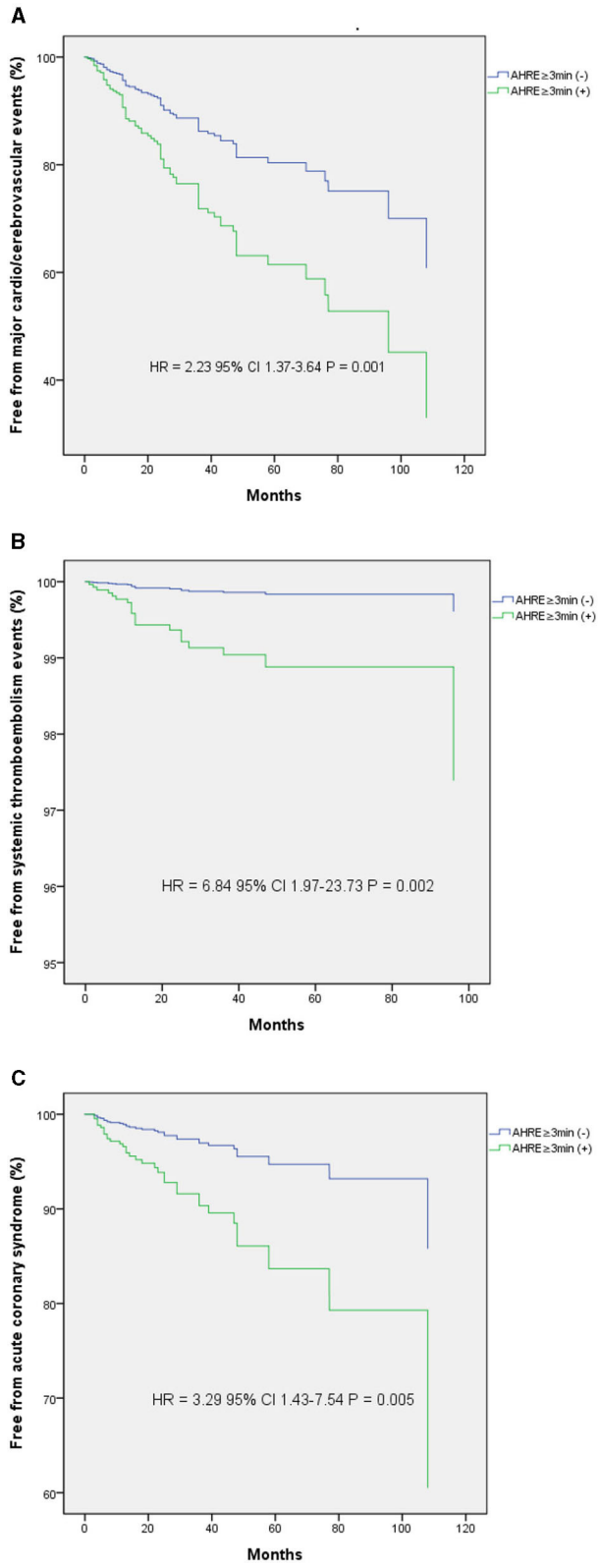

FIGURE 2 | Kaplan-Meier curves depict the accumulative survival rates free from different endpoints regarding AHRE ≥3 min or not. **(A)** For major adverse cardio/cerebrovascular events, a significant higher hazard is seen among the AHRE ≥3 min (+) compared with the AHRE ≥3 min (–) (HR 2.23, log-rank $p = 0.001$). **(B)** For systemic thromboembolism events, a significant higher hazard is seen among the AHRE ≥3 min (+) compared with the AHRE ≥3 min (–) (HR 6.84, log-rank $p = 0.002$). **(C)** For acute coronary syndrome, a significant higher hazard is seen among the AHRE ≥3 min (+) compared with the AHRE ≥3 min (–) (HR 3.29, log-rank $p = 0.005$).

bpm and at least 30 s of atrial tachyarrhythmia recorded by the devices on any day during the study. To evaluate the cutoff threshold for primary endpoints, AHRE was categorized by duration ≥3, ≥6 min, and ≥6 h. If patients had multiple AHREs, the longest AHRE duration was used for analysis. If a patient's longest AHRE duration was 7 min, the result was counted as AHRE ≥3 and ≥6 min.

Statistical Analysis

Categorical variables are presented as percentages, and continuous variables are presented as means and standard deviations for normally distributed values or medians and interquartile interval for non-normally distributed values. The normal distribution for continuous variables was assessed with the Kolmogorov–Smirnov method. Pearson's chi-square test or Fisher's exact test was used to determine differences in baseline characteristics for categorical variables, and a two-sample student's *t*-test or Mann-Whitney U-test was used to analyze continuous variables. Survival was estimated by the Kaplan–Meier method, and differences in survival were evaluated with a log-rank test. Multivariate Cox regression analysis was used to identify variables associated with AHRE occurrence, reported as hazard ratios (HR) with 95% confidence intervals (CI). If the *p*-value in univariable analysis was <0.05, the parameter was entered into multivariable analysis. Indicators of AHRE ≥3 min, 6 min, and 6 h were determined separately as time-dependent covariates in multivariate Cox proportional hazards regression. Because CHA_2DS_2-VASc scores, HASBLED score, C_2HEST score, and HATCH score overlapped many factors in univariate analysis, they were used as an independent factor in multivariate Cox regression analysis. The receiver-operating characteristic (ROC) area under the curve (AUC) of AHRE and the associated 95% CI were evaluated for association with MACCE after CIED implantation. The optimal cutoff values with the highest Youden index were chosen based on the results of ROC curve analysis and used to evaluate the associated values of AHRE in min for determining endpoints and the optimal cutoff values of left atrial size in cm and HATCH score for determining AHRE >3 min. For all comparisons, $p < 0.05$ was considered statistically significant. All data were analyzed using SPSS statistical package version 23.0 (SPSS Inc. Chicago, IL, USA).

RESULTS

Between January 1, 2014, and April 30, 2021, 453 consecutive patients who received Medtronic CIED implantation at National Cheng Kung University Hospital were recruited initially. Patients with previous AF ($n = 139$) were excluded, so the final

TABLE 4 | Baseline characteristics of the overall study group and with/without AHRE ≥3 min.

Variables	All patients (n = 314)	AHRE ≥3 min		Univariate P-value
		Yes (N = 125)	No (N = 189)	
Age (years)	72.5 (62–81)	76 (64–83)	70 (59–79)	0.006
Gender				0.108
Male	194 (61.8%)	84 (67.2%)	110 (58.2%)	
Female	120 (38.2%)	41 (32.8%)	79 (41.8%)	
BMI[a] (kg/m^2)	24.6 (22.5–26.3)	24.5 (22.3–26.0)	24.8 (22.6–26.8)	0.080
Device type				0.001
Dual chamber PM[b]	220 (70.1%)	102 (81.6%)	118 (62.4%)	
Dual chamber ICD[c]	66 (21.0%)	12 (9.6%)	54 (28.6%)	
CRTP[d]	23 (7.3%)	9 (7.2%)	14 (7.4%)	
CRTD[e]	5 (1.6%)	2 (1.6%)	3 (1.6%)	
Primary indication				0.001
Sick sinus syndrome	141 (44.9%)	62 (49.6%)	79 (41.8%)	
Atrioventricular block	79 (25.2%)	40 (32.0%)	39 (20.6%)	
Heart failure/VT[f]/VF[g]	94 (29.9%)	23 (18.4%)	71 (37.6%)	
Atrial pacing (%)	25.0 (5.8–71.4)	29.2 (4.8–70.5)	23.1 (6.2–77.6)	0.937
Ventricular pacing (%)	1.9 (0.2–98.3)	16.5 (0.5–98.9)	0.3 (0.2–86.4)	<0.001
CHA_2DS_2-VASc score[h]	3 (2–4)	3 (2–4)	3 (2–4)	0.027
C_2HEST score[i]	3 (1–3)	3 (1–3)	3 (1–3)	0.016
HATCH score[j]	2 (1–3)	2 (1–3)	2 (1–2)	<0.001
Hypertension	253 (80.6%)	113 (90.4%)	140 (74.1%)	<0.001
Diabetes mellitus	142 (45.2%)	60 (48.0%)	82 (43.4%)	0.421
Hyperlipidemia	241 (76.8%)	108 (86.4%)	133 (70.4%)	0.001
Chronic obstructive pulmonary disease	14 (4.5%)	7 (5.6%)	7 (3.7%)	0.425
Prior stroke	19 (6.1%)	9 (7.2%)	10 (5.3%)	0.487
Prior myocardial infarction	57 (18.2%)	28 (22.4%)	29 (15.3%)	0.112
Heart failure				0.448
Preserved LVEF[k]	44 (14.0%)	21 (16.8%)	23 (12.2%)	
Reduced LVEF[k]	68 (21.7%)	28 (22.4%)	40 (21.2%)	
None	202 (64.38)	76 (60.8%)	126 (66.7%)	
Chronic kidney disease	108 (34.4%)	53 (42.4%)	55 (29.1%)	0.015
Chronic liver disease	15 (4.8%)	7 (5.6%)	8 (4.2%)	0.578
Echo parameters				
LVEF[k] (%)	66.0 (53.8–73.0)	66.0 (53.5–73.0)	66.0 (52.5–73.0)	0.716
Mitral E/e'	11.0 (8.0–13.6)	11.1 (9.0–14.5)	10.7 (7.7–13.0)	0.012
LA[l] diameter (cm)	3.8 (3.2–4.1)	3.9 (3.4–4.3)	3.6 (3.1–4.1)	0.003
RV[m] systolic function (s', m/s)	12.0 (11.0–13.6)	12.0 (11.0–14.0)	12.0 (11.0–13.5)	0.995
Drug prescribed at baseline				
Antiplatelets	121 (38.5%)	52 (41.6%)	69 (36.5%)	0.364
Anticoagulants	30 (9.6%)	20 (16.0%)	10 (5.3%)	0.002
Beta blockers	122 (38.9%)	46 (36.8%)	76 (40.2%)	0.544
Ivabradine	25 (8.0%)	9 (7.2%)	16 (8.5%)	0.685
Amiodarone	58 (16.8%)	21 (16.8%)	37 (19.6%)	0.535
Dronedarone	4 (1.3%)	3 (2.4%)	1 (0.5%)	0.305
Flecainide	1 (0.3%)	0 (0.0%)	1 (0.5%)	1.000
Propafenone	13 (4.1%)	9 (7.2%)	4 (2.1%)	0.040
Digoxin	5 (1.6%)	3 (2.4%)	2 (1.1%)	0.390
Non-DHP CCBs[n]	12 (3.8%)	6 (4.8%)	6 (3.2%)	0.462
RAAS[o] inhibitors	141 (45.0%)	55 (44.0%)	86 (45.7%)	0.761
Diuretics	47 (15.0%)	21 (16.8%)	26 (13.8%)	0.459

(Continued)

TABLE 4 | Continued

Variables	All patients ($n = 314$)	AHRE ≥3 min		Univariate *P*-value
		Yes ($N = 125$)	No ($N = 189$)	
Statins	121 (38.5%)	41 (32.8%)	80 (42.3%)	0.089
Metformin	50 (15.9%)	14 (11.2%)	36 (19.0%)	0.063
SGLT2[p] inhibitors	13 (4.1%)	4 (3.2%)	9 (4.8%)	0.575

Data are presented as medians (interquartile interval) or n (%). Non-parametric continuous variables, as assessed using the Kolmogorov–Smirnov method, were analyzed using the Mann–Whitney U test. Statistical significance is set at $p < 0.05$.

[a] *BMI, body mass index.*

[b] *PM, pacemaker.*

[c] *ICD, implantable cardioverter defibrillator.*

[d] *CRTP, cardiac resynchronization therapy pacemaker.*

[e] *CRTD, cardiac resynchronization therapy defibrillator.*

[f] *VT, ventricular tachycardia.*

[g] *VF, ventricular fibrillation.*

[h] *CHA_2DS_2-Vasc score: Range from 0 to 9. History of heart failure, hypertension, diabetes, vascular disease, age 65–74 years, and female sex each is calculated as 1 point; 75 years or older and prior stroke, TIA, or thromboembolism each is calculated as 2 points.*

[i] *C_2HEST score: Range from 0 to 8. C_2: CAD/COPD (1 point each); H: hypertension (1 point); E: elderly (age ≥75 years, 2 points); S: systolic HF (2 points); and T: thyroid disease (hyperthyroidism, 1 point).*

[j] *HATCH score: Range from 0 to 7. Hypertension, 1 point; age >75 years, 1 point; stroke or transient ischemic attack, 2 points; chronic obstructive pulmonary disease, 1 point; heart failure, 2 points.*

[k] *LVEF, left ventricular ejection fraction.*

[l] *LA, left atrium.*

[m] *RV, right ventricle.*

[n] *Non-DHP CCBs, non-dihydropyridine calcium channel blockers.*

[o] *RAAS, renin-angiotensin-aldosterone system.*

[p] *SGLT2, sodium glucose co-transporters 2.*

analysis included data of 314 patients, of which 77 had experienced MACCE.

The median follow-up period was 32 months after implantation of CIEDs. **Table 1** presents the patients' baseline demographic and clinical characteristics based on whether they had MACCE. Patients' median age was 73 years, and 61.8% of patients were men. Types of CIEDs were dual chamber pacemaker (220, 70.1%), dual chamber ICD (66, 21.0%), CRTP (23, 7.3%), and CRTD (5, 1.6%). The most common indication for CIED implantation was sick sinus syndrome (44.9%), followed by atrioventricular block (25.2%) and ventricular tachyarrhythmia (29.9%). Median atrial pacing was 25.0% and ventricular pacing 1.9%. High percentages of hypertension (80.6%), hyperlipidemia (76.8%), and diabetes (45.2%) suggest relatively high risk of primary endpoints for the entire study cohort. During follow-up, 125 (39.8%) patients developed AHRE ≥3 min, 103 (32.8%) developed AHRE ≥6 min, and 55 (17.5%) developed AHRE ≥6 h.

Components of primary endpoints, including MACCE, time to primary endpoints, incidence rates, and distribution of MACCE, are reported in **Table 2**. The total number of MACCE was 77 (incidence rate 9.20/100 patient-years, 95% CI 5.66–18.39). The endpoints were acute coronary syndrome, systemic thromboembolism events, and all-cause mortality. We also compared the incidence rates between the patients with or without AHRE in **Table 2**. The patients with AHRE had higher incidence rates of MACCE than those without AHRE.

Univariate Analysis and Multivariate Cox Regression Analysis to Identify Associations Between AHRE Durations and MACCE

Univariate analysis revealed that age, male gender, hypertension, diabetes mellitus, hyperlipidemia, prior myocardial infarction, heart failure with reduced ejection fraction, chronic kidney disease, CHA_2DS_2-VASc score, HAS-BLED score, C_2HEST score, and HATCH score were significantly associated with MACCE occurrence. Atrial high-rate episodes lasting ≥3, ≥6 min, and ≥6 h were each significantly associated with MACCE (**Table 1**). Multivariate Cox regression analysis using model A (not including CHA_2DS_2-VASc score, HASBLED score, C_2HEST score, and HATCH score as a confounder) showed that AHRE ≥3 min (HR 3.216, 95% CI 1.745–5.927, $p < 0.001$), AHRE ≥6 min (HR 2.800, 95% CI 1.591–4.931, $p < 0.001$), and AHRE ≥6 h (HR 2.220, 95% CI 1.254–3.927, $p = 0.006$) were independently associated with MACCE, except in heart failure with reduced ejection fraction, which was also associated with MACCE (**Table 3**). In model B (which included CHA_2DS_2-VASc score, HASBLED score, C_2HEST score, and HATCH score as a confounder), AHRE ≥3 min (HR 3.675, 95% CI 2.051–6.586, $p < 0.001$) was still independently associated with MACCE except in the presence of CHA_2DS_2-VASc scores, HASBLED score, C_2HEST score, and HATCH score. We also demonstrated the independent role of AHRE in predicting ischemic thromboembolic events, including ischemic stroke and TIA, in the **Supplementary Tables 1**, **2**.

TABLE 5 | Multivariate logistic regression analysis for independent factors of subsequent atrial high rate episodes ≥3 min.

	Model 1			Model 2			Model 3			Model 4		
	HR	95%CI	*p*	HR	95%CI	*p*	HR	95%CI	*p*	HR	95%CI	*p*
Age (y/o)	0.999	0.977–1.022	0.944									
Indications (SSS)[a]	1.160	0.610–2.209	0.650	1.161	0.606–2.224	0.653	1.224	0.638–2.350	0.543	1.354	0.698–2.624	0.370
Ventricular pacing (%)	1.002	0.996–1.009	0.493	1.002	0.996–1.009	0.495	1.002	0.996–1.009	0.504	1.002	0.995–1.009	0.642
Hypertension (yes)	1.611	0.646–4.017	0.306									
Hyperlipidemia (yes)	1.065	0.467–2.431	0.881	1.208	0.523–2.793	0.658	1.164	0.538–2.516	0.700	0.960	0.435–2.119	0.919
Chronic kidney disease (yes)	1.335	0.780–2.285	0.292	1.334	0.766–2.324	0.308	1.213	0.693–2.124	0.499	1.028	0.588–1.797	0.924
Mitral E/E'	1.017	0.970–1.067	0.486	1.019	0.971–1.070	0.450	1.016	0.968–1.066	0.524	1.002	0.953–1.053	0.935
Left atrial diameter (cm)	1.665	1.111–2.497	0.014	1.651	1.101–2.475	0.015	1.619	1.082–2.422	0.019	1.559	1.038–2.341	0.033
CHA_2DS_2-VASc score[b]				1.028	0.834–1.268	0.793						
C_2HEST score[c]							1.123	0.927–1.360	0.236			
HATCH score[d]										1.546	1.211–1.973	<0.001

[a] *SSS: Sick sinus syndrome.*

[b] *CHA_2DS_2-Vasc score: Range from 0 to 9. History of heart failure, hypertension, diabetes, vascular disease, age 65–74 years, and female sex each is calculated as 1 point; 75 years or older and prior stroke, TIA, or thromboembolism each is calculated as 2 points.*

[c] *C_2HEST score: Range from 0 to 8. C_2: CAD/COPD (1 point each); H: hypertension (1 point); E: elderly (age ≥75 years, 2 points); S: systolic HF (2 points); and T: thyroid disease (hyperthyroidism, 1 point).*

[d] *HATCH score: Range from 0 to 7. Hypertension, 1 point; age >75 years, 1 point; stroke or transient ischemic attack, 2 points; chronic obstructive pulmonary disease, 1 point; heart failure, 2 points.*

ROC-AUC Determination of AHRE Cutoff Values as Predictive Factors for Future MACCE and Survival Analysis

The optimal AHRE cutoff value predictive of MACCE was determined to be 3 min, with the highest Youden index 1.350 (sensitivity, 76.2%; specificity, 70.0%; AUC, 0.716; 95% CI, 0.638–0.793; $p < 0.001$) (**Figure 1**). The survival analysis revealed a significant correlation between an AHRE ≥3 min detection and a shorter event-free survival time. Multivariate Cox proportional hazards analysis further revealed that AHRE ≥3 min were associated with increased risk of MACCE (HR = 2.23, 95% CI 1.37–3.64, $p = 0.001$), systemic thromboembolism events (HR = 6.84, 95% CI 1.97–23.73, $p = 0.002$), and acute coronary syndrome (HR = 3.28% CI 1.43–7.54, $p = 0.005$) (**Figure 2**).

Univariate Analysis and Multivariate Logistic Regression Analysis to Identify Associations Between Risk Models and AHRE ≥3 Min

After a median follow-up of 32 months, 125 (39.8%) patients had AHRE ≥3 min. In univariate analysis, sick sinus syndrome, hypertension, hyperlipidemia, chronic kidney disease, accumulated ventricular pacing loads, left atrial diameter, mitral E/E', CHA_2DS_2-VASc scores, HASBLED score, C_2HEST score, and HATCH score were significantly different between patients with or without AHRE ≥3 min (**Table 4**).

Multivariate logistic regression analysis revealed that among values from the significant variables from the univariate analysis, only HATCH score (HR 1.546, 95% CI 1.211–1.973, $p < 0.001$) and left atrial diameter (HR 1.559, 95% CI 1.038–2.341, $p = 0.033$) were independently associated with AHRE ≥3 min (**Table 5**).

ROC-AUC Determination of HATCH Score and Left Atrial Diameter Cutoff Values Associated With AHRE ≥3 Min

The optimal HATCH score cutoff value for AHRE ≥3 min was 3, with the highest Youden index (sensitivity, 43.2%; specificity, 76.7%; AUC, 0.624; 95% CI, 0.560–0.688; $p < 0.001$) (**Figure 3**). The optimal left atrial diameter cutoff value for subsequent AHRE ≥3 min was 4 cm, with the highest Youden index (sensitivity, 47.2%; specificity, 68.3%; AUC, 0.600; 95% CI, 0.536–0.664; $p = 0.003$) (**Figure 3**). We also found that patients with both left diameter ≥4 cm and HATCH score ≥3 had a higher risk for AHRE ≥3 min than did patients with either left atrial diameter <4 cm or HATCH score <3 (**Figure 4**).

DISCUSSION

The main finding of this study is that AHRE lasting ≥3, ≥6 min, or ≥6 h is significantly and independently associated with MACCE in a Taiwanese population having CIEDs and no history of AF. The optimal cutoff value of AHRE for subsequent MACCE was 3 min. Increased left atrial diameter and HATCH score were independently associated with AHRE duration ≥3 min. These results suggest that early detection of AHRE ≥3 min and measurement of left diameter and calculation of the HATCH score in patients with CIEDs is warranted to prompt early, aggressive therapy to prevent MACCE.

This study was conducted because the optimal cutoff for AHRE duration to predict MACCE in patients with CIEDs

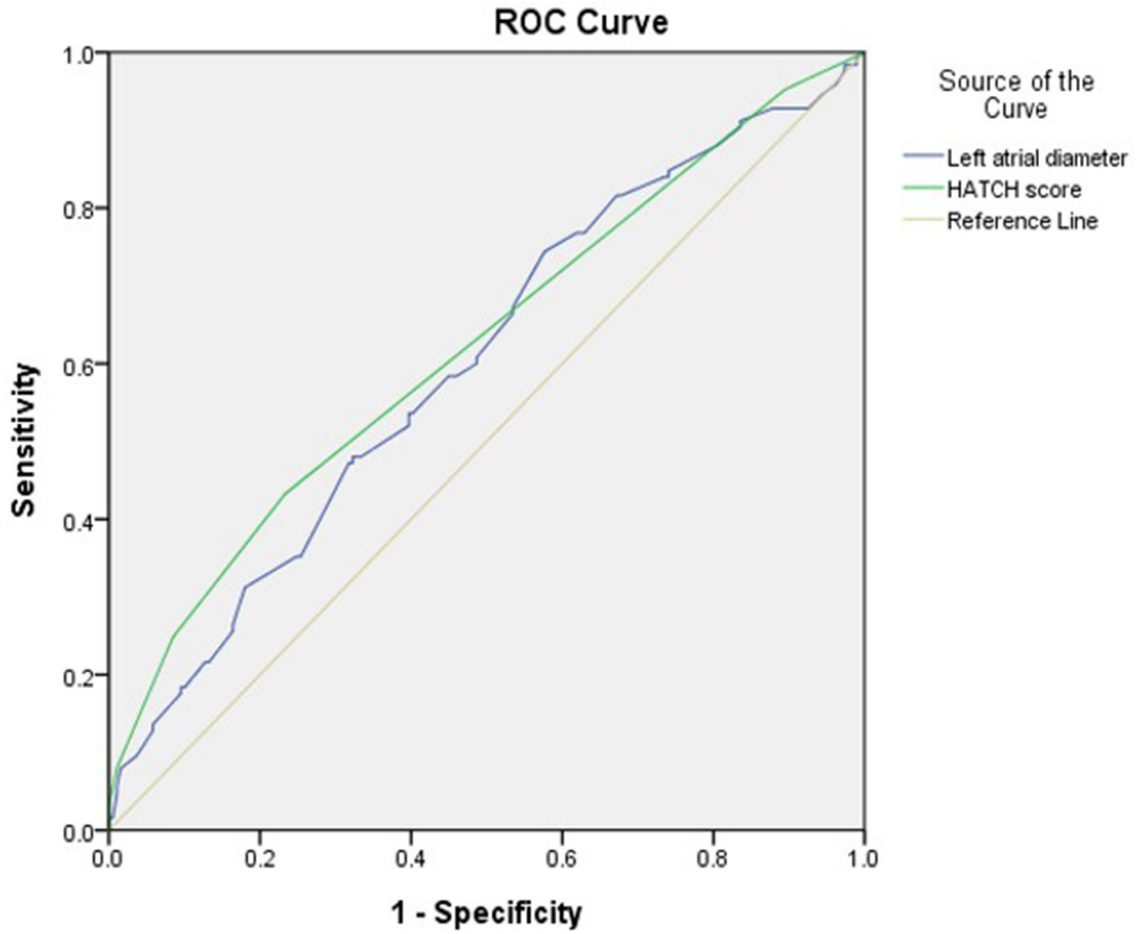

FIGURE 3 | Receiver-operating characteristic curve analysis of factors in patients with CIEDs with subsequent AHRE ≥3 min. Left atrial diameter (cm): the highest Youden index: 4.0 cm, AUC, 0.600; 95% CI, 0.536–0.664; $p = 0.003$. HATCH score: the highest Youden index: 3, AUC, 0.624; 95% CI, 0.560–0.688; $p < 0.001$.

had not been well-studied, and predictive factors were not established. Sometimes, a relative short-duration of atrial tachyarrhythmias, such as <30 s, may be misclassified as AHRE due to artifacts and false detection of far-field R-waves by the atrial lead. European Society of Cardiology guidelines (8) recommend that AF can only be diagnosed by 12-lead electrocardiography or more than 30 s in an electrocardiographic strip. The updated guidelines (8) also recommend that if AHRE ≥6 min with high CHA_2DS_2-VASc score or AHRE ≥24 h occur, more aggressive monitoring of clinical AF is warranted.

Although most studies have focused on systemic embolic or neurological events occurring after AHRE, more recent studies have found that MACCE, including ventricular tachyarrhythmias (6, 7), heart failure (6), myocardial infarction (6), and cardiovascular death (6), also were associated with AHRE ≥5 min, and the association was even stronger for AHRE ≥24 h. Also, the use of different settings for AHRE detection is an important factor that can affect results between these studies. Pastori et al. (6) used 175 beats/min, and Vergara et al. (7) used 200 beats/min as threshold rate. We used 175 beats/min (Medtronic), and at least 30 s of atrial tachyarrhythmia recorded by the CIEDs on any day during the study period. Atrial high-rate episodes ≥3, ≥6 min, and ≥6 h were all significant risk factors for future MACCE. Only the present study has demonstrated that AHRE is an independent risk factor for MACCE, and the optimal cutoff value for predicting MACCE is 3 min.

Several pathophysiological mechanisms of AHRE in MACCE have been proposed (18): (1) AHRE as a precursor of AF, leading to coronary or systemic thromboembolism from the left atrium or left atrial appendage, resulting in acute coronary syndrome or neurologic events; (2) AHRE associated with multiple atherosclerotic risks and associated inflammatory process, yielding a pro-thrombotic state; and (3) AHRE resulting in a supply-demand mismatch between the coronary system and heart function. Hence, the relationship of AHRE duration and MACCE is an

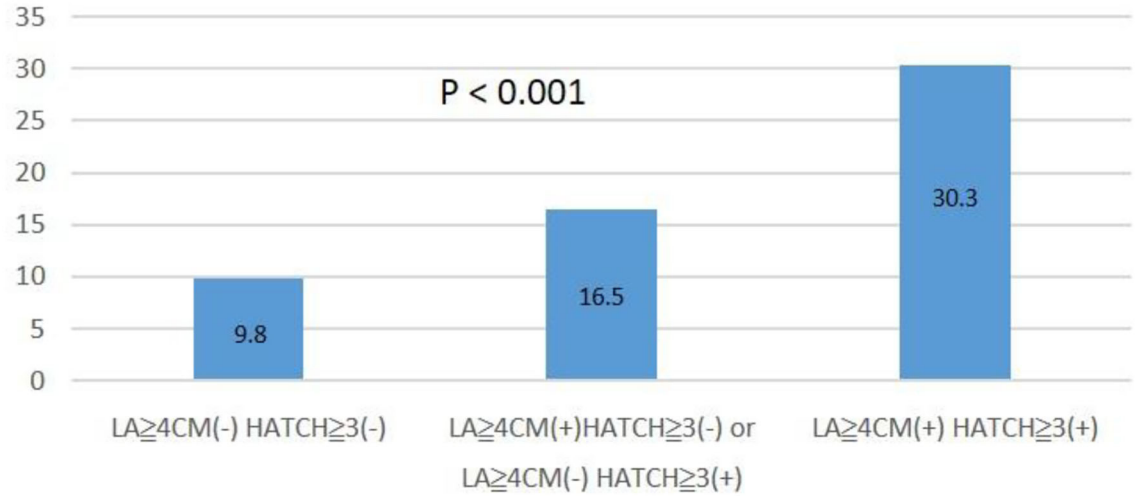

FIGURE 4 | The incidence percentage of AHRE ≥3 min significantly increased with left atrial size ≥4 cm and HATCH score ≥3.

important area of research. Large-scale studies are needed to explore AHRE duration cutoffs, with the goal of establishing a standard cutoff for further evaluation of MACCE in patients with AHRE.

Awareness of risk factors that contribute to the occurrence of AHRE ≥3 min is important for early prevention in patients with CIEDs. Previous studies (13–17) identified several predictors for AHRE; a consistent predictive factor was increased left atrial diameter (14, 15). The Korean study (14) demonstrated that left atrial diameter >41 mm was associated with AHRE ≥6 min, and the Indian study (15) reported that increased left atrial diameter contributed to prolonged AHRE. In the present study, increased left atrial diameter was consistently and significantly associated with AHRE ≥3 min, a finding compatible with results of the two studies above. Our results suggest that evaluation of patients' echocardiographic features before implantation of CIEDs should include measurement of left atrial size, which may provide early prediction of AHRE ≥3 min—a strong predictor for MACCE.

Risk scoring systems, such as CHA_2DS_2-VASc score (9), C_2HEST score (10), and HATCH score (11, 12), have been evaluated for predicting AF, but only the C_2HEST score was evaluated for sustained AHRE >24 h (13). We found that the HATCH score independently predicted sustained AHRE ≥3 min (HR 1.546, $p < 0.001$), but the CHA_2DS_2-VASc score and the C_2HEST score did not. We found also that the percentage of AHRE ≥3 min increased with increasing HATCH score. Recently, Li et al. (19), in China, modified the mC_2HEST score (adding age ≥65 years as one point), which increased the predictive accuracy and discriminative capability for incident AF. We also evaluated the performance of the mC_2HEST score but found it not as suitable as the HATCH score (data not shown).

LIMITATIONS

Our study has limitations. First, this was a single-center, retrospective, observational study with a relatively small number of patients with CIEDs in a hospital setting, and all patients were Taiwanese. Thus, causality cannot be inferred between AHRE and MACCE, and the presence of confounding factors cannot be denied. Also, the results may not be generalizable to other populations. Thus, prospective multicenter studies with larger samples are required to confirm the results of this study. Second, this study did not investigate the nature of heart rhythms at the time of onset of MACCE. Third, in this retrospective analysis of patient data, we could not confirm that patients started anticoagulants due to CIED-detected AHRE, although these patients were not excluded because no significant differences were found between anticoagulants use and the presence (5, 6.5%) or absence (25, 10.5%) of MACCE ($p = 0.293$), as shown in **Table 1**.

CONCLUSIONS

Major cardiovascular events are not uncommon in patients after implantation of CIEDs. Episodes of AHRE lasting ≥3 min to ≥6 h are independent risk factors for MACCE in this population during mid-term follow-up. When AHRE ≥3 min is detected in patients with CIEDs, long-term monitoring to detect clinical AF

and comprehensive assessment of MACCE risk with HATCH score and echocardiography (to determine left atrial size) for risk stratification are indicated. Early detection of AHRE ≥3 min and measurement of left atrial diameter and calculation of HATCH score in patients with CIEDs may be warranted to prompt early, aggressive therapy and prevent MACCE.

DATA AVAILABILITY STATEMENT

The raw data supporting the conclusions of this article will be made available by the authors, without undue reservation.

ETHICS STATEMENT

The studies involving human participants were reviewed and approved by Institutional Review Board of National Cheng Kung University Hospital (B-ER-108-278).

AUTHOR CONTRIBUTIONS

J-YC: conception and design, data analysis and interpretation, statistical analysis, drafting and finalizing the article, and critical revision of the article for important intellectual content. T-WC and W-DL: data acquisition. All authors contributed to the article and approved the submitted version.

FUNDING

The authors thank the Ministry of Science and Technology of the Republic of China, Taiwan, for financially supporting this research under contract MOST 109-2218-E-006-024 and MOST 110-2218-E-006-017.

ACKNOWLEDGMENTS

The authors thank Convergence CT for assistance with English editing of the manuscript.

SUPPLEMENTARY MATERIAL

The Supplementary Material for this article can be found online at: https://www.frontiersin.org/articles/10.3389/fcvm.2021.746225/full#supplementary-material

REFERENCES

1. Khan AA, Boriani G, Lip GYH. Are atrial high-rate episodes (AHREs) a precursor to atrial fibrillation? *Clin Res Cardiol.* (2020) 109:409–16. doi: 10.1007/s00392-019-01545-4
2. Nakano M, Kondo Y, Nakano M, Kajiyama T, Hayashi T, Ito R, et al. Impact of atrial high-rate episodes on the risk of future stroke. *J Cardiol.* (2019) 74:144–9. doi: 10.1016/j.jjcc.2019.01.006
3. Chen JY, Lu WD. Duration of atrial high-rate episodes and CHA_2DS_2-VASc score to predict cardiovascular and cerebrovascular events in patients with dual chamber permanent pacemakers. *J Cardiol.* (2021) 77:166–73. doi: 10.1016/j.jjcc.2020.08.005
4. Uittenbogaart SB, Lucassen WAM, van Etten-Jamaludin FS, de Groot JR, van Weert HCPM. Burden of atrial high-rate episodes and risk of stroke: a systematic review. *Europace.* (2018) 20:1420–7. doi: 10.1093/europace/eux356
5. Lu WD, Chen JY. Atrial high-rate episodes and risk of major adverse cardiovascular events in patients with dual chamber permanent pacemakers: a retrospective study. *Sci Rep.* (2021) 11:5753. doi: 10.1038/s41598-021-85301-7
6. Pastori D, Miyazawa K, Li Y, Székely O, Shahid F, Farcomeni A, et al. Atrial high-rate episodes and risk of major adverse cardiovascular events in patients with cardiac implantable electronic devices. *Clin Res Cardiol.* (2020) 109:96–102. doi: 10.1007/s00392-019-01493-z
7. Vergara P, Solimene F, D'Onofrio A, Pisanò EC, Zanotto G, Pignalberi C, et al. Are atrial high-rate episodes associated with increased risk of ventricular arrhythmias and mortality? *JACC Clin Electrophysiol.* (2019) 5:1197–208. doi: 10.1016/j.jacep.2019.06.018
8. Hindricks G, Potpara T, Dagres N, Arbelo E, Bax JJ, Blomström-Lundqvist C, et al. 2020 ESC Guidelines for the diagnosis and management of atrial fibrillation developed in collaboration with the European Association for Cardio-Thoracic Surgery (EACTS): The Task Force for the diagnosis and management of atrial fibrillation of the European Society of Cardiology (ESC) Developed with the special contribution of the European Heart Rhythm Association (EHRA) of the ESC. *Eur Heart J.* (2021) 42:373–498. doi: 10.1093/eurheartj/ehaa612
9. Hu WS, Lin CL. Role of CHA_2DS_2-VASc score in predicting new-onset atrial fibrillation in patients with type 2 diabetes mellitus with and without hyperosmolar hyperglycaemic state: real-world data from a nationwide cohort. *BMJ Open.* (2018) 8:e020065. doi: 10.1136/bmjopen-2017-020065
10. Li YG, Pastori D, Farcomeni A, Yang PS, Jang E, Joung B, et al. A Simple Clinical Risk Score (C_2HEST) for predicting incident atrial fibrillation in Asian subjects: derivation in 471,446 Chinese subjects, with internal validation and external application in 451,199 Korean subjects. *Chest.* (2019) 155:510–8. doi: 10.1016/j.chest.2018.09.011
11. Suenari K, Chao TF, Liu CJ, Kihara Y, Chen TJ, Chen SA. Usefulness of HATCH score in the prediction of new-onset atrial fibrillation for Asians. *Medicine (Baltimore).* (2017) 96:e5597. doi: 10.1097/MD.0000000000005597
12. Chen K, Bai R, Deng W, Gao C, Zhang J, Wang X, et al. HATCH score in the prediction of new-onset atrial fibrillation after catheter ablation of typical atrial flutter. *Heart Rhythm.* (2015) 12:1483–9. doi: 10.1016/j.hrthm.2015.04.008
13. Li YG, Pastori D, Miyazawa K, Shahid F, Lip GYH. Identifying at-risk patients for sustained atrial high-rate episodes using the C_2 HEST score: the West Birmingham atrial fibrillation project. *J Am Heart Assoc.* (2021) 10:e017519. doi: 10.1161/JAHA.120.017519
14. Kim M, Kim TH Yu HT, Choi EK, Park HS, Park J, et al. Prevalence and predictors of clinically relevant atrial high-rate episodes in patients with cardiac implantable electronic devices. *Korean Circ J.* (2021) 51:235–47. doi: 10.4070/kcj.2020.0393
15. Mathern PG, Chase D. Pacemaker detected prolonged atrial high-rate episodes – incidence, predictors and implications; a retrospective observational study. *J Saudi Heart Assoc.* (2020) 32:157–65. doi: 10.37616/2212-5043.1064
16. Pastori D, Miyazawa K, Li Y, Shahid F, Hado H, Lip GYH. Inflammation and the risk of atrial high-rate episodes (AHREs) in patients with cardiac implantable electronic devices. *Clin Res Cardiol.* (2018) 107:772–7. doi: 10.1007/s00392-018-1244-0
17. Belkin MN, Soria CE, Waldo AL, Borleffs CJW, Hayes DL, Tung R, et al. Incidence and clinical significance of new-onset device-detected atrial

tachyarrhythmia: a meta-analysis. *Circ Arrhythm Electrophysiol.* (2018) 11:e005393. doi: 10.1161/CIRCEP.117.005393
18. Violi F, Soliman EZ, Pignatelli P, Pastori D. Atrial fibrillation and myocardial infarction: a systematic review and appraisal of pathophysiologic mechanisms. *J Am Heart Assoc.* (2016) 5:e003347. doi: 10.1161/JAHA.116.003347
19. Li YG, Bai J, Zhou G, Li J, Wei Y, Sun L, et al. Refining age stratum of the C_2HEST score for predicting incident atrial fibrillation in a hospital-based Chinese population. *Eur J Intern Med*. (2021) 90:37–42. doi: 10.1016/j.ejim.2021.04.014

Conflict of Interest: The authors declare that the research was conducted in the absence of any commercial or financial relationships that could be construed as a potential conflict of interest.

Publisher's Note: All claims expressed in this article are solely those of the authors and do not necessarily represent those of their affiliated organizations, or those of the publisher, the editors and the reviewers. Any product that may be evaluated in this article, or claim that may be made by its manufacturer, is not guaranteed or endorsed by the publisher.

frontiers in Cardiovascular Medicine

ORIGINAL RESEARCH
published: 25 October 2021
doi: 10.3389/fcvm.2021.736042

Malnutrition and Risk of Procedural Complications in Patients With Atrial Fibrillation Undergoing Catheter Ablation

Daehoon Kim[1], Jaemin Shim[2†], Yun Gi Kim[2], Hee Tae Yu[1], Tae-Hoon Kim[1], Jae-Sun Uhm[1], Jong-Il Choi[2], Boyoung Joung[1], Moon-Hyoung Lee[1], Young-Hoon Kim[2] and Hui-Nam Pak[1*†]*

[1] Division of Cardiology, Department of Internal Medicine, Yonsei University Health System, Seoul, South Korea, [2] Korea University Cardiovascular Center, Seoul, South Korea

OPEN ACCESS

Edited by:
Antonio Sorgente,
EpiCURA, Belgium

Reviewed by:
Mario Matta,
Ospedaliero S. Andrea Vercelli, Italy
Philipp Sommer,
Clinic for Electrophysiology, Germany

***Correspondence:**
Jaemin Shim
jaemins@korea.ac.kr
Hui-Nam Pak
hnpak@yuhs.ac

[†]These authors have contributed equally to this work and share senior authorship

Specialty section:
This article was submitted to Cardiac Rhythmology, a section of the journal Frontiers in Cardiovascular Medicine

Received: 04 July 2021
Accepted: 27 September 2021
Published: 25 October 2021

Citation:
Kim D, Shim J, Kim YG, Yu HT, Kim T-H, Uhm J-S, Choi J-I, Joung B, Lee M-H, Kim Y-H and Pak H-N (2021) Malnutrition and Risk of Procedural Complications in Patients With Atrial Fibrillation Undergoing Catheter Ablation. Front. Cardiovasc. Med. 8:736042. doi: 10.3389/fcvm.2021.736042

Background: Little is known about the prognostic value of nutritional status among patients undergoing atrial fibrillation (AF) catheter ablation (AFCA). We compared the risk of procedure-related complications and long-term rhythm outcomes of AFCA according to nutritional status.

Methods: We included 3,239 patients undergoing *de novo* AFCA in 2009-2020. Nutritional status was assessed using the controlling nutritional status (CONUT) score. The association between malnutrition and the risk of AFCA complications or long-term rhythm outcomes was evaluated. We validated the effects of malnutrition using an external cohort of 360 patients undergoing AFCA in 2013-2016.

Results: In the study population (26.8% women, median age: 58 years), 1,005 (31.0%) had malnutrition (CONUT scores $\geq$ 2); 991 (30.6%) had mild (CONUT 2–4) and 14 (0.4%) had moderate-to-severe (CONUT $\geq$ 5) malnutrition. The overall complication rates after AFCA were 3.3% for normal nutrition, 4.2% for mild malnutrition, and 21.4% for moderate-to-severe malnutrition. Moderate-to-severe malnutrition [odds ratio (OR) 6.456, 95% confidence interval (CI) 1.637-25.463, compared with normal nutrition], older age (OR 1.020 per 1-year increase, 95% CI 1.001-1.039), female sex (OR 1.915, 95% CI 1.302-2.817), and higher systolic blood pressure (OR 1.013 per 1-mmHg increase, 95% CI 1.000-1.026) were independent predictors for the occurrence of complications. In the validation cohort, malnutrition (CONUT $\geq$ 2) was associated with a 2.87-fold higher risk of AFCA complications (95% CI 1.174-7.033). The association between malnutrition and a higher risk of AFCA complications was consistently observed regardless of body mass index and sex. Malnutrition did not affect rhythm outcomes during the median follow-up of 40 months (clinical recurrence: 37.0% in normal nutrition vs. 36.5% in malnutrition).

Conclusion: Malnutrition, which is common in patients undergoing AFCA, was associated with a substantially higher risk for complications after AFCA.

Keywords: atrial fibrillation, catheter ablation, complication, malnutrition, rhythm outcome

INTRODUCTION

Malnutrition is prevalent in ∼34% of hospitalized patients, even in developed countries (1). Malnutrition has been reflected by a lower body mass index (BMI) in previous studies and has been shown to be associated with higher incidences of atrial fibrillation (AF) and arrhythmia progression, as well as poor prognosis among those with AF (2–5). However, a recent study reported that malnutrition is common in obese patients with heart failure, suggesting the BMI *per se* does not fully reflect the nutritional status (6).

Atrial fibrillation increases the risk of cardiovascular mortality and morbidity resulting from strokes and heart failure and impairs quality of life (7, 8). Compared with antiarrhythmic drug (AAD) therapy, AF catheter ablation (AFCA) reduces the number of acute episodes and prolongs the duration of sinus rhythm, thereby improving the quality of life (9). AFCA has been found to be associated with a lower risk of mortality and hospitalizations for heart failure (10), a lower risk of stroke (11), and improved cognitive function (12, 13). Among the various screening tools for malnutrition, controlling the nutritional status (CONUT) score has been studied in AF (14, 15). Malnutrition determined by this score is an independent predictor of a poor prognosis, especially hemorrhagic adverse events and AF recurrence after AFCA (14, 15). However, few studies have evaluated the effect of nutritional status on the outcomes of AFCA, and the relationship between the nutritional status and safety of AFCA remains unclear.

We previously reported on poor long-term rhythm outcomes after AFCA in patients with metabolic syndrome and a higher pericardial fat volume (16, 17). The aim of the present study was to investigate the association between nutritional status and the efficacy and safety of catheter ablation in patients with AF. In this study, we compared the risk of procedure-related complications and long-term rhythm outcomes according to CONUT score.

MATERIALS AND METHODS

Study Population

The study protocol adhered to the Declaration of Helsinki and was approved by the institutional review board of the Yonsei University Health System. Written informed consent was obtained from all patients included in the Yonsei AF Ablation Cohort Database (NCT02138695). Among 3,375 patients who underwent *de novo* AFCA for symptomatic drug-refractory AF, 3,239 patients who had available data on their serum albumin, cholesterol, and total lymphocyte count at the time of the ablation procedure were enrolled in this study (cohort 1). All patients stopped their AADs for a period of at least five half-lives before the catheter ablation. The exclusion criteria were as follows: (1) permanent AF refractory to electrical cardioversion, (2) AF with valvular disease ≥grade 2, and (3) a previous cardiac surgery with a concomitant AF surgery or AFCA.

Independent AFCA Cohort

For external validation of the association between nutritional status and outcomes of catheter ablation, we used an independent AF ablation cohort that included 805 patients who underwent their first AFCA at Korea University Cardiovascular Center from 2013 to 2016. From the independent data, we enrolled and analyzed 360 patients who had available data on their serum albumin, cholesterol, and total lymphocyte [median age 57 (interquartile range 50-64) years, 20.8% female, and 46.4% paroxysmal AF] for CONUT score evaluation (cohort 2).

Nutritional Status

A diagnosis of malnutrition was reached using the CONUT score, which is a screening tool for the nutritional status of hospitalized patients (18) and was calculated according to the levels of serum albumin, cholesterol, and total lymphocyte count (**Table 1**). High CONUT score has been known to have a prognostic impact in patients with chronic cardiac disease including heart failure and AF (6, 14). Also, the score has been associated with outcomes after cardiovascular surgery (19) or interventional procedures including transcatheter aortic valve replacement and percutaneous coronary intervention (20, 21). A score of 0–1 was considered normal (good) nutrition, whereas malnutrition could be classified as mild (2–4) or moderate to severe (≥5).

Electrophysiological Mapping and Radiofrequency Catheter Ablation

Intracardiac electrograms were recorded using the Prucka CardioLab Electrophysiology system (General Electric Medical Systems, Inc., Milwaukee, WI, USA). Three-dimensional electroanatomic mapping (NavX, St. Jude Medical, Inc., Minnetonka, Minnesota and CARTO, Biosense-Webster, Inc., Diamond Bar, California) was performed using a circumferential pulmonary vein (PV) mapping catheter (Lasso, Biosense-Webster Inc.) through a long sheath (Schwartz left 1, St. Jude Medical, Inc.). Transseptal punctures were performed, and multi-view pulmonary venograms were obtained. The details of the AFCA technique have been described in our previous studies (22, 23). All patients underwent a circumferential PV isolation (CPVI) during the *de novo* procedure. Most patients (87.8%) underwent the creation of cavotricuspid isthmus block during the *de novo* procedure, unless there was atrioventricular conduction disease. As an extra-PV left atrial (LA) ablation, additional linear ablation, including a roof line, posterior inferior line (posterior box lesion), and anterior line, was performed, especially in patients with persistent AF. A left lateral isthmus ablation, right atrial ablation, or complex fractionated electrogram ablation were performed in a minority of patients at the operator's discretion. An open-irrigated tip catheter [Celsius (Johnson & Johnson, Inc., Diamond Bar, CA); NaviStar ThermoCool (Biosense Webster, Inc); ThermoCool SF (Biosense Webster, Inc); ThermoCool SmartTouch (Biosense Webster, Inc); Coolflex (St. Jude Medical, Inc); 30–35 W; 47°C; FlexAbility (St. Jude Medical, Inc); ThermoCool SmartTouch (Biosense Webster, Inc.); and TactiCath (St. Jude Medical, Inc)] was used. Systemic anticoagulation was attained with intravenous heparin to maintain an activated clotting time of 350–400 s during the procedure.

After completion of the protocol-based ablation, the procedure was completed when no recurrence of AF was

TABLE 1 | Definition of CONUT score.

Parameters	Range and score			
Serum albumin, g/dl	≥3.50	3.00-3.49	2.50-2.99	<2.50
Score	0	2	4	6
Total Cholesterol, mg/dl	≥180	140-179	100-139	<100
Score	0	1	2	3
Total lymphocyte count, /mm^3	≥1,600	1,200-1,599	800-1,199	<800
Score	0	1	2	3
Total CONUT score	0-1 points	2-4 points	5-8 points	9-12 points
Degree of malnutrition	Normal	Mild	Moderate	Severe

CONUT, Controlling nutritional status.

observed within 10 min after cardioversion with an isoproterenol infusion (5–10 μg/min depending on ß-blocker use, target sinus heart rate of 120 bpm). If further AF triggered or frequent unifocal atrial premature beats were observed due to the effect of isoproterenol, extra-PV foci were ablated using quick 3D activation mapping. We defined an extra-PV LA ablation as an additional linear ablation with or without a complex fractionated electrogram ablation following the CPVI. If recurrent AF or atrial tachycardia (AT) were seen repeatedly under AADs after the *de novo* AFCA, we recommended a repeat AFCA. The detailed technique and strategy for repeat ablation procedures were presented in a previous study (22, 23).

Post-ablation Management and Follow-Up

We discharged patients not taking AADs except for those who had recurrent extra-PV triggers after the AFCA procedure, symptomatic frequent atrial premature beats, non-sustained atrial tachycardia, or an early recurrence of AF on telemetry during the admission period (28.7%). Electrocardiography was performed for all patients visiting an outpatient clinic 1, 3, 6, and 12 months after AFCA and every 6 months thereafter or whenever symptoms developed. Twenty-four-hour Holter recordings were performed at 3, 6, and 12 months and every 6 months thereafter. Patients who reported episodes of palpitations suggestive of arrhythmia recurrence underwent Holter monitoring or event monitor recordings. AF recurrence was defined as any episode of AF or AT lasting for at least 30 s. Any ECG documentation of AF recurrence within a 3-month blanking period was diagnosed as an early recurrence, and AF recurrence occurring more than 3 months after the procedure was diagnosed as clinical recurrence.

Statistical Analysis

Continuous variables are summarized as medians (interquartile range) and were compared using the Mann-Whitney *U*-test or Kruskal-Wallis *H*-test. Categorical variables are summarized as frequencies (percentages) and were compared using Fisher's exact test. We used Cochran-Armitage analysis to investigate trends in the complications of AFCA according to CONUT score. Multivariate logistic regression was applied to identify predictors associated with the occurrence of overall and major complications after AFCA. Kaplan–Meier analysis with the log-rank test was used to calculate AF recurrence-free survival over time and to compare recurrence rates across groups. A two-sided *P*-value of <0.05 was considered statistically significant. The statistical analyses were performed using R version 4.0.2 software (The R Foundation, www.R-project.org).

RESULTS

Patient Characteristics and Factors Associated With Malnutrition

Table 2 summarizes the baseline clinical and procedure-related characteristics of the patients undergoing AFCA according to their nutritional status. Of the 3,239 patients included [median age 59 (interquartile range 52-66) years, 26.8% female, and 67.7% paroxysmal AF] (cohort 1), 1,005 (31.0%) had malnutrition; 991 (30.6%) had mild malnutrition (CONUT scores: 2–4), and 14 (0.4%) had moderate-to-severe (CONUT scores: ≥5) malnutrition. Patients with malnutrition were more likely to be older ($P < 0.001$) and male ($P = 0.014$), and had a lower BMI ($P < 0.001$), lower blood pressure ($P < 0.001$), higher CHA_2DS_2-VASc score ($P < 0.001$), and more comorbidities than those with normal nutritional status.

AFCA Complications and Nutritional Status

The rates of complications of AFCA according to CONUT score in cohort 1 are summarized in **Figure 1**. The overall complication (P for trend = 0.037) and major complication rates (P for trend = 0.028) were greater in individuals with higher CONUT scores. Detailed information about the complications of AFCA according to nutritional status are presented in **Table 3**. During the first half of the study period (2009–2015), the overall complication rates after AFCA were 4.0 and 5.1% in those with normal nutrition and malnutrition (CONUT scores: ≥2), respectively. During the second half (2015–2020), the rates slightly decreased to 3.6% for a normal nutrition and 4.9% for a malnutrition. The overall complication rates after AFCA were 3.3% for a normal nutrition, 4.2% for a mild malnutrition, and 21.4% for a moderate-to-severe malnutrition. The major complication rates were 1.9, 2.6, and 14.3% for normal nutrition, mild malnutrition, and moderate-to-severe malnutrition, respectively. In multivariable logistic

TABLE 2 | Baseline clinical and procedure-related characteristics of the patients undergoing a *de novo* catheter ablation of atrial fibrillation according to the nutritional status.

Variables	All subjects ($N = 3,239$)	Normal nutrition: CONUT 0-1 ($n = 2,234$)	Malnutrition: CONUT ≥ 2 ($n = 1,005$)	*P*-value
Clinical characteristics				
Age, years	59 (52-66)	57 (50-64)	63 (56-69)	<0.001
<65 years	2,249 (69.4)	1,676 (75.0)	573 (57.0)	<0.001
65-74 years	794 (24.5)	461 (20.6)	333 (33.1)	
≥75 years	196 (6.1)	97 (4.3)	99 (9.8)	
Female sex	867 (26.8)	627 (28.1)	240 (23.9)	0.014
Paroxysmal AF	2,184 (67.7)	1,530 (68.9)	654 (65.3)	0.048
BMI, kg/m^2	24.8 (23.1-26.8)	25.0 (23.3-26.9)	24.6 (22.7-26.6)	<0.001
CONUT score	1 (0-1)	1 (0-1)	2 (2-3)	<0.001
Serum albumin, g/dl	4.3 (4.1-4.5)	4.3 (4.2-4.5)	4.2 (4.0-4.4)	<0.001
Cholesterol, mg/dl	171 (145-198)	186 (164-207)	133 (119-153)	<0.001
Lymphocyte count, /mm^3	2.03 (1.65-2.47)	2.14 (1.83-2.56)	1.59 (1.30-2.12)	<0.001
eGFR, ml/min/1.73 m^2	82 (71-120)	83 (72-120)	80 (68-108)	<0.001
Systolic BP, mmHg	120 (110-128)	120 (110-128)	119 (109-128)	0.009
Diastolic BP, mmHg	75 (68-83)	76 (70-83)	73 (66-81)	<0.001
CHA_2DS_2-VASc	1 (1-3)	1 (0-2)	2 (1-3)	<0.001
Congestive heart failure	403 (12.4)	247 (11.1)	156 (15.5)	0.001
Hypertension	1509 (46.6)	949 (42.5)	560 (55.7)	<0.001
Diabetes	499 (15.4)	250 (11.2)	249 (24.8)	<0.001
Previous stroke/TIA	375 (11.6)	176 (7.9)	199 (19.8)	<0.001
Previous vascular disease	326 (10.1)	159 (7.1)	167 (16.6)	<0.001
Chronic kidney disease, stage 3–5	306 (9.5)	165 (7.4)	141 (14.0)	<0.001
Anemia	305 (9.4)	130 (5.8)	175 (17.4)	<0.001
LA dimension, mm	41 (37-45)	41 (37-45)	42 (38-46)	<0.001
LVEF, %	64 (59-68)	64 (59-68)	64 (59-69)	0.576
E/Em	9.0 (7.4-12.0)	9.0 (7.1-11.4)	10.0 (8.0-12.7)	<0.001
LA volume index by CT, cm^3/m^2	80.5 (66.5-98.1)	79.9 (65.0-95.7)	85.0 (70.0-102./8)	<0.001
Pericardial fat volume, cm^3	103.1 (71.5-141.5)	102.9 (70.8-140.7)	103.6 (73.1-142.8)	0.209
Mean LA voltage, mV	1.31 (0.82-1.80)	1.31 (0.83-1.82)	1.31 (0.79-1.77)	0.327
Mean LA wall thickness, mm	1.93 (1.73-2.14)	1.93 (1.74-2.14)	1.94 (1.70-2.14)	0.868
Procedure-related characteristics				
Procedure time, min	164 (125-200)	165 (126-201)	160 (124-196)	0.062
Fluoroscopy time, min	32 (24-43)	33 (24-44)	32 (24-43)	0.268
Ablation time, sec	4,112 (2,811-5,344)	4,138 (2,829-5,384)	4,083 (2,752-5,270)	0.161
Ablation lesions				
CPVI	3,235 (99.9)	2,231 (99.9)	1,004 (99.9)	1.000
CTI	2,819 (87.2)	1,943 (87.2)	876 (87.3)	1.000
POBI	749 (23.2)	525 (23.6)	224 (22.4)	0.464
Anterior line	658 (20.4)	450 (20.2)	208 (20.7)	0.764
Use of contact force sensing catheters	262 (8.1)	179 (8.0)	83 (8.3)	0.867

Values are presented as median (interquartile range) or n (%).

AF, atrial fibrillation; BP, blood pressure; BMI, body mass index; CT, computed tomography; CONUT, controlling nutritional status; CPVI, circumferential pulmonary vein isolation; CTI, cavo-tricuspid isthmus; E/Em, ratio of the peak mitral flow velocity of the early rapid filling to the early diastolic velocity of the mitral annulus; eGFR, estimated glomerular filtration rate; LA, left atrium; LVEF, left ventricle ejection fraction; POBI, posterior wall box isolation; RA, right atrial; SVC, superior vena cava; TIA, transient ischemic attack.

regression, moderate-to-severe malnutrition was associated with an increased risk of overall (OR 6.456, 95% CI 1.637–25.463, $P = 0.008$) and major complications (OR 5.845, 95% CI 1.164–29.359, $P = 0.032$), compared to normal nutritional status (**Table 4**). Older age (OR 1.020 per 1-year increase, 95% CI 1.001–1.039), female sex (OR 1.915, 95% CI (1.302–2.817), and higher systolic blood pressure (OR 1.013 per 1-mmHg increase, 95% CI 1.000–1.026) were also independent predictors for the occurrence of complications after AFCA.

Figure 2 shows the effects of nutritional status on incidences of AFCA complications according to body mass index and sex. Even among overweight or obese patients with body mass indices

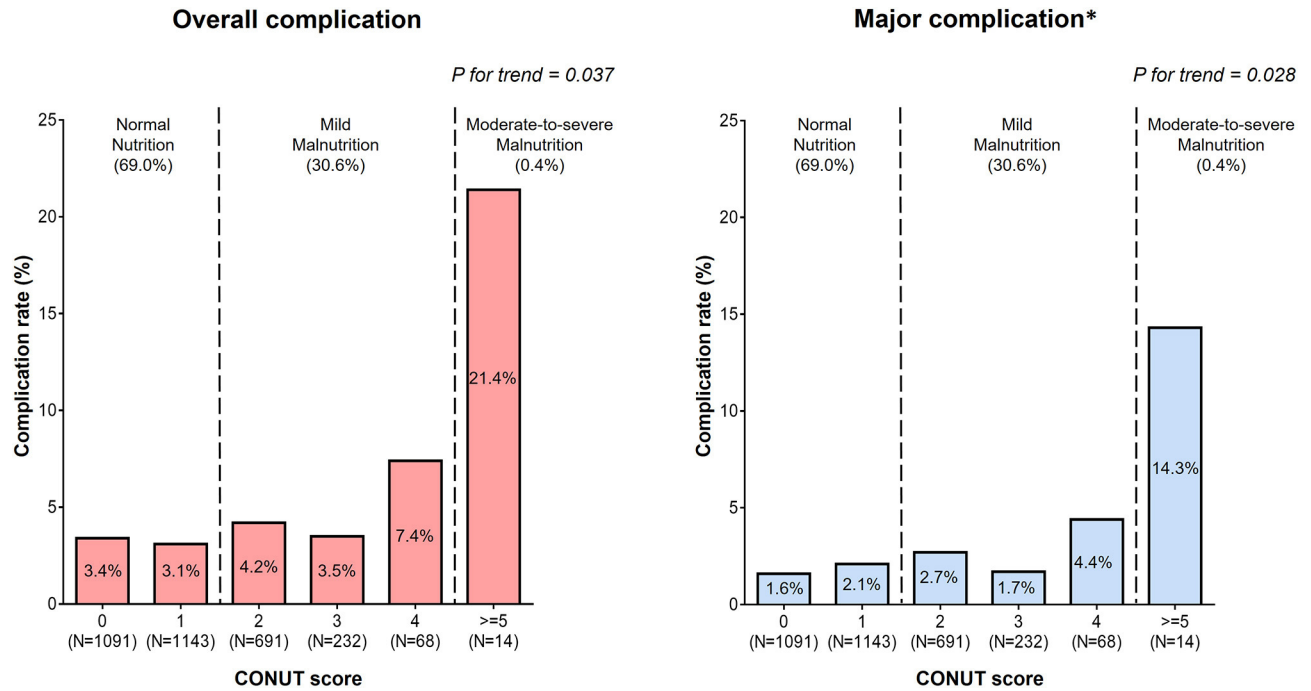

FIGURE 1 | Rates of the overall and major complications according to the CONUT score. *Complications that resulted in permanent injury or death, required intervention, or a prolonged or required hospitalization for more than 48 h.

TABLE 3 | Complications after the de novo catheter ablation of atrial fibrillation.

Complications	Normal nutrition: CONUT 0-1 (n = 2,234)	Malnutrition		
		Overall: CONUT ≥ 2 (n = 1,005)	Mild: CONUT 2-4 (n = 991)	Moderate-to-severe: CONUT ≥ 5 (n = 14)
Overall complications	73 (3.3)	45 (4.5)	42 (4.2)	3 (21.4)
Major complication*	42 (1.9)	28 (2.8)	26 (2.6)	2 (14.3)
Atrioesophageal fistula	1 (0.0)	2 (0.2)	1 (0.1)	1 (7.1)
Vascular access complication	17 (0.8)	9 (0.9)	8 (0.8)	1 (7.1)
Cardiac tamponade/hemopericardium	28 (1.3)	15 (1.5)	14 (1.4)	1 (7.1)
Pulmonary vein stenosis	4 (0.2)	0 (1.5)	0 (0.0)	0 (0.0)
Phrenic nerve paralysis	3 (0.1)	1 (0.1)	1 (0.1)	0 (0.0)
Stroke/transient ischemic attack	4 (0.2)	2 (0.2)	2 (0.2)	0 (0.0)
Complete atrioventricular block	1 (0.0)	1 (0.1)	1 (0.1)	0 (0.0)
Pericarditis	4 (0.2)	3 (0.3)	3 (0.3)	0 (0.0)
Others†	15 (0.7)	12 (1.2)	12 (1.2)	0 (0.0)

Values are presented as number (%).

**Complications that resulted in permanent injury or death, required intervention for treatment, or a prolonged or required hospitalization for more than 48 h.*

†Includes pleural effusion, shock due to unknown etiology, sudden cardiac arrest, and sinus node dysfunction.

at least 25 kg/m^2, malnutrition was prevalent (27.8%). Regardless of body mass index, malnutrition showed trend toward a higher risk of complications compared with normal nutrition (**Figure 2A**). The rates of overall complications after AFCA were highest (7.1%) in malnourished female patients, followed by 5.3% in normally nourished females, 3.7% in malnourished male patients, and 2.5% in normally nourished males (P for trend < 0.001) (**Figure 2B**).

TABLE 4 | Logistic regression analysis for the predictors of the overall and major complications.

	Overall complications				Major complications*			
	Univariable		Multivariable		Univariable		Multivariable	
Variables	**OR (95% CI)**	***P***	**OR (95% CI)**	***P***	**OR (95% CI)**	***P***	**OR (95% CI)**	***P***
Nutritional status by CONUT								
Normal nutrition (0-1)	1 (ref)	-	1 (ref)	-	1 (ref)	-	1 (ref)	-
Mild malnutrition (2-4)	1.310 (0.890-1.930)	0.172	1.191 (0.793-1.790)	0.400	1.400 (0.854-2.297)	0.182	1.162 (0.693-1.950)	0.569
Moderate-to-severe malnutrition (≥5)	8.073 (2.205-29.557)	0.002	6.456 (1.637-25.463)	0.008	8.663 (1.880-39.916)	0.006	5.845 (1.164-29.359)	0.032
Clinical variables								
Age	1.031 (1.013-1.050)	<0.001	1.020 (1.001-1.039)	0.039	1.039 (1.014-1.063)	0.017	1.030 (1.005-1.056)	0.018
Female sex	2.074 (1.427-3.013)	<0.001	1.915 (1.302-2.817)	0.001	1.746 (1.072-2.843)	0.025	1.518 (0.921-2.502)	0.102
Paroxysmal atrial fibrillation	0.878 (0.596-1.294)	0.512			1.195 (0.708-2.017)	0.506		
BMI (kg/m^2)	0.947 (0.891-1.008)	0.087	0.963 (0.904-1.026)	0.245	0.925 (0.853-1.003)	0.060	0.951 (0.877-1.032)	0.228
Systolic BP (mmHg)	1.013 (1.000-1.026)	0.051	1.013 (1.000-1.026)	0.043	1.009 (0.993-1.026)	0.285		
Diastolic BP (mmHg)	1.001 (0.985-1.018)	0.893			1.002 (0.981-1.023)	0.866		
Heart failure	0.945 (0.536-1.668)	0.847			1.054 (0.519-2.139)	0.884		
Hypertension	1.327 (0.918-1.918)	0.133			1.291 (0.803-2.074)	0.292		
Diabetes	1.056 (0.64-1.742)	0.831			1.258 (0.683-2.315)	0.461		
Stroke/TIA	1.117 (0.643-1.941)	0.695			0.843 (0.383-1.854)	0.671		
Vascular disease	1.759 (1.062-2.914)	0.028	1.490 (0.869-2.554)	0.147	0.832 (0.358-1.936)	0.670		
Chronic kidney disease, stage 3–5	1.531 (0.981-2.629)	0.123			1.243 (0.589-2.620)	0.568		
Anemia	2.298 (1.423-3.711)	<0.001	1.576 (0.939-2.644)	0.085	2.247 (1.216-4.154)	0.010	1.466 (0.756-2.842)	0.258
Echocardiographic								
LA dimension (mm)	0.978 (0.950-1.008)	0.145			0.973 (0.936-1.011)	0.159		
LVEF (%)	1.022 (0.997-1.046)	0.082	1.015 (0.991-1.040)	0.217	1.020 (0.989-1.052)	0.215		
E/Em	1.048 (1.016-1.081)	0.003	1.014 (0.974-1.056)	0.505	1.044 (1.003-1.086)	0.034		
Computed tomographic								
Pericardial fat volume (cm^3)	0.998 (0.994-1.002)	0.378			0.996 (0.991-1.001)	0.132		
Mean LA voltage (mV)	1.205 (0.882-1.647)	0.242			1.180 (0.783-1.777)	0.429		
Mean LA wall thickness (mm)	1.270 (0.707-2.282)	0.424			1.323 (0.622-2.814)	0.468		
Procedural								
Procedure time (min)	1.003 (1.000-1.006)	0.079	1.003 (1.000-1.006)	0.060	1.000 (0.995-1.004)	0.832		
Extra-PV LA ablation	1.308 (0.905-1.889)	0.153			1.883 (1.158-3.062)	0.011	1.901 (1.165-3.100)	0.010
Use of contact force sensing catheters	1.175 (0.624-2.216)	0.617			1.481 (0.701-3.127)	0.303		

Factors significant in the univariable analyses (P<0.10) were entered into the multivariable analyses.

**Complications that resulted in permanent injury or death, required intervention for treatment, or a prolonged or required hospitalization for more than 48 hours.*

BMI, body mass index; CI, confidence interval; E/Em, ratio of the peak mitral flow velocity of the early rapid filling to the early diastolic velocity of the mitral annulus; LA, left atrium; LVEF, left ventricular ejection fraction; TIA, transient ischemic attack; OR, odds ratio.

External Validation Cohort

Of the 360 patients in the validation cohort (cohort 2), 120 (33.3%) had malnutrition; 117 (32.5%) had mild and 3 (0.8%) had moderate-to-severe malnutrition. 26 (7.2%) had complications after AFCA. The baseline clinical and procedure-related characteristics of the patients in the validation cohort are presented in **Supplementary Table 1**. The overall complication rates after AFCA were 5.0 and 11.7% for normal nutrition and malnutrition, respectively. Detailed information about the complications of AFCA are presented in **Supplementary Table 2**. After multivariable adjustment, malnutrition (CONUT $\geq$ 2) was an independent predictor (OR 2.874, 95% CI 1.174-7.033) for complications after AFCA (**Supplementary Table 3**). In addition, an increasing CONUT score was associated with a higher risk for complications (OR 1.418 per 1 point increase, 95% CI 1.049-1.916).

AF Recurrence and Nutritional Status

Among 3,239 patients in the main cohort (cohort 1), neither the early recurrence rate within 3 months of the AFCA (32.6 vs. 34.4%, $P = 0.331$) nor the clinical recurrence rate (37.0 vs. 36.6%, $P = 0.829$) differed between the normal nutrition

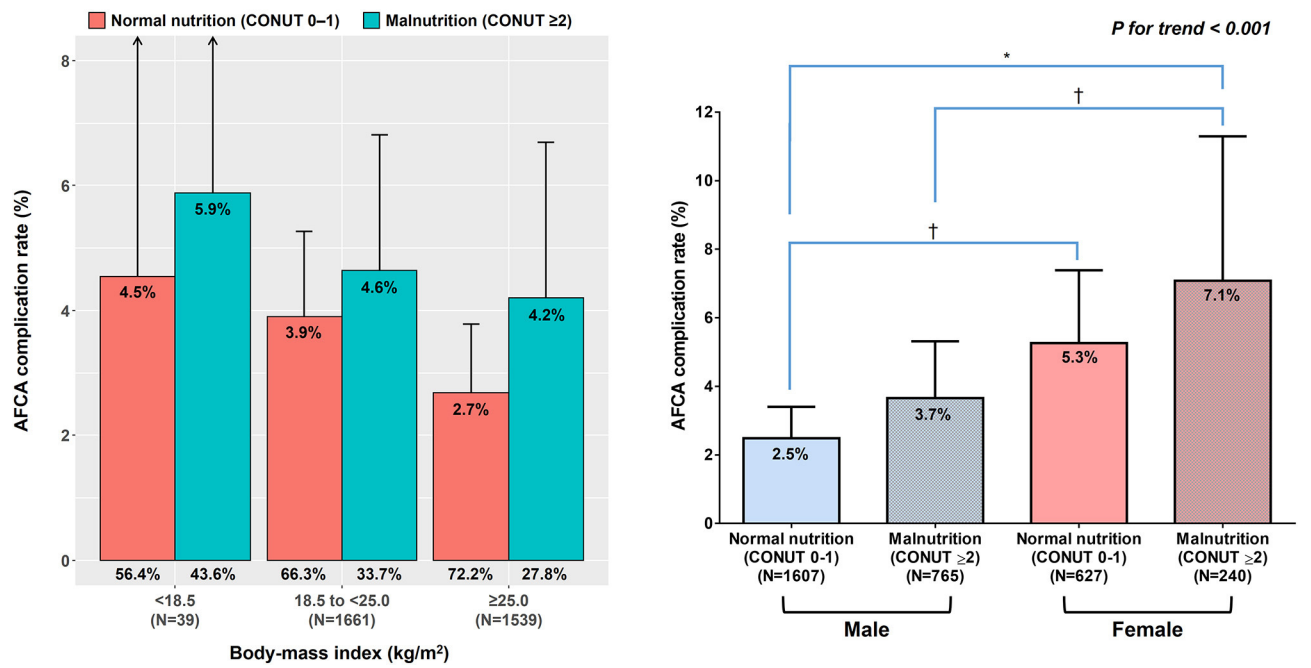

FIGURE 2 | Effects of nutritional status on rates of the overall complications according to body mass index **(A)** and sex **(B).** *Indicates $P < 0.001$ between the two groups. †Indicates $P < 0.05$ between the two groups. AFCA, atrial fibrillation catheter ablation.

and malnutrition groups during the median follow-up of 40 months (interquartile range 18–74 months, **Table 5**). Kaplan–Meier analysis showed no significant difference in overall AF recurrence (log-rank $P = 0.763$; **Figure 3A**) or AAD-free AF recurrence (log-rank $P = 0.148$; **Figure 3B**) between the groups. Repeat ablation procedures were performed in 13.3% of the normally nourished patients and 11.7% of the malnourished patients ($P = 0.230$). In those with a repeat ablation, the proportion of PV reconnections did not differ according to nutritional status ($P = 0.396$, **Table 5**).

In the validation cohort of 360 patients (cohort 2), there were consistently no differences in overall AF recurrence or AAD-free AF recurrence between the normal nutrition and malnutrition groups during the median follow-up of 14 months (interquartile range 6-28 months, **Figures 3C,D**).

DISCUSSION

Main Findings

Malnutrition, defined by CONUT score, is relatively common in patients with AF undergoing catheter ablation. In this study, we noted a trend toward a higher risk of AFCA complications in patients with higher CONUT scores. Patients with moderate-to-severe malnutrition (CONUT scores ≥ 5) and females with CONUT scores ≥ 2 faced a substantially higher risk of complications after AFCA. In an external validation cohort, malnutrition was consistently associated with an increased risk of complications. There was no significant association between nutritional status and AF recurrence after AFCA.

Malnutrition in Patients With AF

Using the same scoring as that in the present study (CONUT score), Zhu et al. reported that 36.6% of patients undergoing AFCA were malnourished, and 2% had moderate-to-severe malnutrition (15). The results of that study are consistent with those of the present study: 31% of the patients undergoing AFCA had malnutrition, although only 0.4% had moderate-to-severe malnutrition. Several studies have investigated the association of BMI with the clinical outcomes in patients with AF, in which they reported that a BMI of at least 25 kg/m^2 was associated with a lower risk of a stroke, cardiovascular death, or all-cause mortality, suggesting an "obesity paradox" in AF (5). However, research evaluating the prognostic value of nutritional status beyond BMI is scarce. Raposeiras-Roubín et al. reported that malnutrition, defined using CONUT score, is more prevalent (43.1%) in octogenarian patients with AF and that malnutrition is associated with a higher risk of mortality, strokes, and major bleeding (14). In this study, malnutrition was prevalent even in those with body mass indices at least 25 kg/m^2. Those findings suggest a discrepancy between BMI and nutritional status and support the importance of assessing and improving nutritional status beyond BMI. The negative impact of malnutrition on the course of AF might be attributable to cardiac cachexia, which leads to the activation of proinflammatory cytokines and neurohormonal

TABLE 5 | Clinical rhythm outcomes.

Outcomes	Normal nutrition: CONUT 0-1 (n = 2,234)	Malnutrition				
		CONUT ≥ 2 Overall (n = 1,005)	P* vs. normal	Mild: CONUT 2-4 (n = 991)	Moderate-to-severe: CONUT ≥ 5 (n = 14)	$P^{\dagger}$ among 0-1, 2-4, and ≥5
Follow-up duration (months)	41 (19-76)	38 (17-72)	0.070	38 (17-71)	36 (27-79)	0.188
Post-ABL medication						
ACEi, or ARB, *n* (%)	697 (31.3)	414 (41.2)	<0.001	407 (41.1)	7 (50.0)	<0.001
Beta blocker, *n* (%)	815 (36.6)	426 (42.4)	0.002	417 (42.1)	9 (64.3)	0.002
Statin, *n* (%)	526 (23.6)	538 (53.5)	<0.001	531 (53.6)	7 (50.0)	<0.001
AAD use						
AADs at discharge, *n* (%)	633 (28.3)	295 (29.4)	0.229	291 (29.4)	4 (28.6)	0.633
AADs after 3 months, *n* (%)	811 (36.3)	391 (38.9)	0.414	383 (38.6)	8 (57.1)	<0.001
AADs at final follow-up, *n* (%)	871 (39.8)	422 (42.8)	0.112	415 (42.7)	7 (50.0)	0.229
Early recurrence, *n* (%)	714 (32.6)	340 (34.5)	0.331	332 (34.1)	8 (57.1)	0.115
Recurrence type AT, *n* (% in recur)	212 (29.7)	107 (31.5)	0.484	107 (32.2)	0 (0.0)	0.493
Clinical recurrence, *n* (%)	811 (37.0)	360 (36.5)	0.829	354 (36.4)	6 (42.9)	0.858
Recurrence type AT, *n* (% in recur)	200 (24.6)	117 (32.4)	0.015	113 (31.9)	4 (66.7)	0.017
Cardioversion, *n* (% in recur)	241 (29.7)	97 (26.9)	0.370	95 (26.8)	2 (33.3)	0.590
Repeat AF ablation, *n* (%)	298 (13.3)	118 (11.7)	0.230	116 (11.7)	2 (14.3)	0.435
PV reconnections (% in redo)	208 (69.8)	88 (74.6)	0.396	86 (74.1)	2 (100.0)	0.454
1∼2 PV reconnections, *n* (% in redo)	122 (40.9)	44 (37.3)		44 (37.9)	0 (0.0)	
3∼4 PV reconnections, *n* (% in redo)	86 (28.9)	44 (37.3)		42 (36.2)	2 (100.0)	

Normal nutrition vs. malnutrition †Normal nutrition vs. mild malnutrition vs. moderate-to-severe malnutrition.
AAD, antiarrhythmic drug; ABL, ablation; ACEi, angiotensin-converting enzyme inhibitor; AF, atrial fibrillation; ARB, angiotensin receptor blocker; AT, atrial tachycardia; PV, pulmonary vein.

dysfunction (24) and a weakened protective effect of adipokines stemming from a reduced fat mass (25).

Malnutrition and AFCA Outcomes

Numerous studies have investigated relationships between nutritional status and AFCA outcomes using BMI to evaluate nutritional status, and all of them have focused on the efficacy of AFCA, that is, the AF recurrence rate. Baek et al. reported that being overweight and having metabolic syndrome were associated with a higher long-term recurrence rate at 2 years after AFCA in Asian populations in which the proportion of patients with a BMI $>$ 30 kg/m^2 was only 5.5% (16). Further, Deng et al. reported that being underweight (BMI $<$ 18.5 kg/m^2) was also associated with a higher AF recurrence (4). However, Bunch et al. reported that there was no significant association between BMI and AF recurrence (26). A recent study in 246 patients undergoing AFCA on the prognostic value of malnutrition using two nutritional status screening tools, including CONUT score, reported that malnutrition was an independent predictor of the recurrence of AF (15). In the present study, we expounded on the prior observations by enrolling a substantially larger number of participants and using longer follow-up durations, showing that the rates of early (<3 months) and clinical (beyond 3 months) AF recurrence did not differ according to nutritional status. However, the complication rates increased significantly as CONUT score increased. Up to 2 out of 10 patients with a CONUT score $\geq$ 5 sustained complications after AFCA. The trend was consistently observed in overweight or obese patients with AF. Female sex has been reported to be a risk factor for AFCA complications (27), which was consistently shown in this study. The present study showed a substantial risk for AFCA complication in malnourished females. Thus, emphasis should be placed on the assessment of nutritional status in patients with AF who are scheduled to undergo catheter ablation.

Limitations

This study had several limitations. First of all, the proportion of those with moderate-to-severe malnutrition was too small (0.4%) in this study. Although they were at significantly higher risk of complications in multivariable analyses, this needs to be interpreted carefully and cannot be generalized. This was a retrospective observational cohort study from two centers that included patients using strict selection criteria referred for AF ablation; hence, our findings cannot be used to establish causal relationships. Also, we were not able to fully exclude selection bias. Nutritional status was measured using CONUT score instead of studying body composition or detailed information on diet. Some patients whose CONUT score elements were

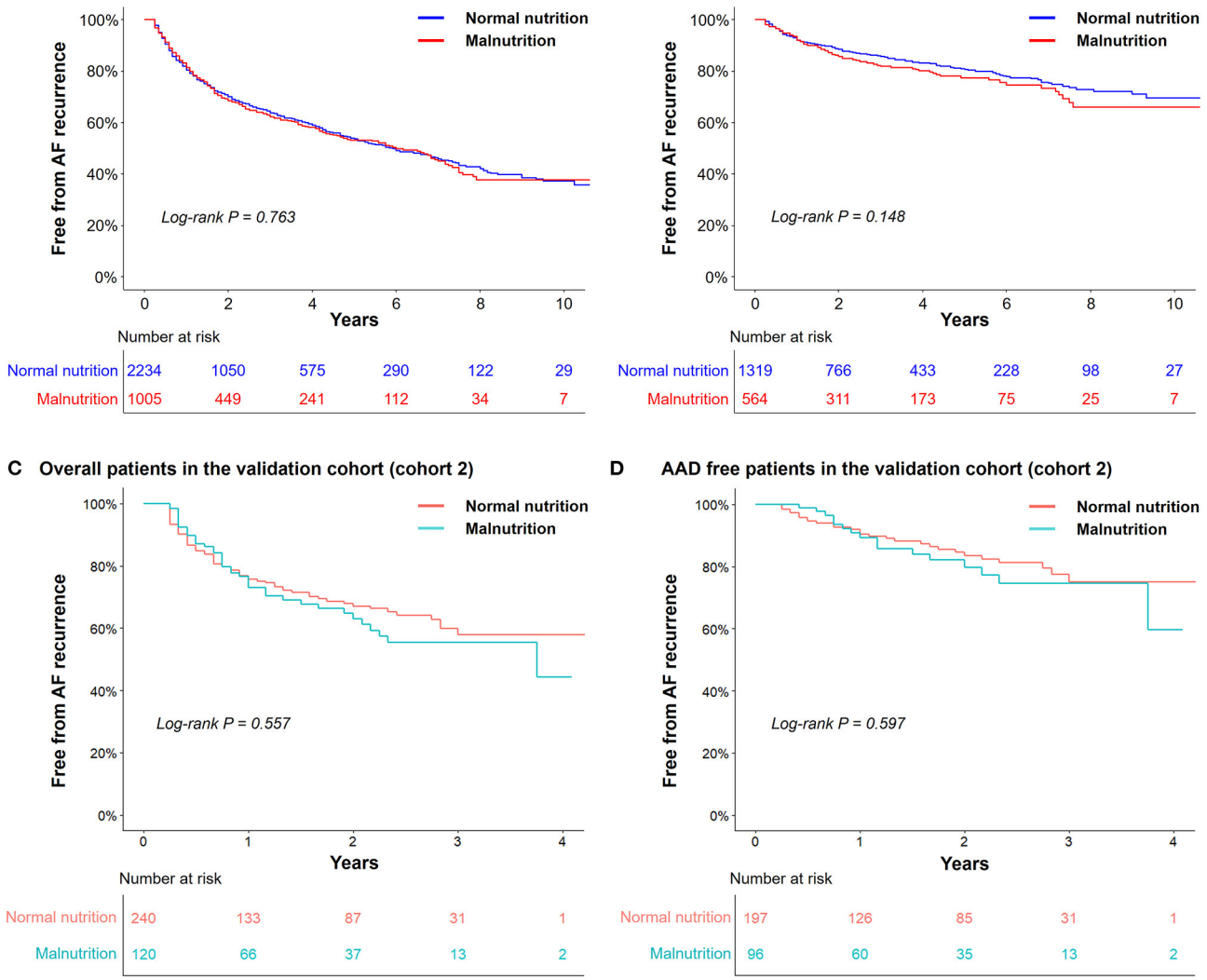

FIGURE 3 | Kaplan–Meier analyses of the atrial fibrillation (AF) recurrence-free survival rate in the cohort 1 (the main cohort) (n = 3,239; **A,B**) and in the cohort 2 (the external validation cohort) (n = 360, **C,D**). AAD, antiarrhythmic drugs.

not available were excluded from this study. We did not compare the prognostic values of other validated screening tools for malnutrition.

CONCLUSIONS

Malnutrition is highly prevalent in patients undergoing AFCA, and patients with malnutrition have a substantially higher risk of procedural complications. Nutritional assessment may provide additional risk stratification for safer AFCA.

DATA AVAILABILITY STATEMENT

The raw data supporting the conclusions of this article will be made available by the authors, without undue reservation.

ETHICS STATEMENT

The studies involving human participants were reviewed and approved by the institutional review board of the Yonsei University Health System. The patients/participants provided their written informed consent to participate in this study.

AUTHOR CONTRIBUTIONS

H-NP and JS contributed to the conception and design of the work and critical revision of the manuscript. DK contributed to the conception and design of the work, interpretation of data, and drafting of the manuscript. JS, YK, HT, T-HK, J-SU, J-IC, and H-NP contributed to the acquisition and analysis of data. BJ, M-HL, and Y-HK contributed to the conception and design of

the work. All authors contributed to the article and approved the submitted version.

FUNDING

This work was supported by Ministry of Health and Welfare (HI19C0114 and HI21C0011) and by the Basic Science Research Program (NRF-2020R1A2B01001695) run by the National Research Foundation (NRF) of Korea, which is funded by the Ministry of Science, ICT & Future Planning (MSIP).

ACKNOWLEDGMENTS

We would like to thank Mr. John Martin for his linguistic assistance.

SUPPLEMENTARY MATERIAL

The Supplementary Material for this article can be found online at: https://www.frontiersin.org/articles/10.3389/fcvm.2021.736042/full#supplementary-material

REFERENCES

1. Westergren A, Wann-Hansson C, Börgdal EB, Sjölander J, Strömblad R, Klevsgård R, et al. Malnutrition prevalence and precision in nutritional care differed in relation to hospital volume–a cross-sectional survey. *Nutr J*. (2009) 8:20. doi: 10.1186/1475-2891-8-20
2. Baek YS, Yang PS, Kim TH, Uhm JS, Park J, Pak HN, et al. Associations of abdominal obesity and new-onset atrial fibrillation in the general population. *J Am Heart Assoc*. (2017) 6:e004705. doi: 10.1161/JAHA.116.004705
3. Wang HJ, Si QJ, Shan ZL, Guo YT, Lin K, Zhao XN, et al. Effects of body mass index on risks for ischemic stroke, thromboembolism, and mortality in chinese atrial fibrillation patients: a single-center experience. *PLoS ONE*. (2015) 10:e0123516. doi: 10.1371/journal.pone.0123516
4. Deng H, Shantsila A, Guo P, Potpara TS, Zhan X, Fang X, et al. A u-shaped relationship of body mass index on atrial fibrillation recurrence post ablation: a report from the guangzhou atrial fibrillation ablation registry. *EBioMedicine*. (2018) 35:40-5. doi: 10.1016/j.ebiom.2018.08.034
5. Sandhu RK, Ezekowitz J, Andersson U, Alexander JH, Granger CB, Halvorsen S, et al. The obesity paradox in atrial fibrillation: observations from the aristotle (apixaban for reduction in stroke and other thromboembolic events in atrial fibrillation) trial. *Eur Heart J*. (2016) 37:2869-78. doi: 10.1093/eurheartj/ehw124
6. Sze S, Pellicori P, Kazmi S, Rigby A, Cleland JGF, Wong K, et al. Prevalence and prognostic significance of malnutrition using 3 scoring systems among outpatients with heart failure: a comparison with body mass index. *JACC Heart Fail*. (2018) 6:476-86. doi: 10.1016/j.jchf.2018.02.018
7. Hindricks G, Potpara T, Dagres N, Arbelo E, Bax JJ, Blomström-Lundqvist C, et al. 2020 ESC guidelines for the diagnosis and management of atrial fibrillation developed in collaboration with the European Association of cardio-thoracic surgery (EACTS). *Eur Heart J*. (2020) 342:373–498. doi: 10.1016/j.rec.2021.03.009
8. January CT, Wann LS, Alpert JS, Calkins H, Cigarroa JE, Cleveland JC, Jr., et al. 2014 AHA/ACC/HRS guideline for the management of patients with atrial fibrillation: a report of the American College of Cardiology/American Heart Association task force on practice guidelines and the heart rhythm society. *Circulation*. (2014) 130:e199-267. doi: 10.1161/CIR.0000000000000041
9. Mark DB, Anstrom KJ, Sheng S, Piccini JP, Baloch KN, Monahan KH, et al. Effect of catheter ablation vs medical therapy on quality of life among patients with atrial fibrillation: the cabana randomized clinical trial. *JAMA*. (2019) 321:1275-85. doi: 10.1001/jama.2019.0692
10. Marrouche NF, Brachmann J, Andresen D, Siebels J, Boersma L, Jordaens L, et al. Catheter ablation for atrial fibrillation with heart failure. *N Engl J Med*. (2018) 378:417-27. doi: 10.1056/NEJMoa1707855
11. Friberg L, Tabrizi F, Englund A. Catheter ablation for atrial fibrillation is associated with lower incidence of stroke and death: data from Swedish health registries. *Eur Heart J*. (2016) 37:2478-87. doi: 10.1093/eurheartj/ehw087
12. Jin MN, Kim TH, Kang KW, Yu HT, Uhm JS, Joung B, et al. Atrial fibrillation catheter ablation improves 1-year follow-up cognitive function, especially in patients with impaired cognitive function. *Circ Arrhythm Electrophysiol*. (2019) 12:e007197. doi: 10.1161/CIRCEP.119.007197
13. Kim D, Yang P-S, Sung J-H, Jang E, Yu HT, Kim T-H, et al. Less dementia after catheter ablation for atrial fibrillation: a nationwide cohort study. *Eur Heart J*. (2020) 41:4483-93. doi: 10.1093/eurheartj/ehaa726
14. Raposeiras-Roubín S, Abu-Assi E, Paz RC, Rosselló X, Barreiro Pardal C, Piñón Esteban M, et al. Impact of malnutrition in the embolic-haemorrhagic trade-off of elderly patients with atrial fibrillation. *Europace*. (2020) 22:878-87. doi: 10.1093/europace/euaa017
15. Zhu S, Zhao H, Zheng M, Peng J. The impact of malnutrition on atrial fibrillation recurrence post ablation. *Nutr Metab Cardiovasc Dis*. (2020) 31:834-40. doi: 10.1016/j.numecd.2020.12.003
16. Baek YS, Yang PS, Kim TH, Uhm JS, Kim JY, Joung B, et al. Delayed recurrence of atrial fibrillation 2years after catheter ablation is associated with metabolic syndrome. *Int J Cardiol*. (2016) 223:276-81. doi: 10.1016/j.ijcard.2016.08.222
17. Kim TH, Park J, Park JK, Uhm JS, Joung B, Lee MH, et al. Pericardial fat volume is associated with clinical recurrence after catheter ablation for persistent atrial fibrillation, but not paroxysmal atrial fibrillation: an analysis of over 600-patients. *Int J Cardiol*. (2014) 176:841-6. doi: 10.1016/j.ijcard.2014.08.008
18. Ignacio de Ulíbarri J, González-Madroño A, de Villar NG, González P, González B, Mancha A, et al. Conut: a tool for controlling nutritional status. First validation in a hospital population. *Nutr Hosp*. (2005) 20:38-45.
19. Cho JS, Shim JK, Kim KS, Lee S, Kwak YL. Impact of preoperative nutritional scores on 1-year postoperative mortality in patients undergoing valvular heart surgery. *J Thorac Cardiovasc Surg*. (2021) 2021:S0022-5223(20)33454-1. doi: 10.1016/j.jtcvs.2020.12.099
20. Lee K, Ahn JM, Kang DY, Ko E, Kwon O, Lee PH, et al. Nutritional status and risk of all-cause mortality in patients undergoing transcatheter aortic valve replacement assessment using the geriatric nutritional risk index and the controlling nutritional status score. *Clin Res Cardiol*. (2020) 109:161-71. doi: 10.1007/s00392-019-01497-9
21. Wada H, Dohi T, Miyauchi K, Doi S, Konishi H, Naito R, et al. Prognostic impact of nutritional status assessed by the Controlling Nutritional Status score in patients with stable coronary artery disease undergoing percutaneous coronary intervention. *Clin Res Cardiol*. (2017) 106:875-83. doi: 10.1007/s00392-017-1132-z
22. Park JW, Yu HT, Kim TH, Uhm JS, Joung B, Lee MH, et al. Mechanisms of long-term recurrence 3 years after catheter ablation of atrial fibrillation. *JACC Clin Electrophysiol*. (2020) 6:999-1007. doi: 10.1016/j.jacep.2020.04.035
23. Park JW, Yu HT, Kim TH, Uhm JS, Joung B, Lee MH, et al. Atrial fibrillation catheter ablation increases the left atrial pressure. *Circ Arrhythm Electrophysiol*. (2019) 12:e007073. doi: 10.1161/CIRCEP.118.007073
24. Guo Y, Lip GY, Apostolakis S. Inflammation in atrial fibrillation. *J Am Coll Cardiol*. (2012) 60:2263-70. doi: 10.1016/j.jacc.2012.04.063
25. Wolf AM, Wolf D, Rumpold H, Enrich B, Tilg H. Adiponectin induces the anti-inflammatory cytokines il-10 and il-1ra in human leukocytes. *Biochem Biophys Res Commun*. (2004) 323:630-5. doi: 10.1016/j.bbrc.2004.08.145
26. Bunch TJ, May HT, Bair TL, Crandall BG, Cutler MJ, Jacobs V, et al. Long-term influence of body mass index on

cardiovascular events after atrial fibrillation ablation. *J Interv Card Electrophysiol.* (2016) 46:259-65. doi: 10.1007/s10840-016-0142-5

27. Linde C, Bongiorni MG, Birgersdotter-Green U, Curtis AB, Deisenhofer I, Furokawa, T, et al. Sex differences in cardiac arrhythmia: a consensus document of the European Heart Rhythm Association, endorsed by the Heart Rhythm Society and Asia Pacific Heart Rhythm Society. *Europace.* (2018) 20:1565ao. doi: 10.1093/europace/euy067

Conflict of Interest: The authors declare that the research was conducted in the absence of any commercial or financial relationships that could be construed as a potential conflict of interest.

Publisher's Note: All claims expressed in this article are solely those of the authors and do not necessarily represent those of their affiliated organizations, or those of the publisher, the editors and the reviewers. Any product that may be evaluated in this article, or claim that may be made by its manufacturer, is not guaranteed or endorsed by the publisher.

frontiers in Cardiovascular Medicine

ORIGINAL RESEARCH
published: 04 November 2021
doi: 10.3389/fcvm.2021.759967

Extra-Pulmonary Vein Triggers at *de novo* and the Repeat Atrial Fibrillation Catheter Ablation

*Daehoon Kim†, Taehyun Hwang†, Min Kim, Hee Tae Yu, Tae-Hoon Kim, Jae-Sun Uhm, Boyoung Joung, Moon-Hyoung Lee and Hui-Nam Pak**

Division of Cardiology, Department of Internal Medicine, Yonsei University Health System, Seoul, South Korea

Background: Extra-pulmonary vein triggers can play a significant role in atrial fibrillation recurrence after catheter ablation. We explored the characteristics of the extra-pulmonary vein (PV) triggers in *de novo* and repeat atrial fibrillation (AF) catheter ablation (AFCA).

Methods: We included 2,118 patients who underwent a *de novo* AFCA (women 27.6%, 59.2 ± 10.9 years old, paroxysmal AF 65.9%) and 227 of them conducted repeat procedures. All included patients underwent isoproterenol provocation tests at the end of the procedure, and then we analyzed extra-PV triggers-related factors.

Results: Extra-PV triggers were documented in 11.7% of patients undergoing *de novo* AFCA (1.22 ± 0.46 foci per patient) and 28.6% undergoing repeat AFCA (1.49 ± 0.73 foci per patient). Older age and higher LA volume index in *de novo* procedures and women, diabetes, and higher parasympathetic nerve activity (heart rate variability) in repeat-AFCA were independently associated with the existence of extra-PV triggers. The septum (19.9%), coronary sinus (14.7%), and superior vena cava (11.2%) were common extra-PV foci. Among 46 patients who were newly found to have mappable extra-PV triggers upon repeat procedures, 15 (32.6%) matched with the previous focal or empirical extra-PV ablation sites. The rate of AF recurrence was significantly higher in patients with extra-PV triggers than in those without after *de novo* (HR 1.91, 95% CI 1.54–2.38, $p < 0.001$) and repeat procedures (HR 2.68, 95% CI 1.63–4.42, $p < 0.001$).

Conclusions: Extra-PV triggers were commonly found in AF patients with significant remodeling and previous empirical extra-PV ablation. The existence of extra-PV triggers was independently associated with poorer rhythm outcomes after the *de novo* and repeat AFCA.

Keywords: atrial fibrillation, catheter ablation, recurrence, extra-pulmonary vein triggers, remodeling

OPEN ACCESS

Edited by:
Jonathan Kalman, Royal Melbourne Hospital, Australia

Reviewed by:
Nicola Tarantino, Montefiore Medical Center, United States
Naotaka Hashiguchi, Japanese Red Cross Narita Hospital, Japan

***Correspondence:**
Hui-Nam Pak
hnpak@yuhs.ac

†These authors have contributed equally to this work

Specialty section:
This article was submitted to Cardiac Rhythmology, a section of the journal Frontiers in Cardiovascular Medicine

Received: *17 August 2021*
Accepted: *05 October 2021*
Published: *04 November 2021*

Citation:
Kim D, Hwang T, Kim M, Yu HT, Kim T-H, Uhm J-S, Joung B, Lee M-H and Pak H-N (2021) Extra-Pulmonary Vein Triggers at de novo and the Repeat Atrial Fibrillation Catheter Ablation. Front. Cardiovasc. Med. 8:759967. doi: 10.3389/fcvm.2021.759967

INTRODUCTION

Catheter ablation is an effective treatment for atrial fibrillation by reducing the number of acute episodes and prolongs the duration of sinus rhythm, thereby improving the quality of life (1). Circumferential pulmonary vein (PV) isolation is considered to be the cornerstone technique of atrial fibrillation (AF) catheter ablation (AFCA) (2). Reports of AF recurrence rates after initial ablation procedures have been variable, ranging from 20 to 80% in several studies, and 30–70% of patients require a repeat ablation

procedure to achieve sinus rhythm during long-term follow-up (3, 4). Previous studies have reported that the mechanism of arrhythmia recurrence after AFCA has a PV origin due to PV reconnections (5, 6). However, in especially persistent AF (PeAF), non-PV triggers play important roles in the pathophysiology through the progression of atriomyopathy and circumferential PV isolation (CPVI) alone generally does not achieve a satisfactory clinical outcome (7–11). The study of Kim et al. found that a larger number of reconnected PVs were paradoxically associated with a lower rate of arrhythmia recurrence after the second AF ablation (12). However, it is unclear whether the existence of extra-PV triggers is directly associated with AF recurrence at the condition of well-maintained PV isolation or after extensive empirical extra-PV ablations. The relationships between extra-PV triggers and multiple known pre-disposing factors or a higher recurrence after *de novo* or redo ablations have not been investigated. It is also unknown whether extensive empirical extra-PV ablation increases extra-PV foci by increasing the atrial damage (13). Therefore, we conducted a comprehensive analysis on the extra-PV triggers in patients who underwent a consistent isoproterenol provocation protocol during AFCA procedures, and assessed their characteristics and the association with the outcomes after both *de novo* and repeat ablation procedures. The purpose of this study was to compare the characteristics and mechanisms of extra-PV triggers and their role in the long-term outcome of AFCA.

MATERIALS AND METHODS

Study Population

This study was performed as a single-center retrospective cohort study. The study protocol adhered to the principles of the Declaration of Helsinki and was approved by the Institutional Review Board at Yonsei University Health System. All patients provided written informed consent for inclusion in the Yonsei AF Ablation Cohort (ClinicalTrials.gov identifier: NCT02138695). Among 3,640 patients who underwent a *de novo* AFCA from March 2009 to December 2020, we included 2,118 patients who underwent post-procedural isoproterenol provocation tests. Among them, 227 patients underwent a repeat AFCA (**Figure 1**). The study exclusion criteria were as follows: (1) permanent AF refractory to electrical cardioversion; (2) AF with valvular disease grade $>$ 2; (3) prior cardiac surgery with a concomitant AF surgery. Before the ablation procedure, the anatomies of the left atrium (LA) and PVs were visually defined on three-dimensional (3D) computed tomography (CT) (64 Channel, Light Speed Volume CT; Brilliance 63; Philips, Best, The Netherlands). We confirmed the absence of any LA thrombi by transesophageal echocardiography, intracardiac echocardiography, or CT. All antiarrhythmic drugs (AADs) were discontinued for at least five half-lives, and amiodarone was stopped at least 4 weeks before the procedure.

Echocardiographic Evaluation

All included patients underwent transthoracic echocardiography (Sonos 5500, Philips Medical System, Andover, MA, USA or Vivid 7, GE Vingmed Ultrasound, Horten, Norway) before undergoing AFCA and at 1 year after the procedure. We acquired the cardiac chamber size, left ventricular ejection fraction, trans-mitral Doppler flow velocity, the ratio of the early diastolic peak mitral inflow velocity, and early diastolic mitral annular velocity (E/Em), following the American Society of Echocardiography guidelines.

Electrophysiological Mapping and AF Catheter Ablation

We recorded the intracardiac electrograms using the Prucka CardioLab^{TM} Electrophysiology system (General Electric Medical Systems, Inc., Milwaukee, WI, USA) and generated 3D electroanatomical maps (NavX, Abbott, Inc., Chicago, IL, USA; CARTO system, Biosense Webster, Diamond Bar, CA, USA) using a circumferential PV-mapping catheter (AFocus, Abbott, Inc., Chicago, IL, USA; Lasso, Biosense-Webster Inc., Diamond Bar, CA, USA) through a long sheath. The 3D geometries of the LA and PVs were generated using the 3D mapping system and then merged with 3D spiral CT images. Blinded to the patient information, a technician analyzed the color-coded CT-merged voltage maps. Then, we performed transseptal punctures. The number of transseptal punctures (single vs. double) was at the discretion of the operator. Afterward, we obtained multi-view pulmonary venograms for the perfect matching of 3D-map, CT, and fluoroscopy in all patients except for significant renal disease. Immediately after the transseptal puncture, systemic anticoagulation was started with an intravenous bolus of heparin 200 IU/kg followed by intermittent boluses to maintain an activated clotting time of 350–400 s.

The details of the AFCA technique and strategy were described previously (12). An open-irrigated tip catheter (Celsius, Johnson & Johnson Inc., Diamond Bar, CA, USA; NaviStar ThermoCool, Biosense Webster Inc., Diamond Bar, CA, USA; ThermoCool SF, Biosense Webster Inc.; ThermoCool SmartTouch, Biosense Webster Inc.; Coolflex, Abbott Inc., Minnetonka, MN, USA; 30–35 W; 47°C; FlexAbility, Abbott Inc.; ThermoCool SmartTouch, Biosense Webster Inc., and TactiCath, Abbott Inc.) was used for the AFCA. Because we included patients over a relatively long period for this study, the radiofrequency power for the AFCA varied between 25 and 60 W. The endpoint of ablation at each site was as the average impedance drop $>$10% of baseline or an $>$80% decrease in the local electrogram voltage amplitude. We generated a CPVI with a bidirectional block in all patients. Most patients (91.6%) underwent the creation of cavotricuspid isthmus block during the *de novo* procedure unless there was atrioventricular conduction disease. Empirical linear ablation, including a roofline, posterior inferior line (posterior box lesion), and anterior line, left lateral isthmus ablation, right atrial ablation, or complex fractionated electrogram ablation were performed at the discretion of the operator.

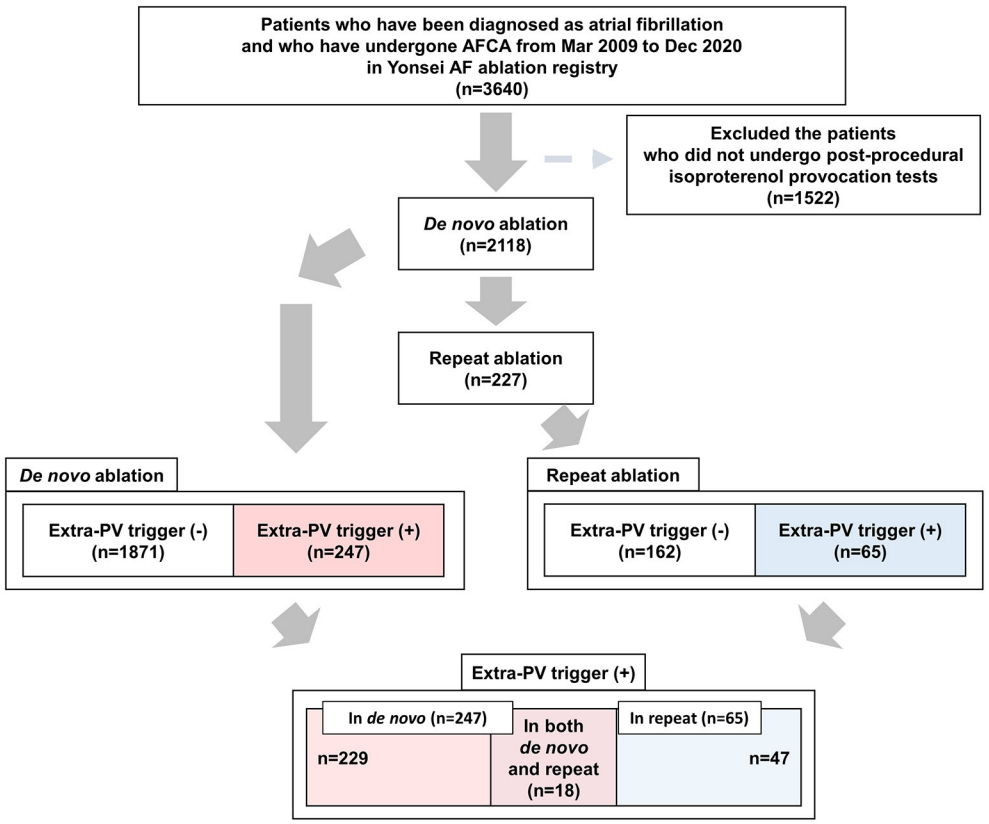

FIGURE 1 | Flow chart of the present study. AFCA, atrial fibrillation catheter ablation; PV, pulmonary vein.

Isoproterenol Provocation and Ablation Endpoint

After completing the protocol-based ablation, AF or atrial tachycardia (AT) was induced by 10-s high-current burst pacing (10 mA, pulse width 5 ms, Bloom Associates, Denver, CO, USA) from the high right atrial (RA) electrodes. This commenced at a pacing cycle length of 250 ms and was gradually reduced to 120 ms as previously described in the procedure (14). We infused isoproterenol (5–20 μg/min depending on ß-blocker use with a target heart rate of 120 bpm) for at least 3 min before induction and maintained this for 3 min after the induction of AF or AT. If sustained AF or AT was induced, internal cardioversion was performed by utilizing biphasic shock (2–20 J) with R wave synchronization (Lifepak12, Physiocontrol Ltd., Redmond, WA, USA). We conducted all the procedures under conscious sedation but induced deep sedation immediately before electrical cardioversion. We ended the procedure when there was no immediate recurrence of AF within the 10 min after the isoproterenol infusion with or without cardioversion. If further AF triggers were observed under the isoproterenol effect, we determined the potential location of the extra-PV triggers based on the contact bipolar electrograms and conducted a quick and detailed 3D-activation mapping with a multielectrode catheter. Based on the 3D mapping of the non-PV foci, we ablated those foci with 35–50 W for 10 s in each lesion until elimination. After the first round ablation, we performed the provocation procedure if it was a highly reproducible extra-PV trigger. However, we did not conduct the second time isoproterenol provocation in general. We defined the extra-PV foci as AF triggering points by isoproterenol provocation after the bidirectional block of CPVI.

Post-ablation Management and Follow-Up

We discharged the patients without taking any AADs except for those who had recurrent extra-PV triggers after the AFCA procedure, symptomatic frequent atrial pre-mature beats, non-sustained atrial tachycardia, or early recurrence of AF on telemetry during admission. Patients visited the outpatient clinic regularly at 1, 3, 6, and 12 months and then every 6 months or whenever symptoms occurred. All patients underwent ECG during every visit and 24-h Holter recordings at 3 and 6 months and every 6 months for 2 years, annually for 2–5 years, and then biannually after 5 years. Holter monitoring or event monitor recordings were obtained when patients reported palpitations suggestive of an arrhythmia recurrence. We defined an AF recurrence as any episode of AF or AT of at least 30 s in duration. Any ECG documentation of an AF recurrence within a 3-month blanking period was diagnosed as an early recurrence, and an AF recurrence occurring more than 3 months after the procedure was diagnosed as a clinical recurrence. We analyzed the clinical

TABLE 1 | Baseline clinical and procedural characteristics according to the existence of extra-PV triggers.

	De novo AF ablation				Repeat AF ablation			
	Overall	**Extra-PV triggers (–)**	**Extra-PV triggers (+)**	***P*-value**	**Overall**	**Extra-PV triggers (–)**	**Extra-PV triggers (+)**	***P*-value**
	(*n* = 2,118)	**(*n* = 1,871)**	**(*n* = 247)**		**(*n* = 227)**	**(*n* = 162)**	**(*n* = 65)**	
Age, years	59.1 ± 11.0	58.8 ± 11.0	60.9 ± 10.3	0.005	61.0 ± 9.9	60.7 ± 9.9	61.6 ± 10.1	0.522
Female, *n* (%)	584 (27.6)	495 (26.5)	89 (36.0)	0.002	63 (27.8)	37 (22.8)	26 (40.0)	0.014
Paroxysmal AF, *n* (%)	1,401 (66.1)	1,240 (66.3)	161 (65.1)	0.788	134 (59.0)	95 (58.6)	39 (60.0)	0.969
AF duration, months	38.1 ± 44.3	35.9 ± 42.3	51.4 ± 53.2	<0.001	75.9 ± 48.9	76.3 ± 48.6	74.9 ± 50.0	0.432
BMI, kg/m^2	24.9 ± 3.0	24.9 ± 3.0	24.6 ± 2.9	0.112	25.0 ± 3.2	25.1 ± 3.2	24.6 ± 3.2	0.277
CHA_2DS_2-VASc score	1.77 ± 1.56	1.75 ± 1.55	1.91 ± 1.66	0.122	1.98 ± 1.52	1.88 ± 1.41	2.22 ± 1.75	0.137
Comorbidities, *n* (%)								
Heart failure	277 (13.1)	243 (13.0)	34 (13.8)	0.810	46 (20.3)	33 (20.4)	13 (20.0)	1.000
Hypertension	958 (45.2)	843 (45.1)	115 (46.6)	0.705	108 (47.6)	72 (44.4)	36 (55.4)	0.179
Diabetes mellitus	312 (14.7)	280 (15.0)	32 (13.0)	0.458	33 (14.5)	18 (11.1)	15 (23.1)	0.035
Stroke	245 (11.6)	214 (11.4)	31 (12.6)	0.683	33 (14.5)	26 (16.0)	7 (10.8)	0.417
Vascular disease	229 (10.8)	213 (11.4)	16 (6.5)	0.026	16 (7.0)	10 (6.2)	6 (9.2)	0.598
Echocardiographic parameters								
LA dimension, mm	41.3 ± 6.1	41.3 ± 6.1	41.2 ± 6.3	0.781	41.5 ± 5.9	41.9 ± 5.8	40.5 ± 6.0	0.103
LA volume index, ml/m^2	37.4 ± 13.4	37.1 ± 13.4	40.0 ± 13.2	0.001	38.9 ± 13.2	38.9 ± 12.0	39.1 ± 15.8	0.913
LV ejection fraction, %	63.3 ± 8.2	63.2 ± 8.3	63.7 ± 7.3	0.345	62.7 ± 7.9	62.8 ± 7.6	62.5 ± 8.7	0.857
E/Em	10.2 ± 4.2	10.2 ± 4.2	10.5 ± 4.4	0.238	10.5 ± 4.2	10.4 ± 4.0	10.9 ± 4.7	0.408
LA volume by CT, ml	151.4 ± 45.7	150.7 ± 45.4	156.4 ± 48.2	0.072	167.9 ± 48.3	166.9 ± 44.0	170.2 ± 57.6	0.646
Pericardial fat volume, cm^3	110.0 ± 56.1	111.4 ± 56.4	99.5 ± 53.3	0.008	116.8 ± 58.3	123.0 ± 60.4	102.5 ± 51.1	0.054
Mean LA voltage, mV (*n* = 1,594)	1.52 ± 0.71	1.54 ± 0.71	1.40 ± 0.70	0.015	1.22 ± 0.67	1.25 ± 0.68	1.14 ± 0.62	0.294
Procedure time, min	175.0 ± 53.6	174.2 ± 53.1	180.5 ± 57.4	0.086	137.6 ± 44.3	132.1 ± 41.7	151.4 ± 47.8	0.003
Ablation time, s	4,530 ± 1,878	4,545 ± 1,865	4,413 ± 1,979	0.297	1,987 ± 1,163	1,927 ± 1,145	2,138 ± 1,201	0.217
Ablation lesions, *n* (%/BDB%)								
CPVI	2,118 (100.0)	1,871 (100.0)	247 (100.0)	NA	227 (100.0)	162 (100.0)	65 (100.0)	NA
CTI ablation	1,940 (91.6)	1,724 (92.2)	216 (87.4)	0.016	212 (93.8)	151 (93.8)	61 (93.8)	1.000
Posterior box isolation	575 (27.2/60.9)	511 (27.3/61.1)	64 (26.0/59.4)	0.717	99 (43.8/51.5)	71 (44.1/53.5)	28 (43.1/46.4)	1.000
Anterior line	443 (20.9/63.9)	388 (20.7/67.0)	55 (22.3/85.9)	0.640	87 (38.3 /64.3)	62 (38.3/59.7)	25 (38.5/76.0)	1.000
Complications, *n* (%)	75 (3.5)	62 (3.3)	13 (5.3)	0.169	10 (4.4)	4 (2.5)	6 (9.2)	0.059
Major complications*, *n* (%)	34 (1.6)	28 (1.5)	6 (2.4)	0.408	5 (2.2)	2 (1.2)	3 (4.6)	0.285

**Complications that resulted in permanent injury or death, required intervention, or a prolonged or required hospitalization for more than 48 h.*

AAD, antiarrhythmic drug; AF, atrial fibrillation; AT, atrial tachycardia; BDB, Bidirectional block; BMI, body mass index; CPVI, Circumferential pulmonary vein isolation; CT, computed tomography; CTI, cavotricuspid isthmus; E/Em, mitral inflow velocity/mitral annulus tissue velocity; HF, high frequency; HRV, Heart rate variability; LA, left atrium; LF, low frequency; LV, left ventricle; NA, not applicable; PV, pulmonary vein; rMSSD, root mean square of successive differences between normal heartbeats.

recurrences depending on the existence of extra-PV triggers and their locations and risk factors.

Holter Monitor Records and Heart Rate Variability Analysis

A GE Marquette MARS 8000 Holter analyzer (General Electric Medical Systems, Chicago, IL, USA) was used to analyze heart rate variability (HRV) based on the 24-h Holter monitor recordings. Pre-mature ventricular beats, pre-mature atrial beats, and electrical artifacts were excluded from the analysis. The mean heart rate and the following time-domain HRV parameters were analyzed as follows: mean RR interval (mean NN interval), SD of NN intervals, SD of the 5 min mean of NN intervals, and root mean square of differences between successive NN intervals (rMSSD). The following parameters were calculated as follows: very-low-frequency components (<0.04 Hz), low-frequency components (LF; 0.04–0.15 Hz), high-frequency components (HF; 0.15–0.4 Hz), and LF:HF ratio. The HF and rMSSD were indicators of parasympathetic nervous activity.

Statistical Analysis

Continuous variables were summarized as the $M \pm SD$ and compared by independent two-sample *t*-test analysis. Categorical variables were summarized as the number (percentage of the group total) and compared by either the chi-square test or Fisher's exact-test. Multivariable logistic regression was applied to identify predictors associated with the existence of extra-PV triggers. Kaplan–Meier analysis with the log-rank-test was used to calculate AF recurrence-free survival over time and to compare

TABLE 2 | Logistic regression analysis for predictors of extra-PV triggers in the *de novo* and repeat AFCA.

	Extra-PV triggers in *de novo* ablation				Extra-PV triggers in repeat ablation					
	Univariable		Multivariable (Model 1)		Univariable		Multivariable (Model 1)		Multivariable (Model 2)	
	OR (95% CI)	*P*	OR (95% CI)	*P*	OR (95% CI)	*P*	OR (95% CI)	*P*	OR (95% CI)	*P*
Age, yrs	1.02 (1.01–1.03)	0.005	1.02 (1.00–1.03)	0.021	1.01 (0.98–1.04)	0.520	1.00 (0.97–1.04)	0.768	1.02 (0.98–1.06)	0.309
Female	1.57 (1.18–2.07)	0.002	1.30 (0.96–1.74)	0.087	2.25 (1.21–4.18)	0.010	2.72 (1.39–5.38)	0.004	2.17 (1.03–4.58)	0.042
Paroxysmal atrial fibrillation	0.97 (0.74–1.29)	0.849	1.08 (0.80–1.48)	0.610	1.08 (0.60–1.97)	0.790	0.91 (0.47–1.77)	0.782	1.31 (0.62–2.85)	0.492
AF duration, month	1.01 (1.00–1.01)	<0.001			1.00 (0.99–1.01)	0.867				
BMI, kg/m^2	0.96 (0.92–1.01)	0.112			0.95 (0.86–1.04)	0.276				
Congestive heart failure	1.07 (0.72–1.55)	0.733			0.98 (0.46–1.97)	0.950				
Hypertension	1.06 (0.81–1.39)	0.656			1.55 (0.87–2.78)	0.137				
Diabetes	0.85 (0.56–1.24)	0.403	0.81 (0.53–1.21)	0.323	2.40 (1.11–5.12)	0.023	2.42 (1.07–5.47)	0.033		
Stroke	1.05 (0.85–1.28)	0.607			0.79 (0.49–1.21)	0.311				
Vascular disease	0.54 (0.31–0.88)	0.021	0.53 (0.30–0.89)	0.023	1.55 (0.51–4.36)	0.419	1.69 (0.51–5.15)	0.366		
CHA_2DS_2-VASc score	1.07 (0.98–1.16)	0.123			1.15 (0.95–1.39)	0.138				
LA diameter, mm	1.00 (0.98–1.02)	0.780			0.96 (0.91–1.01)	0.104				
LAVI, ml/m^2	1.01 (1.01–1.02)	0.001	1.01 (1.00–1.02)	0.015	1.00 (0.98–1.02)	0.912	0.99 (0.96–1.01)	0.259		
LVEF, %	1.01 (0.99–1.03)	0.345			1.00 (0.96–1.03)	0.856				
E/Em	1.02 (0.99–1.05)	0.238			1.03 (0.96–1.10)	0.408				
rMSSD after 3 months *de novo* AFCA					1.02 (1.01–1.04)	0.006			1.02 (1.00–1.04)	0.025
LF after 3 months *de novo* AFCA					1.02 (1.00–1.04)	0.071				
HF after 3 months *de novo* AFCA					1.05 (1.01–1.09)	0.009				
LF-HF ratio after 3 months *de novo* AFCA					1.60 (0.84–3.09)	0.151				
LA volume (by CT), ml	1.00 (1.00–1.01)	0.072			1.00 (1.00–1.01)	0.636				
Pericardial fat volume (by CT), ml	1.00 (0.99–1.00)	0.008			0.99 (0.99–1.00)	0.057				

Variables used in the multivariable analyses: Model 1 includes age, sex, paroxysmal atrial fibrillation, diabetes, vascular disease, and LAVI; Model 2 includes age, sex, paroxysmal atrial fibrillation, and rMSSD.

AF, atrial fibrillation; CT, computed tomography; E/Em; ratio of the peak mitral flow velocity of the early rapid filling to the early diastolic velocity of the mitral annulus; HF, high frequency; LA, left atrium; LAVI, left atrial volume index; LF, low frequency; LVEF, left ventricular ejection fracture; rMSSD, root mean square of successive differences between normal heartbeats.

recurrence rates according to the existence of extra-PV triggers. A multivariable Cox regression analysis was performed to identify the predictors associated with a clinical recurrence of AF. A two-sided $P < 0.05$ was considered statistically significant. The statistical analyses were performed using R version 4.0.2 software (The R Foundation, www.R-project.org, Vienna, Austria).

RESULTS

Characteristics of Extra-PV Triggers

Table 1 summarizes the baseline clinical characteristics of the patients with extra-PV triggers during the *de novo* and repeats AFCA procedures. Regarding *de novo* procedures, the patients with an extra-PV trigger tended to be women

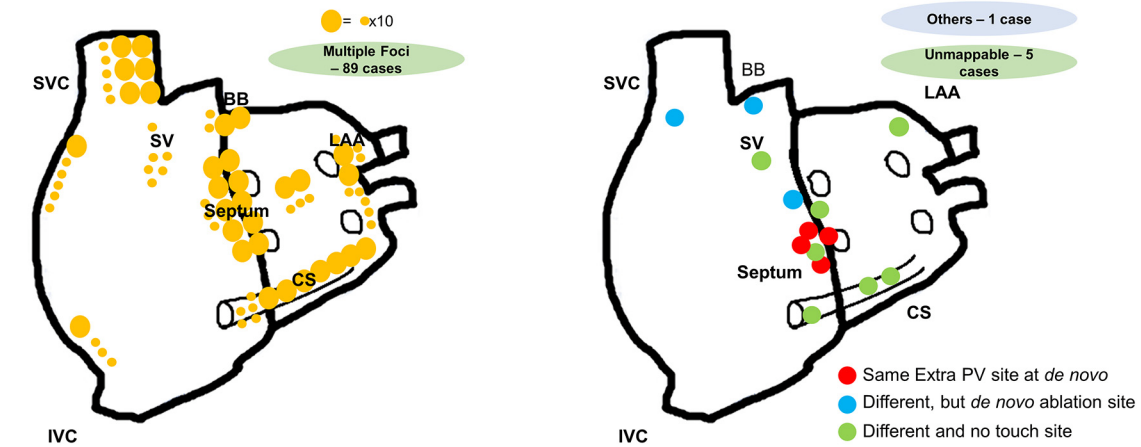

FIGURE 2 | Locations of the extra-PV triggers **(A)** during the *de novo* AFCA; **(B)** during the repeat AFCA in patients who had both extra-PV triggers in the *de novo* and repeat AFCA.

and older and to have a longer AF duration, lesser history of vascular disease, higher LA volume indices on the echocardiogram, lower mean LA voltage, and lower pericardial fat volume. Details of procedural complications are presented in **Supplementary Tables 1**, **2**. In the multivariable logistic regression, an older age [odds ratio (OR) 1.02 per 1-year increase, 95% CI 1–1.03, $p = 0.021$], no history of vascular disease (OR 0.53, 95% CI 0.3–0.89, $p = 0.023$), and a higher LA volume index (OR 1.01, 95% CI 1–1.02, $p = 0.015$) were independently associated with the existence of extra-PV triggers during the *de novo* procedure (**Table 2**). Among the 247 patients who demonstrated an extra-PV trigger in the *de novo* procedure, 19.8% (49/247) underwent a repeat ablation.

The median interval between the *de novo* and repeat procedures was 2 (interquartile range 1.1–4.1) years. The patients with extra-PV triggers in repeat procedures were more likely to be women ($p = 0.014$) and have diabetes ($p = 0.035$, **Table 1**). Being a woman (OR 2.72, 95% CI 1.39–5.38, $p = 0.004$), having diabetes (OR 2.42, 95% CI 1.07–5.47, $p = 0.033$; Model 1), and having higher rMSSD (OR 1.02, 95 CI 1–1.04, $p = 0.025$; Model 2) were independently associated with the existence of extra-PV foci during the repeat procedure (**Table 2**).

TABLE 3 | Characteristics of the extra-PV triggers provoked in repeat ablation procedures.

	Extra-PV triggers in repeat procedures ($n = 65$)	Provoked only in the repeat procedures ($n = 47$)
***De novo* lesion set, *n* (%)**		
CPVI alone, *n* (%)	28 (43.1%)	19 (40.4%)
Empirical LA ablation, *n* (%)	37 (56.9%)	28 (59.6%)
Locations of extra-PV triggers at redo		
Same extra-PV trigger in the *de novo* ablation, *n* (%)	4 (6.2%)	NA
New extra-PV trigger in the repeat ablation, *n* (%)	55 (84.6%)	46 (97.9%)
Sites not ablated at *de novo*, *n* (%)	38/55 (69.1%)	31/46 (67.4%)
Empirical extra-PV LA ablation sites at *de novo*, *n* (%)	17/55 (30.9%)	15/46 (32.6%)
Unmappable extra-PV triggers, *n* (%)	6 (9.2%)	1 (2.1%)

CPVI, Circumferential pulmonary vein isolation; LA, left atrium; NA, not applicable; PV, pulmonary vein.

Locations of Extra-PV Triggers

The proportion of patients who had extra-PV triggers at the end of the procedure was 11.7% (247/2,118) during the *de novo* procedure and 28.6% (65/227) during the repeat procedure ($p < 0.001$). The number of extra-PV trigger foci was significantly higher in the repeat ablation (1.49 ± 0.73 per patient) than in *de novo* procedure (1.22 ± 0.46 per patient, $p < 0.001$; **Supplementary Table 3**). The location of the extra-PV triggers in the *de novo* and repeat ablation procedures are presented in **Figure 2**. The septum (19.9%), coronary sinus (14.7%), and superior vena cava (11.2%) were the most common sites for extra-PV triggers regardless of whether a *de novo* or repeat procedure (**Supplementary Table 3**). Multifocal extra-PV triggers were documented in 21.5% of patients and were more common in the repeat procedures (18.2% in *de novo* vs. 33.8% in repeat ablations, $p = 0.006$; **Supplementary Table 3**). Extra-PV triggers were unmappable in 6.5 and 9.2% of the patients in the *de novo* and repeat ablation procedures, respectively.

TABLE 4 | Clinical rhythm outcomes according to the existence of extra-PV triggers.

	De novo AF ablation				Repeat AF ablation			
	Overall	Extra-PV triggers (–)	Extra-PV triggers (+)	*P*-value	Overall	Extra-PV triggers (–)	Extra-PV triggers (+)	*P*-value
	(*n* = 2,118)	(*n* = 1,871)	(*n* = 247)		(*n* = 227)	(*n* = 162)	(*n* = 65)	
Follow-up duration, months	50.2 ± 37.7	51.5 ± 37.9	40.5 ± 34.4	<0.001	37.3 ± 31.0	37.9 ± 31.5	35.8 ± 29.9	0.656
AAD Use, *n* (%)								
AADs at discharge	394 (18.6)	294 (15.7)	100 (40.5)	<0.001	65 (28.6)	39 (24.1)	26 (40.0)	0.025
AADs after 3 months	621 (31.2)	489 (28.0)	132 (54.1)	<0.001	94 (42.3)	57 (36.3)	37 (56.9)	0.007
Early recurrence, *n* (%)	565 (27.6)	447 (24.8)	118 (47.8)	<0.001	61 (26.9)	35 (21.6)	26 (40.0)	0.008
Clinical recurrence, *n* (%)	680 (33.2)	569 (31.6)	111 (44.9)	<0.001	94 (41.4)	57 (35.2)	37 (56.9)	0.004
At 12 months, *n* (%)	294 (14.4)	240 (13.3)	54 (21.9)	<0.001	43 (18.9)	22 (13.6)	21 (32.3)	0.002
At 24 months, *n* (%)	458 (22.4)	373 (20.7)	85 (34.4)	<0.001	78 (34.4)	44 (27.2)	34 (52.3)	0.001
AT Recurrence, *n* (% in recur/% in overall)	216 (31.8/10.2)	177 (31.1/9.5)	39 (35.1/15.8)	0.470	41 (43.6/18.1)	22 (38.6/13.6)	19 (51.4/29.2)	0.315
Cardioversion, *n* (% in recur/% in overall)	278 (40.9/13.6)	225 (39.5/12.5)	53 (47.7/21.5)	<0.001	46 (48.9/20.2)	30 (52.6/18.5)	16 (43.2/24.6)	0.498

AAD, antiarrhythmic drug; AF, atrial fibrillation; AT, atrial tachycardia; PV, pulmonary vein.

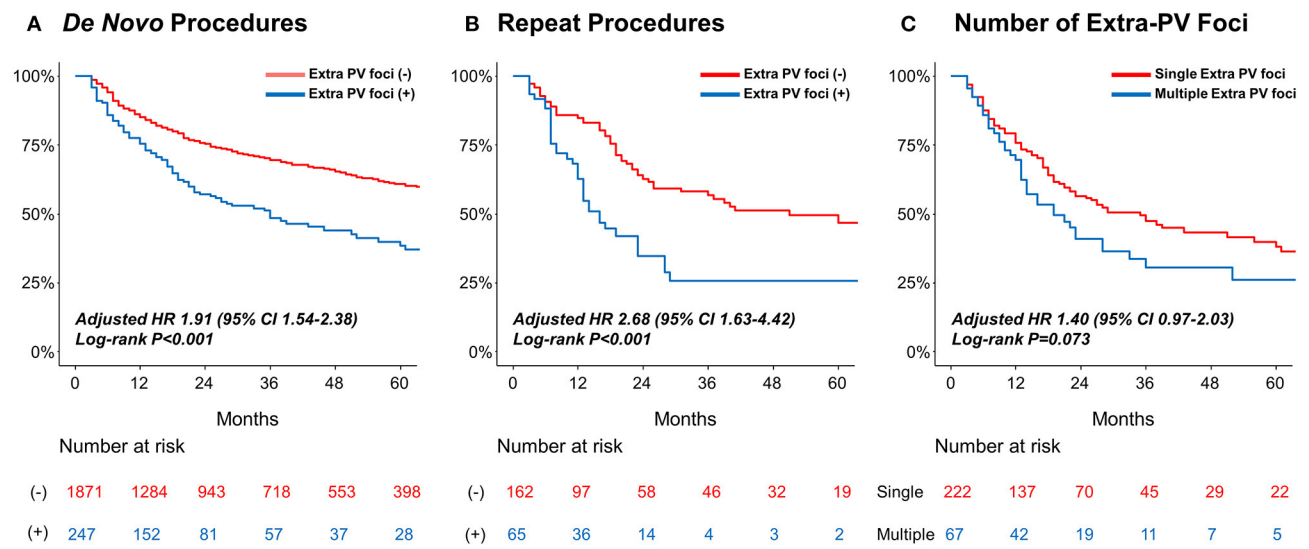

FIGURE 3 | Kaplan–Meier analyses of the AF recurrence-free survival **(A)** according to extra-PV triggers in the *de novo* AFCA; **(B)** according to the extra-PV triggers in the repeat AFCA; and **(C)** according to the number of extra-PV triggers. AF, atrial fibrillation.

Comparisons Between Extra-PV Triggers During the *de novo* vs. Repeat Procedures

Figure 2B displays the locations of the extra-PV foci in the repeat procedures in patients who showed in both *de novo* and repeat ablations. **Table 3** summarizes the characteristics of the extra-PV triggers provoked in repeat procedures. Among the 65 patients revealed to have extra-PV triggers in redo procedures, 6.2% (4/65) had an origin at the same site as the extra-PV foci in the *de novo* procedure, while 84.6% (38/55) had new origins of extra-PV triggers. Among the 46 patients who were newly found to have mappable extra-PV triggers in the redo ablation, 15 (32.6%) patients had extra-PV trigger sites matched with the previous empirical extra-PV ablation sites, whereas 31 (67.4%) had extra-PV trigger sites which were not touched at *de novo* procedures.

Extra-PV Triggers and the Rhythm Outcome After AFCA

Table 4 summarizes the rhythm outcomes after *de novo* and repeat procedures according to the existence of extra-PV foci. AADs were maintained at discharge and 3 months after the repeat procedures more frequently in patients with extra-PV foci than in those without. During the mean follow-up of 50.2 ± 37.7 months, clinical recurrences of AF were significantly higher in the patients with extra-PV triggers (44.9%) than in those without (31.6%) after the *de novo* AFCA (Log-rank $p < 0.001$, **Figure 3A**). During a mean follow-up of 38.8 ± 29.5 months

TABLE 5 | Cox regression analysis of AF recurrence after the *de novo* and repeat ablation procedures.

	Cox regression analysis of AF recurrence in the *de novo* ablation				Cox regression analysis of AF recurrence in the repeat ablation			
	Univariable		Multivariable		Univariable		Multivariable	
	HR (95% CI)	*P*	HR (95% CI)	*P*	HR (95% CI)	*P*	HR (95% CI)	*P*
Age, yrs	1.01 (1.00–1.02)	0.027	1.01 (1.00–1.01)	0.314	1.00 (0.98–1.02)	0.738	0.97 (0.94–1.01)	0.104
Female	1.27 (1.09–1.50)	0.003	1.33 (1.09–1.61)	0.004	1.43 (0.92–2.21)	0.111	1.35 (0.77–2.38)	0.297
Persistent atrial fibrillation	1.79 (1.52–2.08)	<0.001	1.49 (1.25–1.75)	<0.001	1.72 (1.14–2.56)	0.009	1.82 (1.10–3.03)	0.019
AF duration, month	1.02 (1.00–1.00)	0.112			1.00 (1.00–1.01)	0.573		
BMI, kg/m^2	1.02 (0.99–1.04)	0.188			1.07 (1.00–1.14)	0.047		
Congestive heart failure	1.48 (1.19–1.83)	<0.001	1.02 (0.78–1.33)	0.901	1.57 (0.95–2.58)	0.078	1.27 (0.67–2.42)	0.468
Hypertension	1.16 (1.00–1.35)	0.054			1.09 (0.73–1.65)	0.666		
Diabetes	1.04 (0.84–1.28)	0.712			0.85 (0.45–1.61)	0.611		
Stroke	1.05 (0.93–1.17)	0.445			1.08 (0.82–1.41)	0.579		
Vascular disease	1.02 (0.81–1.27)	0.898			1.13 (0.58–2.22)	0.715		
CHA_2DS_2-VASc score	1.07 (1.03–1.12)	0.002	0.99 (0.93–1.06)	0.840	1.07 (0.94–1.22)	0.299	0.97 (0.81–1.17)	0.775
LA diameter, mm	1.05 (1.04–1.06)	<0.001	1.04 (1.02–1.06)	<0.001	1.03 (0.99–1.06)	0.123	1.02 (0.98–1.07)	0.276
LAVI, ml/m^2	1.03 (1.02–1.03)	<0.001			1.01 (0.99–1.02)	0.381		
LVEF, %	0.99 (0.98–1.00)	0.098			0.98 (0.96–1.01)	0.140		
E/Em	1.02 (1.00–1.03)	0.048	0.98 (0.96–1.01)	0.159	1.03 (0.98–1.08)	0.286	1.01 (0.95–1.08)	0.669
LA volume (by CT), ml	1.01 (1.01–1.01)	<0.001			1.00 (1.00–1.01)	0.095		
Pericardial fat volume (by CT), ml	1.00 (1.00–1.00)	0.839			1.00 (1.00–1.01)	0.276		
Prescence of extra PV foci	1.95 (1.59–2.39)	<0.001	1.91 (1.54–2.38)	<0.001	2.32 (1.52–3.56)	<0.001	2.68 (1.63–4.42)	<0.001

Factors significant in the univariable analyses (P < 0.05) were entered into the multivariable analyses.
BMI, body mass index; CI, confidence interval; CT, computed tomography; HR, hazard ratio; E/Em; ratio of the peak mitral flow velocity of the early rapid filling to the early diastolic velocity of the mitral annulus; LA, left atrium; LAVI, left atrial volume index; LVEF, left ventricular ejection fracture; PV, pulmonary vein.

after the repeat ablation procedure, the rhythm outcome was consistently worse in patients with extra-PV triggers (57.5%) than in those without (36.7%) (Log-rank $p < 0.001$, **Figure 3B**). The comparison between the patients with a single extra-PV trigger and multiple extra-PV triggers is presented in **Figure 3C** (Log-rank $p = 0.073$). In the Cox regression analyses (**Table 5**), women [hazard ratio (HR) 1.33 95% CI 1.09–1.61, $p = 0.004$], persistent AF (HR 1.49, 95% CI 1.25–1.75, $p < 0.001$), increasing LA diameter (HR 1.04, 95% CI 1.02–1.06, $p < 0.001$), and the presence of extra-PV triggers (HR 1.91, 95% CI 1.54–2.38, $p < 0.001$) were independently associated with a clinical recurrence of AF after the *de novo* AFCA. The best cut-off value of LA diameter predicting recurrence was ≥44 mm (**Supplementary Figure 1**). The presence of extra-PV triggers (HR 2.68, 95% CI 1.63–4.42, $p < 0.001$) and persistent AF (HR 1.82, 95% CI 1.1–3.03, $p = 0.019$) were associated with an AF recurrence after the repeat procedure (**Table 5**).

DISCUSSION

Main Findings

In this single-center, retrospective cohort study, we analyzed the isoproterenol-induced extra-PV triggers during *de novo* and repeat AF ablation procedures. Extra-PV triggers were more

commonly found in the repeat ablation than in the *de novo* procedure. Older age and LA remodeling were independently associated with the presence of extra-PV triggers in the *de novo* ablation and being a woman, having diabetes, and higher parasympathetic nerve activity were related to the presence of extra-PV triggers in the repeat procedure. One-third of the extra-PV triggers newly found in the repeat ablation matched the empirical extra-PV ablation sites in the *de novo* procedure, and the existence of extra-PV triggers was independently associated with a higher AF recurrence after both the *de novo* and repeat ablation procedures.

Potential Mechanisms of AF Recurrence After AFCA

Continuous long-term AF recurrence after AFCA is a current unmet need. Representative mechanisms of AF recurrence after ablation are PV reconnections, extra-PV triggers, and autonomic neural effects. We expect that the long-lasting PVI issue will be overcome with the development of an upgraded and effective catheter technology (15). However, the extra-PV trigger issue has not only an elusive mechanism but also has limited treatment methods. In this study, we found a significant relationship between an extra-PV trigger and atrial remodelings, such as age and LA volume. The study of Keita Watanabe et al. (16) showed that being a woman, a lower body mass index (BMI < 23.8 kg/m^2), absence of hypertension, and ventricular diastolic dysfunction were independent predictors of extra-PV foci in patients with paroxysmal AF. In this study, the existence of extra-PV triggers in repeat ablations was associated with women, diabetes, and cardiac parasympathetic activity as well as the previous empirical extra-PV ablation sites (32.6%). This suggested that the autonomic nervous activity and previous ablation lesions play some role in extra-PV triggers and the recurrence mechanism. In particular, myofibroblasts, ion current changes, and gap junctional remodeling accompanying matrix remodeling or local fibrosis processes lead to electrophysiological changes such as in the membrane potential, conduction velocity, and refractoriness (17, 18). This atrial substrate remodeling contributes to AF initiation and maintenance mechanisms by the perpetuation of triggers or micro re-entry. Pericardial fat volume was smaller in the patients with extra-PV triggers than those without in this study. Pericardial fat is associated with arrhythmogenicity and AF recurrence in previous studies (19, 20). However, the existence of extra-PV triggers seemed to be more closely related to being a woman rather than to pericardial fat volume or body-mass index in this study. According to the recent study regarding sex differences in the mapping of repeat ablation procedures, extra-PV triggers were more significantly frequent in women than in men. Still, pericardial fat volume was substantially smaller in women (21).

Mapping and Ablation of Extra-PV Triggers

The prevalence of extra PV triggers in the *de novo* AFCA is variable and ranged from 3.2 to 62%, depending on the provocation protocols and punctuality of the mapping procedures (22–24). Unlike PVs, which were anatomically distinct structures, the mapping and ablation method for extra-PV triggers was elusive. A randomized-controlled trial failed to show an improvement in the rhythm outcome by additional empirical ablation for complex fractionated electrograms or rotors that were mapped during sustained AF (25). However, the study of Lee et al. reported that an extra-PV trigger ablation mapped after an isoproterenol provocation significantly lowered the AF recurrence through a randomized clinical trial (26). The work of Kim et al. also reported that the extra-PV ablation lowered the recurrence rate, but the rhythm outcome of the patients who had an extra-PV trigger was significantly worse than that of the patients without, even after an extra-PV trigger ablation (14).

There were several limitations to isoproterenol-provoked extra-PV trigger mapping and ablation. First, immediate trigger mapping was difficult, and the accuracy was decreased when the 3D map was shaken, following the electrical cardioversion due to patient movement. Second, the 3D map defined the exit site of triggers, but the actual foci might exist in the epicardial layer or deep inside the septum. Third, the isoproterenol provocation protocol has not been verified or standardized. We raised the target heart rate to 120 bpm and then induced AF considering the β-blocker effect, but it has not been proven that this dose is appropriate. In this study, there were fewer extra-PV triggers in patients with vascular disease, which might reflect the potential bias of a more careful isoproterenol dosing considering the coronary risk.

Future Directions

The presence of an extra-PV trigger is an important factor that must be overcome in determining long-term prognosis after AFCA. However, it was not easy to eliminate the extra-PV triggers in 11% of the *de novo* and 29% of the repeat procedures or 23% of multiple and 7% of unmappable foci utilizing a contact electrode catheter. Entire chamber mapping such as with the ECGi panoramic map could be a breakthrough for extra-PV mapping but has a limitation of localizing the foci on the septum, which was the most common extra-PV foci site in the current and previous studies (27). Since the AF driver map using computational modeling was an entire chamber map, it can be used as a guide for extra-PV trigger ablation (28). AADs with an appropriate dose are an alternative option to suppress extra-PV triggers by controlling the ion currents. If the presence of an extra-PV trigger could be predicted before the AFCA procedure, it would be useful in selecting an appropriate ablation catheter (balloon or RF), determining the need for an isoproterenol provocation test, and evaluating the prognosis after the procedure.

Limitations

This study had several limitations. First, it was a single-center, retrospective observational cohort study that might have involved selection bias. Further multi-center, prospective studies should be conducted. Second, there was no uniform strategy for the extra PV trigger ablation, and we performed an empirical extra PV ablation based on the discretion of the operators. Finally, we included patients with an isoproterenol provocation

test and excluded those who did not undergo a provocation test. This might have resulted in selection bias.

CONCLUSION

Extra-PV triggers were commonly found in AF patients with older age, in women, and patients with LA remodeling, high parasympathetic nervous activity, and previous empirical extra-PV ablations. The existence of extra-PV triggers was independently associated with a higher recurrence after both the *de novo* and repeat ablations.

DATA AVAILABILITY STATEMENT

The raw data supporting the conclusions of this article will be made available by the authors, without undue reservation.

ETHICS STATEMENT

The studies involving human participants were reviewed and approved by the Institutional Review Board at Yonsei University Health System. The patients/participants provided their written informed consent to participate in this study.

AUTHOR CONTRIBUTIONS

H-NP contributed to the conception and design of the work and critical revision of the manuscript. DK and TH contributed to the conception and design of the work, interpretation of data, and drafting of the manuscript. MK, HY, T-HK, and J-SU contributed to the acquisition and analysis of data. BJ and M-HL contributed to the conception and design of the work and revision of the manuscript. All authors contributed to the article and approved the submitted version.

FUNDING

This study was supported by grants (HI19C0114) and (H21C0011) from the Ministry of Health and Welfare and a grant (NRF-2020R1A2B01001695) from the Basic Science Research Program run by the National Research Foundation of Korea (NRF), which was funded by the Ministry of Science, ICT, and Future Planning (MSIP).

ACKNOWLEDGMENTS

We would like to thank Mr. John Martin for his linguistic assistance.

SUPPLEMENTARY MATERIAL

The Supplementary Material for this article can be found online at: https://www.frontiersin.org/articles/10.3389/fcvm.2021.759967/full#supplementary-material

REFERENCES

1. Mark DB, Anstrom KJ, Sheng S, Piccini JP, Baloch KN, Monahan KH, et al. Effect of catheter ablation vs. medical therapy on quality of life among patients with atrial fibrillation: the CABANA randomized clinical trial. *JAMA.* (2019) 321:1275–85. doi: 10.1001/jama.2019.0692
2. Pappone C, Augello G, Sala S, Gugliotta F, Vicedomini G, Gulletta S, et al. A randomized trial of circumferential pulmonary vein ablation versus antiarrhythmic drug therapy in paroxysmal atrial fibrillation: the APAF Study. *J Am Coll Cardiol.* (2006) 48:2340–7. doi: 10.1016/j.jacc.2006.08.037
3. Tzou WS, Marchlinski FE, Zado ES, Lin D, Dixit S, Callans DJ, et al. Long-term outcome after successful catheter ablation of atrial fibrillation. *Circ Arrhythm Electrophysiol.* (2010) 3:237–42. doi: 10.1161/CIRCEP.109.923771
4. O'Neill MD, Wright M, Knecht S, Jaïs P, Hocini M, Takahashi Y, et al. Long-term follow-up of persistent atrial fibrillation ablation using termination as a procedural endpoint. *Eur Heart J.* (2009) 30:1105–12. doi: 10.1093/eurheartj/ehp063
5. Nilsson B, Chen X, Pehrson S, Køber L, Hilden J, Svendsen JH. Recurrence of pulmonary vein conduction and atrial fibrillation after pulmonary vein isolation for atrial fibrillation: a randomized trial of the ostial versus the extraostial ablation strategy. *Am Heart J.* (2006) 152:537.e1–8. doi: 10.1016/j.ahj.2006.05.029
6. Ouyang F, Antz M, Ernst S, Hachiya H, Mavrakis H, Deger FT, et al. Recovered pulmonary vein conduction as a dominant factor for recurrent atrial tachyarrhythmias after complete circular isolation of the pulmonary veins: lessons from double Lasso technique. *Circulation.* (2005) 111:127–35. doi: 10.1161/01.CIR.0000151289.73085.36
7. Tilz RR, Rillig A, Thum AM, Arya A, Wohlmuth P, Metzner A, et al. Catheter ablation of long-standing persistent atrial fibrillation: 5-year outcomes of the Hamburg sequential ablation strategy. *J Am Coll Cardiol.* (2012) 60:1921–9. doi: 10.1016/j.jacc.2012.04.060
8. Della Rocca DG, Tarantino N, Trivedi C, Mohanty S, Anannab A, Salwan AS, et al. Non-pulmonary vein triggers in nonparoxysmal atrial fibrillation: implications of pathophysiology for catheter ablation. *J Cardiovasc Electrophysiol.* (2020) 31:2154–67. doi: 10.1111/jce.14638
9. Della Rocca DG, Lavalle C, Gianni C, Mariani MV, Mohanty S, Trivedi C, et al. Toward a uniform ablation protocol for paroxysmal, persistent, and permanent atrial fibrillation. *Card Electrophysiol Clin.* (2019) 11:731–8. doi: 10.1016/j.ccep.2019.08.014
10. Briceño DF, Patel K, Romero J, Alviz I, Tarantino N, Della Rocca DG, et al. Beyond pulmonary vein isolation in nonparoxysmal atrial fibrillation: posterior wall, vein of marshall, coronary sinus, superior vena cava, and left atrial appendage. *Card Electrophysiol Clin.* (2020) 12:219–31. doi: 10.1016/j.ccep.2020.01.002
11. Della Rocca DG, Mohanty S, Trivedi C, Di Biase L, Natale A. Percutaneous treatment of non-paroxysmal atrial fibrillation: a paradigm shift from pulmonary vein to non-pulmonary vein trigger ablation? *Arrhythm Electrophysiol Rev.* (2018) 7:256–60. doi: 10.15420/aer.2018.56.2
12. Kim TH, Park J, Uhm JS, Joung B, Lee MH, Pak HN. Pulmonary vein reconnection predicts good clinical outcome after second catheter ablation for atrial fibrillation. *Europace.* (2017) 19:961–7. doi: 10.1093/europace/euw128
13. Shim J, Joung B, Park JH, Uhm JS, Lee MH, Pak HN. Long duration of radiofrequency energy delivery is an independent predictor of clinical recurrence after catheter ablation of atrial fibrillation: over 500 cases experience. *Int J Cardiol.* (2013) 167:2667–72. doi: 10.1016/j.ijcard.2012.06.120
14. Kim IS, Yang PS, Kim TH, Park J, Park JK, Uhm JS, et al. Clinical significance of additional ablation of atrial premature beats after catheter ablation for atrial fibrillation. *Yonsei Med J.* (2016) 57:72–80. doi: 10.3349/ymj.2016.57.1.72
15. Reddy VY, Anter E, Rackauskas G, Peichl P, Koruth JS, Petru J, et al. Lattice-tip focal ablation catheter that toggles between radiofrequency and pulsed field energy to treat atrial fibrillation: a first-in-human trial. *Circ Arrhythm Electrophysiol.* (2020) 13:e008718. doi: 10.1161/CIRCEP.120.008718

16. Watanabe K, Nitta J, Inaba O, Sato A, Inamura Y, Kato N, et al. Predictors of non-pulmonary vein foci in paroxysmal atrial fibrillation. *J Interv Card Electrophysiol.* (2021) 61:71–8. doi: 10.1007/s10840-020-00779-x
17. Park JH, Pak HN, Lee S, Park HK, Seo JW, Chang BC. The clinical significance of the atrial subendocardial smooth muscle layer and cardiac myofibroblasts in human atrial tissue with valvular atrial fibrillation. *Cardiovasc Pathol.* (2013) 22:58–64. doi: 10.1016/j.carpath.2012.05.001
18. Gabbiani G, Chaponnier C, Hüttner I. Cytoplasmic filaments and gap junctions in epithelial cells and myofibroblasts during wound healing. *J Cell Biol.* (1978) 76:561–8. doi: 10.1083/jcb.76.3.561
19. Alí A, Boutjdir M, Aromolaran AS. Cardiolipotoxicity, Inflammation, and arrhythmias: role for interleukin-6 molecular mechanisms. *Front Physiol.* (2018) 9:1866. doi: 10.3389/fphys.2018.01866
20. Kim TH, Park J, Park JK, Uhm JS, Joung B, Lee MH, et al. Pericardial fat volume is associated with clinical recurrence after catheter ablation for persistent atrial fibrillation, but not paroxysmal atrial fibrillation: an analysis of over 600-patients. *Int J Cardiol.* (2014) 176:841–6. doi: 10.1016/j.ijcard.2014.08.008
21. Pak HN, Park JW, Yang SY, Kim M, Yu HT, Kim TH, et al. Sex differences in mapping and rhythm outcomes of a repeat atrial fibrillation ablation. *Heart.* (2021). doi: 10.1136/heartjnl-2020-318282. [Epub ahead of print].
22. Elayi CS, DI Biase L, Bai R, Burkhardt JD, Mohanty P, Sanchez J, et al. Identifying the relationship between the non-PV triggers and the critical CFAE sites post-PVAI to curtail the extent of atrial ablation in longstanding persistent AF. *J Cardiovasc Electrophysiol.* (2011) 22:1199–205. doi: 10.1111/j.1540-8167.2011.02122.x
23. Santangeli P, Zado ES, Hutchinson MD, Riley MP, Lin D, Frankel DS, et al. Prevalence and distribution of focal triggers in persistent and long-standing persistent atrial fibrillation. *Heart Rhythm.* (2016) 13:374–82. doi: 10.1016/j.hrthm.2015.10.023
24. Gianni C, Mohanty S, Trivedi C, Di Biase L, Natale A. Novel concepts and approaches in ablation of atrial fibrillation: the role of non-pulmonary vein triggers. *Europace.* (2018) 20:1566–76. doi: 10.1093/europace/euy034
25. Verma A, Jiang CY, Betts TR, Chen J, Deisenhofer I, Mantovan R, et al. Approaches to catheter ablation for persistent atrial fibrillation. *N Engl J Med.* (2015) 372:1812–22. doi: 10.1056/NEJMoa1408288
26. Lee KN, Roh SY, Baek YS, Park HS, Ahn J, Kim DH, et al. Long-term clinical comparison of procedural end points after pulmonary vein isolation in paroxysmal atrial fibrillation: elimination of nonpulmonary vein triggers versus noninducibility. *Circ Arrhythm Electrophysiol.* (2018) 11:e005019. doi: 10.1161/CIRCEP.117.005019
27. Haissaguerre M, Hocini M, Denis A, Shah AJ, Komatsu Y, Yamashita S, et al. Driver domains in persistent atrial fibrillation. *Circulation.* (2014) 130:530–8. doi: 10.1161/CIRCULATIONAHA.113.005421
28. Lim B, Park JW, Hwang M, Ryu AJ, Kim IS, Yu HT, et al. Electrophysiological significance of the interatrial conduction including cavo-tricuspid isthmus during atrial fibrillation. *J Physiol.* (2020) 598:3597–612. doi: 10.1113/JP279660

Conflict of Interest: The authors declare that the research was conducted in the absence of any commercial or financial relationships that could be construed as a potential conflict of interest.

Publisher's Note: All claims expressed in this article are solely those of the authors and do not necessarily represent those of their affiliated organizations, or those of the publisher, the editors and the reviewers. Any product that may be evaluated in this article, or claim that may be made by its manufacturer, is not guaranteed or endorsed by the publisher.

frontiers in Cardiovascular Medicine

CLINICAL TRIAL
published: 08 December 2021
doi: 10.3389/fcvm.2021.772665

Clinical Outcomes of Computational Virtual Mapping-Guided Catheter Ablation in Patients With Persistent Atrial Fibrillation: A Multicenter Prospective Randomized Clinical Trial

Yong-Soo Baek[1†], Oh-Seok Kwon[2†], Byounghyun Lim[2], Song-Yi Yang[2], Je-Wook Park[2], Hee Tae Yu[2], Tae-Hoon Kim[2], Jae-Sun Uhm[2], Boyoung Joung[2], Dae-Hyeok Kim[1], Moon-Hyoung Lee[2], Junbeom Park[3], Hui-Nam Pak[2*] and the CUVIA-AF 2 Investigators*

[1] Inha University College of Medicine and Inha University Hospital, Incheon, South Korea, [2] Division of Cardiology, Department of Internal Medicine, Yonsei University Health System, Seoul, South Korea, [3] Division of Cardiology, Department of Internal Medicine, Ewha Womans University, Seoul, South Korea

Background: Clinical recurrence after atrial fibrillation catheter ablation (AFCA) still remains high in patients with persistent AF (PeAF). We investigated whether an extra-pulmonary vein (PV) ablation targeting the dominant frequency (DF) extracted from electroanatomical map–integrated AF computational modeling improves the AFCA rhythm outcome in patients with PeAF.

Methods: In this open-label, randomized, multi-center, controlled trial, 170 patients with PeAF were randomized at a 1:1 ratio to the computational modeling-guided virtual DF (V-DF) ablation and empirical PV isolation (E-PVI) groups. We generated a virtual dominant frequency (DF) map based on the atrial substrate map obtained during the clinical AF ablation procedure using computational modeling. This simulation was possible within the time of the PVI procedure. V-DF group underwent extra-PV V-DF ablation in addition to PVI, but DF information was not notified to the operators from the core lab in the E-PVI group.

Results: After a mean follow-up period of 16.3 ± 5.3 months, the clinical recurrence rate was significantly lower in the V-DF than with E-PVI group ($P = 0.018$, log-rank). Recurrences appearing as atrial tachycardias ($P = 0.145$) and the cardioversion rates ($P = 0.362$) did not significantly differ between the groups. At the final follow-up, sinus rhythm was maintained without any AADs in 74.7% in the V-DF group and 48.2% in the E-PVI group ($P < 0.001$). No significant difference was found in the major complication rates ($P = 0.489$) or total procedure time ($P = 0.513$) between the groups. The V-DF ablation was independently associated with a reduced AF recurrence after AFCA [hazard ratio: 0.51 (95% confidence interval: 0.30–0.88); $P = 0.016$].

OPEN ACCESS

Edited by:
Richard Gary Trohman, Rush University, United States

Reviewed by:
Nassir Marrouche, Tulane University, United States
Tilman Maurer, Asklepios Klinik St. Georg, Germany

****Correspondence:***
Hui-Nam Pak
hnpak@yuhs.ac
Junbeom Park
parkjb@ewha.ac.kr

† These authors have contributed equally to this work and share first authorship

Specialty section:
This article was submitted to Cardiac Rhythmology, a section of the journal Frontiers in Cardiovascular Medicine

Received: *08 September 2021*
Accepted: *17 November 2021*
Published: *08 December 2021*

Citation:
Baek Y-S, Kwon O-S, Lim B, Yang S-Y, Park J-W, Yu HT, Kim T-H, Uhm J-S, Joung B, Kim D-H, Lee M-H, Park J, Pak H-N and the CUVIA-AF 2 Investigators (2021) Clinical Outcomes of Computational Virtual Mapping-Guided Catheter Ablation in Patients With Persistent Atrial Fibrillation: A Multicenter Prospective Randomized Clinical Trial. Front. Cardiovasc. Med. 8:772665. doi: 10.3389/fcvm.2021.772665

Conclusions: The computational modeling-guided V-DF ablation improved the rhythm outcome of AFCA in patients with PeAF.

Clinical Trial Registration: Clinical Research Information Service, CRIS identifier: KCT0003613.

Keywords: catheter ablation, computational modeling, recurrence, dominant frequency, atrial fibrillation

INTRODUCTION

Atrial fibrillation (AF) is the most common arrhythmia in clinical practice and has been associated with increased risks of heart failure, strokes, dementia, and cardiovascular death (1). AF catheter ablation (AFCA) is an effective therapy in patients with symptomatic and drug-refractory AF. Because AF is a chronic progressive disease with an annual progression rate of 7.2–15%, appropriate rhythm control by AFCA reduces the heart failure mortality, overall mortality, and hospitalization rates as well as the stroke risk and improves the cognitive function and renal function (2–4). However, clinical long-term AF recurrence after AFCA still remains high in patients with persistent AF (PeAF) and longstanding PeAF (5). This may be because the atrial substrate changes during AF progression and extrapulmonary vein (PV) foci play important roles in AF recurrence after the PeAF ablation (6). Nevertheless, no single empirical extra-PV ablation strategy, such as a linear, electrogram-guided, low voltage–guided, or rotor ablation, has been proven to improve the rhythm outcome of AFCA in patients with non-paroxysmal AF (7–9). In other words, the use of the current sequential atrial substrate mapping technology with a multielectrode catheter is not adequate to find the AF driver, as in contrast to the remarkable improvements made in the catheter technology for a long-lasting PV isolation (PVI). Recently, computational modeling has demonstrated the potential applicability in cardiac arrhythmia interventions (10, 11). Computational modeling allows for high-density, entire-chamber mapping while reflecting the personalized atrial anatomy and physiology (12). It enables a mechanism-based virtual ablation test targeting various AF wave-dynamic parameters and the prediction of the clinical outcomes by a reproducible condition control (10, 11, 13, 14). We previously reported the clinical feasibility and effectiveness of AF ablation lesion sets chosen using an *in silico* ablation relative to that of empirically chosen ablation lesion sets in patients with PeAF in a multicenter prospective clinical study (10, 11). In this study, we improved the existing computational modeling software (CUVIA version 2.5; Laonmed Inc., Seoul, Korea), which enabled one to conduct an entire-chamber mapping of the AF drivers based on the acquired substrate map during atrial pacing. We designed this multicenter prospective randomized clinical trial (RCT) by collaboration between the clinical ablation team and simulation team in real-time. Under this arrangement, the operator acquired the atrial substrate map and sent the data to the simulation team, and then the operator proceeded with the PVI and received the outcome of the simulation for the extra-PV targets after the PVI procedure. We compared the outcomes of the real-time computational modeling–guided extra-PV target ablation and empirical AFCA in patients with non-paroxysmal AF.

MATERIALS AND METHODS

Study Design and Population

This randomized, open-label, multicenter trial included drug-refractory AF patients undergoing AFCA at three tertiary hospitals in Korea (Clinical Research Information Service, CRIS identifier: KCT0003613). The study protocol was approved by the Institutional Review Board of each participating center and complied with the principles of the Declaration of Helsinki. All participants provided written informed consent before study enrollment. **Figure 1** shows the study design of the CUVIA-AF2 study. We enrolled a total of 222 patients with AAD-resistant symptomatic PeAF undergoing catheter ablation. The key exclusion criteria were as follows: (1) an age younger than 20 or older than 80 years, (2) paroxysmal AF, (3) valvular AF, (4) significant structural heart disease other than left ventricular hypertrophy, (5) left atrial (LA) diameter >55 mm, (6) history of AF ablation or cardiac surgery, and (7) the LA voltage map was not available due to recurrent (>3 episodes) or re-initiated AF after cardioversion. In patients with sustaining AF at the beginning of the procedure, we performed internal cardioversion by utilizing biphasic shock (2–20 J) with R wave synchronization (Lifepak12, Physiocontrol Ltd., Redmond, WA, USA) to acquire the LA substrate map. If the cardioversion failed or AF recurred during substrate mapping, we repeated cardioversion without using an antiarrhythmic drug at least 3 times. However, among enrolled a total of 222 patients, 52 (23.4%) were excluded due to failed internal cardioversion or >3 episodes of recurrent AF re-initiated during paced atrial substrate mapping, which provided the mandatory electrophysiologic data for our realistic computation modeling. All patients were treated with antiarrhythmic drugs (AADs) at baseline before AFCA. All antiarrhythmic drugs (AADs) were discontinued for at least five half-lives, and amiodarone was stopped at least 4 weeks before the procedure. Finally, 170 patients (70.6% men; 59.2 ± 11.3 years) were randomly assigned, using a random number table, to the virtual dominant frequency (DF) map-guided catheter ablation (V-DF, 87 patients) and empirical PVI ablation (E-PVI, 83 patients) groups.

CUVIA-AF2 Study Protocol

Figure 2 shows the study process for the CUVIA-AF2 as a real-time collaborative protocol between the clinical procedure

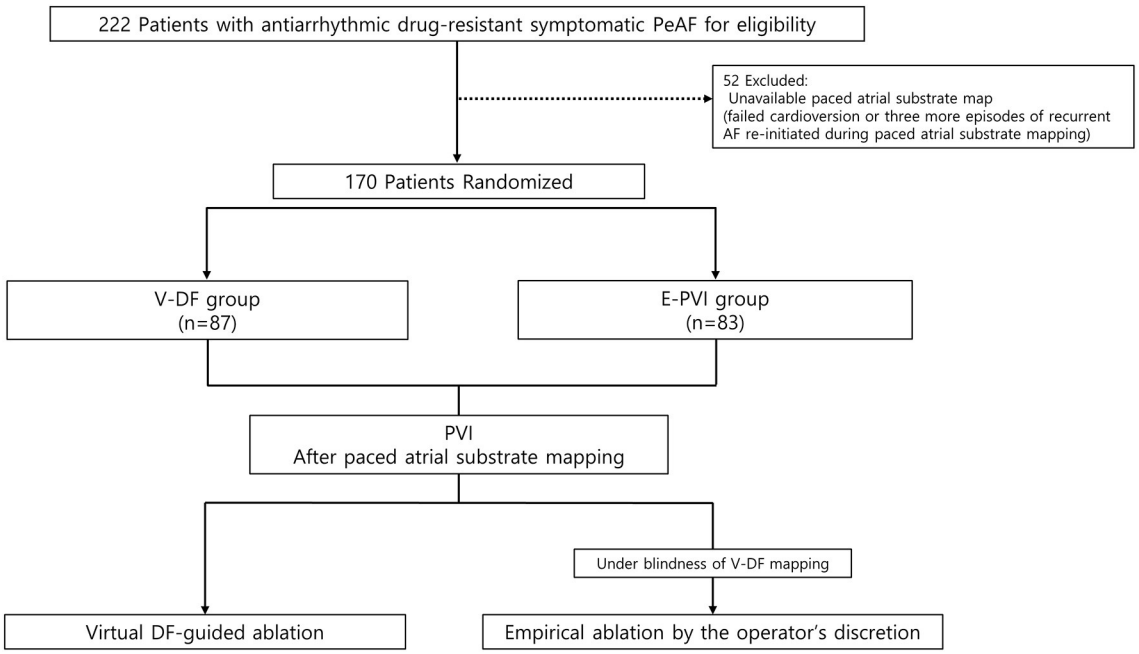

FIGURE 1 | Study flow diagram. The enrolled patients were randomly assigned to either the computational modeling–guided or empirical ablation groups. PeAF, persistent atrial fibrillation; RFCA, radiofrequency catheter ablation.

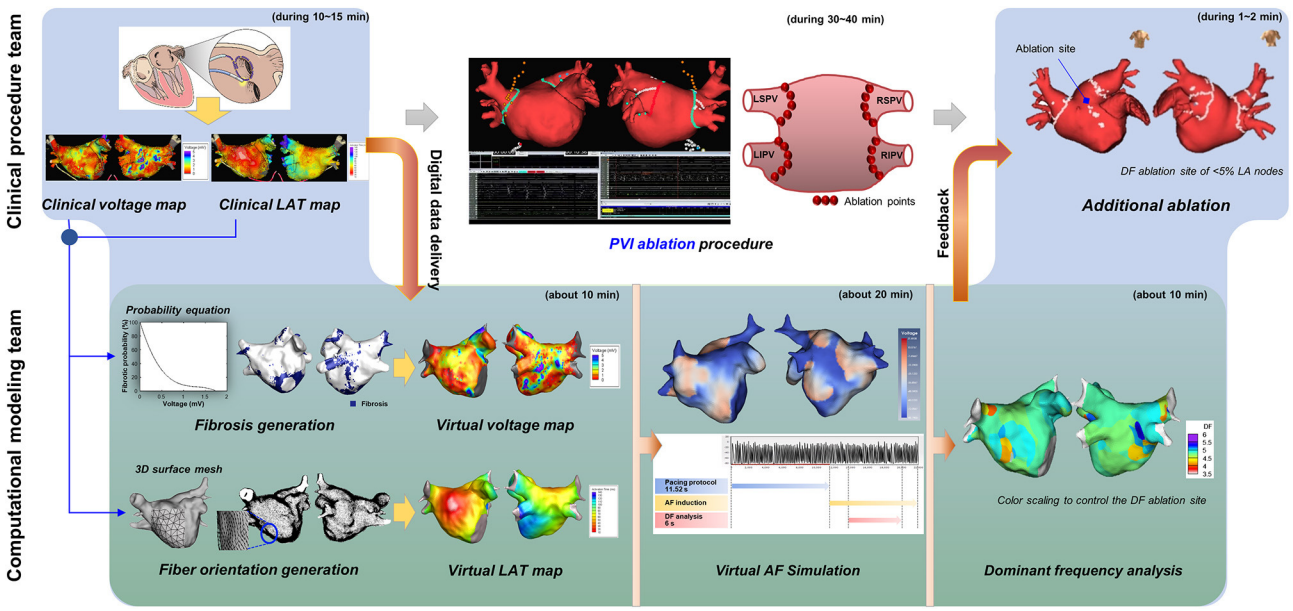

FIGURE 2 | CUVIA-AF 2 approach flowchart.

and computational modeling teams. At the beginning of the AFCA procedure, the clinical procedure team reconstructed the LA substrate map (bipolar voltage and local activation maps) using EnSite™ NavX™ acquired with a multielectrode catheter (AFocus, Abbott, Chicago, IL, USA) during high right atrial pacing with a cycle length of 500 ms. After extracting and transferring the digital data of the atrial substrate map to the computational modeling team, the clinical operator concentrated on conducting the PVI procedure. The substrate mapping data were analyzed in an on-site procedure room or transferred through the in-hospital network. During the 30–40 min PVI procedure, the modeling team conducted a

"virtual AF" induction and DF analysis. "Virtual AF" means AF simulation induced by ramp pacing on the LA substrate map in the computational modeling. This collaborative approach was conducted real-time, and it took <10 min for the integration of the clinical substrate mapping data into the human atrial cell model, including the personalized fibrosis and fiber orientation, about 20 min for inducing and maintaining virtual AF; and <10 min for the virtual DF analysis (11, 15). The computational modeling team provided the analyzed DF color map to the operator in the V-DF group but not in the E-PVI group. The operator then completed additional ablation of DF areas in the V-DF group, but no additional DF ablation was performed in the E-PVI group. However, 14.5% of the E-PVI group underwent an extra-PV ablation in addition to the PVI per the operators' discretion, mostly due to the existence of extra-PV triggers.

Computational Modeling of the AF and DF Analyses

We developed CUVIA version 2.5 for use in real-time AFCA procedures using the computed unified device architecture (CUDA) platform. The CUDA-based design methods and performance have been demonstrated in previous studies (12). The LA geometry was reconstructed with the substrate mapping points provided by the clinical procedure team. The electro-anatomical mapping procedure to acquire approximately over 1,000 mapping points in each patient took ∼10–15 min. Since there was a physical and temporal limitation to the number of mapping points acquired by the operator, we generated and refined the reconstructed high-resolution mesh using the CUVIA software to improve the accuracy of the simulation. The final number of nodes was set at 400,000–500,000 and the adjacent length between the two nodes was ∼300 μm. The LA mesh included the LA appendage and myocardial sleeves of the PV for realistic implementation (16). In the LA mesh, the opening area of the mitral valve and PV vessel was set as a non-conductive area. Then, the personalized fibrosis and fiber orientation were calculated with the clinical substrate mapping data and integrated into the LA mesh node of the human atrial cell model (12).

The cellular ionic currents were calculated based on the modified Courtemanche human atrial model, and electrical wave propagation was simulated with the monodomain equation (12). The following equation was used for the computational modeling of the electric wave propagation on the LA wall (15):

$$\frac{\partial V_m}{\partial t} = \frac{1}{\beta C_m}\left\{\nabla \cdot D\nabla V_m - \beta\left(I_{ion} + I_s\right)\right\}, \quad (1)$$

where Vm (volt) is the membrane potential; β (meter^{-1}) is the membrane surface-to-volume ratio; Cm (farad/meter^2) is the membrane capacitance per unit area; D (siemens/meter) is the conductivity tensor; and I_{ion} and I_s (ampere/meter^2) are the ion and stimulation currents, respectively, the above equation was adopted in parallel on the graphics processing unit as a CUDA kernel using a generalized finite difference system to simulate the electrical wave propagation (15). For the ionic remodeling, the fibrotic cells were initialized in the AF remodeled state and non-fibrotic cells were initialized in the normal state (17, 18). When compared to non-fibrotic cells, the I_{to}, I_{kur}, I_{CaL}, and I_{K1} currents of fibrotic cells changed to −70, −50, −70, and +111%, respectively (**Supplementary Table 1**). The pacing location for AF induction was estimated from the clinical local activation map, and reentry was initiated by rapid pacing. The pacing intervals were set from 200 to 120 ms (total of eight cycles in 10-ms intervals), and the total pacing time was set to 11,520 ms (19). We observed the AF maintenance for 22.5 s and measured the DF values for 6 s after the AF induction. The DF was analyzed as the frequency of the maximum peak power as described in previous research (20). We ablated the total area of the virtual DF sites in the V-DF group, but the DF ablation sites were adjusted to <5% of the LA nodes by color scaling and then delivered to the clinical procedure team. This approach was based on the previous work that ablation in an area of <5% of the critical mass does not change the termination or defragmentation rates (13). The no-flux condition was applied for all boundaries.

Definition of the Fiber Orientation From Atlases

We used an atlases-based mesh from each patient's left atrial (LA) geometry (21, 22) to describe the fiber orientation and performed high-density and entire-chamber atrial fibrillation (AF) mapping using personalized electrophysiological mapping data. The vector of the fiber orientation was generated at each node of the LA mesh along the myocardial fiber direction, and the conduction difference according to the orientation was realized by the fiber tracking method (12). The fiber orientation was adjusted based on the clinical local activation time map. The conductivity in the direction perpendicular to the vector was smaller than the conductivity in the vector direction. The conductivity of the model was applied at 0.1264 S/m (non-fibrotic longitudinal cell), 0.0546 S/m (fibrotic longitudinal cell), 0.0252 S/m (non-fibrotic transverse cell), and 0.0068 S/m (fibrotic transverse cell) (23). This procedure was performed at high speed using graphics processing unit-based software.

Determination of Fibrotic Cells Based on the Clinical Voltage Maps

The fibrosis regions were determined based on a clinically acquired bipolar voltage map. First, the LA mesh was reconstructed with each patient's clinical substrate mapping data, and the clinical bipolar voltage was interpolated into the 3D LA model using the nearest neighbor mapping. To determine the fibrosis or non-fibrosis at each node, we calculated the fibrosis probability through the following equation with the clinical bipolar voltage (24):

$$P_{fibrosis} = \begin{cases} 1, & X<0 \\ -40.0X^3+155X^2-206X+99.8, & 0\le X\le 1.74 \\ 0, & 1.74<X \end{cases}$$

where $P_{fibrosis}$ is the probability of fibrosis at a given node and X is the bipolar voltage at that node. If X is greater than the cutoff value of 1.74 mV, $P_{fibrosis}$ converges to zero. It was developed by comparing the predicted fibrosis rates in a 3D atrial model with pre- and post-ablation fibrosis data. As a result, fibrosis

was determined with a probability of fibrosis between 0 and 1 calculated based on clinically acquired bipolar voltage data at each node.

AFCA

Electrophysiological mapping and AFCA have been described previously (11). Briefly, we used an open irrigated-tip catheter or a contract-force ablation catheter to deliver radiofrequency energy for ablation under three-dimensional electroanatomical mapping (EnSite™ NavX™) merged with three-dimensional spiral computed tomography (CT). All patients in both groups underwent a circumferential PVI. After the PVI, bidirectional block was confirmed in all patients. An extra-PV ablation was performed based on the virtual DF mapping in the V-DF group and at the operator's discretion in the E-PVI group. Examples of determining and the ablation of the CUVIA-AF 2 target in three patients in each randomized group are illustrated in **Figure 3**. We ablated the DF areas marked on the CT-merged 3D electroanatomical map using the focal ablation technique, and not circumferential isolation. We delivered 40–50 W of RF energy for 10–15 s, but used a reduced power and temperature on the posterior side of the LA or LA appendage. DFs located in the LA appendage were mainly at the ostium. After the protocol-based ablation, the procedure ended when no immediate recurrence of AF was observed within 10 min after cardioversion with an isoproterenol infusion (5–10 μg/min depending on ß-blocker use; target sinus heart rate of 120 bpm; AF induction by a ramp pacing cycle length of 120 ms). If further AF triggers or frequent unifocal atrial premature beats were observed under the isoproterenol effect, extra-PV foci were ablated as much as possible. If there were unmappable repetitive AF triggers at the end of the procedure, the operators targeted the potential area of the extra-PV triggers by a linear or CFAE ablation to achieve the endpoint of the protocol.

Post-ablation Management and Follow-Up

We tried to discharge the patients without AADs except for those who had recurrent extra-PV triggers after the AFCA procedure, symptomatic frequent atrial premature beats, non-sustained atrial tachycardia (AT), or early recurrence of AF on telemetry during the admission period (AAD use 34.7% at discharge). Patients visited the outpatient clinic regularly at 1, 3, 6, and 12 months and then every 6 months thereafter or whenever symptoms occurred after AFCA. All patients underwent electrocardiography (ECG) recordings during every visit and 24-h Holter recordings at 3 and 6 months and then every 6 months thereafter, according to the protocol (25). Holter monitoring or event monitor recordings were obtained when patients reported symptoms of palpitations suggestive of an arrhythmia recurrence. A Holter analysis and adjudication were conducted by an individual blinded to the study group assignment. AF recurrence was defined

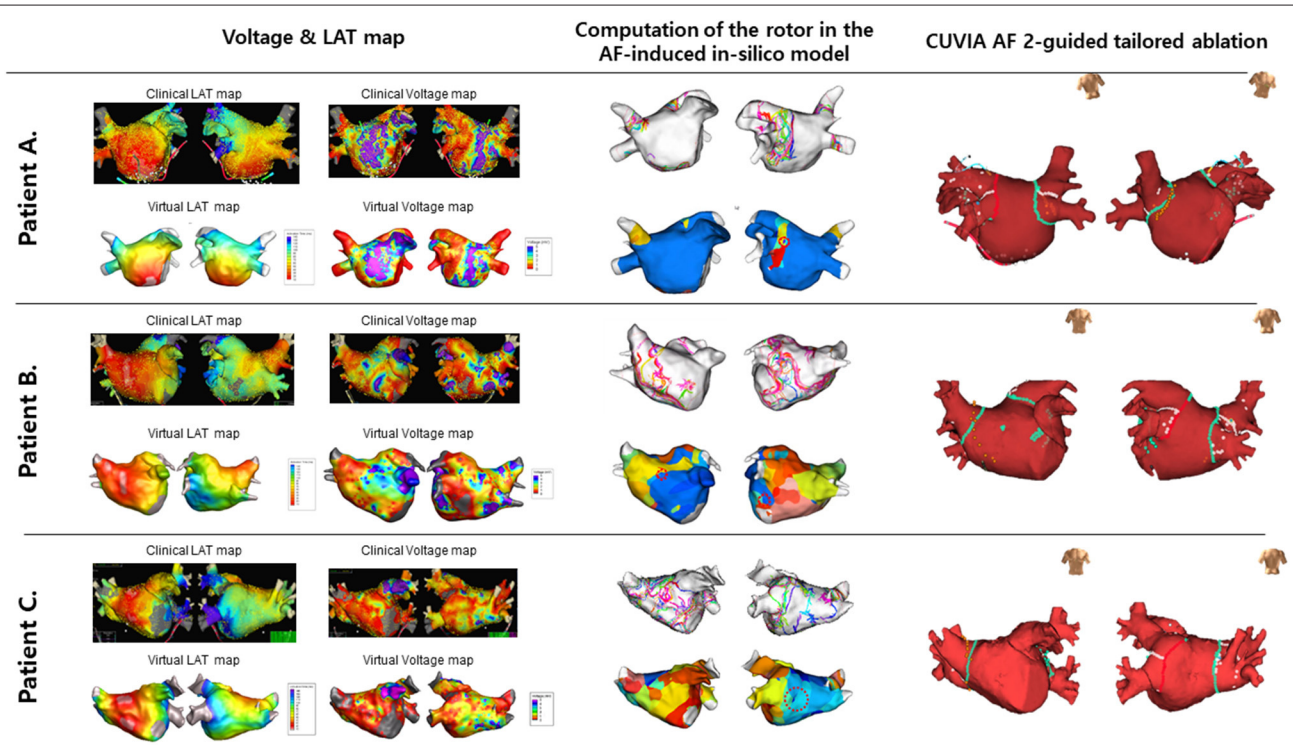

FIGURE 3 | Examples of the process to determine the CUVIA-AF ablation targets in three patients. **(A)** A 52-year-old man with DF located in the left inferior PV in the V-DF group. **(B)** A 56-year-old man with multiple DFs located on the anterior and posterior walls in the V-DF group. **(C)** A 72-year-old man with a DF located on the roof in the E-PVI group.

as any episode of AF or AT of at least 30 s in duration. Any ECG documentation of AF recurrence within a 6-month blanking period was diagnosed as an early recurrence, and AF recurrence occurring more than 6 months after the procedure was diagnosed as a case of clinical recurrence. The primary study endpoint was the freedom from documented episodes of AF or AT lasting longer than 30 s and occurring after a 3-month blanking period after a single ablation procedure. Secondary endpoints were the periprocedural complication rate and responses to AADs or electrical cardioversion rates after postprocedural recurrence.

Statistical Analysis

The continuous variables were compared using Student's *t*-tests, while categorical variables were compared using chi-squared or Fisher's exact tests, as appropriate. The primary endpoint was the freedom from any atrial arrhythmias during the follow-up period after a 3-month blanking period. The time to recurrence and rate of arrhythmia-free survival were assessed by a Kaplan–Meier analysis, with differences calculated using log-rank tests. To assess the factors associated with post-AFCA clinical recurrence of AF, we performed a Cox proportional-hazards model regression analysis. For all variables, *P*-values of <0.05 were considered to be statistically significant. All statistical analyses were performed using the IBM SPSS Statistics for Windows version 26.0 software program (IBM Corp., Armonk, NY, USA).

RESULTS

Patient Characteristics

Among a total of 222 patients with AAD-resistant symptomatic PeAF undergoing catheter ablation, 52 (23.4%) were excluded due to failed internal cardioversion or three episodes of recurrent AF re-initiated during paced atrial substrate mapping, which provided the mandatory electrophysiologic data for our realistic computation modeling (**Figure 1**). The characteristics of the study participants are summarized in **Table 1**. There were 87 patients included in the V-DF group and 83 included in the E-PVI group. The two ablation groups were well-balanced in terms of the baseline demographics. The mean age was 59 years, 70.6% of the study population was male, and the proportion of longstanding PeAF was 62.4%. The mean AF duration and CHA_2DS_2-VASc scores were 40.2 months and 2.1 ± 1.6 points, respectively. The mean LA diameter was 44.8 ± 5.5 mm. No significant difference was found regarding comorbidities between groups (P = NS).

Procedural Characteristics

The procedural results and complications are summarized in **Table 1**. The total procedure ($P = 0.513$) and ablation ($P = 0.894$) times did not differ between the two groups. Circumferential PVI and cavotricuspid isthmus ablation were successfully conducted in all patients. We analyzed the locations of the highest 10% DF in both groups (**Supplementary Table 2**). The highest DF areas were commonly found in the PVs (16.5%, **Figure 3A**), left atrial appendage (11.2%), or roof (10.0%). Multiple DF areas were found in 17.6% of patients and we ablated any extra-PV DF areas in the V-DF ablation group (**Figure 3B**) but not in the E-PVI group (**Figure 3C**). In the V-DF group, 37.6% of the patients (25/87) did not undergo a V-DF ablation because the V-DF was located inside the PVs (20.7%) or there was the absence of any presentation of DFs in the induced virtual ATs (16.9%). In the E-PVI group, an additional posterior box isolation and anterior linear ablation were conducted in 6.0 and 2.4% of the patients, respectively, at the operators' discretion, mostly due to repetitive immediate triggering of AF under an isoproterenol provocation. We conducted linear ablation only in the minority of the patients (4.6% for V-DF group vs. 6.0% for E-PVI group, $p = 0.742$), and the bidirectional block rates did not differ between the two groups (55.6% for V-DF group vs. 44.4% for E-PVI group, $p = 0.099$). The complication rates also did not significantly differ between the groups (3.4 vs. 6.0%; $P = 0.489$). No major thromboembolic complications, including strokes, occurred in either group (**Table 1**).

Primary Outcomes

During the 16.3 ± 5.3 months of follow-up, the early recurrence rates within 3 months of the AFCA did not differ (36.8 vs. 48.2%; $P = 0.132$), but the clinical recurrence rate was significantly lower in the V-DF group than E-PVI group (25.3 vs. 42.2%; $P = 0.023$, **Table 1**). A Kaplan–Meier analysis revealed a significantly lower clinical recurrence rate in the V-DF group than E-PVI group overall ($P = 0.018$, log-rank, **Figure 4A**). The rate of freedom from AF with off-AAD tended to be higher in the V-DF group ($P = 0.051$, log-rank, **Figure 4B**).

Secondary Outcomes and Subgroup Analysis

The AAD prescription rates did not significantly differ between the two groups at discharge (33.3 vs. 36.1%; $P = 0.749$) or 3 months after the procedure (36.8 vs. 49.4%; $P = 0.121$). However, the V-DF group demonstrated a significantly lower rate of AAD prescriptions than that of the E-PVI group at the final follow-up (21.8 vs. 41.0%; $P = 0.008$, **Table 1**). The overall single-procedure success rate was significantly higher in the V-DF group (74.7%) than the E-PVI group (57.8%; $P = 0.023$, **Table 1**). A multivariate Cox regression analysis showed that the V-DF ablation was independently associated with a low clinical recurrence after AFCA (hazard ratio 0.51, 95% confidence interval 0.30–0.88, $P = 0.016$, **Table 2**).

In sub-analysis of DF extra PV ablation, V-DF group showed better rhythm outcome compared to E-PVI group (24.2% recurrence for V-DF vs. 44.1% recurrence for the E-PVI; $p = 0.023$, **Figure 5**) Totally, we conducted the empirical extra-PV ablation in 11 out of 83 patients in the E-PVI group. Although the result of the DF map was not noticed to the operators in the E-PVI group, the DF site and empirical extra-PV ablation site matched in 2 out of 11 patients in the retrospective analysis (**Supplementary Table 3**).

Out of 57 patients with clinical recurrence, 55 experienced AF recurrence and two experienced AT recurrence (**Table 1**).

TABLE 1 | Baseline and procedure-related characteristics and rhythm outcomes of the study participants.

	Overall (*n* = 170)	V-DF (*n* = 87)	E-PVI (*n* = 83)	*P*-value
Age, years	59.2 ± 11.3	58.3 ± 11.5	60.2 ± 11.1	0.269
Male, *n* (%)	120 (70.6)	67 (77.0)	53 (63.9)	0.060
Longstanding persistent AF, *n* (%)	106 (62.4)	52 (59.8)	54 (65.1)	0.528
AF duration, (months)	40.2 ± 41.7	36.7 ± 38.8	43.9 ± 44.5	0.305
Comorbidities, *n* (%)				
Heart failure	40 (23.5)	22 (25.3)	18 (21.7)	0.580
Hypertension	93 (54.7)	51 (58.6)	42 (50.6)	0.294
Diabetes mellitus	39 (22.9)	19 (21.8)	20 (24.1)	0.726
Stroke	27 (15.9)	13 (14.9)	14 (16.9)	0.731
Vascular disease	13 (7.6)	9 (10.3)	4 (4.8)	0.175
CHA2DS2-VASc score	2.1 ± 1.6	2.1 ± 1.5	2.1 ± 1.6	0.719
Echocardiographic parameters				
LA dimension, mm	44.8 ± 5.5	44.9 ± 5.5	44.7 ± 5.5	0.777
LA volume index, ml/m2	40.6 ± 12.9	40.1 ± 13.2	41.0 ± 12.6	0.655
LV ejection fraction, %	60.1 ± 8.3	60.0 ± 7.6	60.1 ± 9.0	0.972
E/Em	10.3 ± 4.4	10.1 ± 4.6	10.4 ± 4.2	0.723
LVEDD, mm	49.7 ± 4.6	50.3 ± 4.8	49.0 ± 4.3	0.069
LVMI, g/m2	94.8 ± 21.7	95.2 ± 24.3	94.3 ± 18.7	0.777
Procedure time, min	166.8 ± 48.8	169.2 ± 43.5	164.3 ± 53.9	0.513
Ablation time, s	2989.4 ± 1067.0	3000.0 ± 958.0	2978.0 ± 1177.5	0.894
Ablation lesions, *n* (%)				
CPVI	170 (100)	87 (100)	83 (100)	–
Cavotricuspid isthmus line	170 (100)	87 (100)	83 (100)	–
Posterior wall isolation	8 (4.7)	3 (3.4)	5 (6.0)	0.489
Anterior line	5 (2.9)	3 (3.4)	2 (2.4)	0.689
Left lateral isthmus line	1 (0.6)	0 (0)	1 (1.2)	0.488
CFAE	2 (1.2)	1 (1.1)	1 (1.0)	0.973
Extra-PV trigger ablation, *n* (%)	4 (2.4)	1 (1.1)	3 (3.6)	0.359
Complications	8 (4.7)	3 (3.4)	5 (6.0)	0.489
Pericardial effusion	1	1	0	
PV stenosis	1	0	1	
Pericarditis	2	1	1	
Others[†]	4	1	3	
Rhythm outcomes				
Follow-up duration (months)	16.3 ± 5.3	16.4 ± 5.6	16.3 ± 5.3	0.903
Post-ABL medication				
ACEi, or ARB, *n* (%)	58 (34.1)	33 (37.9)	25 (30.1)	0.283
Beta blocker, *n* (%)	82 (48.2)	44 (50.6)	38 (45.8)	0.532
Statin, *n* (%)	63 (37.1)	35 (40.2)	28 (33.7)	0.381
AAD use				
At discharge, *n* (%)	59 (34.7)	29 (33.3)	30 (36.1)	0.749
After 3 months, *n* (%)	73 (42.9)	32 (36.8)	41 (49.4)	0.121
At the final follow-up, *n* (%)	53 (31.2)	19 (21.8)	34 (41.0)	0.008
Early recurrence types, *n* (%)	72 (42.4)	32 (36.8)	40 (48.2)	0.132
Clinical recurrence, *n* (%)	57 (33.5)	22 (25.3)	35 (42.2)	0.023
Recurrence type, AT, *n* (% in recur)	2 (3.5)	2 (9.1)	0	0.145
Cardioversion, *n* (% in recur/% overall)	39 (40.4/22.9)	17 (40.9/19.5)	22 (40.0/26.5)	0.362
Single-procedure success, overall, *n* (%)	113 (66.5)	65 (74.7)	48 (57.8)	0.023
Final sinus rhythm, overall, *n* (%)	142 (83.5)	81 (93.1)	61 (73.5)	0.001
Final sinus rhythm without AADs, *n* (%)	105/170 (61.8)	65/87 (74.7)	40/83 (48.2)	<0.001

AF, atrial fibrillation; LA, left atrium; LV, left ventricle; E/Em, mitral inflow velocity/mitral annulus tissue velocity; LVEDD, LV end-diastolic diameter; LVMI, LV mass index; CFAE, complex fractionated atrial electrogram; CPVI, circumferential pulmonary vein isolation; PV, pulmonary vein; AAD, antiarrhythmic drug; ABL, ablation; ACEi, angiotensin-converting enzyme inhibitor; ARB, angiotensin receptor blocker; AT, atrial tachycardia.

[†]*Other complications: sinus node dysfunction, TBS, severe hypotension, puncture site bleeding.*

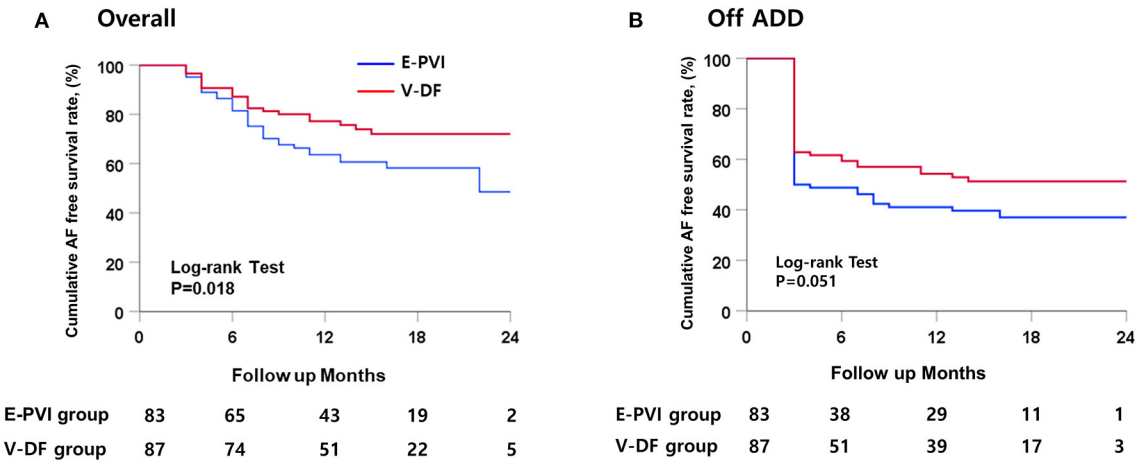

FIGURE 4 | Kaplan–Meier curves for the cumulative AF-free survival. **(A)** Overall patients. **(B)** Patients maintaining AAD use after catheter ablation.

TABLE 2 | Cox regression analysis for clinical recurrence after catheter ablation.

	Univariate		Multivariate	
	HR (95% CI)	***P*-value**	**HR (95% CI)**	***P*-value**
Age, years	1.01 (0.97–1.04)	0.578	1.00 (0.98–1.03)	0.740
Male, *n* (%)	1.09 (0.63–1.90)	0.756	1.35 (0.76–2.40)	0.305
AF duration	1.00 (0.99–1.01)	0.595		
Heart failure	1.01 (0.45–2.27)	0.974		
Hypertension	1.16 (0.57–2.35)	0.681		
Diabetes mellitus	1.10 (0.49–2.50)	0.815		
Stroke	1.26 (0.55–2.88)	0.581		
CHA_2DS_2-VASc score	1.05 (0.89–1.23)	0.601	1.09 (0.88–1.36)	0.423
LA dimension, mm	1.01 (0.96–1.11)	0.666	1.01 (0.96–1.07)	0.654
LVEF, %	0.99 (0.95–1.03)	0.523		
E/Em	0.96 (0.86–1.07)	0.474		
Computational virtual-guided	0.54 (0.31–0.92)	0.022	0.51 (0.30–0.88)	0.016

AF, atrial fibrillation; CHA2DS2-VASc, Congestive heart failure, Hypertension, Age (>65, 1 point; >75, 2 points), Diabetes, previous Stroke/transient ischemic attack (2 points); LA, left atrium; LV, left ventricular ejection fraction; E/Em, mitral inflow velocity/mitral annulus tissue velocity.

Among the patients with clinical recurrence, the proportion of AT [9.1% (2/22) vs. 0% (0/35); $P = 0.145$] and the cardioversion rates [40.9% (9/22) vs. 40.0% (14/35), $P = 0.590$] did not differ between the V-DF and E-PVI groups. Overall, 19.5% (17/87) of the V-DF group and 26.5% (22/83) of the E-PVI group underwent cardioversion to control AAD-resistant recurring atrial arrhythmias ($P = 0.362$). Finally, the proportions of patients who remained in sinus rhythm were 93.1% in the V-DF group and 73.5% in the E-PVI group ($P = 0.001$), respectively, while those who remained in sinus rhythm without AADs totaled 74.7% in the V-DF group and 48.2% in the E-PVI group ($P < 0.001$, **Table 1**).

DISCUSSION

In this prospective RCT comparing real-time computational modeling–guided AFCA and empirical AFCA in patients with PeAF, the intraprocedural virtual DF mapping and ablation targeting DF areas improved the rhythm outcomes without increasing the procedure time or risk of complications. We demonstrated that realistic computational modeling of AF, which reflects a personalized atrial anatomy, electrophysiology, fibrosis, and fiber orientation, is feasible and effective in non-paroxysmal AF ablation.

Heterogeneity and Unmet Needs of AF Ablation in Patients With PeAF

Since AF is a progressive disease, there are various stages of atrial remodeling in the category of PeAF. The current classification of AF is mainly determined by the duration of sustained AF, but the AF duration is often not clear in minimally symptomatic patients. Moreover, depending on the treating institution, some patients with longstanding PeAF undergo AFCA directly, while others undergo AFCA only after changing the AF to the paroxysmal type with AADs and cardioversion (6). Therefore, the current classification does not accurately reflect the pathophysiology of AF, and it is rather natural that prior attempts to conduct a uniform empirical extra-PV ablation for PeAF have failed. All the RCTs and meta-analyses that compared the PVI and other empirical extra-PV ablation procedures, such as the STAR-AF2 (comparing linear ablation and electrogram-guided ablation) and rotor ablation trials, failed to demonstrate the clinical usefulness of additional empirical extra-PV ablation lesions in patients with PeAF (7–9). As for the extra-PV ablation protocol that has been proven effective so far, mapping and ablation of extra-PV triggers after an isoproterenol provocation was the only approach that worked. However, mapping techniques available for provoked extra-PV triggers are still limited (26). In this study, we conducted an isoproterenol provocation and extra-PV trigger mapping and ablation in all patients included.

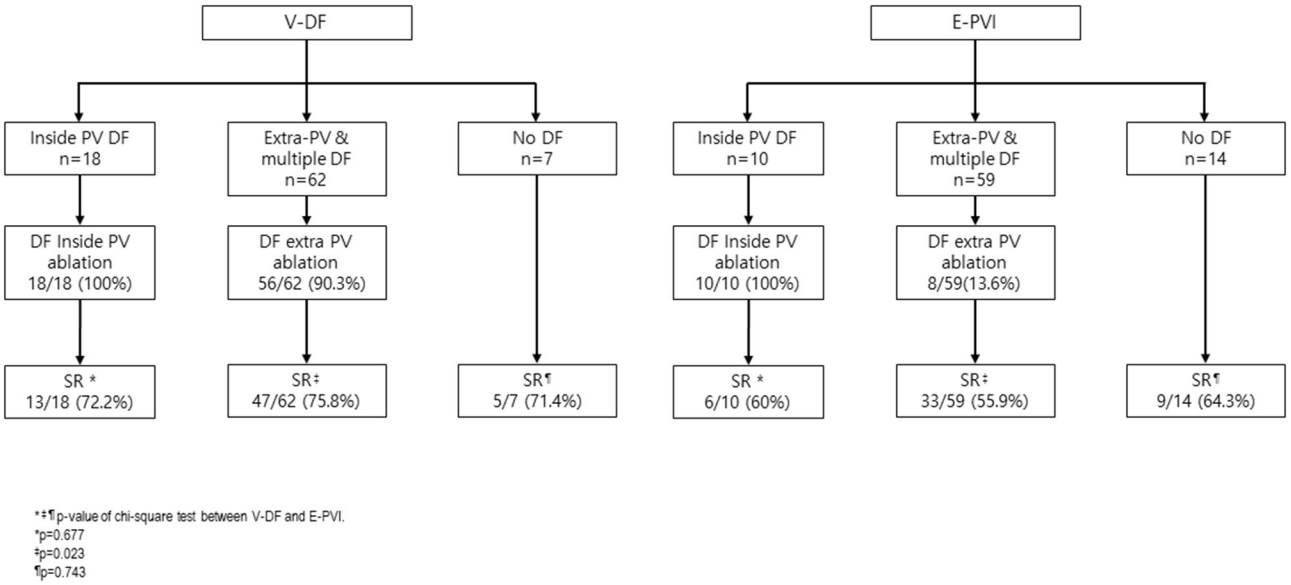

FIGURE 5 | Procedure outcome according to DF location and ablation.

Computational Modeling-Guided AF Ablation

Since Moe et al. (27) published on the subject of human atrial cell modeling in 1964, computational modeling has continued to evolve and innovate, playing an important part in basic electrophysiology research (14, 28). In recent years, sophisticated modeling is possible by reflecting the cardiac magnetic resonance imaging (MRI) late-gadolinium enhancement (29). Nevertheless, the biggest obstacle that exists in applying AF computational modeling to clinical medicine has been the high computational burden. Recently, however, this limitation has been overcome by a parallel computing technology (30), and MRI-based computational modeling has become technically feasible for arrhythmia interventions (29). Simulation-guided AFCA provides precision medical care that reflects the patient's personalized anatomy, histology, and electrophysiological characteristics (31).

The CUVIA-AF 1 trial was the only prospective RCT of computational modeling-guided AFCA published to date (10, 11). Kim et al. (10) conducted a preprocedural virtual ablation to test the optimal linear lesion set using AF modeling (CUVIA version 1.0) (32), which reflected the patient-specific atrial anatomy, and adopted the best lesion set during the clinical AFCA procedure, which was superior to the empirical ablation in patients with PeAF. In the current study, CUVIA version 2.5, which further improved the computational power and calculation efficiency (12), was used to test the effects of the intraprocedural AF driver mapping and ablation in a prospective RCT. After applying the CT-based anatomy, personalized electrophysiology, fibrosis, and fiber orientation inferred from a clinical electroanatomical map, the DF target information was successfully calculated and provided to the operator within 30–40 min while performing the PVI. DF ablation showed the better outcome for AF termination or defragmentation rates as compared to the CFAEs, phase singularities, or Shannon entropy in the previous virtual ablation study (13). It has been reported that a spectral analysis and frequency mapping identify localized sites of high-frequency activity during AF in humans with different distributions in non-paroxysmal AF (8, 11, 33). We targeted the DF sites as extra-PV AF drivers because the AF termination rate was higher after a DF ablation than other parameters representing rotational reentries in the previous simulation study (13). Unlike as seen in this CUVIA-AF2 trial, the RADAR-AF trial (34), which involved an extra-PV DF target ablation, reported negative outcomes as compared to a PVI alone. However, the mapping method in the RADAR-AF trial apparently differs from the entire-chamber DF mapping protocol used in this study. We acquired electrical data by a point-by-point map using a multi-electrode catheter during high right atrial pacing. We did not generate voltage maps in the AF state because AF drivers or rotational reentries meander during AF maintenance. Therefore, we localized virtual DF sites during the virtual AF state after integrating the clinical voltage and activation map to the computational model. The virtual AF analyzed in this study was an entire chamber map, which differs from the point-by-point sequential AF map in the RADAR trial.

Hurdles to Overcome and the Future Direction

Although AF modeling has advanced to the point of intraprocedural simulation and mapping, there are still challenges ahead. First, invasive mapping data are required as an important reference for fibrosis, conduction velocity, and the fiber orientation (12). Second, the dropout rate was 23.4% during the acquisition of clinical paced atrial substrate maps because of cardioversion failure or recurrent re-initiation

of AF. Third, atrial epi- and endocardial dissociation of the activation have to be reflected (35). We improved CUVIA version 3.0 (36) to a stage at which the atrial wall thickness can be applied, but the program still needs to overcome the increased computational burden. Fourth, most of the current modeling is chamber-centric mapping as it is hard to clearly determine the interatrial conduction pattern using medical images or clinical electroanatomical maps. Fifth, AF is a multifactorial disease and future AF modeling requires cardiac autonomic nerve activity, epicardial fat, or metabolic factors in order to apply various pathophysiologies (37). Sixth, it needs considering the possibility in misinterpretation of the results about secondary outcomes and subgroup analysis in this study, because we did not conduct control and adjustment for multiple hypothesis test in the secondary outcomes and subgroup analysis. Seventh, we conducted extra-PV ablation in 11 out of 83 patients in the E-PVI group to achieve the ablation end-point. Finally, it is necessary to expand the clinical application fields of AF modeling—for example, by considering virtual AADs—as well as arrhythmia intervention. With the application of artificial intelligence and the innovation of the hardware, we will overcome such hurdles one by one, however, we will be challenged each time by the computational burden and time.

CONCLUSION

In this prospective RCT comparing the real-time computational modeling–guided AFCA and empirical AFCA, intraprocedural virtual DF mapping and ablation targeting DF areas improved the rhythm outcomes without increasing the procedure time or risk of complications among the patients with PeAF. We proved that realistic computational modeling of AF, which reflects a personalized atrial anatomy, electrophysiology, fibrosis, and fiber orientation, is feasible and effective in non-paroxysmal AF ablation.

DATA AVAILABILITY STATEMENT

The raw data supporting the conclusions of this article will be made available by the authors, without undue reservation.

ETHICS STATEMENT

The studies involving human participants were reviewed and approved by the Institutional Review Board of Yonsei University Health System, Inha University College of Medicine and Inha University Hospital, and Ewha Womans University. The patients/participants provided their written informed consent to participate in this study.

AUTHOR CONTRIBUTIONS

Y-SB and O-SK contributed to writing the manuscript and data analysis. O-SK, BL, and S-YY developed the computational modeling and participate in simulation procedures. J-WP contributed to the data analysis and the manuscript revision. HY, T-HK, J-SU, BJ, D-HK, M-HL, JP, and H-NP conducted a multicenter clinical trial. H-NP and JP controlled all the *in silico* and clinical studies, manuscript preparation, and funding. All authors contributed to the article and approved the submitted version.

FUNDING

This work was supported by grants (HI19C0114 and HI21C0011) from the Ministry of Health and Welfare and grants (NRF-2019R1C1C1009075 and NRF-2020R1A2B01001695) from the Basic Science Research Program run by the National Research Foundation of Korea (NRF), which is funded by the Ministry of Science, ICT & Future Planning (MSIP).

ACKNOWLEDGMENTS

We would like to thank Mr. John Martin for his linguistic assistance.

SUPPLEMENTARY MATERIAL

The Supplementary Material for this article can be found online at: https://www.frontiersin.org/articles/10.3389/fcvm.2021.772665/full#supplementary-material

REFERENCES

1. Benjamin EJ, Wolf PA, D'Agostino RB, Silbershatz H, Kannel WB, Levy D. Impact of atrial fibrillation on the risk of death: the framingham heart study. *Circulation.* (1998) 98:946–52. doi: 10.1161/01.CIR.98.10.946
2. Packer DL, Mark DB, Robb RA, Monahan KH, Bahnson TD, Poole JE, et al. Effect of catheter ablation vs. antiarrhythmic drug therapy on mortality, stroke, bleeding, and cardiac arrest among patients with atrial fibrillation: the CABANA randomized clinical trial. *JAMA.* (2019) 321:1261–74. doi: 10.1001/jama.2019.0693
3. Kim M, Yu HT, Kim J, Kim TH, Uhm JS, Joung B, et al. Atrial fibrillation and the risk of ischaemic strokes or intracranial haemorrhages: comparisons of the catheter ablation, medical therapy, and non-atrial fibrillation population. *Europace.* (2020) 24:529–38. doi: 10.1093/ehjci/ehaa946.0559
4. Park JW, Yang PS, Bae HJ, Yang SY, Yu HT, Kim TH, et al. Five-year change in the renal function after catheter ablation of atrial fibrillation. *J Am Heart Assoc.* (2019) 8:e013204. doi: 10.1161/JAHA.119.013204
5. De With RR, Marcos EG, Van Gelder IC, Rienstra M. Atrial fibrillation progression and outcome in patients with young-onset atrial fibrillation. *Europace.* (2018) 20:1750–7. doi: 10.1093/europace/euy028
6. Pak HN, Park J, Park JW, Yang SY, Yu HT, Kim TH, et al. Electrical posterior box isolation in persistent atrial fibrillation changed to paroxysmal atrial fibrillation: a multicenter, prospective, randomized study. *Circ Arrhythm Electrophysiol.* (2020) 13:e008531. doi: 10.1161/CIRCEP.120.008531
7. Verma A, Jiang CY, Betts TR, Chen J, Deisenhofer I, Mantovan R, et al. Approaches to catheter ablation for persistent atrial fibrillation. *N Engl J Med.* (2015) 372:1812–22. doi: 10.1056/NEJMoa1408288
8. Lee JM, Shim J, Park J, Yu HT, Kim TH, Park JK, et al. The electrical isolation of the left atrial posterior wall in catheter ablation of persistent atrial fibrillation. *JACC Clin Electrophysiol.* (2019) 5:1253–61. doi: 10.1016/j.jacep.2019.08.021

9. Steinberg JS, Shah Y, Bhatt A, Sichrovsky T, Arshad A, Hansinger E, et al. Focal impulse and rotor modulation: acute procedural observations and extended clinical follow-up. *Heart Rhythm.* (2017) 14:192–7. doi: 10.1016/j.hrthm.2016.11.008
10. Kim IS, Lim B, Shim J, Hwang M, Yu HT, Kim TH, et al. Clinical usefulness of computational modeling-guided persistent atrial fibrillation ablation: updated outcome of multicenter randomized study. *Front Physiol.* (2019) 10:1512. doi: 10.3389/fphys.2019.01512
11. Shim J, Hwang M, Song JS, Lim B, Kim TH, Joung B, et al. Virtual in-silico modeling guided catheter ablation predicts effective linear ablation lesion set for longstanding persistent atrial fibrillation: multicenter prospective randomized study. *Front Physiol.* (2017) 8:792. doi: 10.3389/fphys.2017.00792
12. Lim B, Kim J, Hwang M, Song JS, Lee JK, Yu HT, et al. In situ procedure for high-efficiency computational modeling of atrial fibrillation reflecting personal anatomy, fiber orientation, fibrosis, and electrophysiology. *Sci Rep.* (2020) 10:2417. doi: 10.1038/s41598-020-59372-x
13. Hwang M, Song JS, Lee YS, Li C, Shim EB, Pak HN. Electrophysiological rotor ablation in in-silico modeling of atrial fibrillation: comparisons with dominant frequency, shannon entropy, and phase singularity. *PLoS ONE.* (2016) 11:e0149695. doi: 10.1371/journal.pone.0149695
14. Trayanova NA. Mathematical approaches to understanding and imaging atrial fibrillation: significance for mechanisms and management. *Circ Res.* (2014) 114:1516–31. doi: 10.1161/CIRCRESAHA.114.302240
15. Zozor S, Blanc O, Jacquemet V, Virag N, Vesin JM, Pruvot E, et al. A numerical scheme for modeling wavefront propagation on a monolayer of arbitrary geometry. *IEEE Trans Biomed Eng.* (2003) 50:412–20. doi: 10.1109/TBME.2003.809505
16. Li C, Lim B, Hwang M, Song JS, Lee YS, Joung B, et al. The spatiotemporal stability of dominant frequency sites in in-silico modeling of 3-dimensional left atrial mapping of atrial fibrillation. *PLoS ONE.* (2016) 11:e0160017. doi: 10.1371/journal.pone.0160017
17. Narayan SM, Krummen DE, Clopton P, Shivkumar K, Miller JM. Direct or coincidental elimination of stable rotors or focal sources may explain successful atrial fibrillation ablation: on-treatment analysis of the CONFIRM trial (Conventional ablation for AF with or without focal impulse and rotor modulation). *J Am Coll Cardiol.* (2013) 62:138–47. doi: 10.1016/j.jacc.2013.03.021
18. Seemann G, Hoper C, Sachse FB, Dossel O, Holden AV, Zhang H. Heterogeneous three-dimensional anatomical and electrophysiological model of human atria. *Philos Trans A Math Phys Eng Sci.* (2006) 364:1465–81. doi: 10.1098/rsta.2006.1781
19. Kim IS, Kim TH, Shim CY, Mun HS, Uhm JS, Joung B, et al. The ratio of early transmitral flow velocity (E) to early mitral annular velocity (Em) predicts improvement in left ventricular systolic and diastolic function 1 year after catheter ablation for atrial fibrillation. *Europace.* (2015) 17:1051–8. doi: 10.1093/europace/euu346
20. Lim B, Hwang M, Song JS, Ryu AJ, Joung B, Shim EB, et al. Effectiveness of atrial fibrillation rotor ablation is dependent on conduction velocity: an in-silico 3-dimensional modeling study. *PLoS ONE.* (2017) 12:e0190398. doi: 10.1371/journal.pone.0190398
21. Ho SY, Anderson RH, Sanchez-Quintana D. Atrial structure and fibres: morphologic bases of atrial conduction. *Cardiovasc Res.* (2002) 54:325–36. doi: 10.1016/S0008-6363(02)00226-2
22. Pashakhanloo F, Herzka DA, Ashikaga H, Mori S, Gai N, Bluemke DA, et al. Myofiber architecture of the human atria as revealed by submillimeter diffusion tensor imaging. *Circ Arrhythm Electrophysiol.* (2016) 9:e004133. doi: 10.1161/CIRCEP.116.004133
23. Zahid S, Cochet H, Boyle PM, Schwarz EL, Whyte KN, Vigmond EJ, et al. Patient-derived models link re-entrant driver localization in atrial fibrillation to fibrosis spatial pattern. *Cardiovasc Res.* (2016) 110:443–54. doi: 10.1093/cvr/cvw073
24. Hwang M, Kim J, Lim B, Song JS, Joung B, Shim EB, et al. Multiple factors influence the morphology of the bipolar electrogram: an in silico modeling study. *PLoS Comput Biol.* (2019) 15:e1006765. doi: 10.1371/journal.pcbi.1006765
25. Calkins H, Hindricks G, Cappato R, Kim YH, Saad EB, Aguinaga L, et al. 2017 HRS/EHRA/ECAS/APHRS/SOLAECE expert consensus statement on catheter and surgical ablation of atrial fibrillation. *Europace.* (2018) 20:e1–160. doi: 10.1093/europace/eux274
26. Lee KN, Roh SY, Baek YS, Park HS, Ahn J, Kim DH, et al. Long-term clinical comparison of procedural end points after pulmonary vein isolation in paroxysmal atrial fibrillation: elimination of nonpulmonary vein triggers versus noninducibility. *Circ Arrhythm Electrophysiol.* (2018) 11:e005019. doi: 10.1161/CIRCEP.117.005019
27. Moe GK, Rheinboldt WC, Abildskov JA. A computer model of atrial fibrillation. *Am Heart J.* (1964) 67:200–20. doi: 10.1016/0002-8703(64)90371-0
28. McDowell KS, Vadakkumpadan F, Blake R, Blauer J, Plank G, MacLeod RS, et al. Methodology for patient-specific modeling of atrial fibrosis as a substrate for atrial fibrillation. *J Electrocardiol.* (2012) 45:640–5. doi: 10.1016/j.jelectrocard.2012.08.005
29. Boyle PM, Zghaib T, Zahid S, Ali RL, Deng D, Franceschi WH, et al. Computationally guided personalized targeted ablation of persistent atrial fibrillation. *Nat Biomed Eng.* (2019) 3:870–9. doi: 10.1038/s41551-019-0437-9
30. Kwon SS, Yun YH, Hong SB, Pak HN, Shim EB. A patient-specific model of virtual ablation for atrial fibrillation. *Annu Int Conf IEEE Eng Med Biol Soc.* (2013) 2013:1522–5. doi: 10.1109/EMBC.2013.6609802
31. Lim B, Park JW, Hwang M, Ryu AJ, Kim IS, Yu HT, et al. Electrophysiological significance of the interatrial conduction including cavo-tricuspid isthmus during atrial fibrillation. *J Physiol.* (2020) 598:3597–612. doi: 10.1113/JP279660
32. Hwang M, Kwon SS, Wi J, Park M, Lee HS, Park JS, et al. Virtual ablation for atrial fibrillation in personalized in-silico three-dimensional left atrial modeling: comparison with clinical catheter ablation. *Prog Biophys Mol Biol.* (2014) 116:40–7. doi: 10.1016/j.pbiomolbio.2014.09.006
33. Sanders P, Berenfeld O, Hocini M, Jais P, Vaidyanathan R, Hsu LF, et al. Spectral analysis identifies sites of high-frequency activity maintaining atrial fibrillation in humans. *Circulation.* (2005) 112:789–97. doi: 10.1161/CIRCULATIONAHA.104.517011
34. Atienza F, Almendral J, Ormaetxe JM, Moya A, Martinez-Alday JD, Hernandez-Madrid A, et al. Comparison of radiofrequency catheter ablation of drivers and circumferential pulmonary vein isolation in atrial fibrillation: a noninferiority randomized multicenter RADAR-AF trial. *J Am Coll Cardiol.* (2014) 64:2455–67. doi: 10.1016/j.jacc.2014.09.053
35. Parameswaran R, Kalman JM, Royse A, Goldblatt J, Larobina M, Watts T, et al. Endocardial-epicardial phase mapping of prolonged persistent atrial fibrillation recordings: high prevalence of dissociated activation patterns. *Circ Arrhythm Electrophysiol.* (2020) 13:e008512. doi: 10.1161/CIRCEP.120.008512
36. Kwon O-S, Lee J, Lim S, Park J-W, Han H-J, Yang S-H, et al. Accuracy and clinical feasibility of 3D-myocardial thickness map measured by cardiac computed tomogram. *Int J Arrhyt.* (2020) 21:12. doi: 10.1186/s42444-020-00020-w
37. Mahajan R, Nelson A, Pathak RK, Middeldorp ME, Wong CX, Twomey DJ, et al. Electroanatomical remodeling of the atria in obesity: impact of adjacent epicardial fat. *JACC Clin Electrophysiol.* (2018) 4:1529–40. doi: 10.1016/j.jacep.2018.08.014

Conflict of Interest: The authors declare that the research was conducted in the absence of any commercial or financial relationships that could be construed as a potential conflict of interest.

Publisher's Note: All claims expressed in this article are solely those of the authors and do not necessarily represent those of their affiliated organizations, or those of the publisher, the editors and the reviewers. Any product that may be evaluated in this article, or claim that may be made by its manufacturer, is not guaranteed or endorsed by the publisher.

frontiers in Cardiovascular Medicine

ORIGINAL RESEARCH
published: 14 December 2021
doi: 10.3389/fcvm.2021.746820

Predicting Phrenic Nerve Palsy in Patients Undergoing Atrial Fibrillation Ablation With the Cryoballoon—Does Sex Matter?

Alexander Pott, Hagen Wirth, Yannick Teumer, Karolina Weinmann, Michael Baumhardt, Christiane Schweizer, Sinisa Markovic, Dominik Buckert, Carlo Bothner, Wolfgang Rottbauer and Tillman Dahme*

Department of Medicine II, Ulm University Medical Center, Ulm, Germany

OPEN ACCESS

Edited by:
Francesco Santoro, University of Foggia, Italy

Reviewed by:
Christian Hendrik Heeger, University Heart Center Luebeck, Germany
Andreas Rillig, University Heart and Vascular Center Hamburg (UHZ), Germany

***Correspondence:**
Alexander Pott
alexander.pott@uniklinik-ulm.de

Specialty section:
This article was submitted to Cardiac Rhythmology, a section of the journal Frontiers in Cardiovascular Medicine

Received: *24 July 2021*
Accepted: *20 October 2021*
Published: *14 December 2021*

Citation:
Pott A, Wirth H, Teumer Y, Weinmann K, Baumhardt M, Schweizer C, Markovic S, Buckert D, Bothner C, Rottbauer W and Dahme T (2021) Predicting Phrenic Nerve Palsy in Patients Undergoing Atrial Fibrillation Ablation With the Cryoballoon—Does Sex Matter? Front. Cardiovasc. Med. 8:746820. doi: 10.3389/fcvm.2021.746820

Background: Phrenicus nerve palsy (PNP) is a typical complication during pulmonary vein isolation (PVI) using the cryoballoon with the ominous potential to counteract the clinical benefit of restored sinus rhythm. According to current evidence incidence of PNP is about 5–10% of patients undergoing Cryo-PVI and is more frequent during ablation of the RSPV compared to the RIPV. However, information on patient specific characteristics predicting PNP and long-term outcome of patients suffering from this adverse event is sparse.

Aim of the Study: To evaluate procedural and clinical characteristics of AF patients with PNP during cryoballoon PVI compared to patients without PNP.

Methods and Results: Between 2013 and 2019 we included 632 consecutive AF patients undergoing PVI with the cryoballoon in our study. 84/632 (13.3%) patients experienced a total number of 89 PNP during the ablation procedure. 75/89 (84%) cryothermal induced PNP recovered until the end of the procedure (transient PNP, tPNP), whereas 14/89 (16%) PNP hold beyond the end of the procedure (non-transient PNP, ntPNP). Using multivariate logistic regression, we found that sex and BMI are strong and independent predictors of cryothermal induced non-transient PNP during cryoballoon PVI with an odds ratio of 3.9 (CI: 95%, 1.1–14.8, $p = 0.04$) for female gender. Interestingly, all patients (14/14, 100%) with a non-transient PNP experienced complete PNP resolution after a mean recovery time of 68 ± 79 days.

Conclusion: Our data indicate for the first time, that female sex and lower BMI are independent predictors for non-transient PNP caused by cryoballoon PVI. Fortunately, during follow up all PNP patients resolved completely with a median recovery time of 35 days.

Keywords: cryoballoon, phrenic nerve palsy, ablation, atrial fibrillation, female gender

INTRODUCTION

Based on its clinical efficiency and procedural safety cryoballoon pulmonary vein isolation (CB-PVI) has been established as an important therapeutic option for the treatment of patients suffering from atrial fibrillation (AF) (1–4). Severe procedural complications are sparse in patients undergoing CB-PVI with phrenic nerve palsy (PNP) during cryoenergy application of the right-sided pulmonary veins (PV) as the most frequent adverse event (5–7).

The right phrenic nerve (rPN) arises from the right cervical plexus and is located between the right-sided pericardium and the mediastinal pleura at the anterolateral wall of the superior vena cava (SVC) (8). Due to the anatomical proximity between SVC and right sided pulmonary veins rPN is frequently exposed to ablation energy during pulmonary vein isolation (PVI), especially when cryoenergy is applied. In case of phrenic nerve injury diaphragm movement can be limited or even abolished leading to severe dyspnoea counteracting the clinical benefit of restored sinus rhythm (9).

Various data have been published regarding incidence, outcome and clinical impact of PNP depending on ablation technique, balloon size, monitoring of PN activity and PNP definition (10–13). However, patient specific parameters predicting PNP occurrence during cryoballoon-PVI is rather sparse limiting pre-procedural risk evaluation and individualized informed consent of (AF) patients undergoing ablation (14, 15). Furthermore, data on long-term clinical outcome of cryoenergy-induced PNP and its recovery rate is only little studied so far (13).

Hence, the aim of our study was to compare clinical characteristics of AF patients with PNP during cryoballoon PVI compared to patients without PNP and to identify patient specific parameters predicting PNP occurrence. Furthermore, we assessed long-term clinical course of patients suffering from PNP which holds beyond the end of the ablation procedure.

METHODS

Study Population

Between 2013 and 2019 we included 632 consecutive patients undergoing PVI with the 2nd or 3rd generation cryoballoon in this observational study. From 2016 patients were routinely included in our prospective arrhythmia registry ATRIUM (ATrial Fibrillation Registry and BIobank UlM, DRKS-ID: DRKS00013013). Exclusion criteria of ATRIUM are the following:

- Age $<$ 18 years
- permanent atrial fibrillation
- LA $>$ 60 mm
- unable to consent

Beyond these exclusion criteria patients with pre-existing right-sided PNP were retrospectively excluded from our study. Patients with phrenic nerve palsy that occurred during cryoballoon PVI were assigned to the PNP group. PNP that restored within in the ablation procedure was classified as transient PNP (tPNP), whereas PNP that remained beyond the end of the procedure was classified as non-transient PNP (ntPNP). The study complies with the Declaration of Helsinki and was approved by our institutional review committee (342/16 and 05/2017). All patients gave written informed consent to the procedure.

Aim of the Study

To evaluate procedural and clinical characteristics of AF patients experiencing either transient or non-transient PNP during cryoballoon PVI compared to patients without PNP and to assess rate of PNP reconstitution during long-term follow-up.

Periprocedural Management

Intracardiac thrombi were ruled out in every patient by transesophageal echocardiography prior to PVI. No additional pre-procedural imaging was applied. All patients underwent transthoracic echocardiography to rule out pericardial effusion immediately after the procedure and prior to hospital discharge. Periprocedural anticoagulation was conducted as described before (16).

Cryoballoon Ablation Procedure

Cryoballoon ablation procedure was performed either 2nd or 4th generation cryoballoon and has been described in detail before (17). Briefly, a steerable sheeth (Medtronic, Minneapolis, MN, Flexcath Advance) was used to introduce the cryoballoon in the left atrium after single transseptal puncture. After balloon inflation at the PV ostia a 20-mm spiral mapping catheter (Achieve, Medtronic, Minneapolis, MN) was positioned in the PV at the closest achievable proximity to enable real-time observation of PV potentials during PV isolation. PV occlusion was documented by injection of contrast medium.

Phrenic nerve integrity was monitored by stimulation *via* the diagnostic catheter placed in the superior vena cava and palpation of the right-sided diaphragm and with additional recording of compound motor action potentials (CMAP) of the right sided diaphragm (18, 19). Cryoenergy application was aborted in case of reduced palpational feedback and/or reduced CMAP. In general, cryoenergy application was stopped by a single-stop-technique.

Post-procedural Management and Clinical Follow-Up

In patients with ntPNP ultrasound examination and/or x-ray of the chest was performed to evaluate restoration of phrenic movement before discharge and during further follow-up visits in case of ongoing PNP. All patients were scheduled for outpatient clinic visits including clinical assessment, echocardiography, 12-lead ECG, and 7-day-Holter-monitoring at 1, 3, and 6 months after the procedure and thereafter every 6 months.

Statistical Analysis

t-test was used to prove differences of numeric values between the two groups if normal distribution with equal variance was given. Normal distribution was determined by Shapiro-Wilk test and equal variance by Brown-Forsythe test. Numeric variables that were not normally distributed were analyzed by Mann-Whitney

rank sum test. Categorical variables were analyzed by Chi square test or Fisher's exact-test. A p-value < 0.05 was considered significant. Independency of co-variables potentially influencing PNP incidence was proven by uni- as well as multivariate logistic regression. Parameters with a p-value of 0.2 or lower in univariate logistic regression were included in multivariate logistic regression. Statistical assessment was performed with Excel (Version 2016, Microsoft Inc., Redmond, WA), XLStat software (V 2016.02.28430, Addinsoft, New York, NY) and SPSS Statistics 25 software (Version 2017, IBM, Armonk, NY, USA). Applied statistical methods were approved by a statistical expert.

RESULTS

Study Population

Between 2013 and 2019, we included 632 consecutive AF patients undergoing PVI with the cryoballoon in our study. Mean age was 66.1 ± 10.8 years. 352/632 patients (55.7%) were male and 422 (66.8%) had paroxysmal AF. Mean body mass index (BMI) was 29 ± 6 kg/m². Most common comorbidities were arterial hypertension (503/632 patients, 80%), followed by coronary artery disease (CAD, 224/632 patients, 35%). Mean CHA_2DS_2-VAsc score in the study population was 2.7 ± 1.6. Comparison of baseline characteristics between patients with PNP (PNP group) and without PNP (control group, CG) revealed no significant differences and is shown in **Table 1**.

Incidence, Distribution, and Type of Phrenicus Nerve Palsy

Of 632 consecutive patients undergoing Cryo-PVI 84 patients (13%) experienced PNP during ablation of the right sided PV with five patients having PNP at both the RSPV and the RIPV (total PNP number 89). 75/89 cryoenergy-induced PNP (84%) recovered by the end of the procedure (transient PNP, tPNP), whereas in 14/89 (16%) PNP persisted beyond the end of the procedure (non-transient PNP, ntPNP group). 75/89 PNP (84%) occurred during cryoenergy application at the right superior pulmonary vein (RSPV), whereas 14/89 PNP (16%, $p < 0.01$) were registered during PVI of the right inferior pulmonary vein (RIPV). As seen in **Figure 1**, the majority of tPNP as well as ntPNP were registered at the RSPV.

TABLE 1 | Baseline characteristics.

Baseline characteristics	CG	PNP	*p*-value
n (%)	548 (87)	84 (13)	
Age (years), mean ± SD	66 ± 11	66 ± 11	0.75
BMI (kg/m²), mean ± SD	29 ± 5	28 ± 7	0.54
Sex (female), *n* (%)	244 (45)	36 (25)	0.77
Paroxysmal AF, *n* (%)	360 (66)	62 (74)	0.15
EHRA-Score, mean ± SD	2.8 ± 0.8	2.8 ± 0.8	0.46
LAD (mm), mean ± SD	46 ± 6	46 ± 7	0.73
LVEF <45%, *n* (%)	76 (14)	10 (12)	0.19
Arterial hypertension, *n* (%)	434 (79)	69 (82)	0.53
Diabetes, *n* (%)	97 (18)	16 (19)	0.76
Coronary artery disease, *n* (%)	195 (36)	29 (35)	0.84
Stroke, *n* (%)	61 (11)	5 (6)	0.25
CHA_2DS_2VASc, mean ± SD	2.7 ± 1.6	2.7 ± 1.4	0.87
GFR (ml/min), mean ± SD	65 ± 20	66 ± 20	0.96

BMI, body-mass-index; EHRA, European Heart Rhythm Association; LAD, left atrial diameter; LVEF, left ventricular ejection fraction; GFR, glomerular filtration rate.

Procedural Data

Mean number of ablations at the RSPV in patients without PNP was 1.6 ± 0.7 and 1.4 ± 0.5 in the ntPNP group, whereas mean number of ablations in the tPNP group was significantly higher (2.2 ± 0.9, $p < 0.01$). Despite higher number of ablations in the tPNP group total freeze duration was comparable to the control group (tPNP: 323 ± 162s vs. CG: 311 ± 171s, $p = 0.60$). In contrast to patients of the control group, total freeze duration in the ntPNP group was significantly shorter (206 ± 135s, $p = 0.02$). Interestingly, minimal balloon temperature (Tmin) in the ntPNP was significantly higher in comparison to Tmin during cryoenergy application without PNP at the RSPV (ntPNP: −45 ± 7°C vs. noPNP: −49 ± 7°C, $p = 0.04$). Accordingly, mean number of ablations at the RIPV in patients with ntPNP was numerically lower and mean freeze duration tend to be shorter compared to RIPV freeze duration without cryoenergy induced PNP. Incidence of both tPNP and ntPNP was not associated with lower isolation rate of the right sided PV (**Table 2**).

Remarkably, procedural parameters such as number of ablations until PNP, freeze duration until PNP or balloon temperature at PNP were not different in the tPNP and ntPNP group. However, freeze duration until ntPNP was numerically higher compared to freeze duration until tPNP in both the RSPV and RIPV, suggesting that ntPNP might be associated with longer cryoenergy application (**Supplementary Table 1**).

Patient Specific Predictors of Non-transient PNP

To evaluate whether patient-specific constitutional parameters are associated with higher risk of ntPNP during CB-PVI, we compared baseline characteristics that might influence either cryoenergy tissue conduction (e.g., BMI and LAD) or phrenic nerve function such as diabetes or previous stroke in patients with and without ntPNP. Interestingly, we found that incidence of ntPNP is significantly higher in female patients with lower BMI and small atrial size compared to patients without ntPNP (**Table 3**). Uni-and multivariate regression analysis revealed that sex and BMI are strong and independent risk predictors for ntPNP. Remarkably, female patients have an Odds ratio of 3.9 (95%-CI: 1.1–14.8; $p = 0.04$) to experience ntPNP during CB-PVI compared to male patients (**Table 4**).

Long-Term Clinical Outcome of Patients With Non-transient PNP

All patients with non-transient PNP (14/14, 100%) experienced complete reconstitution of phrenic nerve function after a mean recovery time of 2.2 ± 2.6 months (67.8 ± 79 days, median 35

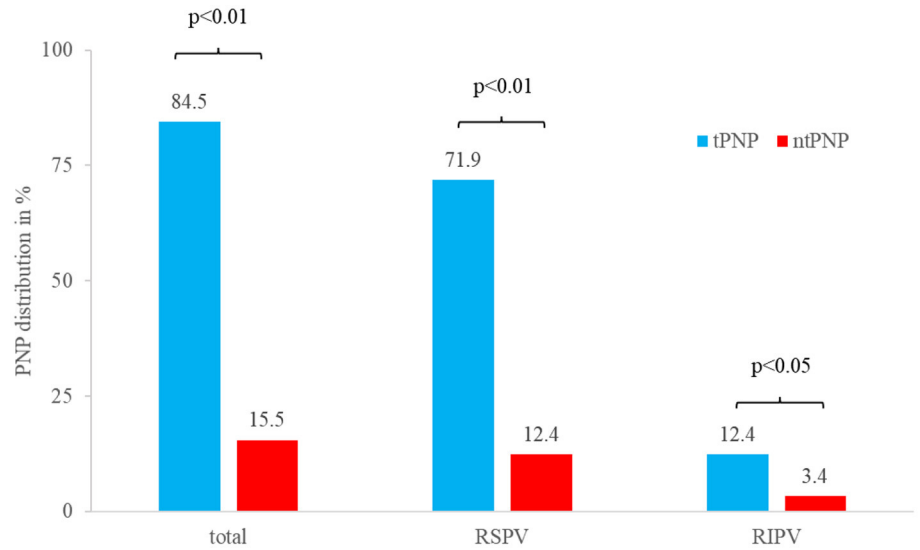

FIGURE 1 | Distribution of tPNP and ntPNP at the right-sided pulmonary veins. Most of the PNP occur during cryoenergy ablation of the RSPV, whereas PNP during ablation of the RIPV is a rare event.

TABLE 2 | Procedural data.

Procedural data	noPNP	tPNP	ntPNP	*p*-value (No vs. tPNP)	*p*-value (No vs. ntPNP)
# RSPV (%)	557 (88)	64 (10)	11 (2)		
# Ablations RSPV	1.6 ± 0.7	2.2 ± 0.9	1.4 ± 0.5	**<0.01**	0.23
Total freeze duration RSPV (s)	311 ± 171	323 ± 162	206 ± 135	0.60	**0.02**
TTI RSPV (s)	40 ± 21	41 ± 26	43 ± 27	0.84	0.83
Tmin RSPV (°C)	−49 ± 7	−52 ± 6	−45 ± 7	**<0.01**	**0.04**
PV isolation rate RSPV (%)	557/557 (100)	63/64 (98)	11/11 (100)	0.97	1.00
# RIPV (%)	618 (98)	11 (2)	3 (<1)		
# Ablations RIPV	1.8 ± 0.9	2.5 ± 1.5	1.3 ± 0.6	0.21	0.27
Total freeze duration RIPV (s)	348 ± 208	365 ± 232	173 ± 57	0.79	0.1
TTI RIPV (s)	48 ± 27	43 ± 6	68 ± 58	0.71	0.65
Tmin RIPV (°C)	−47 ± 9	−48 ± 8	−47 ± 6	0.63	0.96
PV isolation rate RIPV	617/618 (100)	11/11 (100)	3/3 (100)	0.98	1.00

RSPV, right superior pulmonary vein; RIPV, right inferior pulmonary vein; TTI, time-to-isolation; Tmin, minimal balloon temperature; bold values represent values of statistical significance.

days). Three months after index procedure in only 2/14 patients (14%) ntPNP was still documented. Longest period of ntPNP reconstitution was 8.2 months (245 days, **Figure 2**). Symptomatic ntPNP was registered in two patients, which suffered from mild dyspnoea in absence of AF recurrence. Remarkably, symptoms disappeared in these patients after reconstitution of phrenic nerve function.

DISCUSSION

The present study investigated the correlation between procedural parameters, patient specific conditions and the incidence of phrenicus nerve injury, which is a common and typical procedural complication in AF patients undergoing cryoballoon PVI. Furthermore, long-term outcome and time to recovery of patients, which experienced non-transient PNP, was analyzed.

Impact of Procedural Characteristics on Incidence and Type of PNP

Remarkably, comparison of procedural data of cryoballoon PVI between patients with tPNP and ntPNP revealed no significant differences, indicating that the incidence of transient or non-transient phrenic nerve injury cannot be exclusively explained by intensity of cryoenergy application.

However, we found several differences between patients with and without PNP. Interestingly, mean number of freeze applications during RSPV isolation was not different in patients without PNP and in patients with ntPNP, suggesting that thermal induced PNP is not a cryoenergy accumulation effect by high

number of freezes. This finding is well in line with the fact, that the vast majority of ntPNP during RSPV ablation occurred during the first freeze.

Despite a similar number of cryoenergy applications at the RSPV in patients with ntPNP and without PNP, total freeze duration was significantly shorter and mean nadir balloon temperature was significantly higher in the ntPNP group. These findings reflect the fact, that in patients with ntPNP no further cryoenergy applications are performed at the PV, in which the PNP occurred. Hence, less negative balloon temperature and shorter total freeze duration at the RSPV are a consequence of PNP and do not contribute to PNP genesis.

Since number of freezes, freeze duration or nadir balloon temperature was not different or even less extensive in patients with ntPNP compared to patients with tPNP and without PNP, we conclude that procedural parameters such as number of freezes, freeze duration or nadir balloon temperature are not suitable for PNP prediction during cryoballoon PVI.

TABLE 3 | Constitutional Parameter.

Constitutional parameters	No ntPNP	ntPNP	*p*-value
BMI (kg/m²), mean ± SD	29 ± 6	24 ± 4	**<0.01**
Sex (female), *n* (%)	270 (44)	10 (77)	**0.02**
Paroxysmal AF, *n* (%)	413 (67)	11 (85)	0.24
LAD (mm), mean ± SD	46 ± 7	42 ± 6	**0.04**
Diabetes, *n* (%)	112 (18)	1 (8)	0.48
Stroke, *n* (%)	64 (10)	2 (15)	0.46
CHA_2DS_2VASc-Score, mean ± SD	2.7 ± 1.6	3.5 ± 0.9	0.21

BMI, body-mass-index; LAD, left atrial diameter; bold values represent values of statistical significance.

TABLE 4 | Logistic regression.

Predictor	*p*-value: univariate	*p*-value: multivariate	Odds ratio	CI (95%)
Female sex	0.03	**0.04**	**3.9**	**1.1–14.8**
BMI	<0.01	**0.01**	**0.8**	**0.7–0.9**
LAD	0.02	0.12	0.9	0.85–1.0

BMI, body-mass-index; LAD, left atrial diameter; bold values represent values of statistical significance.

Female Sex and Lower Body-Mass-Index as Independent Predictors of Non-transient PNP

In our study cohort, baseline characteristics between patients with and without PNP did not differ significantly. However, comparing patients with clinically relevant phrenic nerve palsy, defined as PNP holding beyond the end of the procedure, revealed that patients with non-transient PNP are mostly female, have smaller left atrial size and lower BMI compared to patients without ntPNP. Accordingly, uni- as well as multivariate regression identified sex and BMI as strong and independent predictors of ntPNP during cryoenergy ablation of the right-sided veins.

Cryoenergy distribution from the cryoballoon to the phrenic nerve depends on the physical phenomenon that energy transfers from tissue with low temperatures to tissue with higher temperature, so called convective cooling. As a result, cold-induced ice-crystal formation as well as derangement of myocardial microcirculation occurs in atrial cardiomyocytes

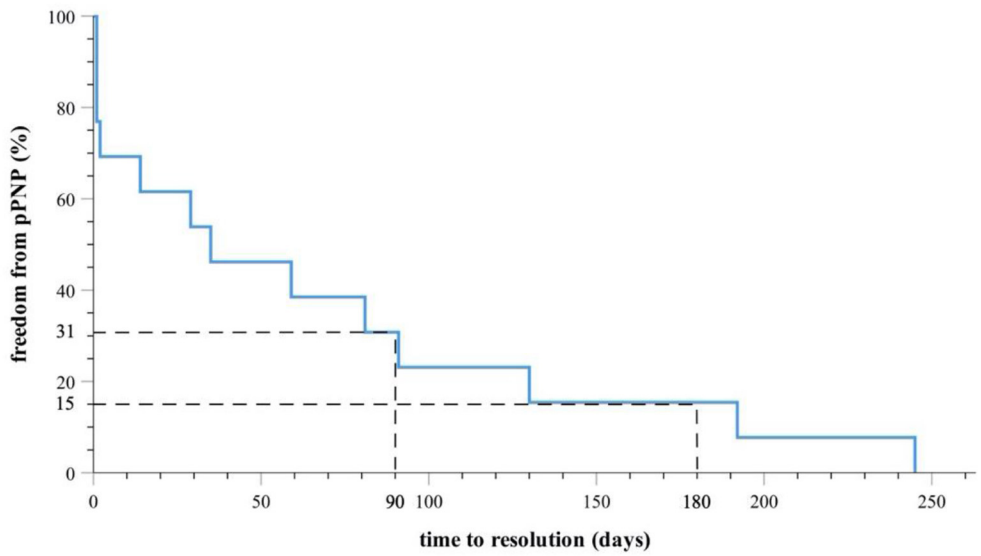

FIGURE 2 | Kaplan-Meier-Survival-Curve indicates complete PNP recovery in all patients during follow-up. Thirty-one percentage of the patients suffered from ntPNP 90 days and 15% of the patients suffered from ntPNP 180 days after index procedure.

surrounding the cryoballoon leading to severe and mostly irreversible tissue damage (20).

The cryoenergy flow strongly depends on the distances between tissues with different temperature as well as on the amount of isolating fatty tissue in between. Despite there are no distinct studies evaluating the interorganic distance between rPN and right-sided PV in the context of AF ablation procedures, one might imagine that in females, which have significant lower chest volumina compared to males (21), rPN and left atrium are in close proximity.

Is There a Protecting Role of Epicardial Fatty Tissue Against Thermal-Induced Phrenic Nerve Injury During Cryoenergy Application?

Epicardial fatty tissue is related to the extent of visceral fatty tissue, rather than to overall adiposity, as shown in several studies (22). Hence, male AF patients, which are more affected from visceral fat compared to female AF patients, might be protected from cryoenergy induced PNP due to the higher extent of isolating epicardial fat tissue. Hence, we conclude that constitutional parameters such as body weight, height and extent of fatty tissue are important factors for incorporal cryoenergy distribution during cryoballoon PVI.

Despite the fact, that our study is non-randomized and data were collected only from one EP center, we propose as a clinical consequence, that female patients with lower BMI should be informed individually about a higher risk of ntPNP during cather ablation using the cryoballoon. Furthermore, in this special patient group, diaphragmatic cMAP monitoring is the method of choice and should be used for the prevention of cryothermal induced PNP in female patients with lower BMI.

DATA AVAILABILITY STATEMENT

The raw data supporting the conclusions of this article will be made available by the authors, without undue reservation.

ETHICS STATEMENT

The studies involving human participants were reviewed and approved by the Ulm University Medical Center Institutional Review Committee (342/16 and 05/2017). The patients/participants provided their written informed consent to participate in this study.

AUTHOR CONTRIBUTIONS

AP: conceptualization, data curation and analysis, methodology, project administration, and writing—review and editing. TD: supervision, conceptualization, project administration, and writing—review and editing. WR: supervision. SM, DB, MB, and KW: data analysis and writing—original draft preparation. CB: data analysis. CS, YT, and HW: data curation and analysis and methodology. All authors contributed to the article and approved the submitted version.

SUPPLEMENTARY MATERIAL

The Supplementary Material for this article can be found online at: https://www.frontiersin.org/articles/10.3389/fcvm.2021.746820/full#supplementary-material

REFERENCES

1. Kirchhof P, Benussi S, Kotecha D, Ahlsson A, Atar D, Casadei B, et al. 2016 ESC guidelines for the management of atrial fibrillation developed in collaboration with EACTS. *Europace.* (2016) 18:1609–78. doi: 10.5603/KP.2016.0172
2. Kirchhof P. Integrated care of patients with atrial fibrillation: the 2016 ESC atrial fibrillation guidelines. *Heart.* (2017) 103:729–31. doi: 10.1136/heartjnl-2016-310843
3. Kirchhof P, Camm AJ, Goette A, Brandes A, Eckardt L, Elvan A, et al. Early rhythm-control therapy in patients with atrial fibrillation. *N Engl J Med.* (2020) 383:1305–16. doi: 10.1056/NEJMoa2019422
4. Hindricks G, Potpara T, Dagres N, Arbelo E, Bax JJ, Blomstrom-Lundqvist C, et al. 2020 ESC guidelines for the diagnosis and management of atrial fibrillation developed in collaboration with the European association of cardio-thoracic surgery (EACTS). *Eur Heart J.* (2020). 42:373–498. doi: 10.1093/eurheartj/ehaa612
5. Parikh V, Kowalski M. Comparison of phrenic nerve injury during atrial fibrillation ablation between different modalities, pathophysiology and management. *J Atr Fibrillation.* (2015) 8:1314. doi: 10.4022/jafib.1314
6. Mol D, Houterman S, Balt JC, Bhagwandien RE, Blaauw Y, Delnoy PH, et al. Complications in pulmonary vein isolation in the Netherlands heart registration differ with sex and ablation technique. *Europace.* (2021) 23:216–25. doi: 10.1093/europace/euaa255
7. De Greef Y, Stroker E, Schwagten B, Kupics K, De Cocker J, Chierchia GB, et al. Complications of pulmonary vein isolation in atrial fibrillation: predictors and comparison between four different ablation techniques: results from the MIddelheim PVI-registry. *Europace.* (2018) 20:1279–86. doi: 10.1093/europace/eux233
8. Sanchez-Quintana D, Cabrera JA, Climent V, Farre J, Weiglein A, Ho SY. How close are the phrenic nerves to cardiac structures? Implications for cardiac interventionalists. *J Cardiovasc Electrophysiol.* (2005) 16:309–13. doi: 10.1046/j.1540-8167.2005.40759.x
9. Mears JA, Lachman N, Christensen K, Asirvatham SJ. The phrenic nerve and atrial fibrillation ablation procedures. *J Atr Fibrillation.* (2009) 2:176. doi: 10.4022/jafib.176
10. Molenaar MMD, Hesselink T, Ter Bekke RMA, Scholten MF, Manusama R, Pison L, et al. Shorter RSPV cryoapplications result in less phrenic nerve injury and similar 1-year freedom from atrial fibrillation. *Pacing Clin Electrophysiol.* (2020) 43:1173–9. doi: 10.1111/pace.14062
11. Furnkranz A, Bordignon S, Schmidt B, Perrotta L, Dugo D, De Lazzari M, et al. Incidence and characteristics of phrenic nerve palsy following pulmonary vein isolation with the second-generation as compared with the first-generation cryoballoon in 360 consecutive patients. *Europace.* (2015) 17:574–8. doi: 10.1093/europace/euu320
12. Okishige K, Aoyagi H, Kawaguchi N, Katoh N, Yamashita M, Nakamura T, et al. Novel method for earlier detection of phrenic nerve injury during cryoballoon applications for electrical isolation of pulmonary veins in patients with atrial fibrillation. *Heart Rhythm.* (2016) 13:1810–6. doi: 10.1016/j.hrthm.2016.05.003

13. Tohoku S, Chen S, Last J, Bordignon S, Bologna F, Trolese L, et al. Phrenic nerve injury in atrial fibrillation ablation using balloon catheters: incidence, characteristics, and clinical recovery course. *J Cardiovasc Electrophysiol.* (2020) 31:1932–41. doi: 10.1111/jce.14567
14. Mugnai G, de Asmundis C, Stroker E, Hunuk B, Moran D, Ruggiero D, et al. Femoral venous pressure waveform as indicator of phrenic nerve injury in the setting of second-generation cryoballoon ablation. *J Cardiovasc Med (Hagerstown).* (2017) 18:510–7. doi: 10.2459/JCM.0000000000000418
15. Maj R, Borio G, Stroker E, Sieira J, Rizzo A, Galli A, et al. Phrenic nerve palsy during right-sided pulmonary veins cryoapplications: new insights from pulmonary vein anatomy addressed by computed tomography. *J Interv Card Electrophysiol*. (2021) 60:85–92. doi: 10.1007/s10840-020-00713-1
16. Pott A, Petscher K, Messemer M, Rottbauer W, Dahme T. Increased rate of observed real-time pulmonary vein isolation with third-generation short-tip cryoballoon. *J Interv Card Electrophysiol.* (2016) 47:333–9. doi: 10.1007/s10840-016-0160-3
17. Pott A, Kraft C, Stephan T, Petscher K, Rottbauer W, Dahme T. Time-to-isolation guided titration of freeze duration in 3rd generation short-tip cryoballoon pulmonary vein isolation - comparable clinical outcome and shorter procedure duration. *Int J Cardiol.* (2018) 255:80–4. doi: 10.1016/j.ijcard.2017.11.039
18. Lakhani M, Saiful F, Parikh V, Goyal N, Bekheit S, Kowalski M. Recordings of diaphragmatic electromyograms during cryoballoon ablation for atrial fibrillation accurately predict phrenic nerve injury. *Heart Rhythm.* (2014) 11:369–74. doi: 10.1016/j.hrthm.2013.11.015
19. Mondesert B, Andrade JG, Khairy P, Guerra PG, Dyrda K, Macle L, et al. Clinical experience with a novel electromyographic approach to preventing phrenic nerve injury during cryoballoon ablation in atrial fibrillation. *Circ Arrhythm Electrophysiol.* (2014) 7:605–11. doi: 10.1161/CIRCEP.113.001238
20. Andrade JG, Wazni OM, Kuniss M, Hawkins NM, Deyell MW, Chierchia GB, et al. Cryoballoon ablation as initial treatment for atrial fibrillation: JACC state-of-the-art review. *J Am Coll Cardiol.* (2021) 78:914–30. doi: 10.1016/j.jacc.2021.06.038
21. Bellemare F, Jeanneret A, Couture J. Sex differences in thoracic dimensions and configuration. *Am J Respir Crit Care Med.* (2003) 168:305–12. doi: 10.1164/rccm.200208-876OC
22. Rosito GA, Massaro JM, Hoffmann U, Ruberg FL, Mahabadi AA, Vasan RS, et al. Pericardial fat, visceral abdominal fat, cardiovascular disease risk factors, and vascular calcification in a community-based sample: the Framingham heart study. *Circulation.* (2008) 117:605–13. doi: 10.1161/CIRCULATIONAHA.107.743062

Conflict of Interest: TD received speaker's honoraria and consulting fees from Medtronic, Biosense Webster, Boerhringer-Ingelheim, Bayer, Daiichi-Sankyo. AP received speaker's honoraria from Medtronic, Biosense Webster, Daiichi-Sankyo and is invited fellow of the Boston Scientific EP training program. CS and YT were funded by the Deutsche Herzstiftung.

The remaining authors declare that the research was conducted in the absence of any commercial or financial relationships that could be construed as a potential conflict of interest.

frontiers in Cardiovascular Medicine

ORIGINAL RESEARCH
published: 04 February 2022
doi: 10.3389/fcvm.2022.810334

Epicardial Adipose Tissue and Postoperative Atrial Fibrillation

Laura Petraglia[1], Maddalena Conte[1,2], Giuseppe Comentale[3], Serena Cabaro[1], Pasquale Campana[1], Carmela Russo[1], Ilaria Amaranto[1], Dario Bruzzese[4], Pietro Formisano[1], Emanuele Pilato[3], Nicola Ferrara[1], Dario Leosco[1] and Valentina Parisi[1]*

[1] Department of Translational Medicine, University of Naples Federico II, Naples, Italy, [2] Clinica San Michele, Maddaloni, Italy, [3] Department of Advanced Biomedical Sciences, University of Naples Federico II, Naples, Italy, [4] Department of Public Health, University of Naples Federico II, Naples, Italy

Background: Atrial fibrillation (AF) often occurs after cardiac surgery and is associated with increased risk of stroke and mortality. Prior studies support the important role of inflammation in the pathogenesis of postoperative atrial fibrillation (POAF). It is known that an increased volume and a pro-inflammatory phenotype of epicardial adipose tissue (EAT) are both associated with AF onset in non surgical context. In the present study, we aim to evaluate whether also POAF occurrence may be triggered by an increased production of inflammatory mediators from EAT.

Methods: The study population was composed of 105 patients, with no history of paroxysmal or permanent AF, undergoing elective cardiac surgery. After clinical evaluation, all patients performed an echocardiographic study including the measurement of EAT thickness. Serum samples and EAT biopsies were collected before surgery. Levels of 10 inflammatory cytokines were measured in serum and EAT conditioned media. After surgery, cardiac rhythm was monitored for 7 days.

Results: Forty-four patients (41.3%) developed POAF. As regard to cardiovascular therapy, only statin use was significantly lower in POAF patients (65.1% vs. 84.7%; *p*-0.032). Levels of Monocyte Chemoattractant Protein-1 (MCP-1), in both serum and EAT, were significantly higher in POAF patients (130.1 pg/ml vs. 68.7 pg/ml; $p = <0.001$; 322.4 pg/ml vs. 153.4 pg/ml; $p = 0.028$ respectively). EAT levels of IL-6 were significantly increased in POAF patients compared to those in sinus rhythm (SR) (126.3 pg/ml vs. 23 pg/ml; $p = < 0.005$).

Conclusion: Higher EAT levels of IL-6 and MCP-1 are significantly associated with the occurrence of POAF. Statin therapy seems to play a role in preventing POAF. These results might pave the way for a targeted use of these drugs in the perioperative period.

Keywords: epicardial adipose tissue, postoperative atrial fibrillation, interleukin-6, Monocyte Chemoattractant Protein-1, inflammation

OPEN ACCESS

Edited by:
Daniel M. Johnson, The Open University, United Kingdom

Reviewed by:
Vishal Vyas, Queen Mary University of London, United Kingdom
Plinio Cirillo, University of Naples Federico II, Italy
Timothy P. Fitzgibbons, University of Massachusetts Medical School, United States

***Correspondence:**
Dario Leosco
dleosco@unina.it

Specialty section:
This article was submitted to Cardiac Rhythmology, a section of the journal Frontiers in Cardiovascular Medicine

Received: *06 November 2021*
Accepted: *06 January 2022*
Published: *04 February 2022*

Citation:
Petraglia L, Conte M, Comentale G, Cabaro S, Campana P, Russo C, Amaranto I, Bruzzese D, Formisano P, Pilato E, Ferrara N, Leosco D and Parisi V (2022) Epicardial Adipose Tissue and Postoperative Atrial Fibrillation. Front. Cardiovasc. Med. 9:810334. doi: 10.3389/fcvm.2022.810334

INTRODUCTION

Atrial fibrillation (AF) is the most common arrhythmia occurring after cardiac surgery. The incidence of postoperative AF (POAF) ranges between 20% and 50% according to the type of surgical procedure, with higher rates after valve replacement or repair respect to isolated coronary artery bypass grafting (CABG) surgery (1–4). Combined procedures (CABG and valvular surgery) present the highest incidence of this complication, reaching up to 80% (5).

POAF occurrence determines a significant increase in stroke risk, morbidity and mortality with consequent increase of hospitalization time and healthcare costs (6).

Although the pathogenesis of POAF remains uncertain, accumulating evidence suggest an important role of inflammatory mechanisms and mediators. In particular, the interleukin- 6 (IL-6), recognized as a primary cytokine in the inflammatory cascade, has been identified as one of the main molecules involved in the development of POAF (4, 7–9). Interestingly, the epicardial adipose tissue (EAT), the visceral fat depot of the heart, produces numerous pro-inflammatory cytokines which can affect the myocardium through paracrine or vasocrine mechanisms (10, 11). Moreover, increased EAT thickness is associated with higher levels of secreted inflammatory mediators and with the onset of atrial fibrillation (10, 12).

The aim of this study was to evaluate the correlation between EAT secretory profile and POAF occurrence in patients undergoing cardiac surgery.

METHODS

Study population: the study population included 105 patients without history of paroxysmal or permanent atrial fibrillation, undergoing elective surgery for CABG or valve replacement for severe aortic stenosis at the cardiac surgery unit of University of Naples "Federico II". The presence of chronic inflammatory diseases and/or cancer represented exclusion criteria, given their association with systemic and/or visceral fat inflammation. Demographic and clinical data including drug therapies were collected from all patients. The study protocol was compliant to the ethical guidelines of the 1975 Declaration of Helsinki. All the study procedures received approval by our institution's human research committee (Protocol n. 301/19). All patients provided written informed consent before their inclusion into the study.

Transthoracic Echocardiography: before cardiac surgery, all patients underwent complete echocardiographic study, performed with a VIVID E9 (GE Healthcare) machine. In addition to the standard parameters, the maximum EAT thickness was evaluated, from the parasternal long-axis view, at end systole, between the right ventricle and the ascending aorta (13). Measurements of EAT thickness were performed offline by two independent blinded echocardiographers. The average value from three cardiac cycles was used for the statistical analysis.

Tissues and serum collection: serum samples and EAT biopsies were collected from all patients undergoing cardiac surgery before the cardiopulmonary bypass (CPB). EAT biopsy samples (average 0.1–0.5 g) were taken between the free wall of the right ventricle and the anterior surface of the ascending aorta. EAT secretomes were obtained as follows: tissues were weighted, cut into small pieces, and transferred into a 12-well plate. According to tissue weight, serum-free Dulbecco modified Eagle medium (DMEM) (1 mL medium/0.1 g tissue) was added to the well and incubated at 37°C in a CO_2 incubator. After 24 h, medium was collected and centrifuged at 14,000g to remove debris and analyzed for cytokines content, as described below.

Serum and EAT conditioned media were screened in duplicate for the concentration of IL-1β, IL-1ra, IL-6, IL-8, IL-13, basic Fibroblast Growth Factor (FGF), Interferon (IFN)-γ, Monocyte Chemoattractant Protein (MCP)-1, Regulated on Activation Normal T-cell Expressed and Secreted (RANTES/CCL5), and Tumor Necrosis Factor (TNF)-α, using the Bio-Plex multiplex Human Cytokine and Growth factor kits (Bio-Rad) according to the manufacturer's protocol.

Materials: Media were from Lonza (Lonza Group Ltd., Basel, Switzerland).

ECG monitoring: after surgery, heart rate and rhythm were monitored for 7 days, by continuous telemetry (ApexPro 7-lead system; General Electric Medical Systems), at the cardiac intensive care unit. Atrial fibrillation has been termed as irregularly atrial rhythm without clear P waves that was confirmed by a 12-lead ECG. In this study, POAF was defined as any episode of atrial fibrillation lasting more than 5 min, with or without symptoms requiring intervention to maintain hemodynamic stability, arisen in the seven days following the cardiac surgery. POAF episodes recorded in condition of hemodynamic and volemic balance were considered for analysis. We excluded POAF episodes potentially related to a sudden fluid loss (diuretic administration, postoperative bleeding, etc…), low blood oxygenation or intravenous high inotropic dose administration.

Anesthesia and surgical technique: surgical technique and perioperative management were the same for all patients according to the specific surgical procedure. Perioperative anesthesiologic management was the same in all cases: according to the institutional protocol, surgical anesthesia was obtained with continuous intravenous infusion of Propofol + Remifentanil + Cisatracurium, while fluid balance was managed paying attention to the hemodynamic conditions, in order to obtain a mean arterial pressure of at least 70 mmHg. Perioperative drugs management was carried out according to the 2017 EACTS Guidelines on perioperative medication in adult cardiac surgery (14). Before CPB, heparin was intravenously administered at a dose of 300 units/Kg in all cases; protamine need was assessed using the HMS Plus Hemostasis Management system (Medtronic, Minneapolis, MN, USA). Transesophageal echocardiography was routinely performed before the surgical incision in order to assess myocardial and cardiac valves function during and after the surgical procedure. All patients underwent surgery through a standard full sternotomy approach and hypothermic CPB. In order to optimize the surgical times and to avoid confounding factors, all tissue collections were performed before the heparin administration and the placement of extracorporeal circulation cannulas. Surgical excision of EAT was performed from the fat pad of right ventricle infundibulum near the atrioventricular groove, using only a surgical scalpel blade no. 11 (without using diathermy) in order to prevent any additional inflammatory damage. After collection, all biopsies were placed in a sterile pipe and quickly transferred to the laboratory to preserve EAT secreting activity. Extracorporeal circulation was performed through aortic and atrio-caval cannulation. All patients requiring high doses of inotropic drugs during their intensive care unit stay were excluded from the

study due to the known pro-arrhythmogenic effect (Epinephrine or Norepinephrine > 0.1 μg/Kg/min or Dobutamine > 5 μg/Kg/min). At the end of surgery, all patients were moved into the cardiac surgery intensive care unit and weaned from the mechanical ventilation after at least 2 h of general postoperative monitoring. Fluid intake was regulated to achieve a central venous pressure of at least 10 mmHg according to the cardiac anatomy and myocardial function. All patients received $MgSO_4$ continuous intravenous infusion in a dose of 17.5 gr in the first 24 h after the surgery as anti-arrhythmia prophylaxis. Packed red cells were transfused only in presence of serum Hemoglobin lower than 8 g/dl while Fresh frozen plasma was used as plasma expander only in case of postoperative bleeding.

Statistical analysis: all statistical analyses were conducted using the statistical platform R (vers. 4.0). Standard descriptive statistics were used to describe the sample. Mean ± standard deviation (std. dev.) with range in case of numerical variables and absolute frequencies and percentages for categorical factors. Numerical variables showing highly skewed distribution were described using median, interquartile range (25–75th percentile). Accordingly, between-groups comparisons were based on the chi-square test (or Fisher exact test where appropriate), the *t*-test for independent samples, or the Mann-Whitney U test. To account for imbalances between the two groups, the inflammatory mediators' levels were log-transformed and the difference between groups were assessed using a linear model

TABLE 1 | Demographic and clinical characteristics of the study population.

	Overall (*n* = 105)	**SR (*n* = 61; 58.7%)**	**POAF (*n* = 44; 41.3%)**	***P*-value**
Gender (female) *n* (%)	29 (27.6)	15 (24.6)	14 (31.8)	0.508
Age *n* (%)	67.8 ± 9.7 (45 to 84)	65 ± 9.9 (45 to 84)	71.6 ± 8 (46 to 83)	<0.001
Hypertension *n* (%)	84 (80.8)	47 (77)	37 (86)	0.317
Diabetes *n* (%)	48 (46.2)	29 (47.5)	19 (44.2)	0.842
Dyslipidemia *n* (%)	62 (60.2)	38 (62.3)	24 (57.1)	0.683
Smokers *n* (%)	40 (38.8)	25 (41)	15 (35.7)	0.492
BMI (kg/m2)	27.8 ± 4.3 (19.7 to 41.2)	28.1 ± 4.4 (21.4 to 41.2)	27.4 ± 4.2 (19.7 to 37.7)	0.474
Previous MI *n* (%)	26 (25.7)	12 (19.7)	14 (31.8)	0.214
Pre-operative WBC count	7.55 ± 1.65 (4.10 to 11.3)	7.38 ± 1.66	7.79 ± 1.62	0.239
CABG *n* (%)	74 (70.5)	42 (68.9)	32 (72.7)	0.669
Valvular Surgery *n* (%)	31 (29.5)	19 (31.1)	12 (27.3)	0.661
Drug therapy				
Beta blockers *n* (%)	88 (87.1)	53 (89.8)	35 (83.3)	0.377
Calcium-channel blockers *n* (%)	41 (40.6)	26 (44.1)	15 (35.7)	0.42
ACE-inhibitors/sartans *n* (%)	73 (72.3)	43 (72.9)	30 (71.4)	1
Statins *n* (%)	78 (76.5)	50 (84.7)	28 (65.1)	0.032
Atorvastatin *n* (%)	45 (42,9)	30 (49.2)	15 (34.1)	0.035
Rosuvastatin *n* (%)	33 (31,4)	20 (32.8)	13 (29.5)	0.589
Antiplatelet *n* (%)	88 (87.1)	54 (91.5)	34 (81)	0.14
Ecochardiographic parameters				
LVEF (%)	59.3 ± 10.6 (33 to 81)	59.1 ± 10.9 (33 to 81)	59.6 ± 10.2 (35 to 79)	0.8
Left Atrial Volume (>34 ml/m2) *n* (%)	35 (33.3)	17 (31.5)	18 (47.4)	0.184
E/A	0.9 [0.8; 1.2] (0.5 to 4.1)	0.9 [0.7; 1.2] (0.5 to 4.1)	0.9 [0.8; 1.3] (0.5 to 3.3)	0.771
E/E'	12 [7.7; 17.4] (4.8 to 32)	10 [6.6; 14] (4.8 to 23)	13.6 [10.4; 20.5] (7.3 to 32)	0.013
LVESD (mm)	29 [28; 31] (2.6 to 38)	28.5 [28; 30.5] (28 to 35)	29 [26.5; 32.5] (2.6 to 38)	0.962
LVEDD (mm)	48 [45; 51] (37 to 61)	48 [44.5; 53] (37 to 58)	48 [45; 51] (40 to 61)	0.918
Interventricular septum (mm)	10 [8; 12] (6 to 15)	10 [8; 12] (6 to 15)	10 [9; 12] (6 to 13)	0.851
Posterior Wall (mm)	9 [7.2; 11] (6 to 14)	9.5 [7; 10.8] (7 to 14)	9 [8; 11] (6 to 11)	0.982
Left ventricular mass (gr)	154.9 [124.1; 190.2] (87.1 to 349)	153 [118.5; 186.1] (87.1 to 349)	156.9 [124.9; 210.4] (90 to 234)	0.85
Left ventricular mass index gr/m^2	69.7 [12.1; 92.9] (0.7 to 163.9)	69.9 [45.7; 92] (0.7 to 163.9)	64.6 [1.3; 98] (0.8 to 131.1)	0.597
RWT	0.39 [0.32; 0.45] (0.22 to 0.58)	0.38 [0.31; 0.48] (0.24 to 0.58)	0.4 [0.33; 0.44] (0.22 to 0.55)	0.704
EAT (mm)	10.7 ± 3.6 (0 to 20)	9.6 ± 3.6 (0 to 15)	11.3 ± 3.5 (5 to 20)	0.099
Pump duration (min)	78 ± 10.9 (60 to 100)	78.7 ± 11.9	77 ± 9.3	0.429

For numerical variables, values are expressed as mean ± standard deviation or median [1st quartile; 3rd quartile] (min to max). SR, sinus rhythm; POAF, postoperative atrial fibrillation; BMI, body mass index; LVEF, left ventricular ejection fraction; LVESD, left ventricular end systolic diameter; LVEDD, left ventricular end diastolic diameter; EAT, epicardial adipose tissue; MI, myocardial infarction; WBC, white blood cells.

where age, statin use, atrial volume and E/e' were entered as covariates.

All tests were two-sided with a p value<0.05 denoting statistical significance. Due to exploratory nature of all the analyses, no adjustments were made for multiple comparison.

RESULTS

Patient Characteristics

Table 1 illustrates demographic, clinical, and echocardiographic characteristics of the study population. In the overall population, the mean age was 67.8 ± 9.7 (range 45–84) years and 27.6% of patients were females. Eighty percent of patients had hypertension, 46.2% were diabetics, 60.2% had dyslipidemia and 38.8% were smokers. Mean body mass index (BMI) was 27.8 ± 4.3. Mean left ventricular ejection fraction (LVEF) was 59.3 ± 10.6%. Mean EAT thickness was 10.7 ± 3.6 mm. As regard to drug therapies, 87.1% of patients assumed beta-blockers, 72.3% ACE-inhibitors/sartans, 40.6% calcium-channel blockers, 87.1% antiplatelet and 76.5% statins.

POAF occurred in 41.3% ($n = 44$ pts) of the study population. Interestingly, patients with POAF were older (71.6 ± 8 vs. 65 ± 9.9; $p = <0.001$) and had a worse diastolic function (E/e' 13.6 vs. 10; $p = 0.01$) compared to SR patients. No differences were found in cardiovascular risk factors, history of prior myocardial infarction, pre-operative inflammatory status, and other clinical characteristics between POAF and SR patients. There were no differences of type of surgical procedure between POAF and SR groups. Further, no patient in both groups underwent CABG plus valve surgery. Of note, as regard to cardiovascular therapy, only statin use was significantly lower in patients who developed POAF (65.1% vs. 84.7%; $p = 0.032$). To note atorvastatin use was higher in sinus rhythm (SR) patients than in POAF patients. All patients were in the hospital for the full 7 days of monitoring.

EAT and Serum Inflammatory Profile

IL-1β, IL-1ra, IL-6, IL-8, IL-13, FGF, IFN-γ, MCP-1, RANTES/CCL5 and TNF-α were detected in serum samples and EAT conditioned media obtained from all patients. No significant differences were found in serum levels of the pro-inflammatory mediators, except for MCP-1 which was significantly higher in patients who developed POAF than in those who remained in SR (130.1 pg/ml vs. 68.7 pg/ml; $p = \leq 0.001$; **Table 2**). Interestingly, also EAT levels of MCP-1 were significantly higher in patients with POAF (322.4 pg/ml vs. 153.4 pg/ml, $p = 0.028$; **Figure 1**; **Table 3**) even after adjusting the analysis for age, statin use and atrial volume, using general linear model ($p = 0.008$). Moreover, EAT levels but not serum levels of IL-6 were significantly increased in patients who developed POAF compared to those in SR patients (126.3 pg/ml vs. 23 pg/ml; $p = 0.005$; **Figure 1**; **Table 3**). The difference remained statistically significant in adjusted analysis ($p = 0.043$).

DISCUSSION

POAF represents one of the most frequent complication after cardiac surgery and accounts for a significant increase of stroke risk, disability and mortality. Although many intraoperative and clinical factors seem to be involved in the development of POAF, its pathogenesis remains still unclear. Recent evidence suggest that inflammation can alter atrial conduction, facilitating multiple re-entry wavelets, thus predisposing to the development of POAF (15, 16).

EAT, the visceral fat depot of the heart, located between the myocardium and the visceral layer of pericardium, is mainly represented in the atrio-ventricular and inter-ventricular grooves, and along the lateral wall of the right ventricle (11). In pathological conditions, EAT produces and secretes numerous inflammatory mediators (12, 17). The absence of fascial boundaries allows a tight connection with surrounding tissues and coronary arterial vessels. Numerous lines of evidence

TABLE 2 | Serum inflammatory profile.

	Overall ($n = 105$)	SR ($n = 61$; 58.7%)	POAF ($n = 44$; 41.3%)	*P*-value
	Median [1st quartile; 3rd quartile] (min to max)			
IL-1b pg/ml	7.6 [6; 8.6] (2.7–28.4)	7.6 [6.9; 8.6] (2.7–11.4)	7.3 [4.8; 9] (2.8–28.4)	0.413
IL-1ra pg/ml	444.9 [251; 803.1] (112.3–2,173)	441.1 [220.2; 660.9] (112.3–1,981.6)	461.2 [321.5; 998.4] (118.6–2,173)	0.13
IL-6 pg/ml	33.5 [28.7; 42.7] (7.6–238.3)	33 [28.7; 41.2] (15.7–93.6)	36.2 [25.9; 51.2] (7.6–238.3)	0.456
IL-8 pg/ml	43.3 [35; 61.4] (21.3–369.7)	39.7 [34.2; 55.8] (21.3–103.7)	45.6 [34.9; 78.8] (26.7–369.7)	0.13
IL-13 pg/ml	13 [9.4; 17.1] (2.9–48)	12.5 [9.4; 16.6] (4.4–23.9)	13.2 [9.4; 18.8] (2.9–48)	0.469
FGF basic pg/ml	105.7 [75; 148.2] (25.2–285.2)	123 [77.4; 148.2] (59.1–174)	81.7 [71.3; 150.6] (25.2–285.2)	0.264
IFN-g pg/ml	194.9 [164.7; 241.2] (76.5–1046.1)	194.9 [171.2; 229.8] (76.5–477.4)	186 [155.7; 318.4] (80.9–1,046.1)	0.969
MCP-1 (MCAF) pg/ml	85 [58.1; 136.5] (49.1–433.3)	68.7 [55.7; 120.7] (49.1–184.8)	130.1 [72.5; 172.3] (53.3–433.3)	0.001
RANTES pg/ml	10,014.6 [5,219.9; 23,118.6] (376.3–109,073.5)	9,473.7 [3,838.4; 23,503.8] (376.3–52,846.2)	10,898.4 [6,373.3; 23,779] (498.2–109,073.5)	0.439
TNF-α pg/ml	97.3 [75.7; 116.1] (21.3–397.6)	97.3 [81.1; 108] (21.3–182.8)	93.3 [55.3; 129.8] (22.6–397.6)	0.973

SR, sinus rhythm; POAF, postoperative atrial fibrillation; IL, Interleukin; FGF, Fibroblast Growth Factor; IFN-γ, Interferon-γ; MCP-1, Monocyte Chemoattractant Protein-1; RANTES/CCL5, Regulated on Activation Normal T-cell Expressed and Secreted; TNF-α, Tumor Necrosis Factor-α.

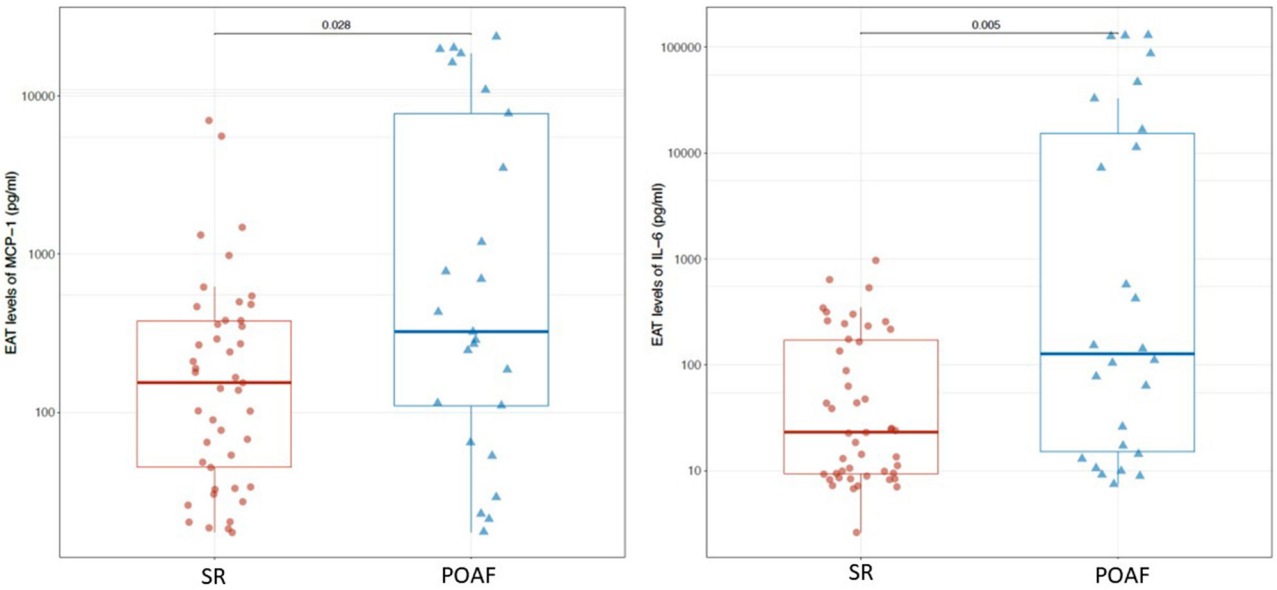

FIGURE 1 | EAT levels of MCP-1 and IL-6 in POAF and SR patients.

TABLE 3 | EAT inflammatory profile.

	Overall ($n = 105$)	SR ($n = 61$; 58.7%)	POAF ($n = 44$; 41.3%)	*P*-value
	Median [1st quartile; 3rd quartile] (min to max)			
IL-1b pg/ml	3.2 [2.1; 20] (1.2–227.7)	2.8 [2; 9.4] (1.2–82.4)	4.1 [2.3; 50.5] (1.2–227.7)	0.07
IL-1ra pg/ml	473.3 [57; 1,445.8] (1.2–21,640.2)	308.7 [51.2; 2,195.9] (1.2–21,640.2)	811.2 [68.5; 1,434.3] (29.7–14,413.5)	0.316
IL-6 pg/ml	38.7 [9.9; 255.9] (2.6–129,652.6)	23 [9.3; 174.5] (2.6–968.5)	126.3 [14; 20,624.3] (7.5–129,652.6)	0.005
IL-8 pg/ml	44.9 [11.3; 274.3] (4.2–335,428.2)	35.1 [10.4; 246.9] (4.4–2,618.9)	81.6 [14.6; 9,216.2] (4.2–335,428.2)	0.087
IL-13 pg/ml	3 [2.5; 3.9] (2.1–136.9)	2.9 [2.4; 3.5] (2.1–44.7)	3.5 [2.4; 10.3] (2.1–136.9)	0.076
FGF basic pg/ml	501.2 [287.4; 942] (40.8–3,416.2)	505 [321.4; 1,041.5] (40.8–3,416.2)	473.6 [273.2; 656] (143.1–3,324.3)	0.485
IFN-g pg/ml	95.6 [40.9; 144.6] (20.8–432.2)	90.2 [36.7; 122.2] (20.8–235.5)	110.6 [44.7; 235.2] (22.4–432.2)	0.057
MCP-1(MCAF) pg/ml	199.2 [53; 531.6] (17.3–23,675.8)	153.4 [39.2; 379.6] (17.3–6,993.6)	322.4 [87.2; 9,341.2] (17.5–23,675.8)	0.028
RANTES pg/ml	166.3 [87.3; 313.4] (24.7–1,065.3)	139.8 [82.6; 275.4] (24.7–1,034.6)	177.8 [115.5; 389.5] (39.4–1,065.3)	0.333
TNF-α pg/ml	28 [20.8; 40.8] (14.9–227.6)	26 [20.3; 34.2] (15.5–77.5)	35 [20.8; 91.9] (14.9–227.6)	0.057

SR, sinus rhythm; POAF, postoperative atrial fibrillation; IL, Interleukin; FGF, Fibroblast Growth Factor; IFN-γ, Interferon-γ; MCP-1, Monocyte Chemoattractant Protein-1; RANTES/CCL5, Regulated on Activation Normal T-cell Expressed and Secreted; TNF-α, Tumor Necrosis Factor-α.

suggest a strong association between increased EAT thickness and atrial fibrillation (11).

This is one of the few studies evaluating the potential association between the levels of EAT-secreted pro-inflammatory cytokines and the development of POAF in patients undergoing elective cardiac surgery, without history of paroxysmal or persistent atrial fibrillation. Viviano et al. have previously described EAT secretome as a possible substrate for POAF indicating the role of gelsolin, involved in inflammation and ion channel regulation, in maintaining sinus rhythm in these patients (18).

Consistent with previous studies, we have found that patients who developed POAF were older than those who remained in sinus rhythm throughout the postoperative period (15, 19). It is known that aging is characterized by a chronic low-grade inflammation and is associated with degenerative and inflammatory modifications in atrial anatomy, such as dilation and fibrosis, which are responsible for the alterations of the atrial electrophysiological properties (20–22). The EAT thickness increases with age and the release of proinflammatory adipocytokines from cardiac visceral fat into the systemic circulation may contribute to the inflammatory state, which in turn promotes the accumulation and inflammation of EAT (22, 23). Furthermore, it is well known that extracorporeal circulation is also characterized by a systemic inflammatory response (4, 24). In the present study, EAT thickness tended to be higher in POAF compared to non POAF patients, although the difference between groups did not reach the statistical significance. To note, EAT thickness mean value in POAF population was higher than that reported as cut-off value (10 mm) in a recent study from

our group that validated, against cardiac magnetic resonance, the echocardiographic assessment of EAT thickness at the level of the Rindfleisch fold (13).

Significantly higher levels of MCP-1, both in serum and in EAT secretomes, were found in patients who developed POAF. The expression of the gene coding for MCP-1 can be induced by a variety of mediators, including numerous interleukins, platelet derived growth factor, and vascular endothelial growth factor (25). MCP-1 is mainly produced by monocytes and macrophages and exerts potent chemotactic and activating effects on CCR2-positive leukocytes. Several studies have reported that serum MCP-1 levels are independently associated with atrial fibrillation (7, 25).

IL-6 levels were significantly higher in EAT secretomes of patients who developed POAF. Numerous evidence have demonstrated elevated serum levels of IL-6 in patients who develop POAF (25–27). IL-6 is a pleiotropic cytokine with a variety of biological activities. It is produced not only by immune cells and immune accessory cells including monocytes and macrophages, but also by endothelial cells, vascular smooth-muscle cells, adipocytes and ischemic cardiomyocytes. It stimulates the synthesis of several acute-phase reaction proteins (7). Of note, in our study, EAT production of this pro-inflammatory cytokine was higher in POAF patients and resulted significantly associated with atrial arrhythmia. Interestingly, Mazurek et al. have previously described the upregulation of MCP-1 and IL-6 in the EAT of CAD patients (17). These previous data reinforce our opinion that these two cytokines may contribute to the EAT pro-inflammatory phenotype. Although left atrial volume is known to be an important factor in conditioning AF occurrence, no differences in this parameter were found between POAF and SR patients. Furthermore, differences in EAT levels of MCP-1 and IL-6 between POAF and SR patients remained significant even after adjusting the analysis for age, statin use prior to surgery, left atrial volume and E/e'. We also excluded the other possible causes of POAF, such as electrolyte imbalance or acid-base disturbances.

Interestingly, statin intake was lower in patients who developed POAF compared with those who remained in SR with a higher use of atorvastatin in SR compared to POAF patients. We hypothesize that this result could be ascribed to the known anti-inflammatory and pleiotropic effect of statins. A randomized, controlled trial (ARMYDA-3) demonstrated that treatment with 40 mg of atorvastatin daily for 7 days significantly reduces the incidence of new-onset POAF and shortens the length of hospital stay in patients undergoing cardiac surgery with CPB (28). Moreover, a recent meta-analysis from Yuan et al., including 20 randomized controlled trials of patients who underwent cardiac surgery, concluded that preoperative statin therapy might be promising for the prevention of POAF, especially for patients undergoing isolated CABG surgery (29). Contrarily, a large randomized controlled trial by Zheng et al. (30) did not demonstrate an association between rosuvastatin assumption and reduction of POAF incidence, thus indicating conflicting evidence on this issue. In this regard, our group has previously demonstrated, both *in vivo* and *in vitro*, that statin administration reduces EAT secretion of IL-6 and IL-8 levels in patients with aortic stenosis (31).

CONCLUSIONS

The present study has evaluated the association of the pro-inflammatory secretory profile of EAT with the onset of POAF in patients undergoing cardiac surgery. It is plausible that the inflammatory substrate is mainly promoted by the EAT secretion of IL-6 and MCP-1. Further studies are needed to establish whether statin therapy could play a protective role, mediated by the reduction of EAT levels of IL-6, thus paving the way for a targeted use of these drugs in the peri-operative period. Further studies will be needed to confirm these findings and investigate the role of cardiac visceral fat in the pathogenesis of POAF.

DATA AVAILABILITY STATEMENT

The raw data supporting the conclusions of this article will be made available by the authors, without undue reservation.

ETHICS STATEMENT

The studies involving human participants were reviewed and approved by Ethical Committee of Federico II. The patients/participants provided their written informed consent to participate in this study.

AUTHOR CONTRIBUTIONS

LP has enrolled patients, has collected clinical/anamnestic data, has performed echocardiograms, and elaborated the manuscript. MC and PC have performed echocardiograms. GC and EP have performed epicardial adipose tissue biopsies during cardiac surgery. SC and PF have analyzed serum samples and epicardial fat biopsies for the concentration of proinflammatory interleukins. CR and IA have enrolled patients and have collected clinical/anamnestic data. DB has performed the statistical analysis. NF, DL, and VP have designed the project and have revised the manuscript. All authors read and approved the final manuscript.

REFERENCES

1. Bessissow A, Khan J, Devereaux PJ, Alvarez-Garcia J, Alonso-Coello P. Postoperative atrial fibrillation in non-cardiac and cardiac surgery: an overview. *J Thromb Haemost.* (2015) 13:S304–12. doi: 10.1111/jth.12974
2. Maisel WH, Rawn JD, Stevenson WG. Atrial fibrillation after cardiac surgery. *Ann Intern Med.* (2001) 135:1061–73. doi: 10.7326/0003-4819-135-12-200112180-00010
3. Zaman AG, Archbold RA, Helft G, Paul EA, Curzen NP, Mills PG. Atrial fibrillation after coronary artery bypass surgery: a model

for preoperative risk stratification. Circulation. (2000) 101:1403–8. doi: 10.1161/01.CIR.101.12.1403
4. Echahidi N, Pibarot P, O'Hara G, Mathieu P. Mechanisms, prevention, and treatment of atrial fibrillation after cardiac surgery. *J Am Coll Cardiol.* (2008) 51:793–801. doi: 10.1016/j.jacc.2007.10.043
5. Helgadottir S, Sigurdsson MI, Ingvarsdottir IL, Arnar DO, Gudbjartsson T. Atrial fibrillation following cardiac surgery: risk analysis and long-term survival. *J Cardiothorac Surg.* (2012) 7:87. doi: 10.1186/1749-8090-7-87
6. Lin MH, Kamel H, Singer DE, Wu YM, Lee M, Ovbiagele B. Perioperative/postoperative atrial fibrillation and risk of subsequent stroke and/or mortality. *Stroke.* (2019) 50:1364–71. doi: 10.1161/STROKEAHA.118.023921
7. Guo Y, Lip GY, Apostolakis S. Inflammation in atrial fibrillation. *J Am Coll Cardiol.* (2012) 60:2263–70. doi: 10.1016/j.jacc.2012.04.063
8. Barnes TC, Anderson ME, Moots RJ. The many faces of interleukin-6: the role of IL-6 in inflammation, vasculopathy, and fibrosis in systemic sclerosis. Int J Rheumatol. (2011) 721608. doi: 10.1155/2011/721608
9. Yuan SM. Interleukin-6 and cardiac operations. *Eur Cytokine Netw.* (2018) 29:1–15. doi: 10.1684/ecn.2018.0406
10. Hatem SN, Sanders P. Epicardial adipose tissue and atrial fibrillation. *Cardiovasc Res.* (2014) 102:205–13. doi: 10.1093/cvr/cvu045
11. Grieco FV, Petraglia L, Conte M, Russo C, Provenzano S, Ferrante L, et al. Cardiac visceral fat as anatomic substrate and functional trigger for the development of atrial fibrillation. *JGG.* (2019) 67:213–8.
12. Parisi V, Rengo G, Pagano G, D'Esposito V, Passaretti F, Caruso A, et al. Epicardial adipose tissue has an increased thickness and is a source of inflammatory mediators in patients with calcific aortic stenosis. *Int J Cardiol.* (2015) 186:167–9. doi: 10.1016/j.ijcard.2015.03.201
13. Parisi V, Petraglia L, Formisano R, Caruso A, Grimaldi MG, Bruzzese D, et al. Validation of the echocardiographic assessment of epicardial adipose tissue thickness at the Rindfleisch fold for the prediction of coronary artery disease. *Nutr Metab Cardiovasc Dis.* (2020) 30:99–105. doi: 10.1016/j.numecd.2019.08.007
14. Sousa-Uva M, Head SJ, Milojevic M, Collet JP, Landoni G, Castella M, et al. 2017 EACTS Guidelines on perioperative medication in adult cardiac surgery. *Eur J Cardiothorac Surg.* (2018) 53:5–33. doi: 10.1093/ejcts/ezx314
15. Ishii Y, Schuessler RB, Gaynor SL, Yamada K, Fu AS, Boineau JP, et al. Inflammation of atrium after cardiac surgery is associated with inhomogeneity of atrial conduction and atrial fibrillation. *Circulation.* (2005) 111:2881–8. doi: 10.1161/CIRCULATIONAHA.104.475194
16. Tselentakis EV, Woodford E, Chandy J, Gaudette GR, Saltman AE. Inflammation effects on the electrical properties of atrial tissue and inducibility of postoperative atrial fibrillation. *J Surg Res.* (2006) 135:68–75. doi: 10.1016/j.jss.2006.03.024
17. Mazurek T, Zhang LF, Zalewski A, Mannion JD, Diehl JT, Arafat H, et al. Human epicardial adipose tissue is a source of inflammatory mediators. *Circulation.* (2003) 108:2460–6. doi: 10.1161/01.CIR.0000099542.57313.C5
18. Viviano A, Yin X, Zampetaki A, Fava M, Gallagher M, Mayr M, et al. Proteomics of the epicardial fat secretome and its role in post-operative atrial fibrillation. *EP Europace.* (2017) 20:1201–8. doi: 10.1093/europace/eux113
19. Mathew JP, Parks R, Savino JS, Friedman AS, Koch C, Mangano DT, et al. Atrial fibrillation following coronary artery bypass graft surgery: predictors, outcomes, and resource utilization. MultiCenter Study of Perioperative Ischemia Research Group. *JAMA.* (1996) 276:300–6. doi: 10.1001/jama.1996.03540040044031
20. Allessie MA, Boyden PA, Camm AJ, Kléber AG, Lab MJ, Legato MJ, et al. Pathophysiology and prevention of atrial fibrillation. *Circulation.* (2001) 103:769–77. doi: 10.1161/01.CIR.103.5.769
21. Leitch JW, Thomson D, Baird DK, Harris PJ. The importance of age as a predictor of atrial fibrillation and flutter after coronary artery bypass grafting. *J Thorac Cardiovasc Surg.* (1990) 100:338–42. doi: 10.1016/S0022-5223(19)35525-4
22. Packer M. Epicardial adipose tissue may mediate deleterious effects of obesity and inflammation on the myocardium. *J Am Coll Cardiol.* (2018) 71:2360–72. doi: 10.1016/j.jacc.2018.03.509
23. Patel VB, Shah S, Verma S, Oudit GY. Epicardial adipose tissue as a metabolic transducer: role in heart failure and coronary artery disease. *Heart Fail Rev.* (2017) 22:889–902. doi: 10.1007/s10741-017-9644-1
24. Abdelhadi RH, Gurm HS, Van Wagoner DR, Chung MK. Relation of an exaggerated rise in white blood cells after coronary bypass or cardiac valve surgery to development of atrial fibrillation postoperatively. *Am J Cardiol.* (2004) 93:1176–8. doi: 10.1016/j.amjcard.2004.01.053
25. Li J, Solus J, Chen Q, Hee Rho Y, Milne G, Stein CM, et al. Role of inflammation and oxidative stress in atrial fibrillation. *Heart Rhythm.* (2010) 7:438–44. doi: 10.1016/j.hrthm.2009.12.009
26. Leftheriotis DI, Fountoulaki KT, Flevari PG, Parissis JT, Panou FK, Andreadou IT, et al. The predictive value of inflammatory and oxidative markers following the successful cardioversion of persistent lone atrial fibrillation. *Int J Cardiol.* (2009) 135:361–9. doi: 10.1016/j.ijcard.2008.04.012
27. Kaireviciute D, Blann AD, Balakrishnan B, Lane DA, Patel JV, Uzdavinys G, et al. Characterisation and validity of inflammatory biomarkers in the prediction of postoperative atrial fibrillation in coronary artery disease patients. *Thromb Haemost.* 104:122–7. (2010). doi: 10.1160/TH09-12-0837
28. Patti G, Chello M, Candura D, Pasceri V, D'Ambrosio A, Covino E, et al. Randomized trial of atorvastatin for reduction of postoperative atrial fibrillation in patients undergoing cardiac surgery: results of the ARMYDA-3 (Atorvastatin for Reduction of MYocardial Dysrhythmia After cardiac surgery) study. *Circulation.* (2006) 114:1455–61. doi: 10.1161/CIRCULATIONAHA.106.621763
29. Yuan X, Du J, Liu Q, Zhang L. Defining the role of perioperative statin treatment in patients after cardiac surgery: a meta-analysis and systematic review of 20 randomized controlled trials. *Int J Cardiol.* (2017) 228:958–66. doi: 10.1016/j.ijcard.2016.11.116
30. Zheng Z, Jayaram R, Jiang L, Emberson J, Zhao Y, Li Q, et al. Perioperative rosuvastatin in cardiac surgery. *N Engl J Med.* (2016) 374:1744–53. doi: 10.1056/NEJMoa1507750
31. Parisi V, Petraglia L, D'Esposito V, Cabaro S, Rengo G, Caruso A, et al. Statin therapy modulates thickness and inflammatory profile of human epicardial adipose tissue. *Int J Cardiol.* (2019) 274:326–30. doi: 10.1016/j.ijcard.2018.06.106

Conflict of Interest: The authors declare that the research was conducted in the absence of any commercial or financial relationships that could be construed as a potential conflict of interest.

The reviewer PC declared a shared affiliation, with several of the authors to the handling editor at the time of the review.

Publisher's Note: All claims expressed in this article are solely those of the authors and do not necessarily represent those of their affiliated organizations, or those of the publisher, the editors and the reviewers. Any product that may be evaluated in this article, or claim that may be made by its manufacturer, is not guaranteed or endorsed by the publisher.

frontiers in Cardiovascular Medicine

ORIGINAL RESEARCH
published: 04 February 2022
doi: 10.3389/fcvm.2021.777463

Dopamine D1/D5 Receptor Signaling Is Involved in Arrhythmogenesis in the Setting of Takotsubo Cardiomyopathy

Mengying Huang[1], Zhen Yang[1], Yingrui Li[1], Huan Lan[2], Lukas Cyganek[3,4], Goekhan Yuecel[1,5,6], Siegfried Lang[1,5,6], Karen Bieback[7], Ibrahim El-Battrawy[1,5,6], Xiaobo Zhou[1,2,5,6], Martin Borggrefe[1,5,6†] and Ibrahim Akin[1,5,6†]*

[1] First Department of Medicine, Medical Faculty Mannheim, University Medical Centre Mannheim (UMM), University of Heidelberg, Mannheim, Germany, [2] Key Laboratory of Medical Electrophysiology of Ministry of Education and Medical Electrophysiological Key Laboratory of Sichuan Province, Institute of Cardiovascular Research, Southwest Medical University, Luzhou, China, [3] DZHK (German Center for Cardiovascular Research), Partner Site, Göttingen, Germany, [4] Stem Cell Unit, Clinic for Cardiology and Pneumology, University Medical Center Göttingen, Göttingen, Germany, [5] DZHK (German Center for Cardiovascular Research), Partner Site, Heidelberg, Germany, [6] DZHK (German Center for Cardiovascular Research), Partner Site, Mannheim, Germany, [7] Institute of Transfusion Medicine and Immunology, University Medical Centre Mannheim (UMM), University of Heidelberg, Mannheim, Germany

OPEN ACCESS

Edited by:
Antonio Zaza,
University of Milano-Bicocca, Italy

Reviewed by:
Markéta Bébarová,
Masaryk University, Czechia
Tomoe Y. Nakamura,
Wakayama Medical University, Japan

***Correspondence:**
Xiaobo Zhou
xiaobo.zhou@medma.uni-heidelberg.de

† These authors share senior authorship

Specialty section:
This article was submitted to Cardiac Rhythmology, a section of the journal Frontiers in Cardiovascular Medicine

Received: *15 September 2021*
Accepted: *29 December 2021*
Published: *04 February 2022*

Citation:
Huang M, Yang Z, Li Y, Lan H, Cyganek L, Yuecel G, Lang S, Bieback K, El-Battrawy I, Zhou X, Borggrefe M and Akin I (2022) Dopamine D1/D5 Receptor Signaling Is Involved in Arrhythmogenesis in the Setting of Takotsubo Cardiomyopathy. Front. Cardiovasc. Med. 8:777463. doi: 10.3389/fcvm.2021.777463

Background: Previous studies suggested involvement of non-ß-adrenoceptors in the pathogenesis of Takotsubo cardiomyopathy (TTC). This study was designed to explore possible roles and underlying mechanisms of dopamine D1/D5 receptor coupled signaling in arrhythmogenesis of TTC.

Methods: Human-induced pluripotent stem cell-derived cardiomyocytes (hiPSC-CMs) were challenged by toxic concentration of epinephrine (Epi, 0.5 mM for 1 h) for mimicking the catecholamine excess in setting of TTC. Specific receptor blockers and activators were used to unveil roles of D1/D5 receptors. Patch clamp, qPCR, and FACS analyses were performed in the study.

Results: High concentration Epi and two dopamine D1/D5 receptor agonists [(±)-SKF 38393 and fenoldopam] reduced the depolarization velocity and prolonged the duration of action potentials (APs) and caused arrhythmic events in iPSC-CMs, suggesting involvement of dopamine D1/D5 receptor signaling in arrhythmogenesis associated with QT interval prolongation in the setting of TTC. (±)-SKF 38393 and fenoldopam enhanced the reactive oxygen species (ROS)-production. H_2O_2 (100 μM) recapitulated the effects of (±)-SKF 38393 and fenoldopam on APs and a ROS-blocker *N*-acetylcysteine (NAC, 1 mM) abolished the effects, suggesting that the ROS-signaling is involved in the dopamine D1/D5 receptor actions. A NADPH oxidases blocker and a PKA- or PKC-blocker suppressed the effects of the dopamine receptor agonist, implying that PKA, NADPH oxidases and PKC participated in dopamine D1/D5 receptor signaling. The abnormal APs resulted from dopamine D1/D5 receptor activation-induced dysfunctions of ion channels including the Na^+ and L-type Ca^{2+} and I_{Kr} channels.

Conclusions: Dopamine D1/D5 receptor signaling plays important roles for arrhythmogenesis of TTC. Dopamine D1/D5 receptor signaling in cardiomyocytes might be a potential target for treating arrhythmias in patients with TTC.

Keywords: Takotsubo cardiomyopathy, arrhythmia, catecholamine excess, D1/D5 dopamine receptor, human-induced pluripotent stem cell-derived cardiomyocytes

INTRODUCTION

Takotsubo cardiomyopathy (TTC) was initially described ∼25 years ago (1). The main feature of the disease is temporary and reversible systolic abnormalities in the apex of the left ventricle and/or involvement of right ventricle with clinical manifestations similar to myocardial infarction (2, 3). The most common symptoms of patients with TTC are chest pain and dyspnea. In severe cases, patients suffer from cardiac arrest, cardiogenic shock and ventricular arrhythmia (4). About 90% of patients with TTC are postmenopausal women who experience multiple stresses before the onset (3, 5). Although several possible causes have been proposed, such as catecholamine cardiotoxicity, metabolic disorders, coronary microvascular injury, multivessel epicardial coronary artery spasm and thyroidal dysfunction, the pathophysiology of TTC has not been fully established (6). A commonly accepted hypothesis is the surge of catecholamines caused by intense psychological or physical stress (4, 7).

So far, the TTC model has been successfully simulated on animal and human induced pluripotent stem cell-derived cardiomyocytes (hiPSC-CMs) by using high concentrations of catecholamines and demonstrated that both beta and alpha adrenoceptors related signaling are important for the pathogenesis of TTC (8–11). However, some clinical reports indicate that the plasma dopamine level in patients with stress cardiomyopathy is significantly increased (12–14). Moreover, high concentration of dopamine successfully induced TTC-like cardiac dysfunction in animal model (15). More importantly, studies showed that some TTC-patients did not profit from use of ß-blocker (16–18). All of these evidences suggest that dopamine-receptor activation may contribute to the pathogenesis of TTC.

Dopamine receptors are a subclass of the super family of G protein-coupled receptors and consisting of two families (19). The D1 family include of D1- and D5-receptor subtypes and the D2 family include of D2-, D3-, and D4-receptor subtypes, which have been identified in a number of organs and tissues in human (20). Among them, D1, D2, D4, and D5 are found in the native human heart (21), but only D1-like receptors (D1 and D5) exist in endocardium that are linked to adenylyl-cyclase stimulation, which can mediate the functional activity of Ca^{2+}, K^+, Na^+ channels by regulating G protein coupling (19, 21–23). However, in human cardiomyocytes, studies on the potential mechanism of ion channel dysfunction and arrhythmias caused by dopamine receptor activation in TTC have not been conducted. Therefore, we designed the current study to assess the importance of dopamine D1/D5 receptor related signaling for the pathogenesis of TTC, focusing on the mechanisms of arrhythmias.

Abbreviations: TTC, Takotsubo cardiomyopathy; hiPSC-CMs, Human-induced pluripotent stem cell-derived cardiomyocytes; Epi, Epinephrine; DCFH-DA, 2′,7′-Dichlorofluorescin diacetate; Chele, chelerythrine; I_{Ca-L}, L-type (I_{Ca-L}) calcium channel current; I_{Kr}, rapidly activating delayed rectifier; EAD, early afterdepolarization; DAD, delayed afterdepolarization; APs, action potentials; APD10, action potential duration at 10% repolarization; APD50, action potential duration at 50% repolarization; APD90, action potential duration at 90% repolarization; Vmax, maximal depolarization velocity; RP, resting potential; APA, amplitude of action potential; ROS, reactive oxygen species; PKA, protein kinase A; PKC, protein kinase C; cAMP, cyclic adenosine monophosphate.

MATERIALS AND METHODS

Generation of Human iPS Cells

The human-induced pluripotent stem cells (hiPSCs) from three male healthy donors were created by integration-free methods under feeder-free culture conditions, as descripted previously (24). In brief, the hiPSC line UMGi014-B clone 1 (ipWT1.1) was generated from dermal fibroblasts by using non-integrated episomal 4-in-1 CoMiP reprogramming plasmids (Addgene, #63726), hiPSC line UMGi124-A clone 11 (isVHFx-R1) was generated from dermal fibroblasts by integration-free Sendai virus, and hiPSC line UMGi130-A clone 5 (isWT11.5) was generated from peripheral mononuclear blood cells by integration-free Sendai virus.

Generation of hiPSC Derived Cardiomyocytes (hiPSC-CMs)

In our previous studies, the generation of hiPSC-CMs has been described (25). Briefly, culture dishes and wells coated with matrigel (Corning, Kaiserslautern, Germany) as well as the culture medium TeSR-E8 (Stemcell Technologies, Köln, Germany) were used for culturing hiPSCs. For culturing hiPSC-CMs, the medium RPMI 1640 Glutamax (Life Technologies, Darmstadt, Germany) containing sodium pyruvate, penicillin/streptomycin, B27 (Life Technologies) and ascorbic acid (Sigma Aldrich, Taufkirchen, Germany) was used. In the first 2 weeks, CHIR99021 (MiltenyiBiotec, Bergisch Gladbach, Germany), BMP-4 (R&D Systems, Wiesbaden, Germany), Activin A (R&D Systems), FGF-2 (MiltenyiBiotec), and IWP-4 (MiltenyiBiotec) were used at several times for inducing the cells to be differentiated into hiPSC-CMs. In the 3rd week, a cardiomyocyte-selection medium containing sodium lactate (Sigma Aldrich) and RPMI-medium without glucose and glutamine (Biological Industries, Cromwell, USA) was used for 4–7 days (usually 5 days) for selecting cardiomyocytes. Then, the survived cardiomyocytes were cultured in cardiac medium. At 40–60 days of differentiation, hiPSC-CMs were used for different experiments. To confirm the successful differentiation of hiPSC-CMs, the expression of different cardiac markers was examined

as shown in our recent study (26). The differentiation was performed every 3–4 weeks, cells from different differentiations were measured and data were combined.

Quantitative Polymerase-Chain-Reaction Assays

RNA was reverse transcribed and converted to cDNA with oligo $(dT)_{15}$ primers with AMV reverse transcriptase following the protocol. Relative mRNA level was calculated as: the mRNA level of the gene of interest relative to that of the housekeeping gene GAPDH in samples from treated or untreated (Control) cells was obtained from the $\Delta\Delta$CT method, based on the threshold cycle (CT), as fold change $= 2^{-\Delta(\Delta CT)}$, where $\Delta CT = CT_{geneofinterest} - CT_{GAPDH}$ and $\Delta(\Delta CT) = \Delta CT_{treated} - \Delta CT_{Control}$ (27). For each experimental group, the cDNA amount of three or more cell culture wells were examined as biological replicates. The sample of each cell culture well was measured two times as technical replicates. The information of used primers is provided in **Supplementary Table 1**.

Fluorescence-Activated Cell Sorting (FACS)

The ROS generation of hiPSC-CM was assessed with 2′,7′-Dichlorofluorescin diacetate (DCFH-DA, sigma) technique following the ROS assay kit instructions. DCFH-DA is a non-polar fluorescence probe that can enter a cell, and in the cell, it is changed into DCFH and can be detected by flow cytometry. The hiPSC-CMs were detached by 0.05% Trypsin-EDTA (Life Technologies) for 2–4 min at 37°C. Thereafter, RPMI medium containing 10% FBS was added. Then, a centrifugation of 250 × *g* was performed for 4 min at room temperature. Next, the supernatant was taken away and the hiPSC-CMs were resuspended in basic culture medium. The hiPSC-CMs were transferred into the 15 ml tubes with 1×10^6 cells/tube and incubated with 10 μM DCFH-DA at 37°C for 30 min in the dark. The hiPSC-CMs were then washed thrice by PBS and measured by BD FACSCanto™ II (Becton Dickinson, Heidelberg, Germany). Analyses were conducted with a quantitative method *via* BD FACS Diva software (Version 8.0.1). More than 25,000 events were sampled and analyzed per experimental condition.

Immunofluorescence (IF) Staining

The hiPSC-CMs were detached by 0.05% Trypsin-EDTA (Life Technologies) for 2–4 min at 37°C. The RPMI medium containing 10% FBS was added. The hiPSC-CMs were then centrifuged at 250 × *g* for 4 min at room temperature. Thereafter, the supernatant was taken away and the hiPSC-CMs were resuspended in basic culture medium and pipetted onto culture slides (FALCON 354114). The slides stayed at room temperature for overnight. On next day, hiPSC-CMs were washed by PBS thrice, and then fixed by 4% Paraformaldehyde (Sigma) at room temperature for 20 min. Then, cells were washed thrice by PBS and were permeabilized by 0.1% Triton-X100 (Carl Roth) for 10 min. Next, hiPSC-CMs were washed trice by PBS and blocked by 5% bovine serum albumin (BSA; Sigma-Aldrich) in PBS at 4°C for 1 h. Primary antibodies were incubated at 4°C in 5% BSA overnight. Then, hiPSC-CMs were washed twice by PBS and incubated with secondary antibodies conjugated to Alexa Fluor 488 or 642 (1:200) at room temperature for 1 h. Finally, hiPSC-CMs were washed twice by PBS and incubated with DAPI (Biozol) at room temperature for 10 min in the dark. Images were analyzed by the Confocal Microscope TCS SP-8 upright (Leica, Germany) with Plan-Apochromat 40×/0.6 objective.

The information of antibodies used in the study is provided in **Supplementary Table 2**.

Patch-Clamp

For patch-clamp measurements, cardiomyocytes at 40–60 days of differentiation were dissociated from 6 well plates by collagenase type I and plated on matrigel-coated 3.5 cm petri dishes as single cells. The patch-clamp whole-cell recording technique was employed to measure the action potential (AP) and channel currents at RT (22–24°C). Pipette resistance ranged from 1 to 2 MΩ and 4 to 5 MΩ for current and AP measurements, respectively. The electrode offset potential was zero-adjusted before a Giga-seal was formed. When a Giga-seal was formed, the fast capacitance was first compensated and then the membrane under the pipette tip was broken by negative pressure to obtain the whole-cell configuration. The signal was sampled at 10 kHz and filtered at 2 kHz using the EPC10 Patch-master digitizer hardware (HEKA Germany) and Fit-master software (HEKA Germany). The action potential was measured by current clamp mode. The spontaneous AP was measured in CC-mode in spontaneously beating hiPSC-CMs. For measuring the APs at a fixed frequency, brief current pulses (2 ms, 1 nA) of 1 Hz were employed for evoking APs. The junction potential (4–6 mV) in AP recordings was not corrected. Recordings of currents and paced APs were started when currents and APs became stable. The spontaneous AP was recorded within the first 100 s after a whole-cell configuration was obtained since after 100 s the spontaneous APs may terminate. To analyze the arrhythmic events, all the events including normal APs, early afterdepolarization (EAD)-like events, which were defined as depolarizations in repolarization phase (phase 3) of AP, delayed afterdepolarization (DAD)-like events, which were defined as under-threshold depolarizations in phase 4 of APs, and triggered activity, which was defined as APs triggered by abnormal over-threshold triggers/stimulations, were counted in control and drug-treated hiPSC-CMs. The number of every type of events in each group was divided by the number of all events (normal and arrhythmic events) to obtain the percentage of arrhythmic events. The number of cells showing arrhythmic evens either EAD-like or DAD-like or triggered activity was divided by the total number of counted cells in a group to obtain the ratio of cells showing arrhythmic events (**Table 1**).

The bath solution (PSS) for AP measurements consists of (mmol/l): 130 NaCl, 5.9 KCl, 2.4 $CaCl_2$, 1.2 $MgCl_2$, 11 glucose, 10 HEPES, pH 7.4 (NaOH). The pipette solution contains (mmol/l): 10 HEPES, 126 KCl, 6 NaCl, 1.2 $MgCl_2$, 5 EGTA, 11 glucose, and 1 MgATP, pH 7.2 (KOH).

The bath solution for peak sodium current recording consists of 20 mmol/L NaCl, 130 mmol/L CsCl, 1.8 mmol/L $CaCl_2$, 1

TABLE 1 | Analysis of arrhythmic events relating to dopamine receptors.

Group	Control	Epi	Epi+SCH23390	SKF 38393	Fenoldopam
Cell number	12	12	12	12	12
Number of cells showing arrhythmia	6	12	9	12	12
Beating rate (bpm)	26.1 ± 3.7	20.5 ± 1.7	23.9 ± 1.8	35.1 ± 2.2	46.8 ± 5.8**
Arrhythmic events (%)	8.1% ± 3.1%	26.5 ± 2.1**	9.3 ± 2.5	26.3% ± 4%**	29.7% ± 4.4%**
Arrhythmia counts	20	65	27	102	144
Number of DAD-like events	16	35	14	65	88
Number of EAD-like events	2	20	9	15	23
Number of triggered activities	2	10	4	22	33
Normal rhythm counts	258	181	254	248	417

*** p < 0.01. The p-values vs. control were determined by one-way ANOVA with Holm-Sidak post-test.*

mmol/L $MgCl_2$, 10 mmol/L HEPES, 10 mmol/L glucose, and 0.001 mmol/L nifedipine. The pH value was adjusted to 7.4 with CsOH. The pipette solution for peak sodium current consists of 10 mmol/L NaCl, 135 mmol/L CsCl, 2 mmol/L $CaCl_2$, 3 mmol/L Mg-ATP, 5 mmol/L EGTA, 10 mmol/L HEPES, and pH 7.2 (CsOH).

The extracellular solution for measuring L-type (I_{Ca-L}) calcium channel current consists of (mmol/l): 140 TEA-Cl, 5 $CaCl_2$, 1 $MgCl_2$, 0.001 E-4031, 10 HEPES, 0.02 TTX, 3 4-AP, pH 7.4 (CsOH). The intracellular solution consists of (mmol/l): 6 NaCl, 135 CsCl, 2 $CaCl_2$, 3 Mg ATP, 2 TEA-Cl, 5 EGTA, 10 HEPES, and pH7.2 (CsOH).

To isolate I_{Kr} from other K^+ channel currents, the Cs^+ currents conducted by I_{Kr} channels were measured. The extracellular and intracellular solution for the Cs^+ current measurement consists of (mmol/L): 140 CsCl, 2 $MgCl_2$, 10 HEPES, 10 Glucose, and pH = 7.4 (CsOH).

The information of drugs and reagents is provided in the **Supplementary Table 3**.

Statistics

Data are shown as means ± SEM and were analyzed using InStat© (GraphPad, San Diego, CA, USA) and SigmaPlot 11.0 (Systat GmbH, Erkrath Germany). To decide whether parametric or non-parametric tests were to be used for analysis, the Kolmogorov Smirnov test was first performed. Outliers in data were excluded in analyses. To determine outliers, the first quantile (Q1), the third quantile (Q3) and the interquartile range (IQR) were calculated by Software Excel. The lower limit and upper limit were defined as Q1-(1.5*IQR) and Q3+(1.5*IQR), respectively. All the data below the lower limit or over the upper limit were defined as outliers. Student's *t*-test was used to compare continuous variables with normal distributions, while the Mann–Whitney *U*-test was used to compare continuous variables with non-normal distributions. For comparing categorical variables, the Fisher-test was used. For comparing parametric data of more than two groups, one-way ANOVA with a Holm-Sidak post-test for multiple comparisons was carried out. An unpaired Student's *t*-test was performed for comparing two independent groups with normal distributions. $p < 0.05$ (two-tailed) was considered significant.

RESULTS

The Dopamine D1/D5 Receptor Activation Contributes to Occurrence of Arrhythmic Events Induced by High-Concentration of Epinephrine

The study used hiPSC-CMs from three healthy donors. Our recent publications confirmed the successful differentiation of hiPSCs into hiPSC-CMs by using qPCR, immunofluorescence and FACS analysis regarding the expression of cardiac markers (26). In this study, the cardiac marker cTnT (TNNT2) was also shown by immunofluorescence (**Supplementary Figure 1B**) and FACS (**Figures 5A,B**) analyses. It has been shown that dopamine receptors exist in cardiomyocytes (21). We next examined the mRNA expression levels of dopamine receptors in our hiPSC-CMs by qPCR (**Supplementary Figure 1A**). We observed that DRD1 and DRD5 are highly expressed in hiPSC-CMs. Furthermore, the immunostaining analysis confirmed the expression of D1 dopamine receptor in hiPSC-CMs (**Supplementary Figure 1B**). It has been proven that high concentrations of epinephrine can cause arrhythmia (11). In order to verify whether dopamine receptor activation could also be involved in the occurrence of arrhythmia, we first treated the spontaneously beating cells with Epi (500 μM) in the presence or absence of 10 μM SCH 23390 (a dopamine D1/D5 receptor blocker). The result showed that SCH 23390 prevented the Epi-induced arrhythmia events (**Figures 1A–C**). Therefore, two kinds of dopamine D1/D5 receptor-specific agonists (±)-SKF 38393 (50 μM) and fenoldopam (5 μM) were used to spontaneously beating cells and arrhythmic events including EAD- (early afterdepolarization) like, DAD- (delayed afterdepolarization) like events, failed APs and triggered activity were analyzed. The results showed that (±)-SKF 38393 and fenoldopam significantly increased the occurrence of arrhythmic events (**Figures 1A,D,E**; **Table 1**). In addition, both (±)-SKF 38393 and fenoldopam increased the cell beating, especially fenoldopam showed a significant effect (**Table 1**). In the

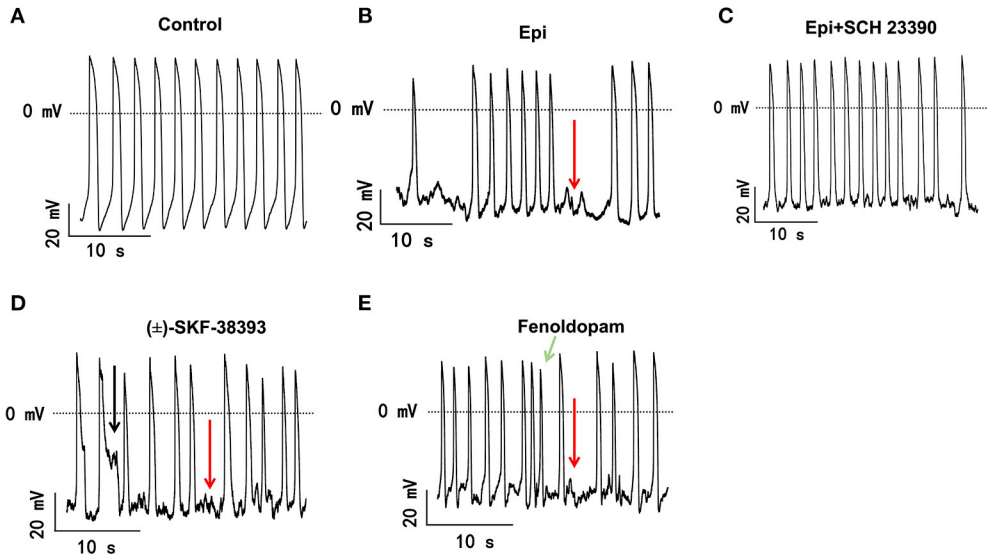

FIGURE 1 | The dopamine D1/D5 receptor activation contributes to occurrence of arrhythmic events. hiPSC-CMs were treated by vehicle (Control) or 500 μM Epi or Epi plus 10 μM SCH 23390 or 50 μM (±)-SKF 38393 or 5 μM fenoldopam for 1 h. Spontaneous APs of spontaneously beating hiPSC-CMs were measured in the first 100 s after the whole cell configuration was obtained. The arrhythmic events including EAD-like (black arrows) or DAD-like and failed AP (red arrows) events or triggered activity (green arrows) in each cell were counted and divided by total events to obtain the percentage of arrhythmic events. Data were summarized in **Table 1**. **(A)** Representative traces of spontaneous APs recorded in a cell of control group. **(B)** Representative AP traces in a cell of Epi-group. **(C)** Representative AP traces in a cell of Epi+SCH 23390 group. **(D)** Representative AP traces in a cell of (±)-SKF 38393 group. **(E)** Representative AP traces in a cell of fenoldopam group.

presence of (±)-SKF 38393 and fenoldopam, more cells showed arrhythmic events (**Table 1**).

The Dopamine D1/D5 Receptor Activation Is Involved in Toxic Effects of Epinephrine on Action Potentials

Arrhythmias are usually related to changes of action potentials (APs). So, APs were measured in hiPSC-CMs challenged by a toxic concentration of epinephrine (Epi, 500 μM) for 1 h in the absence or presence of a dopamine D1/D5 receptor blocker (SCH 23390, 10 μM). The results showed that Epi prolonged the duration of action potential at 10% repolarization (APD10) from 12.9 ± 0.40 to 14.55 ± 0.60 ms, the duration of action potential at 50% repolarization (APD50) from 210.86 ± 27.40 to 461.22 ± 68.22 ms and the duration of action potential duration at 90% repolarization (APD90) from 369.15 ± 36.58 to 667.98 ± 80.18 ms, respectively (**Figures 2A–D**). Interestingly, the dopamine D1/D5 receptors blocker prevented the Epi-effect on action potentials (**Figures 2A–D**). The dopamine D1/D5 receptor blocker alone showed no effect on APDs (**Figures 2A–D**). The maximal depolarization velocity (Vmax) of APs was attenuated by Epi and the Epi-effect was reversed by SCH 23390 (**Figure 2E**). Epi or the dopamine D1/D5 receptor blocker alone showed no effect on the resting potential (RP) and the AP amplitude (APA) (**Figures 2F,G**). These data indicate that dopamine D1/D5 receptor activation plays a key role in Epi-induced effects on APs.

To further confirm the role of dopamine D1/D5 receptor for AP-changes, (±)-SKF 38393 (50 μM) and fenoldopam (5 μM), the dopamine D1/D5 receptor specific agonists, were applied to hiPSC-CMs. Indeed, they mimicked Epi-effects (APD-prolongation and Vmax-suppression) (**Figure 3**). Taking all the data together, dopamine D1/D5 receptor signaling contributed to the Epi-effects on APs.

ROS Mediated the Effects of the Dopamine D1/D5 Receptor Activation

Our previous study detected that the activation of both α and β-adrenoceptors contributed to the ROS (reactive oxygen species) generation induced by the high concentration of isoprenaline and epinephrine, which led us to examine whether ROS also participates in the effects of dopamine D1/D5 receptor activation in catecholamine surge. First, we examined the effects of a ROS blocker *N*-acetylcysteine (NAC) on APs in presence of (±)-SKF 38393 or fenoldopam. Actually, NAC reduced and H_2O_2 (the main form of endogenous ROS) recapitulated the (±)-SKF 38393 and fenoldopam effects on APDs (**Figure 4**; **Table 2**), which are indicative of an involvement of ROS in effects of dopamine D1/D5 receptor activation. NAC alone displayed no effect on APs.

Next, the ROS level was measured by FACS in hiPSC-CMs in presence of (±)-SKF 38393 or fenoldopam. The ROS-level was increased in (±)-SKF 38393- or fenoldopam-treated cells (**Figures 5C–E,H**), suggesting that (±)-SKF 38393 or fenoldopam may affect APs through ROS. As expected, the dopamine D1/D5 receptor blocker reduced the (±)-SKF 38393 or fenoldopam-induced ROS generation in hiPSC-CMs

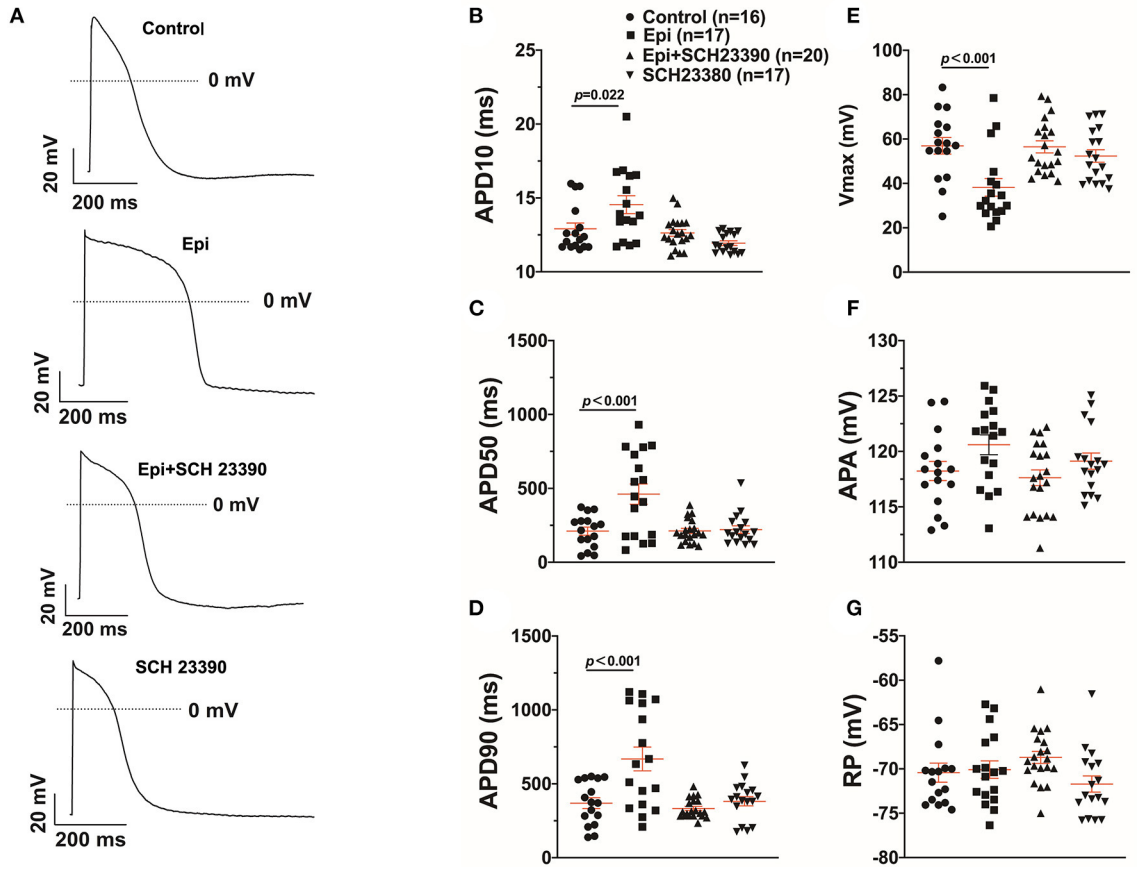

FIGURE 2 | Dopamine D1/D5 receptor signaling contributed to effect of epinephrine on action potential. hiPSC-CMs were challenged by either vehicle (Control) or 500 μM epinephrine (Epi) or epinephrine plus 10 μM SCH 23390 or SCH 23390 alone for 1 h. Action potentials (APs) were recorded at 1 Hz. **(A)** Examples of APs in a cell of each group. **(B)** Mean values of APD10 in each group cells. **(C)** Mean values of APD50 in each group cells. **(D)** Mean values of APD90 in each group cells. **(E)** Mean values of Vmax of APs in each group cells. **(F)** Mean values of AP amplitude (APA) in each group cells. **(G)** Mean values of resting potential (RP) in each group cells. "*n*" numbers in **(B)** are for **(B–G)**. The *p*-values vs. Control were decided by the analysis of one-way ANOVA with Holm-Sidak post-test.

(**Figures 5F–H**), which suggests that that ROS signaling may contribute to effects of dopamine D1/D5 receptor activation.

NADPH Oxidases Were Involved in Effects of Dopamine D1/D5 Receptor Activation

Considering that ROS generation is linked to numerus intracellular signaling, we intended to explore a signaling factor that may be responsible for the elevated ROS generation caused by activation of dopamine D1/D5 receptor. We found that diphenyleneiodonium (DPI), an inhibitor of NADPH oxidase, abolished the effects of (±)-SKF 38393 or fenoldopam on APs, suggesting that NADPH oxidases were involved in effects of dopamine D1/D5 receptor activation (**Figures 6A–C,J,K**; **Table 3**).

Protein Kinase A (PKA) and C (PKC) Were Involved in the Effects of Dopamine D1/D5 Receptor Activation

It has already been demonstrated that stimulation of the D1-like receptors can activate the cyclic adenosine monophosphate (cAMP) and protein kinase A (PKA) signaling pathway (28, 29). But some studies also found that dopamine D1/D5 receptor can be coupled to Gq-PLC signaling and protein kinase C (PKC) is an important downstream signaling protein (30–32). We examined the possible roles of PKC and PKA for AP-changes. We found that a PKC-inhibitor (chelerythrine, 10μM) reduced the effect of dopamine D1/D5 receptor agonists on APs**,** similar to H89 (1 μM), a PKA-inhibitor (**Figures 6A–C,G,H,L**, **Table 3**). Using chelerythrine alone showed no effect on APs (**Figure 6F**). In addition, a PKC stimulator (PMA, 10 μM) displayed effects on APs similar to that of (±)-SKF 38393 (50 μM) or fenoldopam (5 μM) (**Figures 6A–C,E**; **Table 3**), implying that both PKA and PKC are required for the effect of dopamine D1/D5 receptor activation.

Given that ROS is a well-known downstream factor of PKA (33), we tried to clarify relationship between PKC and ROS in dopamine D1/D5 receptor activation. The hiPSC-CMs were treated with H_2O_2 with and without the PKC-inhibitor. Indeed, the PKC-inhibitor suppressed the effects of H_2O_2 (**Figures 6D,I**;

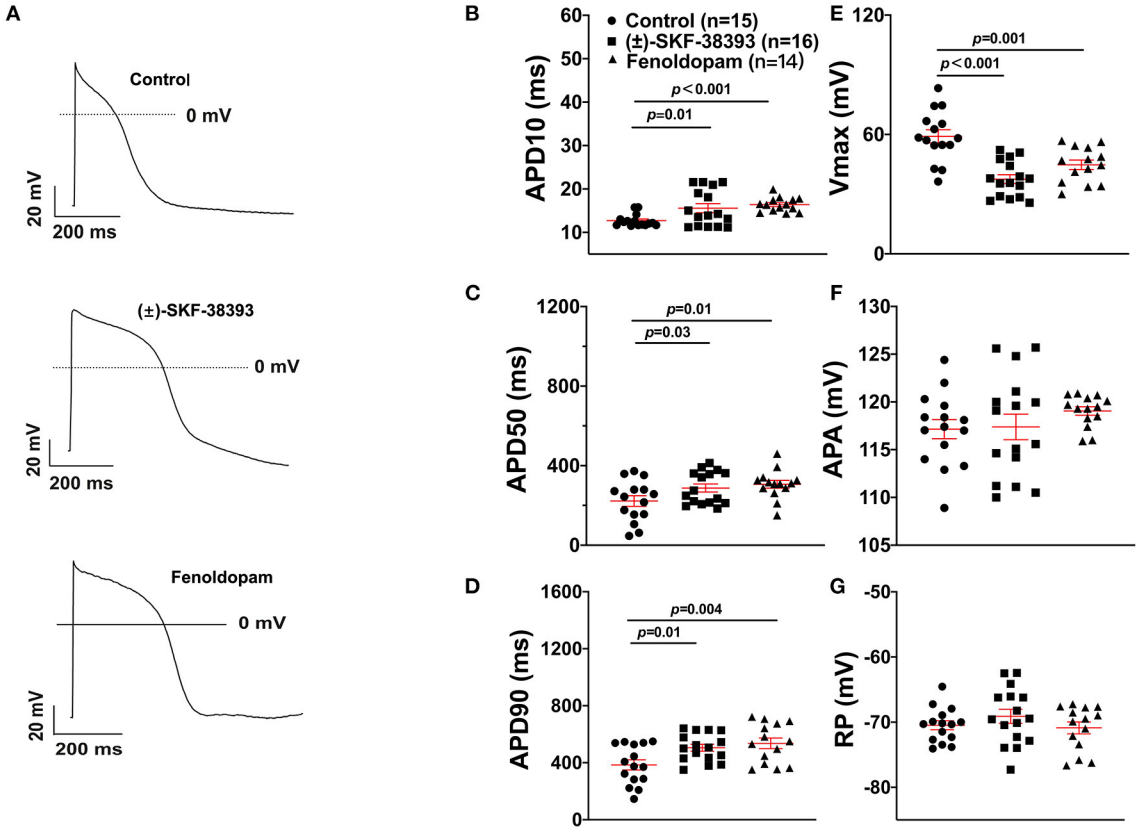

FIGURE 3 | Dopamine D1/D5 receptor agonists mimicked epinephrine effects on the action potential (AP). hiPSC-CMs were challenged by either vehicle (Control) or 50 μM (±)-SKF 38393 or 5 μM fenoldopam for 1 h and action potentials (APs) were recorded. **(A)** Examples of AP traces in each group cells. **(B)** Mean values of APD10 in each group cells. **(C)** Mean values of APD50 in each group cells. **(D)** Mean values of APD90 in each group cells. **(E)** Mean values of AP Vmax in each group cells. **(F)** Mean values of AP amplitude (APA) in each group cells. **(G)** Mean values of resting potential (RP) in each group cells. "*n*" numbers in **(B)** are for **(B–G)**. The *p*-values vs. Control were determined by the analysis of one-way ANOVA with Holm-Sidak post-test.

Table 3), suggesting that PKC was a downstream signaling factor of ROS in the signal pathway.

The Ionic Mechanisms of AP-Changes Caused by Dopamine D1/D5 Receptor Activation

To examine which ion channel dysfunctions may contribute to arrhythmogenesis mediated by dopamine receptors in the setting of TTC, we first assessed the ion channel expression profile in hiPSC-CMs challenged by high concentration (500 μM) epinephrine (Epi) plus dopamine D1/D5 receptor blocker SCH 23390 (**Supplementary Figure 2**). The expression level of CACNA1C (coding L-type calcium channel) genes was increased by Epi (**Supplementary Figure 2A**), but the expression level of SCN5A (coding Nav1.5 sodium channel) and KCNH2 (coding I_{Kr} channel) gene was reduced by Epi (**Supplementary Figures 2B,C**). The dopamine D1/D5 receptor blocker SCH 23390 (10 μM) attenuated the Epi-effect on gene expression level (**Supplementary Figure 2**), suggesting that the dopamine D1/D5 signaling may contribute to ion channel dysfunctions *via* changing ion channel expression levels in the setting of TTC.

Furthermore, we evaluated the effects of (±)-SKF 38393 on ion channel currents. First, the effects of (±)-SKF 38393 on inward currents including I_{Na}, I_{CaL} were examined in vehicle-(control) or (±)-SKF 38393-treated cells. (±)-SKF 38393 reduced the peak I_{Na} (**Figures 7A–D**) without influencing the voltage-dependent inactivation and activation and recovery of channels (**Supplementary Figure 3**).

(±)-SKF 38393 significantly increased the L-type calcium channel current (I_{Ca-L}) (**Figures 7E–H**) without influencing the channel activation and inactivation of I_{Ca-L} (**Supplementary Figures 4A–D**). However, (±)-SKF 38393 strongly accelerated the time course of recovery of I_{Ca-L} (**Supplementary Figures 4E,F**).

Next, we observed that (±)-SKF 38393 decreased I_{Kr} (the rapidly activating delayed rectifier) and inhibited the channel activation by shifting the activation curve to a more positive potential (**Supplementary Figures 5A–E**).

In order to examine possible variations of experimental results among different cell lines, we repeated some pivotal experiments in hiPSC-CMs from other two healthy donors (H2 and H3).

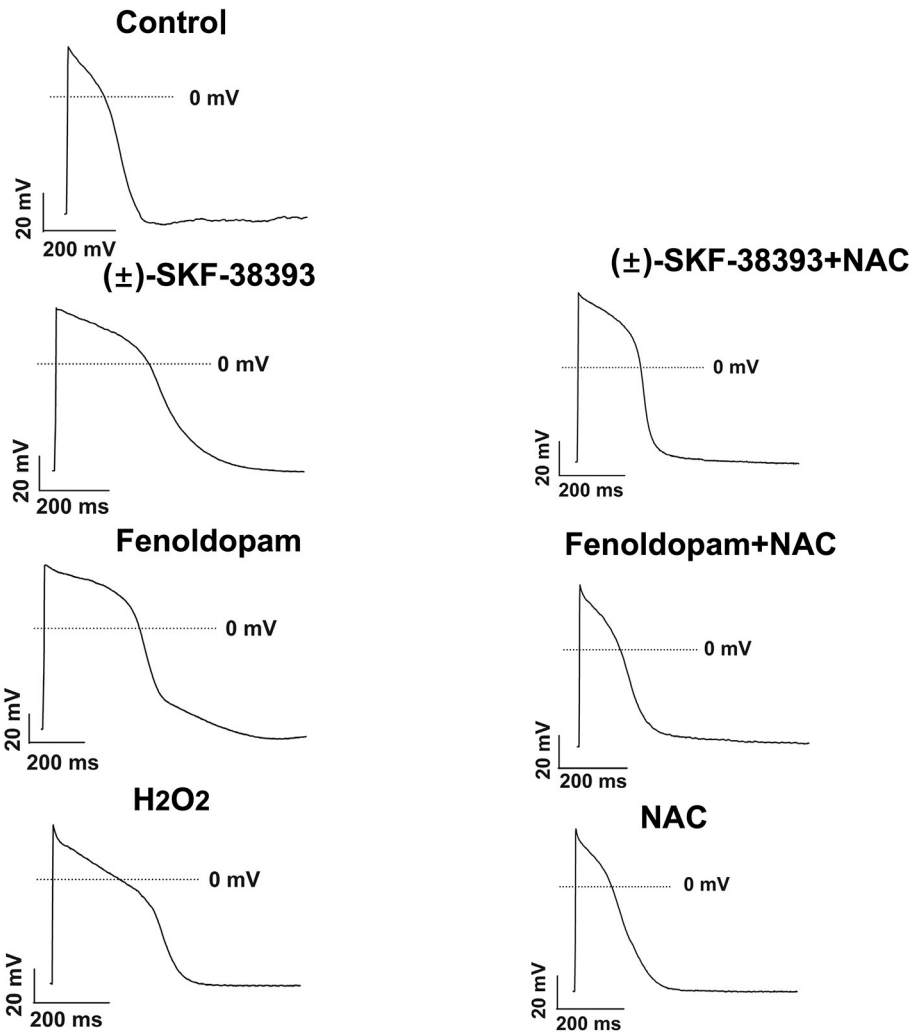

FIGURE 4 | ROS mediated the effects of (±)-SKF 38393 or fenoldopam on action potentials. hiPSC-CMs were challenged by vehicle (Control) or 50 μM (±)-SKF 38393 and 5 μM fenoldopam or 100 μM H_2O_2 (H_2O_2) in the presence or absence of a ROS-blocker (1 mM NAC), or NAC alone for 1 h. APs were recorded at 1 Hz. Shown are examples of APs in each group cells. Statistical data were summarized in **Table 2**.

TABLE 2 | Analysis of action potentials influenced by ROS in presence of dopamine receptor agonists.

Group	Cell number	APD10	APD50	APD90	Vmax	APA	RP
Control	16	12.9 ± 0.4	210.9 ± 27.4	369.2 ± 36.9	56.9 ± 3.8	117.6 ± 1.0	−70.4 ± 1.1
(±)-SKF-38393	18	16.2 ± 1.3**	333.3 ± 44*	566.1 ± 47.4**	39.1 ± 2.2**	118.1 ± 2.9	−71.6 ± 1.6
Fenoldopam	14	16.4 ± 0.4*	328.3 ± 29.8*	535.9 ± 36.9**	44.7 ± 2.4**	119.1 ± 0.4	−70.9 ± 0.9
H_2O_2	15	16.4 ± 0.5*	335.8 ± 16.7*	544.9 ± 35.8**	33.1 ± 1.2**	117.3 ± 1.5	−71.9 ± 0.8
(±)-SKF-38393+NAC	16	12.9 ± 0.3	220.7 ± 4.9	417.4 ± 5.2	47.4 ± 50.	117.8 ± 0.7	−69.5 ± 0.4
Fenoldopam + NAC	16	12.8 ± 0.26	233.6 ± 5.9	420.1 ± 7.6	47.6 ± 0.99	118.91 ± 0.5	−69.8 ± 0.5
NAC	16	12.8 ± 0.3	227.9 ± 5.5	433.7 ± 14.6	54.9 ± 1.31	118.5 ± 1.7	−68.3 ± 0.6

**p<0.05, **p<0.01. The p-values vs. control were determined by one-way ANOVA with Holm-Sidak post-test.*

The results exhibited that in both H2 (**Supplementary Figure 6**) and H3 (**Supplementary Figure 7**) hiPSC-CMs, the dopamine D1/D5 receptor activators (±)-SKF 38393 and fenoldopam altered APs in the same manner as in the first healthy donor (H1) hiPSC-CMs. Either the positive (significant effects) and negative (no effects) result observed in H1-hiPSC-CMs was

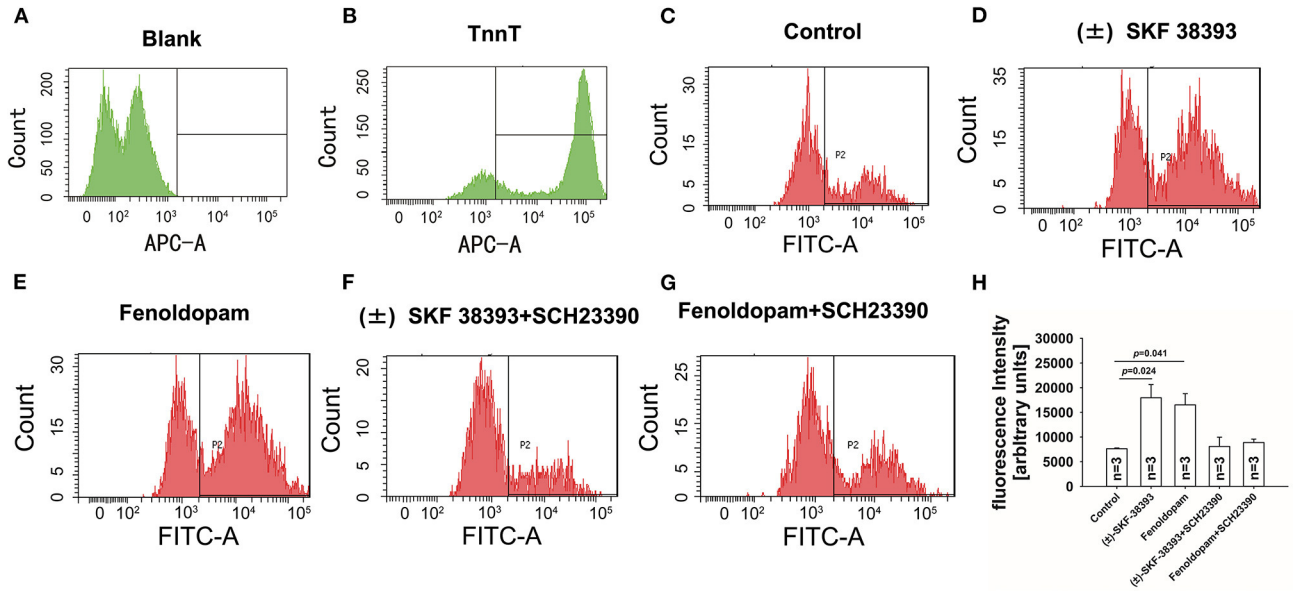

FIGURE 5 | Dopamine D1/D5 receptor activation increased ROS-production. hiPSC-CMs were treated with or without antibody against troponin T (cTnT) and ROS fluorescence dye was applied to measure ROS production. Vehicle (Control) **(C)** or 50 μM (±)-SKF 38393 or 5 μM fenoldopam or (±)-SKF 38393 plus 10 μM SCH 23390 or fenoldopam plus 10 μM SCH 23390 **(D–G)** was applied to cells for 1 h before measurements. ROS-generation was analyzed by FACS. **(A,B)** A representative recoding indicating cardiac troponin T (cTnT) in hiPSC-CMs. **(D,E)** A representative recoding indicating enhancement of ROS generation by (±)-SKF 38393 or fenoldopam. **(F,G)** A representative recoding indicating that SCH 23390 prevented the effect of (±)-SKF 38393 or fenoldopam on ROS generation. **(H)** Averaged values of fluorescence intensity showing the ROS-levels in cells. "blank" means control measurements in cells that were not treated by the ROS fluorescence dye. "*n*" numbers in **(H)** are numbers of different independent experiments using cells from different differentiations. The *p*-values vs. Control were determined by the analysis of one-way ANOVA with Holm-Sidak post-test.

successfully recapitulated in H2- and H3-hiPSC-CMs, which means that the interindividual variation is not large under our experimental conditions.

DISCUSSION

Although there are clinical case reports demonstrating that dopamine injection can induce TTC or the plasma dopamine concentration of TTC patients increases, and experimental data showing that the use of high concentrations of dopamine successfully induced TTC in animal models, it is still unclear how dopamine receptor activation causes TTC in the human body. To our knowledge, this is the first study to explore the roles and mechanisms of dopamine D1/D5 receptor activation for APD/QT-prolongation and arrhythmias induced by toxic concentration of catecholamine using hiPSC-CMs.

It has been confirmed in animals that the stimulatory effect of epinephrine can be inhibited by the D1 antagonist SCH 23390 (34), suggesting that epinephrine can also activate dopamine receptors. Another study showed that norepinephrine and epinephrine both increased (35) SGTPgammaS binding at dopamine D4 receptors (35), suggesting an agonism of norepinephrine and epinephrine at the dopamine D4 receptor. Conversely, dopamine can also activate adrenoceptors (36, 37). These data may suggest an important cross-reactivity among the different monoamine neurotransmitter systems. To investigate the possible contributions of dopamine D1/D5 receptor signaling to catecholamine effects in the setting of TTC, we first used high concentration of epinephrine (Epi) to establish the TTC-model and examined effects of dopamine D1/D5 receptor blockers in the study. The D1/D5 antagonist SCH 23390 attenuated the Epi-induced arrhythmia in hiPSC-CMs. Moreover, both D1/D5 dopamine receptor agonist, (±)-SKF 38393 and fenoldopam, increased the arrhythmic events, indicative of the involvement of dopamine D1/D5 receptor signaling in occurrence of arrhythmias in the setting of TTC. The contribution of dopamine receptors in TTC can be understood in two aspects: (1) High concentration epinephrine can activate dopamine receptor through cross-activation; (2) In stress, catecholamine including dopamine release is largely increased and the stimulation of dopamine receptors by dopamine *per se* is enhanced, which enhances catecholamine effects.

Abnormal APs are usual substrates of arrhythmias, leading us to examine changes of APs caused by dopamine receptor activation. The dopamine receptor blocker SCH 23390 attenuated the effects of epinephrine and two specific agonists of dopamine D1/D5 receptor [(±)-SKF38393 and fenoldopam] mimicked the effect of Epi on APs. These data imply that dopamine D1/D5 receptor signaling can contribute to effects of epinephrine, promoting the changes of APs caused by high doses of catecholamine. The reduction of Vmax may cause conduction defect. The APD-prolongation may cause EADs. Both changes caused by D1/D5 receptor activation may contribute to occurrence of arrhythmic events, which is

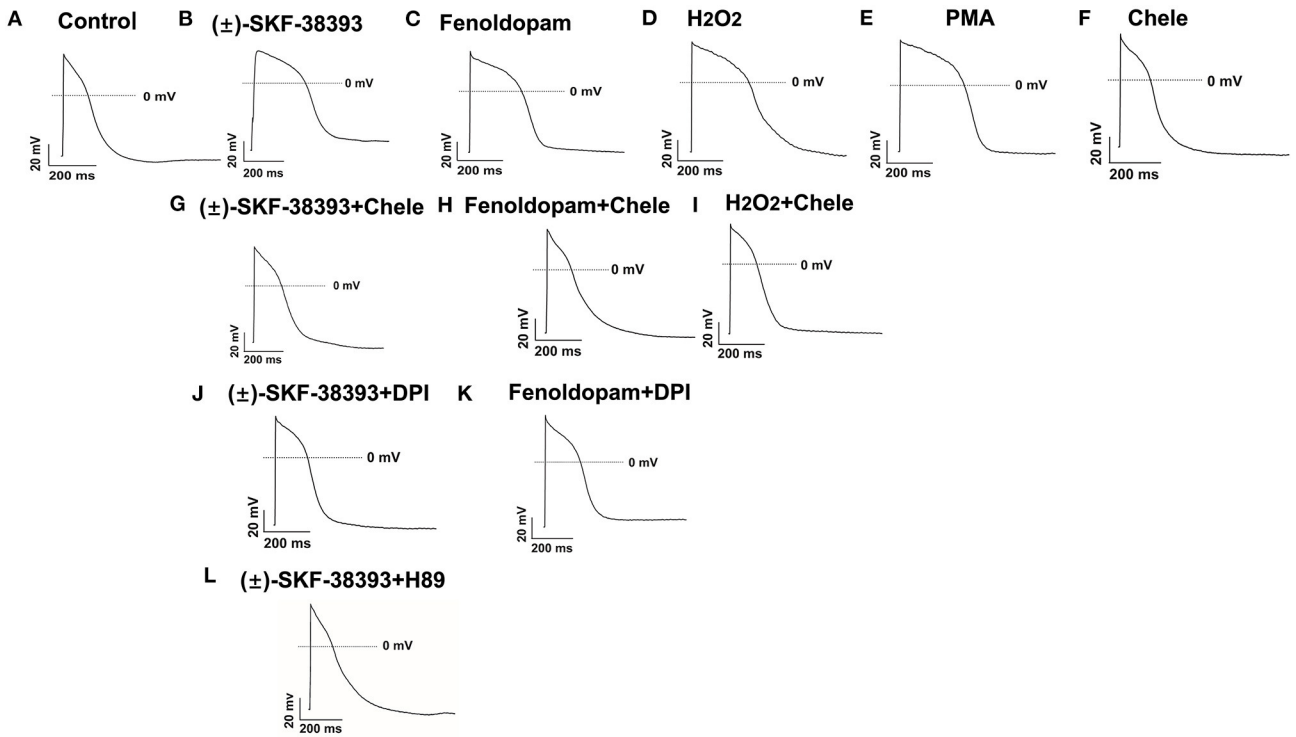

FIGURE 6 | Protein kinases and NADPH oxidases participating in dopamine D1/D5 receptor and ROS signaling. hiPSC-CMs were challenged for 1 h by vehicle [Control, **(A)**] or 50 μM (±)-SKF 38393 **(B)** or 5 μM fenoldopam **(C)** or 100 μM H_2O_2 [H_2O_2, **(D)**] or 10 μM PKC activator PMA [PMA, **(E)**] or 10 μM Chele **(F)** or (±)-SKF 38393 plus 10 μM chelerythrine (Chele), an inhibitor of protein kinase C **(G)**, or fenoldopam plus Chele **(H)** or H_2O_2 plus Chele **(I)** or (±)-SKF38393 plus 10 μM DPI **(J)** or fenoldopam plus DPI **(K)** or (±)-SKF 38393 plus 1 μM H89, an inhibitor of protein kinase A **(L)**. Action potentials paced at 1 Hz were recorded. Statistical data are summarized in **Table 3**. **(A–L)** Examples of AP-traces in each group cells.

reported by TTC cases in up to 12% of patients (38, 39). Of note, epinephrine and dopamine agonists caused also DAD-like events and failed APs. The former suggests abnormal calcium-release or abnormal inward current, while the latter suggests abnormal automaticity in hiPSC-CMs challenged by toxic catecholamine.

The APD-prolongation induced by epinephrine is not consistent with previous reported data showing a shortening of APD by adrenergic stimulators (40). It is well-known that adrenergic stimulation increases heart rate and shortens QT interval and APD, which is a physiological frequency-adaptation. The heart rate acceleration results from activation of I_f channels by increased cAMP due to ß1-Gs activation. The QT/APD-shortening was shown to be caused by enhanced I_{Ks} (41). Of note, those effects result from adrenergic stimulation under physiological condition or at low level of catecholamine. Toxic effects of high level of catecholamine can be different from the physiological effects of catecholamine. Indeed, our study detected an opposite effect, i.e., an APD-prolongation in presence of high concentration of epinephrine. The reasons for the difference between physiological and toxic effects might be: (1) Receptor signaling switch. Low concentration catecholamine predominantly stimulates ß1-Gs-signaling, while high concentration catecholamine mainly stimulates ß2-Gi-siganling (42, 43); (2) Target switch. Low concentration catecholamine activates I_{Ks} (41), while high concentration catecholamine inhibits I_{to} (10) and I_{Kr} (this study); (3) Multiple effects. High concentration catecholamine stimulates more receptors and more signaling than low concentration catecholamine. Different signaling may interact each other and lead to either an enhancing or a counteracting effect. Therefore, the result in the current study can be understood as: high concentration epinephrine stimulates ß- (mainly ß2), α- and D1/D5-receptors. The ß1- (frequency enhancing, I_{Ks} enhancing and APD-shortening) effect was counteracted by ß2- or α- or even D1/D5-effects. The ß2- or α- or even D1/D5-effects on I_{to}, I_{Kr}, I_{Na}, and I_{Ca-L}, all facilitate APD-prolongation (10, 11).

Here, a question is whether the result difference between this and previous studies was caused by the immaturity of hiPSC-CMs. Our recent study showed that our hiPSC-CMs displayed frequency enhancement and APD-shortening when they were stimulated by a low (10 μM) concentration of isoprenaline (44), which are in agreement with previously reported data. This strongly supports that hiPSC-CMs have basic properties similar to human native cardiomyocytes and can provide helpful information in researches regarding cardiac physiology or pathophysiology.

Another question is what the importance and relationship of different receptor activation are in presence of high

TABLE 3 | Analysis of action potentials influenced by ROS, PKC, and PKA signaling in presence of dopamine receptor agonists.

Group	Cell number	APD10	APD50	APD90	Vmax	APA	Baseline
Control	16	12.9 ± 0.4	210.9 ± 27.4	369.2 ± 36.9	56.9 ± 3.8	117.6 ± 1.0	−70.4 ± 1.1
(±)-SKF-38393	18	16.2 ± 1.3**	333.3 ± 44**	566.1 ± 47.4**	39.1 ± 2.2**	118.1 ± 2.9	−71.6 ± 1.6
Fenoldopam	14	16.4 ± 0.4**	328.3 ± 29.8**	535.9 ± 36.9**	44.7 ± 2.4**	119.1 ± 0.4	−70.9 ± 0.9
H_2O_2	15	16.4 ± 0.5**	335.8 ± 16.7**	544.9 ± 35.8**	33.1 ± 1.2**	117.3 ± 1.5	−71.9 ± 0.8
PMA	11	15.8 ± 0.5**	303.7 ± 9.4**	533.0 ± 6.9**	42.6 ± 2.1**	117.8 ± 1.3	−68.4 ± 0.8
(±)-SKF-38393+H89	15	12.7 ± 0.3	170.5 ± 10.9	410.5 ± 24.7	60.9 ± 4.3	116.1 ± 0.9	−69.0 ± 0.6
(±)-SKF38393+Chele	18	13.2 ± 0.3	178.2 ± 24.7	386.3 ± 25.9	56.4 ± 2.2	117.4 ± 0.6	−69.5 ± 0.5
Fenoldopam+Chele	15	12.7 ± 0.4	221.3 ± 9.1	354.8 ± 30.9	59.6 ± 2.3	117.2 ± 1.1	−70.4 ± 0.7
H_2O_2+Chele	15	13.2 ± 0.3	211.6 ± 4.5	419.5 ± 9.2	52.6 ± 1.1	117.3 ± 0.7	−68.2 ± 0.4
(±)-SKF-38393+DPI	16	13.6 ± 0.3	218.9 ± 3.9	411.6 ± 9.4	44.1 ± 2.2	117.9 ± 0.6	−70.0 ± 0.8
Fenoldopam+DPI	13	12.6 ± 0.4	233.9 ± 5.8	429.5 ± 8.2	41.1 ± 1.5	118.9 ± ±0.5	−69.0 ± 0.5
Chele	8	11.9 ± 0.6	214.6 ± 5.5	400.3 ± 6.5	54.6 ± 0.3	118.3 ± 0.3	−71.2 ± 0.4

*** p<0.01. The p-values vs. Control were determined by one-way ANOVA with Holm-Sidak post-test.*

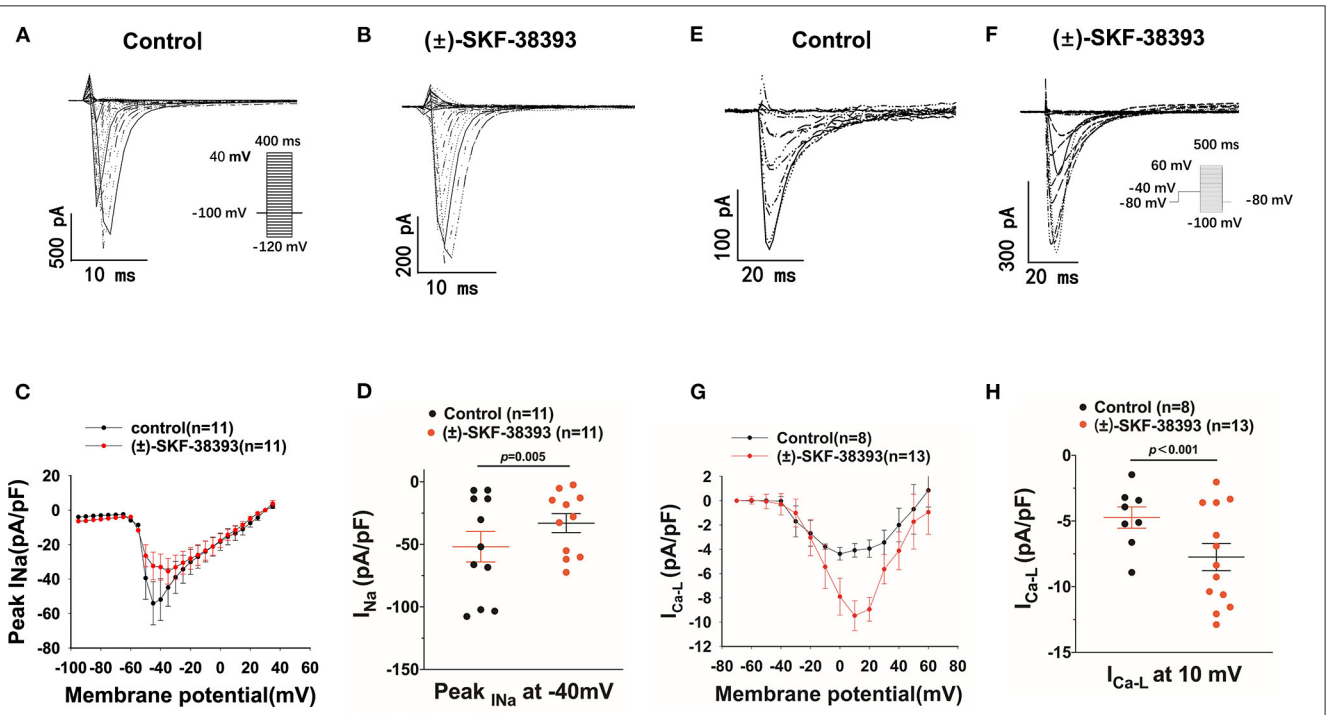

FIGURE 7 | Effects of (±)-SKF 38393 or fenoldopam on ion channel currents. hiPSC-CMs were challenged for 1 h by vehicle (Control) or 50 μM (±)-SKF 38393 and 5 μM fenoldopam. Sodium channel current (I_{Na}) was recorded with the patch clamp (voltage-clamp) protocol indicated in **(A)** (inset). The L-type calcium channel current (I_{Ca-L}) was recorded with the voltage-clamp protocol indicated in **(F)** (inset). **(A,B)** Representative traces of I_{Na} in absence (Control) and presence of (±)-SKF38393. **(C)** I–V curves of peak I_{Na}. **(D)** Mean values of peak I_{Na} at −40 mV. **(E,F)** Examples of traces of I_{Ca-L} in absence (Control) and presence of (±)-SKF38393. **(G)** I–V curves of I_{Ca-L}. **(H)** Mean values of I_{Ca-L} at 10 mV. "*n*" numbers represent the number of analyzed cells. The *p*-values vs. Control were determined by *t*-test.

concentration catecholamine. Notably, our recent studies showed that blockade of ß-receptor or α-receptor could completely prevent the APD-prolongation by high concentration of isoprenaline and epinephrine, respectively (10, 11). High concentration of isoprenaline can probably activate multiple types of adrenoceptors. These data together with results of the current study demonstrated that the APD-prolongation induced by toxic catecholamine needs activation of multiple receptors because blockade of one type receptor can lead to loss of the effect. It implies that every involved receptor is important and activation of only one type of the receptor is not enough for causing APD-prolongation and arrhythmias.

Next, we investigated the ionic mechanism that causes AP changes. Inhibitory effects of Epi on SCN5A expression level and peak I_{Na} were reversed by dopamine D1/D5 receptor blocker

(SCH 23390), Moreover, the (±)-SKF 38393 suppressed peak I_{Na} but did not change the channel gating kinetics. All data together indicated that the activation of dopamine D1/D5 receptors suppressed peak I_{Na} mainly *via* reducing the channel expression level. The inhibition of peak I_{Na} is the main reason for the observed reduction of Vmax of APs.

The L-type Ca channel current (I_{Ca-L}) was increased by dopamine D1/D5 receptor activation *via* enhancing the channel activation and reducing the recovery time after inactivation. The mRAN level of L-type Ca channel (CACNA1C) was also elevated by Epi and inhibited by SCH 23390, which is consistent with the increase in I_{Ca-L} and suggests that dopamine D1/D5 receptor signaling can modulate both the channel activity and channel expression. The increase in I_{Ca-L} can explain the prolongation of APD. The enhanced I_{Ca-L} can increase the intracellular Ca^{2+} concentration, which may stimulate Ca^{2+} release from intracellular Ca^{2+}-storage and in turn causes DADs or trigger activity.

I_{Kr} channels are important in cardiac repolarization, and their dysfunction can lead to prolongation of APD and QT interval, which can cause arrhythmias. It is well-known that some clinically used drugs have anti- or proarrhythmic effect (a side effect) due to their effect on I_{Kr}. Therefore, examination of effect on I_{Kr} is widely performed in drug-screening for therapeutic or toxic effect. In hiPS-CMs, I_{Kr} blockers like sotalol and E-4031 prolonged APD (44), and gain-of-function of I_{Kr} due to a mutation in I_{Kr} gene shortened APD in hiPSC-CMs (24), indicating that I_{Kr} is an important repolarizing current in hiPSC-CMs. Hence, for exploring the reason for APD-prolongation by dopamine receptor activation, we examined I_{Kr}. We observed that high concentration of Epi reduced KCNH2 (gene of I_{Kr}) expression and dopamine receptor blocker attenuated Epi effect and that dopamine receptor agonist (±)-SKF 38393 suppressed significantly I_{Kr}. The reduction of I_{Kr} can prolong APD and contribute to occurrence of arrhythmic events. Therefore, the suppression of I_{Kr} by dopamine D1/D5 receptor activation may contribute to APD/QT prolongation and arrhythmogenesis of TTC.

Besides I_{Na}, I_{Ca-L}, and I_{Kr} other currents may also be affected by high level catecholamine and dopamine receptor signaling. Our recent study showed that hiPSC-CMs express almost all the ion channels reported in human native cardiomyocytes (44). I_{Na}, I_{Ca-L}, I_{Ca-T}, I_f, I_{NCX}, I_{K1}, I_{to}, I_{Kr}, I_{Ks} I_{KATP}, I_{K-pH}, I_{SK1-3}, and I_{SK4}, I_{KACh} (acetylcholine activated K^+ current) and I_{KNa} (Na^+-activated K^+ current), I_{K-pH} (pH-sensitive K^+ current), I_{Cl-vol} (volume-regulated Cl^- current) and I_{Cl-Ca} (calcium-activated Cl^- current), and TRPV channel current could be detected in hiPSC-CMs. We did not examine other currents because the enhanced I_{Ca-L} and reduced I_{Kr} can explain the APD-prolongation. It is possible that some other currents could be also affected and contribute to the APD-prolongation in presence of high concentration catecholamine.

There is a remarkable relationship between dopamine D1/D5 receptor and oxidative stress in abnormal dopamine signaling in animal models (45, 46). To further investigate the signaling factors linked to dopamine D1/D5 receptor activation, we first assessed the ROS generation, which has been shown to be linked to dopamine D1/D5 receptor (32). After treating the hiPSC-CMs with (±)-SKF 38393 or fenoldopam, the ROS production was increased obviously. In addition, SCH 23390 abolished the increase of ROS production. To further confirm the relationship between ROS and dopamine receptors activation, we next examined the effect of ROS blocker NAC on APs in the presence of (±)-SKF 38393 and fenoldopam. The NAC attenuated and H_2O_2 (endogenous ROS) mimicked the effects of (±)-SKF 38393 and fenoldopam on APs. These data indicate an important role of ROS for AP-changes linked to dopamine D1/D5 receptor activation.

However, the increase in ROS level is related to many factors, and it is currently known that NADPH oxidases plays an important role in the process of ROS production. Therefore, we next analyzed the effect of DPI (a NADPH oxidase blocker) on the activation of dopamine D1/D5 receptor. The DPI attenuated the effects of (±)-SKF 38393 and fenoldopam, which means that NADPH oxidase is involved in the signal transduction of AP changes caused by the activation of dopamine D1/D5 receptors.

A large number of studies have shown that activation of G protein-linked pathways by dopamine can inhibit Na-K-ATPase activity involving protein kinase C (PKC) and ROS activation will cause PKC pathway activation (47, 48). So, we next examined the PKC effects in dopamine D1/D5 receptor activation. The PKC blocker and activator were used. The PKC-blocker (chelerythrine) reduced the effects of both (±)-SKF 38393 and fenoldopam and the PKC activator (PMA) recapitulated their effects on APs. These data confirmed an important role of PKC in dopamine D1/D5 receptor mediated effects.

Since we observed that PKA, PKC and ROS all were involved in the effect of D1/D5 receptor activation, we tried to unveil the signal transduction process. PKA is a known upstream regulator of ROS (33). Therefore, the question is whether PKC is a downstream or upstream factor of ROS when D1/D5 receptors are activated. We found that the PKC blocker abolished the ROS effect, indicating that PKC is a downstream factor of ROS. Considering that NADPH oxidases were also involved in effects of dopamine D1/D5 receptor activation since DPI prevented the effects of (±)-SKF 38393 and fenoldopam, we may interpret the signaling in dopamine D1/D5 receptor activation by high concentration of catecholamine as: dopamine D1/D5 receptor-Gs-PKA-NADPH-ROS-PKC. However, how PKA causes NADPH oxidase activation is unknown and further studies are required to answer the question.

CONCLUSION

The study showed that excessive catecholamines can cause abnormal ion channel function and arrhythmias *via* activating dopamine D1/D5 receptor signaling. Activation of dopamine D1D5 receptors is related to PKA, ROS, and PKC related signals. Dopamine D1/D5 receptors may contribute to the occurrence of arrhythmia in patients with TTC and may be possible therapeutic targets for treating the disease.

STUDY LIMITATIONS

In this study, we only studied the role of D1/D5 receptor, and the role of D2 receptor family was not investigated in this study. Possible contributions of D2 family to toxic effects of catecholamine cannot be excluded. In addition, there are many different PKC isozymes for protein kinase C (PKC). This study did not clarify the subtypes of PKC responsible for the observed effects mediated by D1/D5 receptor signaling.

Besides, this study used hiPSC-CMs only from healthy people. Whether hiPSC-CMs from TTC patients show different results is still unknown. Moreover, differences exist between hiPSC-CMs and adult cardiomyocytes, which should also be considered when interpreting the data from hiPSC-CMs. The hiPSC-CMs have automaticity and a relatively high percentage of control cells exhibited the arrhythmic events. This might reflect a limitation of hiPSC-CMs comparing with adult human cardiomyocytes.

Another limitation of the study is that the APs and currents were measured at room temperature. The possibility that at higher temperature different effects of catecholamine may appear cannot be excluded.

DATA AVAILABILITY STATEMENT

The original contributions presented in the study are included in the article/**Supplementary Material**, further inquiries can be directed to the corresponding author/s.

ETHICS STATEMENT

The skin biopsies were obtained from three healthy donors after written informed consent was accumulated. The Ethics Committee of the Medical Faculty Mannheim, University of Heidelberg (approval number: 2018-565N-MA) and the Ethics Committee of the University Medical Center Göttingen (approval number: 10/9/15) have approved the study. The study was performed following the approved guidelines and carried out according to the Helsinki Declaration of 1975 (https://www.wma.net/what-we-do/medical-ethics/declaration-of-helsinki/), revised in 2013. The patients/participants provided their written informed consent to participate in this study.

AUTHOR CONTRIBUTIONS

MH, YL, ZY, LC, HL, GY, and KB contributed to experiments, data collection, and data analysis. SL contributed to data analysis. SL, IE-B, LC, MB, XZ, and IA contributed to the conception or design of the work, interpretation of data, and writing the paper. All authors have read and approved the manuscript.

FUNDING

This study was supported by the DZHK (German Center for Cardiovascular Research), the BMBF (German Ministry of Education and Research) (Nos. 81Z0500204 and 81X2500208), and the Hector Foundation (MED 1814).

ACKNOWLEDGMENTS

We would like to thank Stefanie Uhlig for supporting FACS analysis. We thank the Chinese Scholarship Council (CSC) for the financial support for MH. We thank the technical support by the Stem Cell Unit, Göttingen. We acknowledge the financial support by the Baden-Württemberg Ministry of Science, Research and the Arts and by Ruprecht-Karls-Universität Heidelberg.

SUPPLEMENTARY MATERIAL

The Supplementary Material for this article can be found online at: https://www.frontiersin.org/articles/10.3389/fcvm.2021.777463/full#supplementary-material

REFERENCES

1. Dote K, Sato H, Tateishi H, Uchida T, Ishihara M. Myocardial stunning due to simultaneous multivessel coronary spasms: a review of 5 cases. *J Cardiol.* (1991) 21:203–14.
2. Patankar GR, Choi JW, Schussler JM. Reverse takotsubo cardiomyopathy: two case reports and review of the literature. *J Med Case Rep.* (2013) 7:84. doi: 10.1186/1752-1947-7-84
3. Templin C, Ghadri JR, Diekmann J, Napp LC, Bataiosu DR, Jaguszewski M, et al. Clinical features and outcomes of takotsubo (stress) cardiomyopathy. *N Engl J Med.* (2015) 373:929–38. doi: 10.1056/NEJMoa1406761
4. Pelliccia F, Kaski JC, Crea F, Camici PG. Pathophysiology of Takotsubo syndrome. *Circulation.* (2017) 135:2426–41. doi: 10.1161/CIRCULATIONAHA.116.027121
5. Pelliccia F, Parodi G, Greco C, Antoniucci D, Brenner R, Bossone E, et al. Comorbidities frequency in Takotsubo syndrome: an international collaborative systematic review including 1109 patients. *Am J Med.* (2015) 128:654.e11–9. doi: 10.1016/j.amjmed.2015.01.016
6. Ono R, Falcão LM. Takotsubo cardiomyopathy systematic review: pathophysiologic process, clinical presentation and diagnostic approach to Takotsubo cardiomyopathy. *Int J Cardiol.* (2016) 209:196–205. doi: 10.1016/j.ijcard.2016.02.012
7. Bhat S, Gazi H, Mwansa V, Chhabra L. Catecholamine-induced reverse takotsubo cardiomyopathy. *Proc Bayl Univ Med Cent.* (2019) 32:567–9. doi: 10.1080/08998280.2019.1634229
8. Borchert T, Hübscher D, Guessoum CI, Lam TD, Ghadri JR, Schellinger IN, et al. Catecholamine-dependent β-adrenergic signaling in a pluripotent stem cell model of Takotsubo cardiomyopathy. *J Am Coll Cardiol.* (2017) 70:975–91. doi: 10.1016/j.jacc.2017.06.061
9. Redfors B, Shao Y, Wikström J, Lyon AR, Oldfors A, Gan LM, et al. Contrast echocardiography reveals apparently normal coronary perfusion in a rat model of stress-induced (Takotsubo) cardiomyopathy. *Eur Heart J Cardiovasc Imaging.* (2014) 15:152–7. doi: 10.1093/ehjci/jet079
10. El-Battrawy I, Zhao Z, Lan H, Schünemann JD, Sattler K, Buljubasic F, et al. Estradiol protection against toxic effects of catecholamine on electrical properties in human-induced pluripotent stem cell derived cardiomyocytes. *Int J Cardiol.* (2018) 254:195–202. doi: 10.1016/j.ijcard.2017.11.007
11. Huang M, Fan X, Yang Z, Cyganek L, Li X, Yuecel G, et al. Alpha 1-adrenoceptor signalling contributes to toxic effects of catecholamine on electrical properties in cardiomyocytes. *Europace.* (2021) 23:1137–48. doi: 10.1093/europace/euab008

12. Nakagawa N, Fukawa N, Tsuji K, Nakano N, Kato A. Takotsubo cardiomyopathy induced by dopamine infusion after carotid artery stenting. *Int J Cardiol.* (2016) 205:62–4. doi: 10.1016/j.ijcard.2015.12.023
13. Wittstein IS, Thiemann DR, Lima JA, Baughman KL, Schulman SP, Gerstenblith G, et al. Neurohumoral features of myocardial stunning due to sudden emotional stress. *N Engl J Med.* (2005) 352:539–48. doi: 10.1056/NEJMoa043046
14. Madias JE. Blood norepinephrine/epinephrine/dopamine measurements in 108 patients with takotsubo syndrome from the world literature: pathophysiological implications. *Acta Cardiol.* (2020) 2020:1–9. doi: 10.1080/00015385.2020.1826703
15. Redfors B, Ali A, Shao Y, Lundgren J, Gan LM, Omerovic E. Different catecholamines induce different patterns of takotsubo-like cardiac dysfunction in an apparently afterload dependent manner. *Int J Cardiol.* (2014) 174:330–6. doi: 10.1016/j.ijcard.2014.04.103
16. Isogai T, Matsui H, Tanaka H, Fushimi K, Yasunaga H. Early β-blocker use and in-hospital mortality in patients with Takotsubo cardiomyopathy. *Heart.* (2016) 102:1029–35. doi: 10.1136/heartjnl-2015-308712
17. Santoro F, Ieva R, Musaico F, Ferraretti A, Triggiani G, Tarantino N, et al. Lack of efficacy of drug therapy in preventing takotsubo cardiomyopathy recurrence: a meta-analysis. *Clin Cardiol.* (2014) 37:434–9. doi: 10.1002/clc.22280
18. Singh K, Carson K, Usmani Z, Sawhney G, Shah R, Horowitz J. Systematic review and meta-analysis of incidence and correlates of recurrence of takotsubo cardiomyopathy. *Int J Cardiol.* (2014) 174:696–701. doi: 10.1016/j.ijcard.2014.04.221
19. Sidhu A. Coupling of D1 and D5 dopamine receptors to multiple G proteins: implications for understanding the diversity in receptor-G protein coupling. *Mol Neurobiol.* (1998) 16:125–34. doi: 10.1007/BF02740640
20. Sibley DR, Monsma FJ Jr. Molecular biology of dopamine receptors. *Trends Pharmacol Sci.* (1992) 13:61–9. doi: 10.1016/0165-6147(92)90025-2
21. Cavallotti C, Mancone M, Bruzzone P, Sabbatini M, Mignini F. Dopamine receptor subtypes in the native human heart. *Heart Vessels.* (2010) 25:432–7. doi: 10.1007/s00380-009-1224-4
22. Laitinen JT. Dopamine stimulates K+ efflux in the chick retina *via* D1 receptors independently of adenylyl cyclase activation. *J Neurochem.* (1993) 61:1461–9. doi: 10.1111/j.1471-4159.1993.tb13641.x
23. Mahan LC, Burch RM, Monsma FJ Jr, Sibley DR. Expression of striatal D1 dopamine receptors coupled to inositol phosphate production and Ca^{2+} mobilization in *Xenopus oocytes*. *Proc Natl Acad Sci USA.* (1990) 87:2196–200. doi: 10.1073/pnas.87.6.2196
24. El-Battrawy I, Lan H, Cyganek L, Zhao Z, Li X, Buljubasic F, et al. Modeling short QT syndrome using human-induced pluripotent stem cell-derived cardiomyocytes. *J Am Heart Assoc.* (2018) 7:e007394. doi: 10.1161/JAHA.117.007394
25. Kleinsorge M, Cyganek L. Subtype-directed differentiation of human iPSCs into atrial and ventricular cardiomyocytes. *STAR Protoc.* (2020) 1:100026. doi: 10.1016/j.xpro.2020.100026
26. El-Battrawy I, Zhao Z, Lan H, Cyganek L, Tombers C, Li X, et al. Electrical dysfunctions in human-induced pluripotent stem cell-derived cardiomyocytes from a patient with an arrhythmogenic right ventricular cardiomyopathy. *Europace.* (2018) 20:f46–56. doi: 10.1093/europace/euy042
27. Schmittgen TD, Livak KJ. Analyzing real-time PCR data by the comparative C(T) method. *Nat Protoc.* (2008) 3:1101–8. doi: 10.1038/nprot.2008.73
28. Beninger RJ, Miller R. Dopamine D1-like receptors and reward-related incentive learning. *Neurosci Biobehav Rev.* (1998) 22:335–45. doi: 10.1016/S0149-7634(97)00019-5
29. Li Q, Wu N, Cui P, Gao F, Qian WJ, Miao Y, et al. Suppression of outward K(+) currents by activating dopamine D1 receptors in rat retinal ganglion cells through PKA and CaMKII signaling pathways. *Brain Res.* (2016) 1635:95–104. doi: 10.1016/j.brainres.2016.01.039
30. Undie AS, Weinstock J, Sarau HM, Friedman E. Evidence for a distinct D1-like dopamine receptor that couples to activation of phosphoinositide metabolism in brain. *J Neurochem.* (1994) 62:2045–8. doi: 10.1046/j.1471-4159.1994.62052045.x
31. Opazo F, Schulz JB, Falkenburger BH, PKC. links Gq-coupled receptors to DAT-mediated dopamine release. *J Neurochem.* (2010) 114:587–96. doi: 10.1111/j.1471-4159.2010.06788.x
32. Banday AA, Lokhandwala MF. Oxidative stress reduces renal dopamine D1 receptor-Gq/11alpha G protein-phospholipase C signaling involving G protein-coupled receptor kinase 2. *Am J Physiol Renal Physiol.* (2007) 293:F306–15. doi: 10.1152/ajprenal.00108.2007
33. Zhang J, Xiao H, Shen J, Wang N, Zhang Y. Different roles of β-arrestin and the PKA pathway in mitochondrial ROS production induced by acute β-adrenergic receptor stimulation in neonatal mouse cardiomyocytes. *Biochem Biophys Res Commun.* (2017) 489:393–8. doi: 10.1016/j.bbrc.2017.05.140
34. Vanderheyden P, Ebinger G, Kanarek L, Vauquelin G. Epinephrine and norepinephrine stimulation of adenylate cyclase in bovine retina homogenate: evidence for interaction with the dopamine D1 receptor. *Life Sci.* (1986) 38:1221–7. doi: 10.1016/0024-3205(86)90177-3
35. Czermak C, Lehofer M, Liebmann PM, Traynor J. [35S]GTPgammaS binding at the human dopamine D4 receptor variants hD42, hD44, and hD47 following stimulation by dopamine, epinephrine and norepinephrine. *Eur J Pharmacol.* (2006) 531:20–4. doi: 10.1016/j.ejphar.2005.11.063
36. Zhang XH, Zhang XF, Zhang JQ, Tian YM, Xue H, Yang N, et al. Beta-adrenoceptors, but not dopamine receptors, mediate dopamine-induced ion transport in late distal colon of rats. *Cell Tissue Res.* (2008) 334:25–35. doi: 10.1007/s00441-008-0661-1
37. Rey E, Hernández-Díaz FJ, Abreu P, Alonso R, Tabares L. Dopamine induces intracellular Ca2+ signals mediated by alpha1B-adrenoceptors in rat pineal cells. *Eur J Pharmacol.* (2001) 430:9–17. doi: 10.1016/S0014-2999(01)01250-X
38. El-Battrawy I, Santoro F, Stiermaier T, Möller C, Guastafierro F, Novo G, et al. Prevalence, management, and outcome of adverse rhythm disorders in takotsubo syndrome: insights from the international multicenter GEIST registry. *Heart Fail Rev.* (2020) 25:505–11. doi: 10.1007/s10741-019-09856-4
39. El-Battrawy I, Lang S, Ansari U, Tülümen E, Schramm K, Fastner C, et al. Prevalence of malignant arrhythmia and sudden cardiac death in takotsubo syndrome and its management. *Europace.* (2018) 20:843–50. doi: 10.1093/europace/eux073
40. Tovar OH, Jones JL. Epinephrine facilitates cardiac fibrillation by shortening action potential refractoriness. *J Mol Cell Cardiol.* (1997) 29:1447–55. doi: 10.1006/jmcc.1997.0387
41. Volders PG, Stengl M, van Opstal JM, Gerlach U, Spätjens RL, Beekman JD, et al. Probing the contribution of IKs to canine ventricular repolarization: key role for beta-adrenergic receptor stimulation. *Circulation.* (2003) 107:2753–60. doi: 10.1161/01.CIR.0000068344.54010.B3
42. Paur H, Wright PT, Sikkel MB, Tranter MH, Mansfield C, O'Gara P, et al. High levels of circulating epinephrine trigger apical cardiodepression in a β2-adrenergic receptor/Gi-dependent manner: a new model of Takotsubo cardiomyopathy. *Circulation.* (2012) 126:697–706. doi: 10.1161/CIRCULATIONAHA.112.111591
43. Heubach JF, Ravens U, Kaumann AJ. Epinephrine activates both Gs and Gi pathways, but norepinephrine activates only the Gs pathway through human beta2-adrenoceptors overexpressed in mouse heart. *Mol Pharmacol.* (2004) 65:1313–22. doi: 10.1124/mol.65.5.1313
44. Zhao Z, Lan H, El-Battrawy I, Li X, Buljubasic F, Sattler K, et al. Ion channel expression and characterization in human induced pluripotent stem cell-derived cardiomyocytes. *Stem Cells Int.* (2018) 2018:6067096. doi: 10.1155/2018/6067096
45. Banday AA, Marwaha A, Tallam LS, Lokhandwala MF. Tempol reduces oxidative stress, improves insulin sensitivity, decreases renal dopamine D1 receptor hyperphosphorylation, and restores D1 receptor-G-protein coupling and function in obese Zucker rats. *Diabetes.* (2005) 54:2219–26. doi: 10.2337/diabetes.54.7.2219
46. Marwaha A, Lokhandwala MF. Tempol reduces oxidative stress and restores renal dopamine D1-like receptor- G protein coupling and function in hyperglycemic rats. *Am J Physiol Renal Physiol.* (2006) 291:F58–66. doi: 10.1152/ajprenal.00362.2005
47. Hussain T, Lokhandwala MF. Renal dopamine receptor function in hypertension. *Hypertension.* (1998) 32:187–97. doi: 10.1161/01.HYP.32.2.187

48. Muscella A, Vetrugno C, Antonaci G, Cossa LG, Marsigliante S. PKC-δ/PKC-α activity balance regulates the lethal effects of cisplatin. *Biochem Pharmacol.* (2015) 98:29–40. doi: 10.1016/j.bcp.2015.08.103

Conflict of Interest: The authors declare that the research was conducted in the absence of any commercial or financial relationships that could be construed as a potential conflict of interest.

Publisher's Note: All claims expressed in this article are solely those of the authors and do not necessarily represent those of their affiliated organizations, or those of the publisher, the editors and the reviewers. Any product that may be evaluated in this article, or claim that may be made by its manufacturer, is not guaranteed or endorsed by the publisher.

frontiers in Cardiovascular Medicine

ORIGINAL RESEARCH
published: 16 February 2022
doi: 10.3389/fcvm.2022.813914

Machine Learning-Predicted Progression to Permanent Atrial Fibrillation After Catheter Ablation

Je-Wook Park[1†], Oh-Seok Kwon[1†], Jaemin Shim[2], Inseok Hwang[1], Yun Gi Kim[2], Hee Tae Yu[1], Tae-Hoon Kim[1], Jae-Sun Uhm[1], Jong-Youn Kim[1], Jong Il Choi[2], Boyoung Joung[1], Moon-Hyoung Lee[1], Young-Hoon Kim[2] and Hui-Nam Pak[1*]*

[1] Division of Cardiology, Yonsei University Health System, Seoul, South Korea, [2] Department of Internal Medicine, Korea University Cardiovascular Center, Seoul, South Korea

OPEN ACCESS

Edited by:
Christoph Sinning,
University Medical Center
Hamburg-Eppendorf, Germany

Reviewed by:
Hangsik Shin,
Chonnam National University,
South Korea
Prabhat Kumar,
University of North Carolina at Chapel
Hill, United States
Carlo de Asmundis,
University Hospital Brussels, Belgium

***Correspondence:**
Jaemin Shim
jaemins@korea.ac.kr
Hui-Nam Pak
hnpak@yuhs.ac

[†] These authors have contributed equally to this work and share first authorship

Specialty section:
This article was submitted to Cardiac Rhythmology, a section of the journal Frontiers in Cardiovascular Medicine

Received: 12 November 2021
Accepted: 25 January 2022
Published: 16 February 2022

Citation:
Park J-W, Kwon O-S, Shim J, Hwang I, Kim YG, Yu HT, Kim T-H, Uhm J-S, Kim J-Y, Choi JI, Joung B, Lee M-H, Kim Y-H and Pak H-N (2022) Machine Learning-Predicted Progression to Permanent Atrial Fibrillation After Catheter Ablation. Front. Cardiovasc. Med. 9:813914. doi: 10.3389/fcvm.2022.813914

Introduction: We developed a prediction model for atrial fibrillation (AF) progression and tested whether machine learning (ML) could reproduce the prediction power in an independent cohort using pre-procedural non-invasive variables alone.

Methods: Cohort 1 included 1,214 patients and cohort 2, 658, and all underwent AF catheter ablation (AFCA). AF progression to permanent AF was defined as sustained AF despite repeat AFCA or cardioversion under antiarrhythmic drugs. We developed a risk stratification model for AF progression (STAAR score) and stratified cohort 1 into three groups. We also developed an ML-prediction model to classify three STAAR risk groups without invasive parameters and validated the risk score in cohort 2.

Results: The STAAR score consisted of a stroke (2 points, $p = 0.003$), persistent AF (1 point, $p = 0.049$), left atrial (LA) dimension $\geq$43 mm (1 point, $p = 0.010$), LA voltage $<$1.109 mV (2 points, $p = 0.004$), and PR interval $\geq$196 ms (1 point, $p = 0.001$), based on multivariate Cox analyses, and it had a good discriminative power for progression to permanent AF [area under curve (AUC) 0.796, 95% confidence interval (CI): 0.753–0.838]. The ML prediction model calculated the risk for AF progression without invasive variables and achieved excellent risk stratification: AUC 0.935 for low-risk groups (score = 0), AUC 0.855 for intermediate-risk groups (score 1–3), and AUC 0.965 for high-risk groups (score $\geq$ 4) in cohort 1. The ML model successfully predicted the high-risk group for AF progression in cohort 2 (log-rank $p < 0.001$).

Conclusions: The ML-prediction model successfully classified the high-risk patients who will progress to permanent AF after AFCA without invasive variables but has a limited discrimination power for the intermediate-risk group.

Keywords: atrial fibrillation, catheter ablation, progression, machine learning, risk score

INTRODUCTION

Atrial fibrillation catheter ablation (AFCA) is known to be effective for rhythm control management, which can improve symptoms and quality of life in atrial fibrillation (AF) patients (1). Recent study and guideline reported a beneficial effect of AFCA on mortality and heart failure hospitalization in AF patients with left ventricular dysfunction (1, 2). Although there is a substantial recurrence rate after AFCA, a positive clinical impact can be expected from a reduction in AF

burden itself unless sustained AF continues after a procedure (3, 4). Recurrence after AFCA is defined as AF or atrial tachycardia (AT) of 30 s or more regardless of symptoms (1). At this point, although it is important to reduce a recurrence rate of atrial arrhythmias lasting 30 s, it might also be very important to identify progression to permanent AF in which it is difficult to control sustained AF even after repeated procedures or with use of antiarrhythmic drugs (AADs). By predicting progression to permanent AF before a *de novo* AFCA procedure, we can select patients who are not likely to progress to permanent AF, thereby reducing any unnecessary risk and cost and potentially improving a success rate of a procedure. Therefore, pre-discovery of patients who are likely to progress to permanent AF using pre-procedural parameters may contribute to improvements in AFCA rhythm and clinical outcomes. However, many peri-procedural predictors, including both non-invasive and invasive parameters, contribute in a complex manner to AFCA rhythm outcomes (5). So variable studies reported or validated the risk model for AF recurrence in the patients who underwent repeat ablations (5). Those studies showed the range of ACU from 0.487 to 0.833. However, only a study reported risk model derived from over 1,000 patient population (6), but the follow-up duration was relatively short of investigating the progression to permanent AF (mean 2.5 years). Based on a variety of sources of complex patient information, including electronic medical records (EMRs) and imaging data, artificial intelligence (AI) has been used to detect AF and to predict ablation outcomes (7–12). Furthermore, AI has been suggested for predicting invasive parameters or invasive cardiovascular outcomes (13).

In this retrospective analysis of prospective AFCA cohort data, we aimed to develop a machine learning (ML)-prediction model to identify patients with progression to permanent AF using the pre-procedural non-invasive factors. As an intermediate step for developing the ML prediction model, we used a risk score derived from this study population and identified the high-risk group for progression to permanent AF. Therefore, we developed and used an ML prediction model to classify the patients into risk score-based groups associated with progression to permanent AF.

Abbreviations: AFCA, atrial fibrillation catheter ablation; AAD, antiarrhythmic drugs; RF, random forest; STAAR, risk model consisting of previous history of a stroke or transient ischemic attack, type of AF, left atrial dimension, left atrial voltage, PR interval; Eem, peak transmitral flow velocity (E), and tissue Doppler echocardiography of the peak septal mitral annular velocity (em); ALARMEc, risk model consisting of type of AF, metabolic syndrome, eGFR, and normalized left atrial area; APPLE, risk model consisting of age, type of AF, eGFR, left atrial diameter, and left ventricular ejection farction; ATLAS, risk model consisting of age, sex, type of AF, current smoking, and indexed left atrial volume; CAAP-AF, risk model consisting of age, sex, type of AF, LAD, coronary artery disease, and number of antiarrhythmic drugs failed; HATCH, risk model consisting of age, heart failure, hypertension, chronic obstructive pulmonary disease, and stroke/transient ischemic attack; BASE-AF2, risk model consisting of type of AF, LAD, body mass index, current smoking, AF history, and early recurrence; MB-LATER, risk model consisting of sex, type of AF, LAD, early recurrence, and bundle branch block.

METHODS

Study Population

This study protocol adhered to the principles of the Declaration of Helsinki and was approved by the Institutional Review Board of the Yonsei University Health System. All patients provided written informed consent for inclusion in the Yonsei AF Ablation Cohort Database (registered at ClinicalTrials.gov, Identifier: NCT02138695). **Figure 1** shows the enrollment into this study. A total of 1,850 patients who underwent AFCA from 2009 to 2018 were registered in the Yonsei AF ablation cohort. The cohort was adjusted based on the following exclusion criteria: (1) permanent AF refractory to electrical cardioversion, (2) AF with rheumatic valvular disease, or any mechanical or bioprosthetic heart valve, (3) prior cardiac surgery with concomitant AF surgery or AF catheter ablation, and (4) the absence of a mean left atrial (LA) voltage that could be obtained during the *de novo* ablation procedure. Finally, 1,214 patients {mean age: 58.7 ± 10.9 years, 26.5% female, 31.4% persistent AF, median follow-up duration [interquartile range (IQR)]: 51.4 months (26.9, 83.7)} were enrolled and used to develop risk score and ML prediction models in this study.

Among the 1,214 patients in the development data, 791 remained in sinus rhythm after the first AFCA during the follow-up period [median 38.5 months (23.9, 70.7)]. Among the 423 patients who experienced AF/AT recurrences after the first AFCA, 143 underwent repeat ablation sessions and 280 underwent electrical cardioversion under AADs to restore sinus rhythm. We considered the progression to permanent AF, which is the endpoint of this study, as sustaining AF detected on an electrocardiogram (ECG) or Holter/event-monitor after last ablation procedures with AADs or electrical cardioversion. For example, the patient was considered as progression to permanent AF group when the rhythm status was AF in an ECG or Holter-monitoring at last visit of outpatient clinics on AADs for recurred AF after the last ablation procedures. We defined the controlled arrhythmia group as consisting of those patients who experienced no AF/AT recurrences or intermittent AF/AT after the repeat ablation sessions, AADs, or electrical cardioversion during the follow-up period. Finally, we obtained the following groups from the development data: 1,122 patients with controlled arrhythmias and 92 with progression to permanent AF.

Electrocardiographic, Echocardiographic, and Cardiac Computed-Tomography Evaluations

In order to develop a risk model, we used 12-lead ECG, in which the sinus rhythm and PR interval can be identified, that was be obtained most recently before AFCA, as previously described (14). In brief, the 12-lead ECG of all patients (GE Healthcare, Marquette, MAC5500, Waukesha, WI) was obtained in this study. The paper speed was 25 mm/s and calibration 10 mm/mV. All patients underwent transthoracic echocardiography before the *de novo* procedure. We obtained the echocardiographic parameters according to the American Society of Echocardiography guidelines. The patients underwent three-dimensional (3D) spiral CT scans (64 Channel, LightSpeed

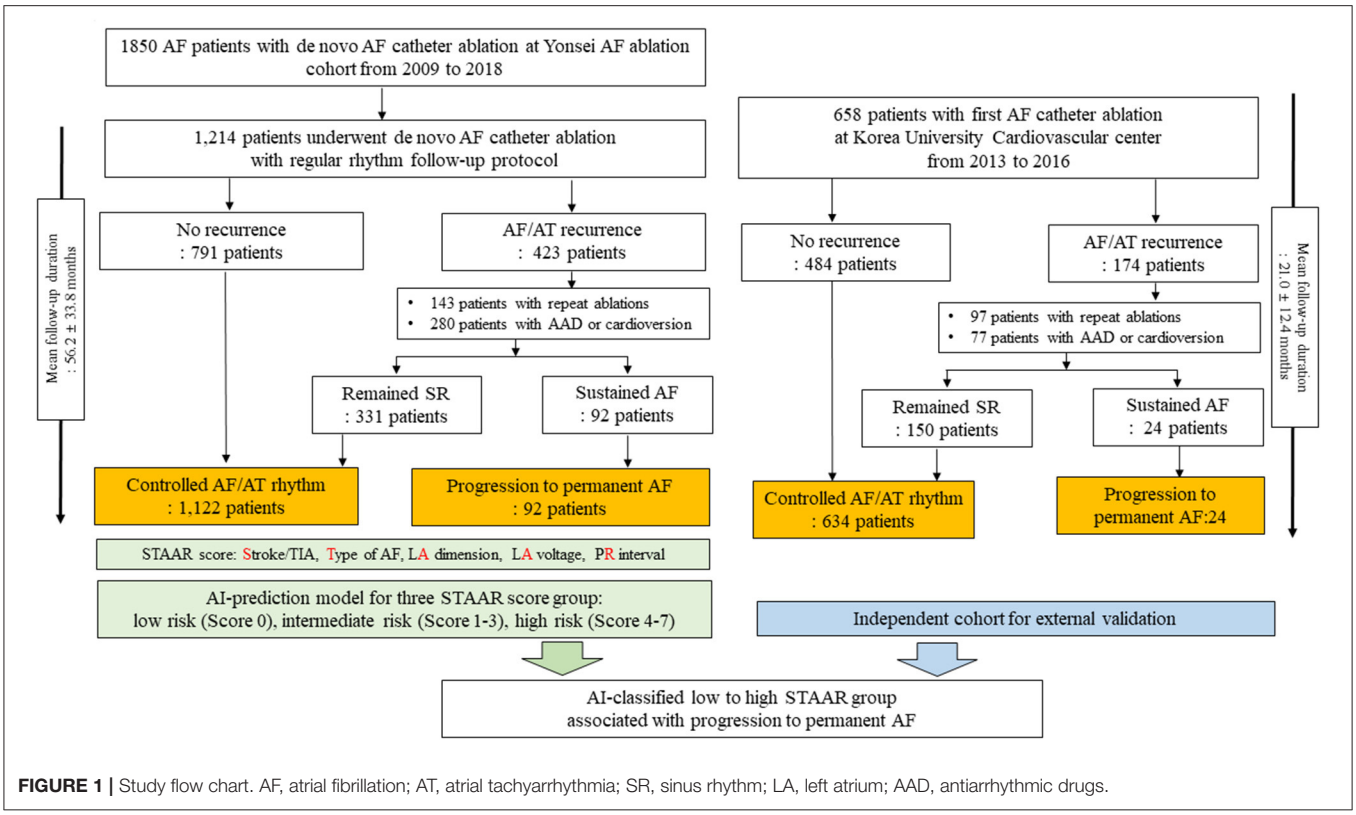

FIGURE 1 | Study flow chart. AF, atrial fibrillation; AT, atrial tachyarrhythmia; SR, sinus rhythm; LA, left atrium; AAD, antiarrhythmic drugs.

Volume CT, Philips, Brilliance 63, Amsterdam, Netherlands) to define the pulmonary vein (PV) anatomy. The 3D spiral CT images of the LA were analyzed on an imaging processing workstation (Aquarius, TeraRecon Inc., Foster City, California, United States).

Electrophysiological Mapping and Radiofrequency Catheter Ablation

AFCA was performed by using a 3D electroanatomical mapping system (NavX, St. Jude Medical, Inc., Minnetonka, Minnesota, United States; CARTO, Biosense-Webser, Inc., Diamond Bar, California, United States). We conducted multi-view pulmonary venograms after the transseptal puncture. The 3D electroanatomical geometry of both the LA and PVs was constructed and merged with the 3D spiral CT images. An LA voltage map was obtained during sinus rhythm using bipolar electrograms from 350 to 500 points on the LA endocardium during atrial pacing at 500 ms, and the mean LA voltage was calculated according to previous reports (15, 16). The LA voltage data was obtained in all patients of the dependent cohort. If the initial rhythm was AF before the ablation procedure, we restored sinus rhythm using internal electrical cardioversion. If the AF was frequently reinitiated after recurrent electrical cardioversion before the ablation procedure, we obtained LA voltage map after the ablation procedure.

An open-irrigated tip catheter (Celsius, NaviStar ThermoCool, ThermoCool SF, and ThermoCool SmartTouch, Johnson & Johnson Inc., Diamond Bar, California, United States; CoolFlex, FlexAbility, and TactiCath, St. Jude Medical Inc., Minnetonka, Minnesota, United States) was used for the AFCA. All patients underwent a *de novo* procedure with a circumferential pulmonary vein isolation (CPVI). The majority of the patients (91.8%) underwent a cavotricuspid isthmus (CTI) block procedure during the *de novo* procedure unless there was atrioventricular conduction disease. We added additional linear ablation such as a roof line, posterior inferior line (posterior box lesion), or anterior line, especially in patients with persistent AF. A left lateral isthmus ablation, right atrial ablation, and complex fractionated electrogram ablation were performed in a minority of the patients at the operator's discretion. We ended the *de novo* procedure when there was no immediate recurrence of AF within 10 min after the cardioversion with an isoproterenol infusion (5–10 μg/min depending on ß-blocker use and target sinus heart rate of 120 bpm). In the case of mappable AF triggers or premature atrial beats, the extra-PV foci were carefully mapped and ablated as much as possible. Systemic anticoagulation was achieved using intravenous heparin to maintain an activated clotting time of 350–400 s during the procedure.

Post-ablation Management and Follow-Up

Patients visited an outpatient clinic at 1, 3, 6, and 12 months and every 6 months thereafter or whenever symptoms developed after AFCA. Patients underwent an ECG at every visit. Twenty-four-hour Holter monitoring was performed at 3, 6, and 12 months and then every 6 months after the AFCA according to the 2012 Heart Rhythm Society/European Heart

Rhythm Association/European Cardiac Arrhythmia Society expert consensus statement guidelines. Whenever the patients suffered from symptoms of palpitations, Holter/event-monitor examinations were performed to investigate the possibility of an arrhythmia recurrence. We defined an AF/AT recurrence as any episode of AT or AF lasting for 30 s or more. Any electrocardiography documentation of an AF recurrence after a 3-month blanking period was classified as a clinical recurrence.

Management of Recurrence and Progression to Permanent AF

Patients who experienced AF/AT recurrences after the first AFCA were prescribed AADs or electrical cardioversion based on the rhythm condition. If a recurrent atrial arrhythmia could not be controlled by medications, we recommended a repeat ablation to the patients and their family members. We previously reported the detailed technique and strategy for repeat ablation procedures (17). In brief, if there were reconnections of the PV potentials, a CTI or additional linear lines that were created in the index procedure, we first completed them as much as possible. Then, we provoked extra-PV foci with an isoproterenol infusion (5–10 μg /min) and carefully mapped and ablated any mappable AF triggers or frequent atrial premature beats.

After the repeat ablation procedures, we performed a serial rhythm follow-up, adhering to the above-mentioned protocol. We defined patients with progression to permanent AF as those patients who remained in a sustained AF/AT rhythm at the final follow-up date despite a repeat ablation, AADs, or electrical cardioversion.

Risk Score for Progression to Permanent AF: STAAR Score

We performed Cox regression analysis using clinical variables to develop the risk score for progression to permanent AF. First, we decided on the optimal cut-off values for the LA dimension (43 mm), PR interval (196 ms), and mean LA voltage (<1.109 mV) by using the Youden index. The predictors with p-values < 0.05 in the univariate Cox regression model and age were included in the multivariate Cox regression model without any stepwise methods. Finally, five predictors including persistent AF at baseline, a history of a stroke or TIA, an enlarged LA (≥43 mm), a prolonged PR interval (≥196 ms), and a low mean LA voltage (<1.109 mV) were associated with progression to permanent AF (**Supplementary Table 1**). Then, the STAAR score was developed using the following five predictors: a previous history of a stroke or transient ischemic attack (TIA, S), type of AF (T), LA dimension (A), LA voltage (A), and PR interval (R). The STAAR score was calculated based on the beta coefficients, which were divided by the smallest absolute value of the regression coefficient and rounded to the nearest integer. And each patient was calculated by summing the points assigned to each predictor (**Supplementary Table 2**): a previous history of a stroke or TIA (2 points), the AF type (1 point for persistent AF at the time of the diagnosis), LA size (1 point for an enlarged LA ≥ 43 mm), mean LV voltage (2 points for a low mean LA voltage < 1.109 mV), and PR interval (1 point for a prolonged PR interval ≥ 196 ms).

Random Forest for Developing the ML-Prediction Model to Classify Three STAAR Risk Groups

Using the median and interquartile value of STAAR score in the overall population, the patients with individual STAAR scores were divided into three STAAR risk groups which had each risk level for progression to permanent AF; low risk (score 0) for progression to permanent AF, intermediate-risk (score 1–3) for progression to permanent AF, and high risk (score 4–7) for progression to permanent AF. Because the STAAR score needed the invasive parameter such as LA voltage, we developed an ML-prediction model for predicting three STAAR risk groups for progression to permanent AF using non-invasive parameters. For a risk stratification model of AF progression to permanent AF (STAAR score), we developed a model based on the Random Forest (RF) (18) and implemented the software with a Scikit-learn library (version 1.0.1). The input parameters (15×1) used non-invasive clinical features [age, female sex, AF type, body mass index (BMI), congestive heart failure (CHF), hypertension, diabetes mellitus, stroke or TIA, vascular disease, LA dimension, left ventricular ejection fraction (LVEF), Eem [peak transmitral flow velocity (E) divided by tissue Doppler echocardiography of the peak septal mitral annular velocity (Em)], creatinine, hemoglobin, and pre-ablation PR interval]. Before hyperparameter selection by cross-validation, the training and test sets were randomly divided at an 8:2 ratio. Then, an optimal model was induced with 20-fold cross-validation from the training set (0.8) and the predictive performance of the RF classifier was evaluated with the test set (0.2). However, it may still induce overlooked biases as the data sets provided for cross-validation may not be representative of patient or population diversity (19). Therefore, we performed the nested cross-validation with five "outer" test sets consisting of 5 iterations. Finally, we identify the best RF classifier with this nested cross-validation procedure. The output Y_{class} consisted of three classes and each class was divided into the following criteria:

$$Y_{class}(z) = \begin{cases} Low-risk\ group, & z < 1 \\ Intermediate-risk\ group, & 1 \le z \le 3 \\ High-risk\ group, & z > 3 \end{cases},$$

where z is the STAAR score, and Y_{class} has a higher risk when it increases from 0 to 2. Hyperparameters for optimal performance of the RF model were carefully selected by grid search algorithm (20) using the GridSearchCV function of the Scikit-learn library. The selected hyperparameters are bootstrap: true, the maximum depth of the tree (max_depth: 8), the number of features to consider when looking for the best split (max_feature: 5), the minimum number of samples required to be at a leaf node (min_samples_leaf: 4), the minimum number of samples required to split an internal node (min_samples_split: 10), and the number of trees in the forest (n_estimators: 100). The selected hyperparameters and search ranges are shown in **Supplementary Table 3**. **Supplementary Figure 1** shows an

example of a trained first decision tree. To check for overfitting (using the Scikit-learn library version 1.0.1), the results using a method of High Energy Physics showed that the effect of the class imbalance is not significant with the distance of the points (test set) to the bars (training set) (**Supplementary Figure 2**). For the reproducibility, all model training was performed for five iterations with a random sample.

Independent AFCA Cohort to Predict the Ablation Outcome

For external validation of the ML-prediction model to classify three STAAR risk groups, we used an independent AF ablation cohort that included 805 patients who underwent their first AFCA at Korea University Cardiovascular Center between 2013 and 2016. From this independent data, we enrolled and analyzed 658 patients who were classified into three risk groups for progression to permanent AF based on the ML-prediction model that classified three STAAR risk groups. Among the 658 patients in the independent cohort, 484 remained in sinus rhythm after the first AFCA during the follow-up period. Of the 174 patients who experienced an AF/AT recurrences after the first AFCA, 97 underwent repeat ablation sessions and 77 underwent AADs or electrical cardioversion during the follow-up period. Finally, we identified 634 patients as the controlled arrhythmia group and 24 as the progression to permanent AF group for the external validation. There were significant size and follow-up duration discrepancies between training and external validation cohorts, but the ablation procedure data of two cohorts were similar to each other.

Statistical Analysis

Continuous variables are reported as means ± standard deviations (SD) and were analyzed using an independent *t*-tests. Categorical variables are reported as numbers (percentages) and were analyzed using a Chi-square or Fisher's exact test. We defined a cut-off value of the LA dimension, PR interval, and LA voltage using the Youden index. The Youden index decides a cut-off point at the specific value where the amount of sensitivity plus specificity was maximal value (21, 22). As a result, the Youden index yielded the highest value of the following equation at the specific point: sensitivity + specificity-1. To develop STAAR risk model, we included the predictors with p-values < 0.05 in the univariate Cox regression analysis and age in the multivariate Cox regression analysis without any stepwise methods. CHA2DS2VASc score was excluded in multivariate Cox regression analysis because the score already included age, previous history of congestive heart failure, and stroke/TIA (**Supplementary Table 1**). We confirmed the proportional hazard assumption of the STAAR risk model using log-minus-log Kaplan-Meier plot. Linear regression analysis was performed to investigate the relationship between pre-procedural factors and the STAAR score (**Supplementary Table 4**). The ANOVA test for continuous variables or a Chi-square or Fisher's exact test for categorical variables were performed to investigate characteristics among three STAAR risk groups before developing the ML-risk model to classify three STAAR risk groups (**Supplementary Table 5**). An independent *t*-test for continuous variables or a Chi-square or Fisher's exact test for categorical variables were used to investigate the difference in baseline characteristics between the controlled AF/AT group and progression to permanent AF group in the independent cohort (**Supplementary Table 6**). The STAAR score performance was assessed with a C-statistic representing the area under the curve (AUC) of the receiver operating characteristic (ROC) curve. Because the STAAR score included invasive parameters, the ML prediction model was developed based on the RF algorithm using non-invasive parameters to classify the patients into three risk groups for progression to permanent AF. A Kaplan-Meier analysis was used to investigate the freedom from progression to permanent AF in the three STAAR groups of the development cohort and the three ML-predicted risk groups in the independent cohort. A p-value < 0.05 was considered statistically significant. All statistical analyses were performed using SPSS (Statistical Package for Social Sciences, Chicago, Illinois, United States) software for Windows (version 23.0) and the R package (3.1.0, R Foundation for Statistical Computing, Boston, Massachusetts, United States).

RESULTS

Baseline Characteristics

The comparison of the baseline characteristics between the controlled AF/AT group ($n = 1{,}122$; 92.4%) and progression to permanent AF group ($n = 92$, 7.6%) is presented in **Table 1**. Patients with progression to permanent AF had a higher proportion of baseline persistent AF ($p < 0.001$), higher BMI ($p = 0.039$), higher number of previous stroke or TIA events, and longer PR interval than the controlled AF/AT group. In terms of the echocardiographic parameters, the LA dimension ($p < 0.001$) was larger in the progression group than in the rhythm-controlled group. The invasive parameters acquired during *de novo* ablation procedures showed that the LA voltage was lower ($p < 0.001$), ablation time was longer ($p = 0.036$), and extra-PV LA ablation more commonly performed ($p = 0.001$) in the progression group than its counterpart (**Table 2**). In the independent cohort with median 18.9 (IQR: 11.4, 30.3) months of follow-up, mean age was 56.8 ± 10.7 years, the proportion of female was 20.8%, and the proportion of persistent AF was 40.3%.

Association Between the STAAR Score and Progression to Permanent AF

In the development data, an AUC of ROC curve of the STAAR score, which showed the discriminative power for progression to permanent AF, was 0.796 (95% CI: 0.753–0.838, **Figure 2A**). The STAAR score ranged from 0 to 7 points. There was a significantly increased proportion of patients who progressed to permanent AF in those with a higher risk score (0% at a risk score of 0 to 50% at a risk score of 7, p-value for the trend < 0.001, **Figure 2B**). The patients were classified into three risk groups which had each risk level for progression to permanent AF: low (0 points), intermediate (1–3 points), and high (>3 points). The population and baseline characteristics in the three risk groups are presented in **Supplementary Table 5**. The high-risk group for progression to permanent AF was older ($p < 0.001$),

TABLE 1 | Baseline characteristics during the *de novo* ablation procedure.

	Overall patients (n = 1,214)	Controlled AF/AT (n = 1,122)	Progression to permanent AF (n = 92)	p-value
Age, years	58.7 ± 10.9	58.6 ± 11.0	60.1 ± 10.0	0.193
Female	322 (26.5%)	298 (26.6%)	24 (26.1%)	0.921
Persistent AF at diagnosis	381 (31.4%)	325 (29.0%)	56 (60.9%)	**<0.001**
Body mass index, kg/m^2	25.0 ± 3.2	25.0 ± 3.2	25.7 ± 3.1	**0.039**
CHA_2DS_2VASc score	1.7 ± 1.6	1.7 ± 1.5	2.0 ± 1.7	0.053
CHF	126 (10.4%)	114 (10.2%)	12 (13.0%)	0.383
Hypertension	575 (47.4%)	527 (47.0%)	48 (52.2%)	0.336
Diabetes mellitus	176 (14.5%)	161 (14.3%)	15 (16.3%)	0.609
Stroke/TIA	143 (11.8%)	123 (11.0%)	20 (21.7%)	**0.002**
Vascular disease	150 (12.4%)	142 (12.7%)	8 (8.7%)	0.267
LA dimension, mm	41.3 ± 6.1	41.0 ± 6.0	45.2 ± 5.9	**<0.001**
LVEF, %	63.3 ± 8.4	63.4 ± 8.3	62.2 ± 9.2	0.208
EEm (n = 1,159)	10.2 ± 4.2	10.1 ± 4.1	10.9 ± 5.2	0.111
Creatinine, mg/dL	0.9 ± 0.3	0.9 ± 0.3	0.9 ± 0.3	0.737
Hemoglobin, g/dL	14.4 ± 1.5	14.4 ± 1.5	14.5 ± 1.3	0.355
Pre-ECG PR interval, ms	184.0 ± 31.8	182.6 ± 29.7	201.4 ± 40.6	**<0.001**

AF, atrial fibrillation; AT, atrial tachyarrhythmia; CHF, congestive heart failure; TIA, transient ischemic attack; LA, left atrium; LVEF, left ventricular ejection fraction; Eem, peak transmitral flow velocity (E), and tissue Doppler echocardiography of the peak septal mitral annular velocity (Em); ECG, electrocardiography. The bold values represents p-value <0.05.

TABLE 2 | Ablation characteristics and outcomes during the *de novo* ablation procedure.

	Overall patients (n = 1,214)	Controlled AF/AT (n = 1,122)	Progression to permanent AF (n = 92)	p-value
Mean LA voltage, mV	1.3 ± 0.6	1.3 ±0.6	0.9 ± 0.5	**<0.001**
Ablation time, min	81.4 ± 27.5	81.0 ± 27.3	87.3 ± 29.3	**0.036**
Procedure time, min	181.2 ± 53.3	180.2 ± 52.7	193.2 ± 58.7	**0.025**
Contact force sensing catheter	95 (7.8%)	89 (7.9%)	6 (6.5%)	0.628
Extra-PV LA ablation	442 (36.4%)	393 (35.1%)	49 (53.3%)	**0.001**
Roof line	436 (36%)	387 (34.6%)	49 (53.3%)	**<0.001**
Postero-inferior line	373 (30.8%)	334 (29.8%)	39 (42.4%)	**0.012**
Left latera isthmus	48 (4.0%)	42 (3.8%)	6 (6.5%)	0.171
Anterior line	325 (26.8%)	283 (25.2%)	42 (45.7%)	**<0.001**
Bidirectional block of linear ablation				
Roof line	378/436 (86.7%)	334/387 (86.3%)	44/49 (86.3%)	0.498
Postero-inferior line	218/373 (58.4%)	202/334 (60.5%)	16/39 (41%)	**0.020**
Left lateral isthmus line	10/48 (20.8%)	10/42 (23.8%)	0 (0%)	0.320
Anterior line	231/325 (65.5%)	187/283 (66.1%)	26/42 (61.9%)	0.595
CFAE ablation	63 (5.2%)	54 (4.8%)	9 (9.8%)	**0.049**
Post-ablation AAD use	194 (16%)	161 (14.4%)	33 (35.9%)	**<0.001**
Type of AAD after recurrence (n = 249)				
Class Ic drug	90 (36.1%)	73 (38.2%)	17 (29.3%)	0.216
Class III drug	159 (63.9%)	118 (61.8%)	41 (70.7%)	
Number of repeat ablations (in 143 patients)	2.0 ± 0.3 (n = 143)	2.1 ± 0.3 (n = 118)	2.0 ± 0.4 (n = 25)	0.203
Duration between 1st and 2nd AFCA, months (n = 143)	35.7 ± 26.6	36.4 ± 26.8	31.8 ± 25.5	0.443
AF/AT recurrence after repeat ablations	55/143 (38.5%)	30/118 (25.4%)	25 (100%)	**<0.001**
Progression to permanent AF after repeat ablations	25/143 (17.5%)	0 (0%)	25 (100%)	**<0.001**

AF, atrial fibrillation; AT, atrial tachyarrhythmia; PV, pulmonary vein; LA, left atrium; CFAE, complex fractionated atrial electrogram; AAD, antiarrhythmic drugs; AFCA, AF catheter ablate. The bold values represents p-value <0.05.

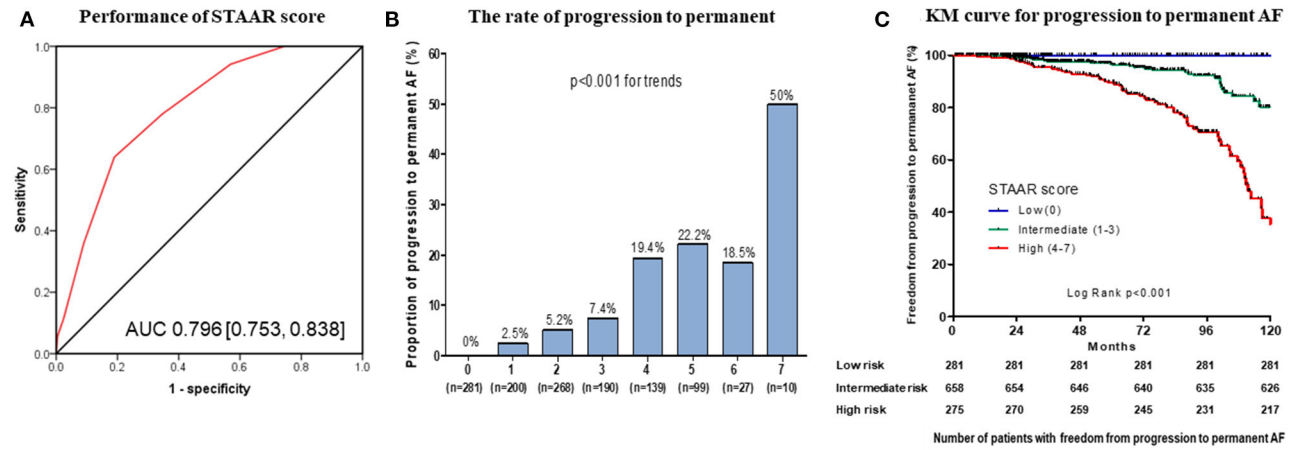

FIGURE 2 | Performance and Kaplan-Meier (KM) analysis of the STAAR score. Performance of the STAAR score for the discrimination of the progression to permanent AF **(A)**. The rate of progression to permanent AF according to the STAAR score **(B)**. KM analysis with censor marker (black vertical line) of the progression to permanent AF according to the STAAR group **(C)**. AF, atrial fibrillation; AUC, area under the curve.

had more proportion of comorbidities, more enlarged LA ($p < 0.001$), and more prolonged PR interval on ECG before ablation ($p < 0.001$) as compared to low and intermediate-risk group. The high-risk group for progression to permanent AF had a significantly greater progression to permanent AF than the low-risk and intermediate-risk groups for progression to permanent AF in the Kaplan-Meier analysis (log-rank $p < 0.001$, **Figure 2C**).

ML-Prediction Model Predicting the Progression to Permanent AF

Using pre-procedural non-invasive variables (age; female sex; AF type; BMI; comorbidities including CHF, hypertension, diabetes mellitus, stroke or TIA, vascular disease; LA dimension; LVEF; EEm creatinine; hemoglobin; and pre-ablation PR interval), we developed an ML prediction model to stratify the risk for the progression to permanent AF in cohort 1. We chose those 15 variables based on a linear regression analysis without multicollinearity among the variables (**Supplementary Table 4**). The training and test set were derived from randomly selected samples in each test. All tests were performed five times. The mean ROC curves of the five tests, which had a discriminative power for the three risk groups for progression to permanent AF, are presented in **Figure 3A**. The performance of the five ML prediction models to classify three STAAR risk groups is presented in **Table 3**. Among the five randomly tested models, we chose the best prediction model, Test 4 in **Supplementary Table 7** (performance predicting low risk: AUC 0.935, sensitivity 0.945, specificity 0.847; performance predicting intermediate risk: AUC 0.855, sensitivity 0.717, specificity 0.848; and performance predicting high risk: AUC 0.965, sensitivity 0.960, specificity 0.890) for the verification in the independent cohort 2. In the independent cohort 2, the ML prediction model using pre-procedural non-invasive variables successfully classified the three risk groups for progression to permanent AF, and the patients in the ML-predicted high-risk group had a significantly higher rate of progression to permanent AF than those in the low-risk (log-rank $p < 0.001$, **Figure 3B**) and the intermediate-risk (log-rank $p = 0.001$, **Figure 3B**) groups.

DISCUSSION

Main Findings

In this study, we investigated that the high STAAR score group (4–7) had a higher rate of progression to permanent AF after AFCA. However, the STAAR score was derived from an invasive parameter that could be obtained during the procedure. Using STAAR score as a labeling criterion, an ML prediction model based on a RF algorithm was developed to classify patients into risk groups for progression to permanent AF using non-invasive pre-AFCA variables. ML-predicted high-risk patients had a higher rate of progression to permanent AF than non-high-risk patients in an independent cohort.

Mechanisms of AF Progression After AFCA

As a mechanism of recurrent AF after AFCA, technical factors such as an incomplete or inefficient ablation and disease factors such as substrate remodeling can be considered. Among the technical factors, there are operator factors and limitations of the current ablation technology. The operator-dependent variability of ablation success has been gradually decreasing due to development of contact force catheter technology and software such as an ablation index, lesion index, and one-shot technologies including cryoballoon ablation (23, 24). However, reconnections of PV potentials are still commonly observed in patients with recurrent AF, and we need to recognize limitations of the current ablation technology in generating a permanent conduction block during AFCA (17, 25, 26).

Nevertheless, AF is a progressive disease, and substrate remodeling is an important mechanism of AF progression and a long-term AF recurrence. Sustained AF aggravates atrial structural and electrical remodeling itself, which leads

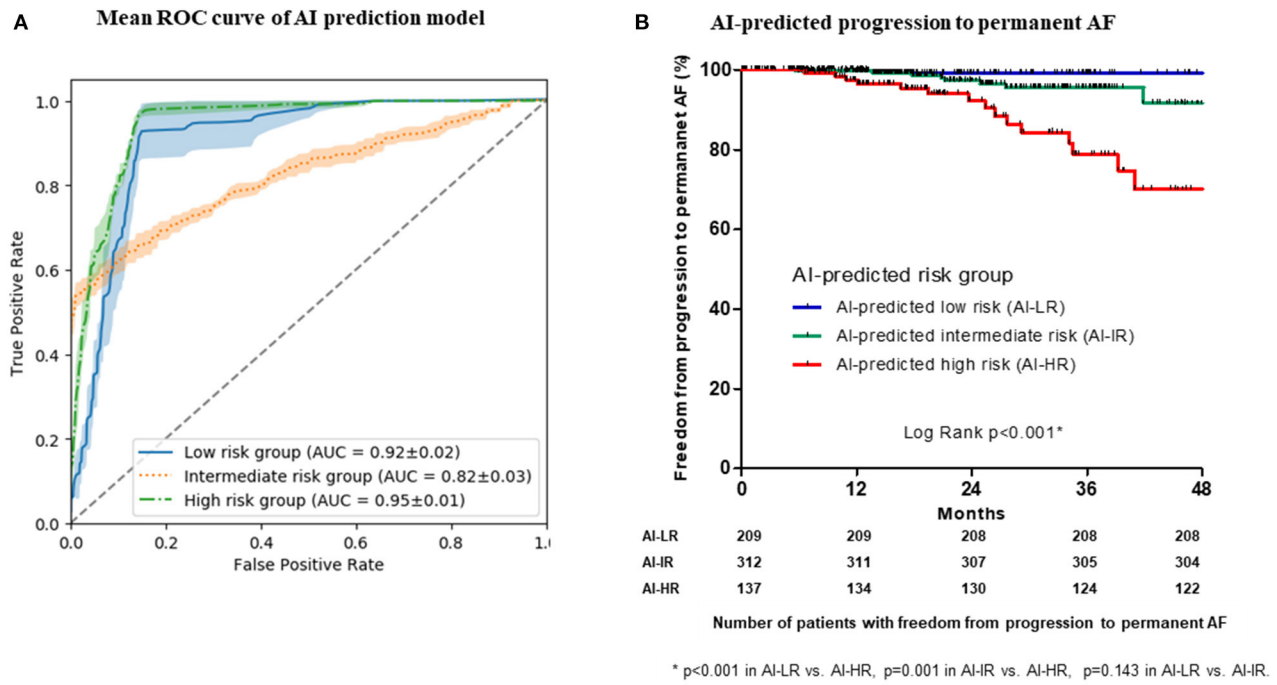

FIGURE 3 | The mean area under the curve (AUC) of the receiver operating characteristic (ROC) curves of the machine learning (ML) prediction model to classify three STAAR risk groups **(A)**. Kaplan-Meier analysis with censor marker (black vertical line) of the progression to permanent AF according to the ML-predicted risk groups in the independent cohort **(B)**. AF, atrial fibrillation.

to a persistent AF burden (27). Pre-existing atrial remodeling, including an atrial low voltage substrate (28), magnetic resonance imaging (MRI)-detected atrial fibrosis (29), and elevated atrial pressure (30), have been proven to have negative effects on the rhythm outcome after AFCA. The PR interval reflects atrial remodeling with electrophysiological heterogeneity and a conduction delay throughout the atrium, which results from atrial fibrosis and inflammation (31) The fact that patients without PV reconnections in the redo mapping more commonly have extra-PV triggers and a higher chance of recurrence after the repeat ablation suggests the important role of the atrial substrate as a mechanism of a long-term recurrence (17, 32).

STAAR Score and ML Risk Model to Classify Three STAAR Risk Groups Compared to Other Risk Models

Several risk models have been developed for AF recurrence after AFCA (5). Among them, there are two types of models: non-invasive and invasive risk models. Non-invasive risk models, which consist of non-invasive predictors, are ALARMEc, APPLE, ATLAS, CAAP-AF, and HATCH. These non-invasive risk models have discriminative power of AUC from 0.44 to 0.75. Invasive risk models, which consist of invasive predictors, are BASE-AF2 and MB-LATER. The AUC of these invasive risk models are between 0.57 and 0.94. However, a primary endpoint was progression to permanent AF in the current STAAR score and ML model in contrast with AF recurrence in other previous risk models. Because of this difference in an ablation outcome, we could not directly compare the performance for predicting ablation outcomes in the current model and other risk models. Although the highest AUC of invasive risk model is 0.94, early recurrence is an essential predictor for both BASE-AF2 and MB-LATER. Early recurrence can be obtained after AF ablation and may be underestimated in the patients with asymptomatic AF recurrence.

As compared to the published risk model and studies including repeat ablations (5), the current risk model was developed in the largest AF population who had the longest follow-up duration (**Supplementary Table 8**). We developed the current risk model using an ML algorithm to predict the high-risk patients progress to permanent AF despite AFCA using non-invasive non-imaging parameters. Therefore, the current ML-risk model can quickly discriminate the high-risk patient who might progress to permanent AF before the invasive ablations or expensive cardiac imaging at the outpatient clinics.

Prognostic Value of AI in Cardiovascular Disease

Few AI models have been reported in other studies to predict the rhythm outcome of AFCA. Shade et al. (10) reported an AI model combined with late gadolinium enhancement (LGE)-MRI images to assess a probability of AF recurrence during a median 1-year follow-up period in patients with paroxysmal AF. Firouznia et al. (33) and Liu et al. (34) suggested an AI model using CT images of the LA or PVs to predict AF recurrence after AF ablation (33) or non-PV triggers in paroxysmal AF patients

TABLE 3 | Summary of prediction performance of the five machine learning-prediction model for the three STAAR groups in the development cohort*.

	AUC	Sens	Spec	PPV	NPV	Gini	Loss	MSE	ACC
LRG	0.923 (0.896, 0.935)	0.927 (0.927, 0.945)	0.842 (0.836, 0.847)	0.646 (0.638, 0.658)	0.974 (0.974, 0.980)	0.846 (0.791, 0.870)	0.862 (0.858, 0.871)	0.923 (0.896, 0.935)	0.927 (0.927, 0.945)
IRG	0.828 (0.786, 0.852)	0.717 (0.661, 0.724)	0.800 (0.705, 0.848)	0.814 (0.752, 0.850)	0.697 (0.661, 0.706)	0.656 (0.572, 0.704)	0.759 (0.724, 0.772)	0.828 (0.786, 0.852)	0.717 (0.661, 0.724)
HRG	0.946 (0.943, 0.950)	0.940 (0.900, 0.960)	0.857 (0.846, 0.874)	0.649 (0.616, 0.671)	0.981 (0.969, 0.987)	0.892 (0.885, 0.901)	0.879 (0.858, 0.888)	0.946 (0.943, 0.950)	0.940 (0.900, 0.960)

**Each value of each risk group is presented as median (interquartile range) among five prediction model.*

AI, articial intelligence; LRG, low risk group; IRG, intermediate risk group; HRG, high risk group; AUC, area under the curve; Sens, sensitivity; Spec, specificity; PPV, positive predictive value; NPV, negative predictive value; Gini, gini coefficient; Loss, logit loss; MSE, mean squared error; ACC, accuracy.

without AF recurrence during a 1-year follow-up period (34). Budzianowski et al. (11) reported an AI model that investigated predictors of early AF recurrence after cryoballoon ablation in numerous EMR data. Image-based AI models for AF recurrence or AF triggers need complex preprocessing procedures because MRI and CT images should be adjusted for the AI algorithms (10, 33, 34). As shown in this study, the ML prediction model may identify patients who are poor responders or super-responders to the specific treatment modalities over the long-term.

In the present study, although the STAAR score could well predict patients with progression to permanent AF over the long-term follow-up period, the STAAR score included the invasive parameters that could be obtained during an ablation procedure. An ML prediction model to classify three STAAR risk groups, which used non-invasive variables that were obtained in EMR, could replace the STAAR score. Furthermore, the ML prediction model could classify the patients into three risk groups with long-term progression to permanent AF in the development cohort. In an independent cohort, it could identify patients at a high risk for progression to permanent AF.

Limitations

This study was an observational cohort study from two centers that included patients who were referred for AF ablation. There might be a selection bias. Due to the long duration of enrollment and follow-up, catheter technology and ablation strategies including additional linear ablation and extra-pulmonary foci ablation have been changed. It should be considered that those changes might affect the ablation results. Due to the different time of enrollment and follow-up duration between development and independent cohorts, it should be considered for the differences in type of catheter, ablation lesion set, and AF recurrence between the two cohorts. However, we found a time discrepancy of enrollment in training cohort and validation cohort in the previous AI-related studies (33, 35). Although PR interval can be influenced by medication, such as β-blockers or calcium channel blockers, and their dose, specific medication information at the time of sinus rhythm ECG was not available in this cohort study. Because the cut-off values of this study were derived from the patients in this single-cohort database, the values could not be fully applied to a wider population of AF. The number of the patients with progression to permanent AF was small in the replication cohort compared with an overall large population. Because the current ML model was validated in the independent cohort with a small number of events, this model may not be applied to the generalized AF population. Although it is common to set the label with the ground truth in the development of ML model, we used a STAAR score which is a processed risk score model. Therefore, a prospective randomized clinical trial is going on to prove the robustness of our ML model (ClinicalTrials.gov, NCT04997824). Because of using a one-vs.-all strategy for three groups of STAAR scores (low, intermediate, and high), the intermediate-risk group showed a relatively low AUC and the limited classification power from the low and high groups (**Supplementary Figure 3**). Although the current ML prediction model to classify three STAAR risk groups has been faithfully verified with 20-fold cross-validation and an external

test set, actual predictive performance may differ in actual clinical application and needs future prospective study. Since we could not obtain the exact duration of maintaining sinus rhythm, there might be some patients who experienced relatively less AF recurrence, even among patients with progression to permanent AF. Holter or ECG monitoring might be insufficient to detect the subclinical AF recurrence and the rate of progression to permanent AF could be underestimated. The assessment of the last rhythm status in this study was variable because of different tools and intermittent time intervals for checking rhythm status. So, the progression to permanent AF, the endpoint in this study, should not be the same meaning to continuous AF all day. Operator or technical factors that could occur during AFCA were excluded from the risk score developed in this study. Because the definition of permanent AF might vary depending on the medical environment or physicians, the number of patients with progression to permanent AF was small even in the high-risk group, and also it needed long-term follow-up periods to identify the high-risk patients for progression to permanent AF. Due to the strict criteria of insurance coverage for AFCA in Korea, physicians generally start AADs first, and then recommend a repeat ablation when a recurrent atrial arrhythmia cannot be controlled by medication. Moreover, ML outcome is dependent on the data quality and the amount of training set. Therefore, the outcome of this study cannot be generalized to all patients with AF.

CONCLUSIONS

An ML-prediction model successfully classified three risky groups that showed different risk levels of progression to permanent AF for long-term periods before an ablation procedure. Using pre-procedural and non-invasive variables, the ML prediction model can identify patients at high risk for progression to permanent AF before an ablation procedure but has a limited discrimination power for the patients with intermediate-risk.

DATA AVAILABILITY STATEMENT

The raw data supporting the conclusions of this article will be made available by the authors, without undue reservation.

ETHICS STATEMENT

The studies involving human participants were reviewed and approved by the Institutional Review Board of the Yonsei University Health System. The patients/participants provided their written informed consent to participate in this study.

AUTHOR CONTRIBUTIONS

J-WP, O-SK, H-NP, and JS designed the current study, performed data analysis, and wrote the manuscript. IH performed the data analysis. YK, HY, T-HK, J-SU, J-YK, JC, BJ, M-HL, and Y-HK contributed to organize the database. H-NP and JS interpreted and discussed the results. All authors contributed to manuscript revision and approved the final version of the manuscript.

FUNDING

This work was supported by Grant (HI21C0011 to H-NP) from the Korea Health 21 R&D Project, Ministry of Health and Welfare and a Grant (NRF-2020R1A2B01001695) from the Basic Science Research Program run by the National Research Foundation of Korea (NRF).

ACKNOWLEDGMENTS

We thank Mr. John Martin for his linguistic assistance.

SUPPLEMENTARY MATERIAL

The Supplementary Material for this article can be found online at: https://www.frontiersin.org/articles/10.3389/fcvm.2022.813914/full#supplementary-material

Supplementary Figure 1 | Example of a trained first decision tree.

Supplementary Figure 2 | Results of overfitting checks for three STAAR groups. **(A–C)** Each group was divided by a one-vs.-all strategy and identified by the frequency of predicted value in the training and test sets.

Supplementary Figure 3 | Confusion matrix result of artificial intelligence model (Test 4) for three STAAR group.

Supplementary Table 1 | Cox regression analysis of the pre-procedural variables for the progression to permanent AF.

Supplementary Table 2 | Prediction model and risk scores for the progression to permanent AF (STAAR score).

Supplementary Table 3 | Optimal hyperparameters selected by grid search.

Supplementary Table 4 | Linear regression analysis of the pre-procedural variables associated with the STAAR score.

Supplementary Table 5 | Baseline characteristics during the *de novo* ablation according STAAR risk groups.

Supplementary Table 6 | Baseline characteristics during the *de novo* ablation procedure in the independent cohort.

Supplementary Table 7 | Prediction performance of the ML-prediction model for the three STAAR groups in the development cohort.

Supplementary Table 8 | The previous studies and risk model predicting AF recurrence in the patients with repeat ablations for AF (1–9).

REFERENCES

1. Hindricks G, Potpara T, Dagres N, Arbelo E, Bax JJ, Blomström-Lundqvist C, et al. 2020 ESC Guidelines for the diagnosis and management of atrial fibrillation developed in collaboration with the European Association for Cardio-Thoracic Surgery (EACTS). *Eur Heart J.* (2021) 42:373–498. doi: 10.1093/eurheartj/ehaa945
2. Marrouche NF, Brachmann J, Andresen D, Siebels J, Boersma L, Jordaens L, et al. Catheter ablation for atrial fibrillation with heart failure. *N Engl J Med.* (2018) 378:417–27. doi: 10.1056/NEJMoa1707855

3. Jin MN, Kim TH, Kang KW, Yu HT, Uhm JS, Joung B, et al. Atrial fibrillation catheter ablation improves 1-year follow-up cognitive function, especially in patients with impaired cognitive function. *Circ Arrhythm Electrophysiol.* (2019) 12:e007197. doi: 10.1161/CIRCEP.119.007197
4. Park JW, Yang PS, Bae HJ, Yang SY, Yu HT, Kim TH, et al. Five-year change in the renal function after catheter ablation of atrial fibrillation. *J Am Heart Assoc.* (2019) 8:e013204. doi: 10.1161/JAHA.119.013204
5. Dretzke J, Chuchu N, Agarwal R, Herd C, Chua W, Fabritz L, et al. Predicting recurrent atrial fibrillation after catheter ablation: a systematic review of prognostic models. *Europace.* (2020) 22:748–60. doi: 10.1093/europace/euaa041
6. Winkle RA, Jarman JW, Mead RH, Engel G, Kong MH, Fleming W, et al. Predicting atrial fibrillation ablation outcome: the CAAP-AF score. *Heart Rhythm.* (2016) 13:2119–25. doi: 10.1016/j.hrthm.2016.07.018
7. Attia ZI, Noseworthy PA, Lopez-Jimenez F, Asirvatham SJ, Deshmukh AJ, Gersh BJ, et al. An artificial intelligence-enabled ECG algorithm for the identification of patients with atrial fibrillation during sinus rhythm: a retrospective analysis of outcome prediction. *Lancet.* (2019) 394:861–7. doi: 10.1016/S0140-6736(19)31721-0
8. Bumgarner JM, Lambert CT, Hussein AA, Cantillon DJ, Baranowski B, Wolski K, et al. Smartwatch algorithm for automated detection of atrial fibrillation. *J Am Coll Cardiol.* (2018) 71:2381–8. doi: 10.1016/j.jacc.2018.03.003
9. Tison GH, Sanchez JM, Ballinger B, Singh A, Olgin JE, Pletcher MJ, et al. Passive detection of atrial fibrillation using a commercially available smartwatch. *JAMA Cardiol.* (2018) 3:409–16. doi: 10.1001/jamacardio.2018.0136
10. Shade JK, Ali RL, Basile D, Popescu D, Akhtar T, Marine JE, et al. Preprocedure application of machine learning and mechanistic simulations predicts likelihood of paroxysmal atrial fibrillation recurrence following pulmonary vein isolation. *Circ Arrhythm Electrophysiol.* (2020) 13:e008213. doi: 10.1161/CIRCEP.119.008213
11. Budzianowski J, Hiczkiewicz J, Burchardt P, Pieszko K, Rzezniczak J, Budzianowski P, et al. Predictors of atrial fibrillation early recurrence following cryoballoon ablation of pulmonary veins using statistical assessment and machine learning algorithms. *Heart Vessels.* (2019) 34:352–9. doi: 10.1007/s00380-018-1244-z
12. Hung M, Lauren E, Hon E, Xu J, Ruiz-Negrón B, Rosales M, et al. Using machine learning to predict 30-day hospital readmissions in patients with atrial fibrillation undergoing catheter ablation. *J Pers Med*. (2020) 10:82. doi: 10.3390/jpm10030082
13. Al'Aref SJ, Anchouche K, Singh G, Slomka PJ, Kolli KK, Kumar A, et al. Clinical applications of machine learning in cardiovascular disease and its relevance to cardiac imaging. *Eur Heart J.* (2019) 40:1975–86. doi: 10.1093/eurheartj/ehy404
14. Park J, Kim TH, Lee JS, Park JK, Uhm JS, Joung B, et al. Prolonged PR interval predicts clinical recurrence of atrial fibrillation after catheter ablation. *J Am Heart Assoc.* (2014) 3:e001277. doi: 10.1161/JAHA.114.001277
15. Lin YJ, Tai CT, Kao T, Chang SL, Wongcharoen W, Lo LW, et al. Consistency of complex fractionated atrial electrograms during atrial fibrillation. *Heart Rhythm.* (2008) 5:406–12. doi: 10.1016/j.hrthm.2007.12.009
16. Park JH, Pak HN, Kim SK, Jang JK, Choi JI, Lim HE, et al. Electrophysiologic characteristics of complex fractionated atrial electrograms in patients with atrial fibrillation. *J Cardiovasc Electrophysiol.* (2009) 20:266–72. doi: 10.1111/j.1540-8167.2008.01321.x
17. Kim TH, Park J, Uhm JS, Joung B, Lee MH, Pak HN. Pulmonary vein reconnection predicts good clinical outcome after second catheter ablation for atrial fibrillation. *Europace.* (2017) 19:961–7. doi: 10.1093/europace/euw128
18. Breiman L. Random forests. *Mach Learn.* (2001) 45:5–32. doi: 10.1023/A:1010933404324
19. Jamet B, Morvan L, Nanni C, Michaud AV, Bailly C, Chauvie S, et al. Random survival forest to predict transplant-eligible newly diagnosed multiple myeloma outcome including FDG-PET radiomics: a combined analysis of two independent prospective European trials. *Eur J Nucl Med Mol Imaging.* (2021) 48:1005–15. doi: 10.1007/s00259-020-05049-6
20. LaValle SM, Branicky MS, Lindemann SR. On the relationship between classical grid search and probabilistic roadmaps. *Int J Rob Res.* (2004) 23:673–92. doi: 10.1177/0278364904045481
21. Youden WJ. Index for rating diagnostic tests. *Cancer.* (1950) 3:32. doi: 10.1002/1097-0142(1950)3:1<32::AID-CNCR2820030106>3.0.CO;2-3
22. Schisterman EF, Perkins NJ, Liu A, Bondell H. Optimal cut-point and its corresponding Youden Index to discriminate individuals using pooled blood samples. *Epidemiology.* (2005) 16:73–81. doi: 10.1097/01.ede.0000147512.81966.ba
23. Reddy VY, Dukkipati SR, Neuzil P, Natale A, Albenque JP, Kautzner J, et al. Randomized, controlled trial of the safety and effectiveness of a contact force-sensing irrigated catheter for ablation of paroxysmal atrial fibrillation: results of the tacticath contact force ablation catheter study for atrial fibrillation (TOCCASTAR) study. *Circulation.* (2015) 132:907–15. doi: 10.1161/CIRCULATIONAHA.114.014092
24. Chen S, Schmidt B, Bordignon S, Perrotta L, Bologna F, Chun KRJ. Impact of cryoballoon freeze duration on long-term durability of pulmonary vein isolation: ICE Re-map study. *JACC Clin Electrophysiol.* (2019) 5:551–9. doi: 10.1016/j.jacep.2019.03.012
25. Kim TH, Park J, Uhm JS, Kim JY, Joung B, Lee MH, et al. Challenging achievement of bidirectional block after linear ablation affects the rhythm outcome in patients with persistent atrial fibrillation. *J Am Heart Assoc.* (2016) 5:3894. doi: 10.1161/JAHA.116.003894
26. Nilsson B, Chen X, Pehrson S, Kober L, Hilden J, Svendsen JH. Recurrence of pulmonary vein conduction and atrial fibrillation after pulmonary vein isolation for atrial fibrillation: a randomized trial of the ostial versus the extraostial ablation strategy. *Am Heart J.* (2006) 152:537.e1–8. doi: 10.1016/j.ahj.2006.05.029
27. Walters TE, Nisbet A, Morris GM, Tan G, Mearns M, Teo E, et al. Progression of atrial remodeling in patients with high-burden atrial fibrillation: implications for early ablative intervention. *Heart Rhythm.* (2016) 13:331–9. doi: 10.1016/j.hrthm.2015.10.028
28. Vlachos K, Efremidis M, Letsas KP, Bazoukis G, Martin R, Kalafateli M, et al. Low-voltage areas detected by high-density electroanatomical mapping predict recurrence after ablation for paroxysmal atrial fibrillation. *J Cardiovasc Electrophysiol.* (2017) 28:1393–402. doi: 10.1111/jce.13321
29. Marrouche NF, Wilber D, Hindricks G, Jais P, Akoum N, Marchlinski F, et al. Association of atrial tissue fibrosis identified by delayed enhancement MRI and atrial fibrillation catheter ablation: the DECAAF study. *JAMA.* (2014) 311:498–506. doi: 10.1001/jama.2014.3
30. Park J, Joung B, Uhm JS, Young Shim C, Hwang C, Hyoung Lee M, et al. High left atrial pressures are associated with advanced electroanatomical remodeling of left atrium and independent predictors for clinical recurrence of atrial fibrillation after catheter ablation. *Heart Rhythm.* (2014) 11:953–60. doi: 10.1016/j.hrthm.2014.03.009
31. Hocini M, Sanders P, Deisenhofer I, Jaïs P, Hsu LF, Scavée C, et al. Reverse remodeling of sinus node function after catheter ablation of atrial fibrillation in patients with prolonged sinus pauses. *Circulation.* (2003) 108:1172–5. doi: 10.1161/01.CIR.0000090685.13169.07
32. Lin WS, Tai CT, Hsieh MH, Tsai CF, Lin YK, Tsao HM, et al. Catheter ablation of paroxysmal atrial fibrillation initiated by non-pulmonary vein ectopy. *Circulation.* (2003) 107:3176–83. doi: 10.1161/01.CIR.0000074206.52056.2D
33. Firouznia M, Feeny AK, LaBarbera MA, McHale M, Cantlay C, Kalfas N, et al. Machine learning-derived fractal features of shape and texture of the left atrium and pulmonary veins from cardiac CT scans are associated with risk of recurrence of atrial fibrillation post-ablation. *Circ Arrhythm Electrophysiol.* (2021) 14:e009265. doi: 10.1161/CIRCEP.120.009265
34. Liu CM, Chang SL, Chen HH, Chen WS, Lin YJ, Lo LW, et al. The clinical application of the deep learning technique for predicting trigger origins in patients with paroxysmal atrial fibrillation with catheter ablation. *Circ Arrhythm Electrophysiol.* (2020) 13:e008518. doi: 10.1161/CIRCEP.120.008518
35. Feeny AK, Rickard J, Trulock KM, Patel D, Toro S, Moennich LA, et al. Machine learning of 12-lead QRS waveforms to identify cardiac

resynchronization therapy patients with differential outcomes. *Circ Arrhythm Electrophysiol.* (2020) 13:e008210. doi: 10.1161/CIRCEP.119.008210

Conflict of Interest: The authors declare that the research was conducted in the absence of any commercial or financial relationships that could be construed as a potential conflict of interest.

Publisher's Note: All claims expressed in this article are solely those of the authors and do not necessarily represent those of their affiliated organizations, or those of the publisher, the editors and the reviewers. Any product that may be evaluated in this article, or claim that may be made by its manufacturer, is not guaranteed or endorsed by the publisher.

frontiers in Cardiovascular Medicine

ORIGINAL RESEARCH
published: 10 March 2022
doi: 10.3389/fcvm.2021.759563

The Roles of Fractionated Potentials in Non-Macroreentrant Atrial Tachycardias Following Atrial Fibrillation Ablation: Recognition Beyond Three-Dimensional Mapping

Yu-Chuan Wang[1,2], *Li-Bin Shi*[2,3], *Song-Yun Chu*[1,2,4], *Eivind Solheim*[2], *Peter Schuster*[2,3] *and Jian Chen*[2,3]*

[1] Department of Geriatrics, Peking University First Hospital, Beijing, China, [2] Department of Heart Disease, Haukeland University Hospital, Bergen, Norway, [3] Department of Clinical Science, University of Bergen, Bergen, Norway, [4] Department of Cardiology, Peking University First Hospital, Beijing, China

OPEN ACCESS

Edited by:
Matteo Anselmino, University of Turin, Italy

Reviewed by:
Naotaka Hashiguchi, Japanese Red Cross Narita Hospital, Japan
Xin Li, University of Leicester, United Kingdom
Antonio Frontera, Vita-Salute San Raffaele University, Italy

***Correspondence:**
Jian Chen
jian.chen@med.uib.no

Specialty section:
This article was submitted to Cardiac Rhythmology, a section of the journal Frontiers in Cardiovascular Medicine

Received: *16 August 2021*
Accepted: *31 December 2021*
Published: *10 March 2022*

Citation:
Wang Y-C, Shi L-B, Chu S-Y, Solheim E, Schuster P and Chen J (2022) The Roles of Fractionated Potentials in Non-Macroreentrant Atrial Tachycardias Following Atrial Fibrillation Ablation: Recognition Beyond Three-Dimensional Mapping. Front. Cardiovasc. Med. 8:759563. doi: 10.3389/fcvm.2021.759563

Introduction: Non-macroreentrant atrial tachycardia (nAT) following atrial fibrillation (AF) ablation is being increasingly reported. Many issues remain to be elucidated. We aimed to characterize the fractionated potentials (FPs) in nAT and introduce a new method of cross-mapping for clarifying their roles.

Methods and Results: Forty-four nATs in 37 patients were enrolled and classified into focal AT (FAT, 12), microreentrant AT (MAT, 14), and small-loop-reentrant AT (SAT, 18) groups, according to activation pattern. FP was found on all targets except in nine FATs. The ratio of FP duration to AT cycle length (TCL) was different among groups (28 ± 7% in FAT, 53 ± 11% in MAT, and 42 ± 14% in SAT, $p < 0.05$), and ablation duration were longer in SATs (313 ± 298 vs. 111 ± 125 s, $p < 0.05$). The ratio of mappable cycle length to TCL was lower in the FAT group (63 ± 22% vs. 90 ± 9% and 89 ± 8%, $p < 0.05$). When cross-mapping was employed, trans-potential time differences in both longitudinal and transverse direction were longer around the culprit FP for MAT ($p < 0.01$). After Receiver Operating Characteristic curve analysis, it is best to adopt the sum of time difference ratios in both directions ≥60% as a cut-off value for discrimination of the FPs responsible for MAT with a sensitivity of 92% and specificity of 87%.

Conclusions: FP could be found on target in most nATs following a previous AF ablation. The ratio of FP duration to TCL may help for differentiation. A simple method of cross-mapping could be employed to clarify the roles of FPs.

Keywords: atrial tachycardia, atrial fibrillation, fractionated potential, mapping, ablation

INTRODUCTION

Catheter ablation has become an important therapy for atrial fibrillation (AF). Pulmonary vein isolation is a cornerstone for AF ablation technique (1). Expansive ablation techniques, including linear ablation and complex fractionated atrial electrogram (CFAE) ablation, have been employed to improve clinical outcomes of ablation for persistent AF (2, 3). As a consequence, atrial

tachycardia (AT) post AF ablation has been increasingly observed. Compared with the incidence of <5% after segmental pulmonary vein ablation (4, 5), the incidence increases to 10–31% after circumferential pulmonary vein ablation (6, 7), to >20% after CFAE ablation (8), and to nearly 50% after an extensive stepwise approach of AF ablation (9). Among the post AF ablation ATs, 25% was accounted for non-macroreentrant ATs (nATs), with almost 75% for macroreentrant ATs, whose reentry circuit diameter was ≥30 mm and involved more than two parts of the atria (6, 10). In patients with post AF ablation AT, symptoms are often significant due to a rapid and regular ventricular response and are refractory to antiarrhythmic drugs. Therefore, catheter ablation has been playing an increasingly important role for these ATs. Meanwhile, great challenges of procedures are presented by the complexity, variability, and unpredictability of these ATs, especially in nATs (11). Although nATs have been reported, many issues have not yet been elucidated. In this study, we systematically investigated and compared the electrophysiological characteristics of different nATs.

METHODS

Study Population

Patients with AT were retrospectively enrolled when the following criteria were satisfied: (i) There was clinical evidence for AT on surface electrocardiogram or/and Holter and diagnoses were confirmed by electrophysiological study; (ii) patients had undergone at least one ablation procedure for AF prior to AT ablation; (iii) AT was successfully eliminated by ablation during the procedure. All patients provided informed consent before the ablation procedure. The study protocol was approved by the Ethics Committee of Western Norway.

Electrophysiological Study and Ablation

All antiarrhythmic medications, except for amiodarone, were discontinued for at least five half-lives. All procedures were performed under conscious sedation. A 20-pole catheter (Abbott, Minneapolis, MN, USA) with 2–10–2 mm spacing was advanced into the high right atrium (RA) and looped around the tricuspid annulus with the distal dipoles in the coronary sinus (CS). After a single transseptal puncture, an ablation catheter (Thermocool, Biosense Webster, Diamond Bar, CA, USA or Therapy Cool Path, Abbott, Minneapolis, MN, USA) and a circular mapping catheter (Lasso, Biosense Webster or Inquiry Optima, Abbott) were advanced into the left atrium (LA). The procedure was performed step by step as follows: (i) AT was induced by electrical stimulation if sinus rhythm presented before the procedure; (ii) three-dimensional activation mapping was performed by means of CARTO (Biosense Webster) or EnSite NavX system (Abbott); (iii) entrainment maneuvers were employed to identify the mechanism of AT, if possible, but was not performed in patients for whom there was concern regarding AT converting to another form or degenerating into AF; (iv) as a complement, a new method of cross-mapping was used at areas of interest to differentiate diagnoses when entrainment could not be applied or produced an unsatisfactory result; (v) radiofrequency energy was delivered at the identified essential locations; (vi) electrical stimulation was implemented for re-induction after the termination of AT by ablation (**Figure 1**).

After overall activation mapping, the areas of interest, including suspicious reentrant circuits and fractionated potential (FP), were meticulously mapped with a distance between points ≤5 mm. FP was defined as a multi-component electrogram with ≥3 deflections (12, 13). When an FP was recorded, cross-mapping with four recording sites evenly and closely distributed (pairwise facing and vertical to each other) around the FP (**Figure 1**) was used to identify the possible role of FP in tachycardia. The time difference was measured across the FP in two perpendicular directions. The direction with the longer time difference was defined as longitudinal, and the shorter as transverse. Any region with a voltage of ≤0.05 mV was defined as a scar. All intracardiac electrograms were recorded and analyzed in a recording system (ProLab, BARD Electrophysiology, Lowell, MA, USA) and filtered with 30 to 300 Hz. The variation in cycle length of tachycardia (TCL) was calculated by the maximum minus minimum of TCL, which was counted continuously for 1 min after AT had stabilized for at least 5 min. The fluctuations in TCL were assessed by using the ratio of TCL variation to the mean minimum value of TCL.

Radiofrequency energy was applied in a temperature-control mode with a cut-off of 50°C and an irrigation rate of 20 ml/min. At the posterior wall or in the CS, energy was limited to a maximum of 30 or 25 W, respectively.

Classifications of Non-Macroreentrant AT and Localization of AT

According to the global activation patterns, we classified nATs into three types: focal AT (FAT, a radial mode of conduction from the earliest activation site was displayed; **Figure 2**), microreentrant AT (MAT, a centrifugal mode of reentrant activation around a tiny core without any scar was shown in an area with a diameter of ≤10 mm; **Figure 3**), and small-loop-reentrant AT (SAT, a centrifugal mode of reentrant activation around a defined scar was presented in an area with a diameter of >10 mm, but ≤30 mm; **Figure 4**). We localized the site of AT according to the anatomical structure, including the pulmonary vein area (inside or within the antra ≤10 mm from the pulmonary vein ostia), the anterior, posterior, lateral, inferior way, roof, and septum of the LA, CS, and RA (10).

Follow-Up

After discharge, all patients were regularly followed up in an outpatient clinic. Holter was performed for every patient after 3, 6, and 12 months. If a patient experienced symptoms suggestive of recurrence, a surface electrocardiogram and Holter would be taken at any time.

Statistical Analysis

Continuous variables were reported as mean ± SD and compared by a one-way ANOVA with a Tukey *post-hoc* test. Categorical variables were reported as absolute or relative frequency and compared by using the chi-square test or Fisher's exact test. All analyses were conducted with the use of SPSS Statistics 25.0

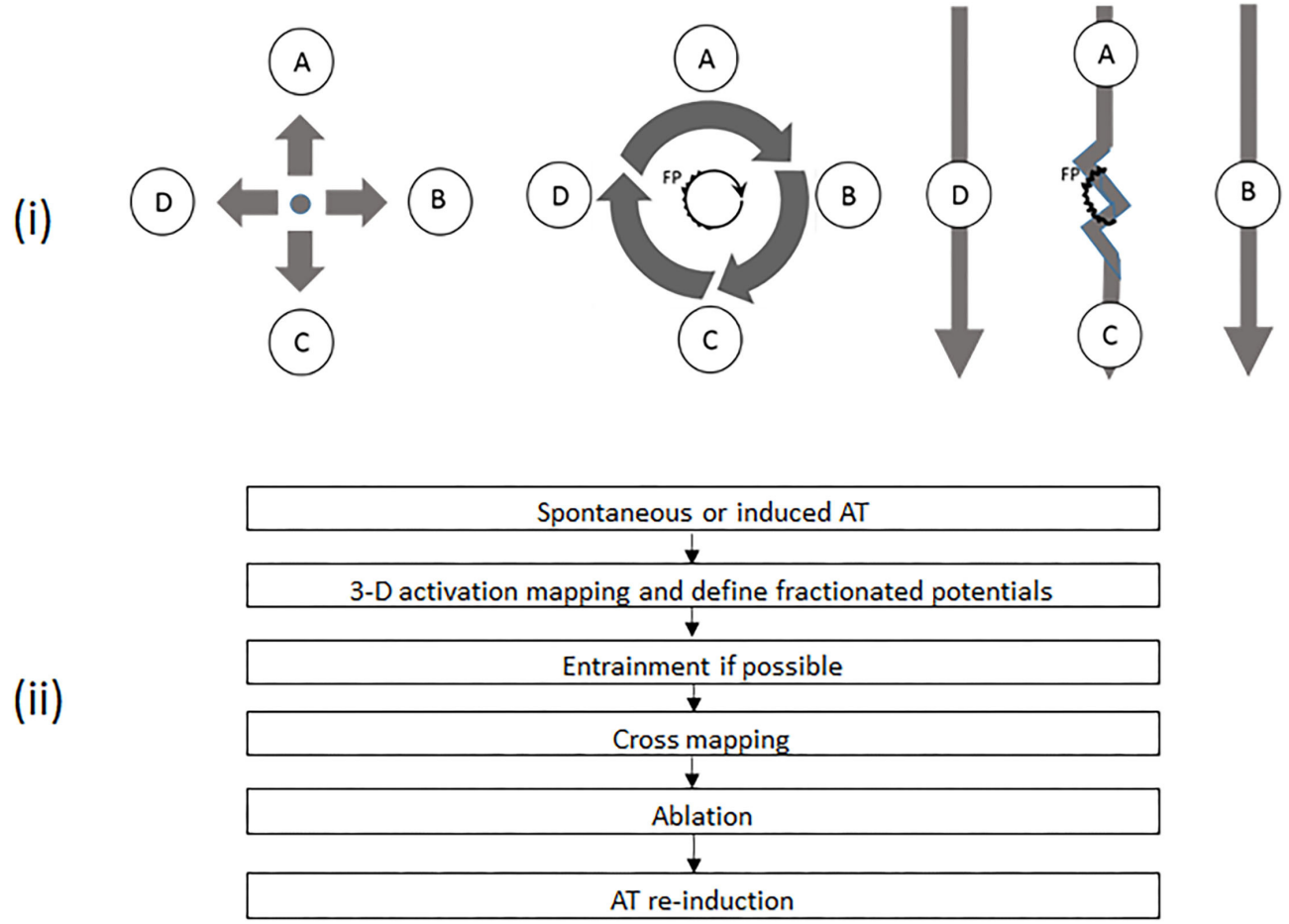

FIGURE 1 | (i) Schematic diagrams demonstrating different activation patterns in various atrial tachycardias (ATs) and the principles of cross-mapping for the differentiation of different ATs with fractionated potentials (FPs). The left panel shows a focal AT with sites A, B, C, and D activated almost at the same time. The middle panel demonstrates a microreentrant AT, with sites A, B, C, and D activated sequentially. The core with a FP is the source for maintenance of tachycardia. In the right panel, FP is a bystander potential. Thus, Sites A and C are activated sequentially due to slow conduction through FP. Sites B and D are activated almost simultaneously. The twisted line represents an area with FP. The heavy arrow shows the direction of activation. A, B, C, and D represent mapping sites around an FP, respectively. (ii) Workflow chart of mapping and ablation. AT,atrial tachycardia; FP, fractionated potential.

(IBM, Armonk, NY, USA). A p-value of <0.05 was considered statistically significant.

RESULTS

Thirty-seven patients (31 men and mean age 62 ± 9 years) were included in this study according to the criteria. Coronary artery disease was observed in 3 patients, hypertension in 13, hypertrophic cardiomyopathy in 1, and sick sinus syndrome in 1. The mean left ventricular ejection fraction was 51 ± 6%, and the mean antero-posterior dimension of LA was 42 ± 4 mm. An average of 2 ± 1 ablation procedures for AF were performed on the patients before the AT ablation, including 16 paroxysmal, 7 persistent, and 14 longstanding persistent AF.

In total, 44 nATs were treated, while 31 macroreentrant ATs in 37 patients were ablated during the same procedure. Mapping with CARTO or EnSite NavX system was performed in 15 and 22 patients, respectively, with mean mapping points of 247 ± 36. The mean TCL of these 44 nATs was 316 ± 89 ms (range 208–547 ms). Seventeen ATs were localized within the pulmonary vein areas, 21 in the LA (4 anterior, 5 lateral, 2 inferior, 2 roof, and 8 septum), and 6 in the RA. Compared with the earlier ablation procedures, only 6 ATs were not localized in proximity to the previously ablated areas, including 3 in the anterior LA, 2 in the superior vena cava, and 1 in the RA. Entrainment was performed in 33 ATs, and a postpacing interval of ≤30 ms longer than the TCL was demonstrated in 19 ATs. In the remaining 14 ATs, no postpacing interval of ≤30 ms longer than the TCL was observed in 12 ATs, and arrhythmia changed after pacing in 2 ATs.

All clinical information and electrophysiological data for three different ATs are listed in **Tables 1** and **2**. There were no differences among FAT, MAT, and SAT regarding the mode of AT initiation, earlier ablation strategies, TCL and its fluctuation. FP

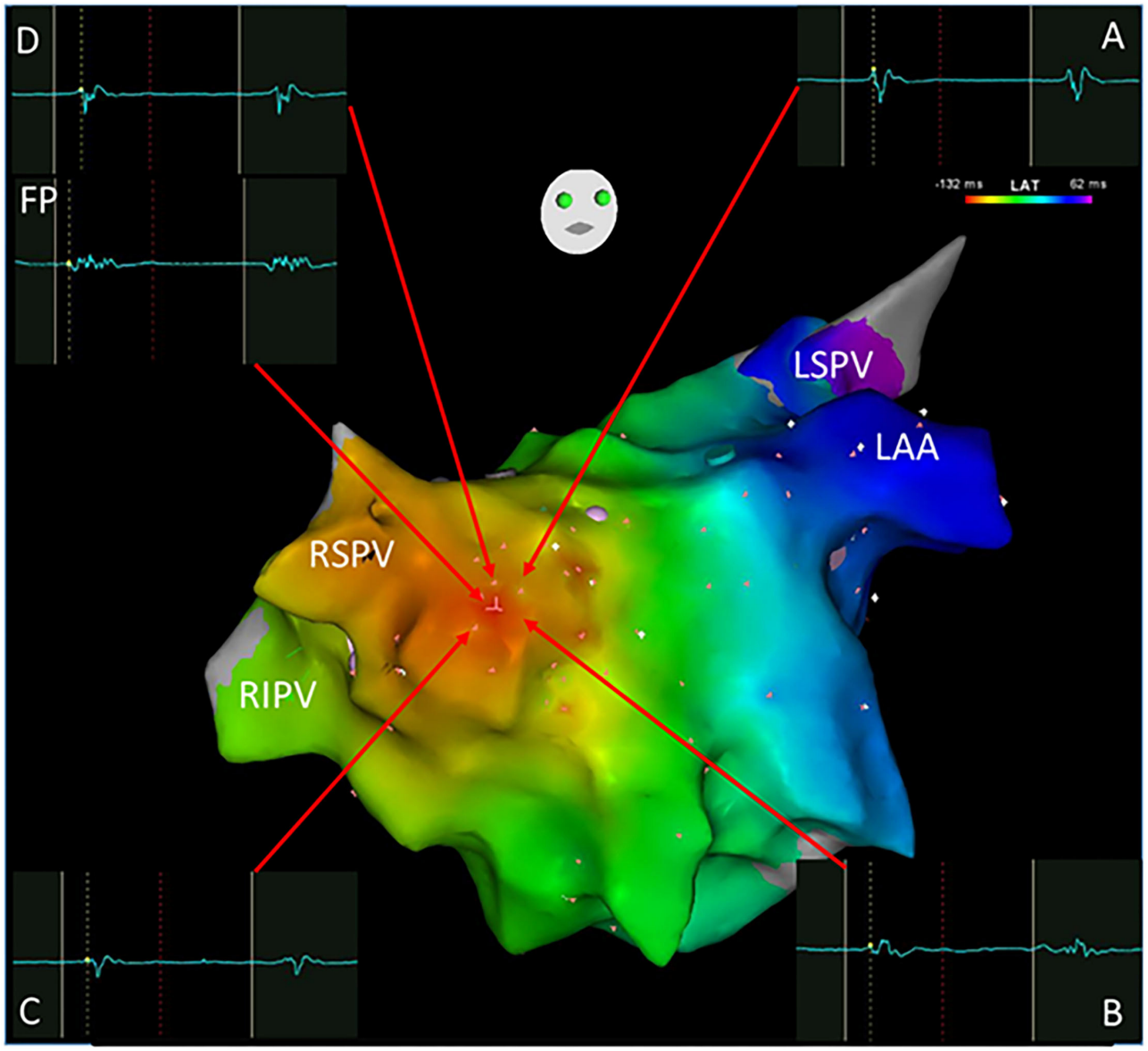

FIGURE 2 | A focal atrial tachycardia located in front of the right superior pulmonary vein with a radiation activation pattern was mapped using the Carto system. The earliest activation point was shown with an FP (-132 ms) as the ablation target. Cross-mapping was employed with local activation time at sites A, B, C, and D for -120,-122,-122, and -122 ms, respectively. FP, fractionated potential; LAA, left atrial appendage; LSPV, left superior pulmonary vein; RSPV, right superior pulmonary vein; RIPV, right inferior pulmonary vein.

was found at a successful ablation target in only 3 out of 12 FATs but all MATs and SATs. Compared to MAT and SAT, mappable TCL was shorter and the FP duration ratio to TCL in the FAT group was lower ($p < 0.05$). Compared to MAT, the ratio of FP duration to TCL was shorter, and more ablation applications were needed to terminate the AT in SAT group ($p < 0.05$). No statistically significant difference was found with respect to FP amplitude ($p > 0.05$).

When cross-mapping was used to differentiate focal sources and bystander FPs, no difference was found in the time difference between the longitudinal and transverse directions in the FAT group, but great differences in the MAT ($p < 0.01$) and bystander groups ($p < 0.01$). Compared to the bystander, trans-potential time differences in both directions were longer in the culprit FP for MAT ($p < 0.01$, **Table 3**). After Receiver Operating Characteristic curve analysis using different parameters, we regard it as best to adopt the sum of time-difference ratios in both the longitudinal and transverse directions, with ≥60% as a cut-off value for the FPs responsible for MAT with a sensitivity of 92%, specificity of 87%, and area under the curve of 0.94 (**Figure 5**). The positive predictive value, negative predictive value, and likelihood were 0.87, 0.81, and 6.88, respectively.

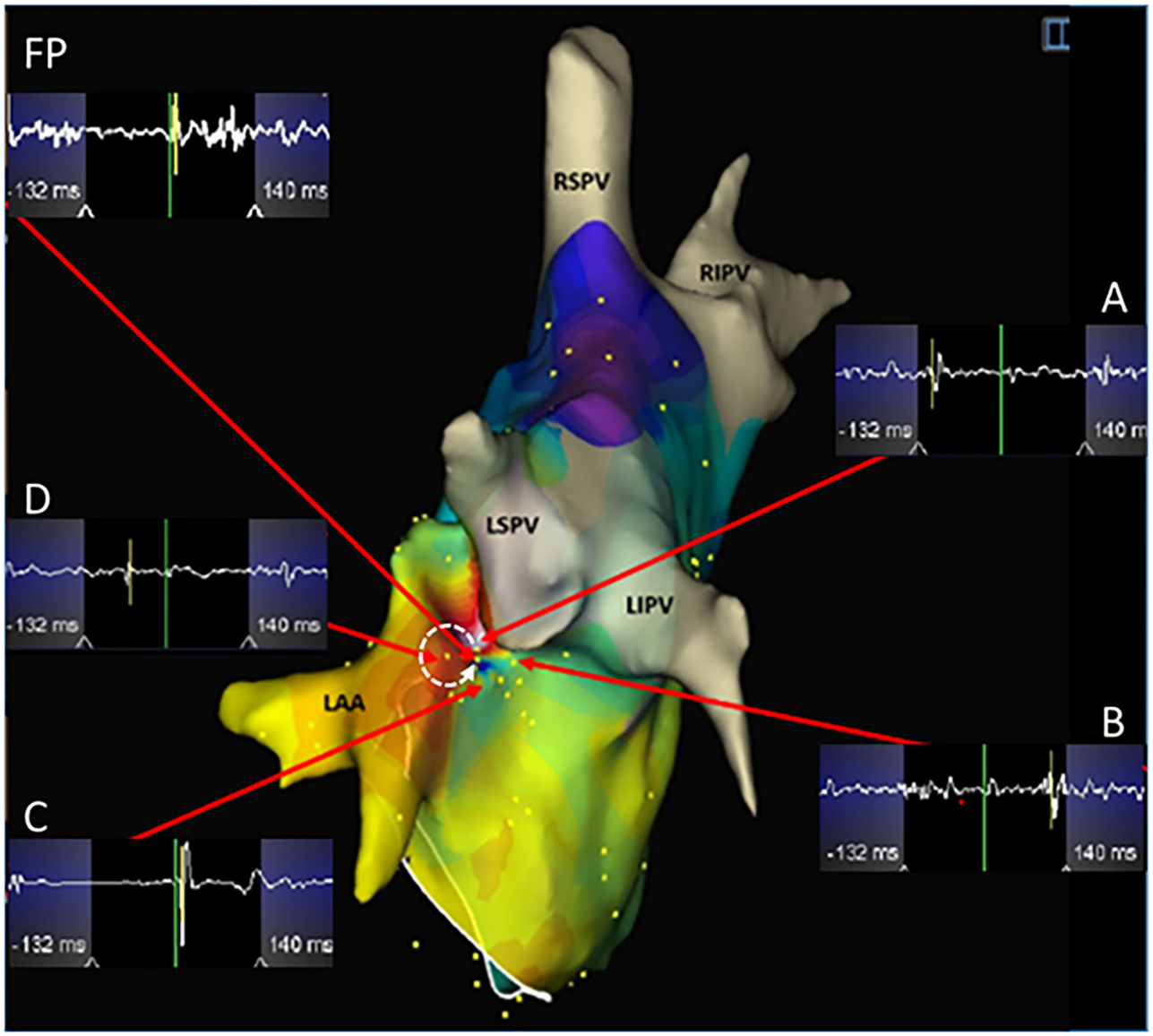

FIGURE 3 | A microreentrant atrial tachycardia located between the left atrial appendage and the left superior pulmonary vein was shown by the EnSite NavX system. A whirlpool-like reentry around a tiny core was displayed with the earliest (white) connected to the latest activation (purple) in an area with a diameter of <10 mm. A wide fractionated potential was recorded connecting the earliest and the latest activation sites. Cross-mapping was used and the local activation time at sites A, B, C, and D measured at -110, 112, 14, and -56 ms, respectively. The dotted arrow shows the activation direction from A to D and further to C and B in sequence. Ablation targeting the FP terminated the atrial tachycardia. LIPV, left inferior pulmonary vein. Abbreviations as shown in **Figures 1**, **2**.

There were no periprocedural or delayed postprocedural complications, including thromboembolism, in any patient. After a long-term follow-up period of 69 ± 20 months, six patients experienced AF recurrence, and four had episodes of AT, in which macroreentry was demonstrated during a repeat procedure, while nAT was not documented in any patient. One patient with AT recurrence died of cancer during the follow-up period.

DISCUSSION

In this study, the electrophysiological characteristics of nAT, especially of FPs, were demonstrated systematically and a new method of cross-mapping was introduced to clarify the roles of FPs.

The ATs following AF ablation usually include the mechanisms of macroreentry and non-macroreentry. Macroreentrant AT is frequently present and can be quickly identified by using three-dimensional mapping combined with entrainment pacing maneuvers (14), while non-macroreentrant AT is more difficult to identify due to its variability, individuality, and diversity. In this study, we focused primarily on three-dimensional activation mapping and the new cross-mapping with weighting less the entrainment pacing maneuvers. The reasons for doing so were based on the difficulties in

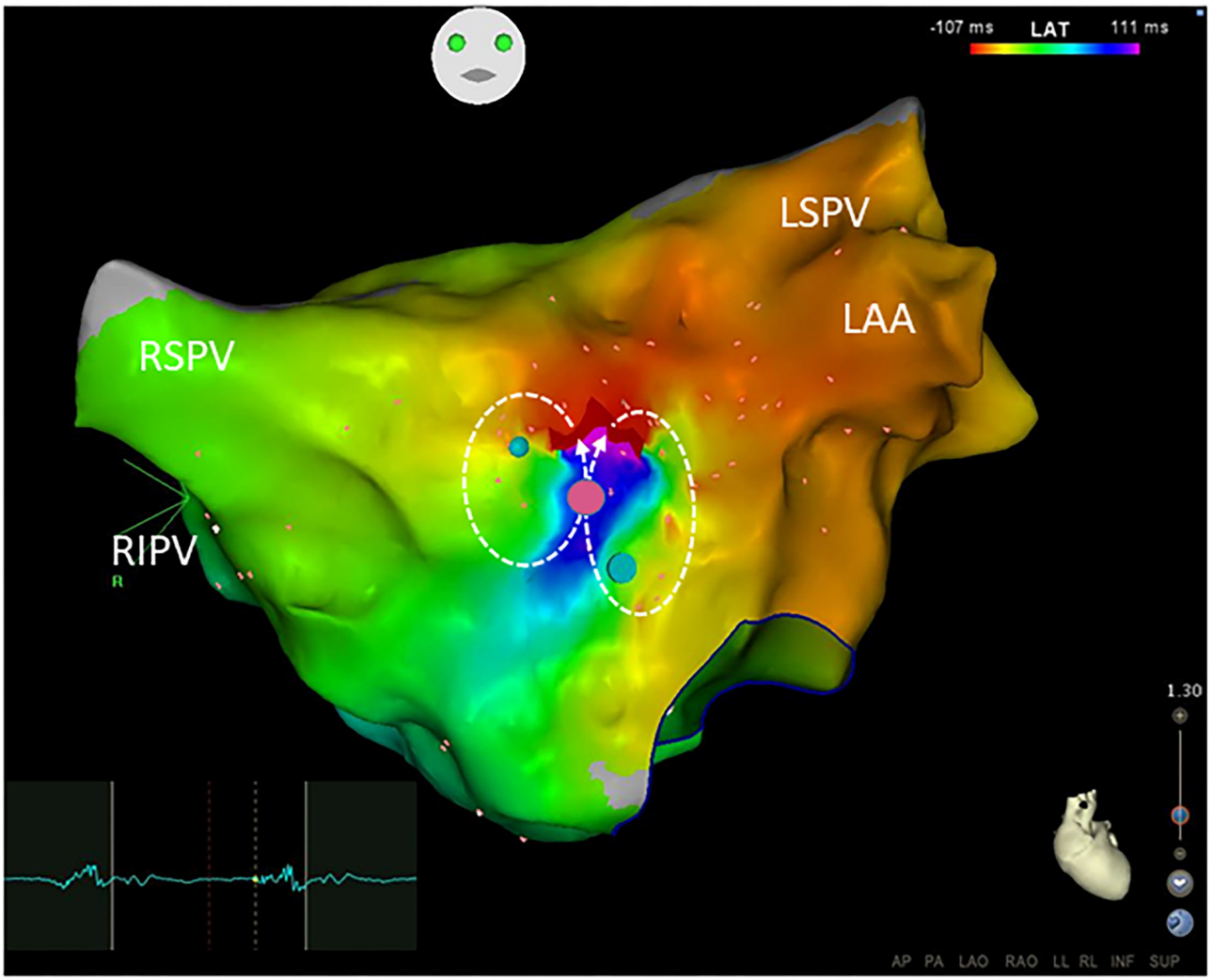

FIGURE 4 | Small-loop-reentrant atrial tachycardia with a figure-of-eight pattern was demonstrated by the Carto system. The reentrant circuits located at the anterior wall of the left atrium were within an area with a diameter of <30 mm but >10 mm. The phenomenon of early (red) meeting late (purple) wavefront was shown in the activation map. A narrow isthmus area with an FP (electrogram on the left) at a pink dot was shown and confined by small regions of the scar. Blue dots define double potentials and dotted arrows show the activation directions. Ablation targeting on the FP terminated the atrial tachycardia. Abbreviations as shown in **Figures 1**, **2**.

clinical practice such as (i) rapid stimulation can change the tachycardia to a different arrhythmia (e.g., AF) if the TCL is very short; (ii) stimulation can be hard to capture in a locally injured myocardium (with low voltage) after the previous ablation; (iii) the TCL can be variable, making interpretation of entrainment difficult.

Compared to FAT or SAT, it could be even more challenging to recognize the MAT even though three-dimensional mapping was employed. In our series, 7 out of 14 MATs were differentiated by entrainment pacing. However, only one of them was verified by the entrainment criterion of postpacing interval-TCL of $\leq$30 ms. The key point of recognizing MAT may be to interpret and identify the essential FPs which represent the fundamentally slow conduction areas for maintenance of MAT. It has been shown that FP is a prerequisite for some of the reentrant arrhythmias (15). Our results demonstrate that FAT could be simply separated from the other nATs based on the short duration of FP and mappable TCL. Although there were no statistically significant differences between MAT and SAT regarding the FP duration, the ratio of FP duration to TCL may separate these two groups. The FP covered more than half of the TCL, which suggests that local slow conduction might be taking place. In this setting, a high-density mapping may be critical. **Figure 3** shows that both the earliest and latest activation sites can be localized within a distance of 5 mm from each other. Reducing the size of the mapping catheter electrodes and of the distance between electrodes can certainly increase the resolution of mapping and further increase the chances of recognizing SAT and MAT.

FP may not always present a critical part of the reentrant arrhythmia but is sometimes just a bystander that is passively

activated (16, 17). It could be time-consuming if several FPs need to be checked. As a supplement, we introduced a simple method of cross-mapping around the FP to differentiate the bystander FP from the culprit in MAT, and from FAT as well (**Figure 1**). After four points with local activation time around an FP had been recorded, the ratios of time difference to TCL between two opposite points could be easily obtained and further different nAT or bystander FP could be quickly recognized by using the cutoff sum values of the time-difference ratio in both directions (<10% for FAT; ≥60% for MAT). This finding can be shared with the concept of the new multiple-electrode mapping catheter (18) and potentially developed into new application software. This method can also play an important role when entrainment is impossibly or unsuccessfully performed, or as an additional approach to confirm a diagnosis even while a three-dimensional mapping is employed. Besides being the cause of myocardial degeneration, FP is probably an iatrogenic consequence of non-transmural injury after ablation (17). In the present study, FPs were found on the target sites in 34 out of 44 ATs, which were located in or adjacent to the previous ablation sites. Moreover, there was no difference regarding earlier ablation strategies among the three groups. Thus, a non-transmural injury, no matter what strategy was involved, might create an essential substrate for nAT (19). This indicated that extensive ablation in the atria other than pulmonary vein isolation must be carefully considered.

Being consistent with previous studies, this study has demonstrated that the pulmonary veins, septum, LA appendage, and CS were the common harbors for nAT after AF ablation (20–22). In some patients, the ridges between the pulmonary veins and LA or appendage are steep, which may make the

TABLE 1 | Clinical data of different atrial tachycardias.

	FAT group ($n = 12$)	MAT group ($n = 14$)	SAT group ($n = 18$)
The mode of AT initiation			
Spontaneous	3	8	7
Induced	8	5	9
Converted from another arrhythmia	1	1	2
Prior strategies for AF ablation			
PVI	3	1	1
PVI+CFAE	1	5	5
PVI+lines	6	5	9
PVI+CFAE+lines	2	3	3
Termination pattern			
Restore sinus rhythm	12	12	14
Converted to another atrial tachycardia	0	2	4

AF, atrial fibrillation; CFAE, complex fractionated atrial electrogram; FAT, focal atrial tachycardia; MAT, micro-reentrant atrial tachycardia; PVI, pulmonary vein isolation; SAT, small-loop-reentrant atrial tachycardia.

TABLE 2 | Comparison of electrophysiological data between different atrial tachycardia groups.

	FAT group ($n = 12$)	MAT group ($n = 14$)	SAT group ($n = 18$)	*P* value
TCL (ms)	323 ± 86 (227–493)	301 ± 93 (208–547)	323 ± 90 (221–500)	0.764
Fluctuation of TCL (%)	2 ± 1 (1–4)	4 ± 2 (1–7)	3 ± 2 (1–8)	0.166
Ratio of mappable CL vs. TCL (%)	63 ± 22 (27–98)	90 ± 9† (64–100)	89 ± 8† (73–100)	**0.009**
Duration of FP (ms)	89 ± 17* (78–108)	161 ± 69 (101–352)	135 ± 48 (60–240)	0.099
Ratio of FP duration versus TCL (%)	28 ± 7* (20–35)	53 ± 11† (34–74)	42 ± 14†‡ (19–68)	**0.013**
Amplitude of FP (mV)	0.11 ± 0.04* (0.07–0.15)	0.09 ± 0.04 (0.04–0.19)	0.10 ± 0.06 (0.05–0.28)	0.755
Duration of ablation for AT termination (s)	167 ± 183 (2–558)	111 ± 125 (5–472)	313 ± 298‡ (12–945)	**0.045**

**FP was observed in only three out of 12 patients. $^{\dagger}p < 0.05$ compared with FAT; $^{\ddagger}p < 0.05$ compared with MAT; AT, atrial tachycardia; TCL, atrial tachycardia cycle length; FAT, focal atrial tachycardia; FP, fractionated potential; MAT, micro-reentrant atrial tachycardia; SAT, small-loop-reentrant atrial tachycardia. The bold values are < 0.05 meaning significantly different.*

TABLE 3 | Cross-mapping measurement around fractionated potentials with different roles.

	Culprit FP for FAT ($n = 3$)	Culprit FP for MAT ($n = 14$)	Bystander FP ($n = 17$)
Trans-potential measurement, longitudinal			
Time difference (ms)	10 ± 2	183 ± 90	71 ± 57‡
Time-difference ratio (%)	4 ± 1	60 ± 20	22 ± 21‡
Trans-potential measurement, transverse			
Time difference (ms)	5 ± 1	107 ± 73*	15 ± 15†‡
Time-difference ratio (%)	2 ± 1	35 ± 23†	6 ± 5†‡
TCL (ms)	285 ± 52	301 ± 93	355 ± 118

$p < 0.05$, $^{\dagger}p < 0.01$, compared to the longitudinal direction. $^{\ddagger}p > 0.001$, compared to the MAT group. Time-difference ratio: the ratio of the activation-time difference to atrial tachycardia cycle length (TCL). Abbreviation as in **Tables 1, **2**. See also **Figure 1**.*

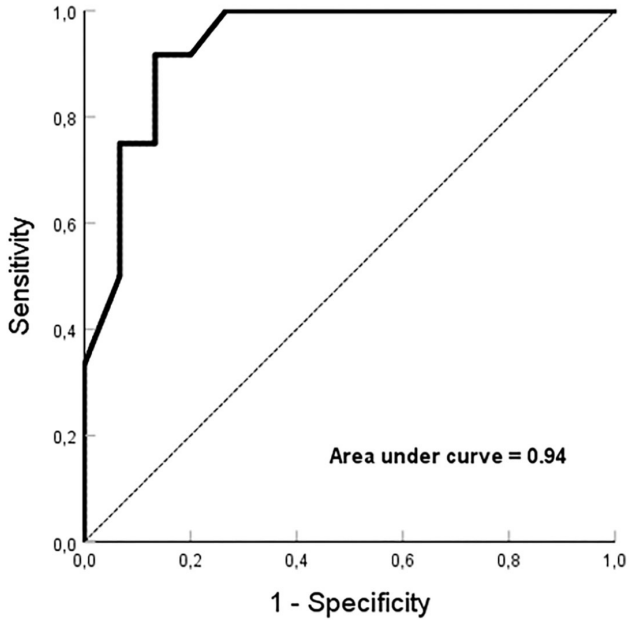

FIGURE 5 | Receiver Operating Characteristic curve analysis. The sum of ≥60% for time-difference ratios in both the longitudinal and transverse directions, is employed as a cut-off value for the fractionated potentials responsible for microreentrant atrial tachycardia with an area under the curve of 0.94.

catheter unstable. For this reason, ablation is often performed in these areas with a low contact force (23). The thickness of the myocardium is another factor. The superior parts of the left lateral ridge and septum are the thickest areas in the LA (24, 25). Thus, transmural lesions in these areas are difficult to achieve through endocardial ablation. Furthermore, heterogeneous fiber orientation also provides a milieu for the formation of conduction block/slow conduction and initiation of reentry (26). In CS, complicated connections within the musculature provide an important substrate for reentrant AT (27). Unlike previous studies, the ratio of mappable cycle length to TCL in the FAT group was significantly lower than that in the other groups, but even so, we found a mean of 63%. This may be a characteristic difference from idiopathic focal AT. Although the fluctuation of TCL >15% was reported as a characteristic of focal AT (28), only a mean 2–4% fluctuation was found in our study. The statistically significant difference in ablation duration between the MAT and SAT groups provided further evidence of the tiny circuit size involved in MAT.

LIMITATIONS

This was a retrospective study with a relatively small number of patients. In most cases, multiple ATs coexisted in a single patient post AF ablation. Therefore, it was difficult to select a homogeneous patient population for each type of AT. Notably, high-resolution mapping catheters were not available at the time when the study was performed. Entrainment pacing maneuvers were not obtained in all ATs for various reasons as indicated in the Discussion. These two factors may influence the interpretation and analysis. However, all diagnoses were made based on global mapping in the atria, and not dependent only on a local electrogram. Furthermore, all mappings were verified by the successful ablation outcomes. Additionally, we performed a detailed mapping with help of cross-mapping which could overcome some flaws. It is important to note that interpretation of cross-mapping can be affected in cases where there are existing lines of block in a contiguous area. The cross-mapping method needs to be further confirmed by prospective and randomized studies.

CONCLUSION

In this study, characteristic FPs were observed on targets in most nATs following previous AF ablation. The ratio of FP duration to TCL may be of help for differentiation. A simple method of cross-mapping could be employed to clarify the roles of FPs.

DATA AVAILABILITY STATEMENT

The data analyzed in this study is subject to the following licenses/restrictions: Data related to patients' information cannot be published publicly. Data of this study are saved in the lab and patients' medical recordings. Requests to access these datasets should be directed to eivind.solheim@helse-bergen.no.

ETHICS STATEMENT

The studies involving human participants were reviewed and approved by Regional Ethics Committee of Western Norway. Written informed consent for participation was not required for this study in accordance with the national legislation and the institutional requirements.

AUTHOR CONTRIBUTIONS

Y-CW, L-BS, and JC: conception of the study. Y-CW, L-BS, S-YC, and JC: design and interpretation of data, as well as revising of the manuscript. Y-CW, L-BS, S-YC, ES, PS, and JC have significantly contributed to this manuscript, data collection, data analysis, and drafting of the manuscript. All authors have read and approved submission of the manuscript and the manuscript has not been published and is not being considered for publication elsewhere in whole or part in any language except as an abstract. All authors contributed to the article and approved the submitted version.

FUNDING

The author L-BS was supported by Helse Vest, Norway, Research Fellowship, and S-YC was supported by the Research Council of Norway.

REFERENCES

1. Calkins H, Kuck KH, Cappato R, Brugada J, Camm AJ, Chen SA, et al. HRS/EHRA/ECAS Expert Consensus Statement on Catheter and Surgical Ablation of Atrial Fibrillation: recommendations for patient selection, procedural techniques, patient management and follow-up, definitions, endpoints, and research trial design. *Europace.* (2012). 14:528–606. doi: 10.1093/europace/eus027
2. Knecht S, Hocini M, Wright M, Lellouche N, O'Neill MD, Matsuo S, et al. Left atrial linear lesions are required for successful treatment of persistent atrial fibrillation. *Eur Heart J.* (2008) 29:2359–2366. doi: 10.1093/eurheartj/ehn302
3. De Bortoli A, Ohm OJ, Hoff PI, Sun LZ, Schuster P, Solheim E, et al. Long-term outcomes of adjunctive complex fractionated electrogram ablation to pulmonary vein isolation as treatment for non-paroxysmal atrial fibrillation. *J Interv Card Electrophysiol.* (2013) 38:19–26. doi: 10.1007/s10840-013-9816-4
4. Karch MR, Zrenner B, Deisenhofer I, Schreieck J, Ndrepepa G, Dong J, et al. Freedom from atrial tachyarrhythmias after catheter ablation of atrial fibrillation: a randomized comparison between 2 current ablation strategies. *Circulation.* (2005) 111:2875–80. doi: 10.1161/CIRCULATIONAHA.104.491530
5. Derval N, Takigawa M, Frontera A, Mahida S, Konstantinos V, Denis A, et al. Characterization of complex atrial tachycardia in patients with previous atrial interventions using high-resolution mapping. *JACC Clin Electrophysiol.* (2020) 6:815–26. doi: 10.1016/j.jacep.2020.03.004
6. Gerstenfeld EP, Callans DJ, Dixit S, Russo AM, Nayak H, Lin D, et al. Mechanisms of organized left atrial tachycardias occurring after pulmonary vein isolation. *Circulation.* (2004) 110:1351–7. doi: 10.1161/01.CIR.0000141369.50476.D3
7. Deisenhofer I, Estner H, Zrenner B, Schreieck J, Weyerbrock S, Hessling G, et al. Left atrial tachycardia after circumferential pulmonary vein ablation for atrial fibrillation: incidence, electrophysiological characteristics, and results of radiofrequency ablation. *Europace.* (2006) 8:573–82. doi: 10.1093/europace/eul077
8. Oral H, Chugh A, Good E, Wimmer A, Dey S, Gadeela N, et al. Radiofrequency catheter ablation of chronic atrial fibrillation guided by complex electrograms. *Circulation.* (2007) 115:2606–12. doi: 10.1161/CIRCULATIONAHA.107.691386
9. Matsuo S, Lim KT, Haissaguerre M. Ablation of chronic atrial fibrillation. *Heart Rhythm.* (2007) 4:1461–3. doi: 10.1016/j.hrthm.2007.07.016
10. Takigawa M, Derval N, Frontera A, Martin R, Yamashita S, Cheniti G, et al. Revisiting anatomic macroreentrant tachycardia after atrial fibrillation ablation using ultrahigh-resolution mapping: Implications for ablation. *Heart Rhythm.* (2018) 15:326–33. doi: 10.1016/j.hrthm.2017.10.029
11. Anter E, Duytschaever M, Shen C, Strisciuglio T, Leshem E, Contreras-Valdes FM, et al. Activation mapping with integration of vector and velocity information improves the ability to identify the mechanism and location of complex scar-related atrial tachycardias. *Circ Arrhythm Electrophysiol.* (2018) 11:e006536. doi: 10.1161/CIRCEP.118.006536
12. Nademanee K, McKenzie J, Kosar E, Schwab M, Sunsaneewitayakul B, Vasavakul T, et al. A new approach for catheter ablation of atrial fibrillation: mapping of the electrophysiologic substrate. *J Am Coll Cardiol.* (2004) 43:2044–2053. doi: 10.1016/j.jacc.2003.12.054
13. Lee G, Kumar S, Teh A, Madry A, Spence S, Larobina M, et al. Epicardial wave mapping in human long-lasting persistent atrial fibrillation: transient rotational circuits, complex wavefronts, and disorganized activity. *Eur Heart J.* (2014) 35:86–97. doi: 10.1093/eurheartj/eht267
14. Saoudi N, Anselme F, Poty H, Cribier A, Castellanos A. Entrainment of supraventricular tachycardias: a review. *Pacing Clin Electrophysiol.* (1998) 21:2105–25. doi: 10.1111/j.1540-8159.1998.tb01131.x
15. Ban JE, Chen YL, Park HC, Lee HS, Lee DI, Choi JI, et al. Relationship between complex fractionated atrial electrograms during atrial fibrillation and the critical site of atrial tachycardia that develops after catheter ablation for atrial fibrillation. *J Cardiovasc Electrophysiol.* (2014) 25:146–53. doi: 10.1111/jce.12300
16. Navoret N, Jacquir S, Laurent G, Binczak S. Detection of complex fractionated atrial electrograms using recurrence quantification analysis. *IEEE Trans Biomed Eng.* (2013) 60:1975–82. doi: 10.1109/TBME.2013.2247402
17. Frontera A, Takigawa M, Martin R, Thompson N, Cheniti G, Massoullie G, et al. Electrogram signature of specific activation patterns: Analysis of atrial tachycardias at high-density endocardial mapping. *Heart Rhythm.* (2018) 15:28–37. doi: 10.1016/j.hrthm.2017.08.001
18. Tan VH, Lyu MZ, Tan PC, Wong LC, Yeo C, Wong KCK. Utility of directional high-density mapping catheter (Advisor(TM) HD Grid) in complex scar-related atrial tachycardia. *J Arrhythm.* (2020) 36:180–3. doi: 10.1002/joa3.12256
19. Kitamura T, Takigawa M, Derval N, Denis A, Martin R, Vlachos K, et al. Atrial tachycardia circuits include low voltage area from index atrial fibrillation ablation relationship between RF ablation lesion and AT. *J Cardiovasc Electrophysiol.* (2020) 31:1640–8. doi: 10.1111/jce.14576
20. Rostock T, O'Neill MD, Sanders P, Rotter M, Jais P, Hocini M, et al. Characterization of conduction recovery across left atrial linear lesions in patients with paroxysmal and persistent atrial fibrillation. *J Cardiovasc Electrophysiol.* (2006) 17:1106–11. doi: 10.1111/j.1540-8167.2006.00585.x
21. Hocini M, Shah AJ, Nault I, Sanders P, Wright M, Narayan SM, et al. Localized reentry within the left atrial appendage: arrhythmogenic role in patients undergoing ablation of persistent atrial fibrillation. *Heart Rhythm.* (2011) 8:1853–1861. doi: 10.1016/j.hrthm.2011.07.013
22. Kurotobi T, Shimada Y, Kino N, Inoue K, Kimura R, Okuyama Y, et al. Inducible atrial tachycardias with multiple circuits in a stepwise approach are associated with increased episodes of atrial tachycardias after catheter ablation. *J Electrocardiol.* (2012) 45:102–8. doi: 10.1016/j.jelectrocard.2011.07.011
23. Makimoto H, Lin T, Rillig A, Metzner A, Wohlmuth P, Arya A, et al. In vivo contact force analysis and correlation with tissue impedance during left atrial mapping and catheter ablation of atrial fibrillation. *Circ Arrhythm Electrophysiol.* (2014) 7:46–54. doi: 10.1161/CIRCEP.113.000556
24. Hall B, Jeevanantham V, Simon R, Filippone J, Vorobiof G, Daubert J. Variation in left atrial transmural wall thickness at sites commonly targeted for ablation of atrial fibrillation. *J Interv Card Electrophysiol.* (2006) 17:127–32. doi: 10.1007/s10840-006-9052-2
25. Cabrera JA, Ho SY, Climent V, Sanchez-Quintana D. The architecture of the left lateral atrial wall: a particular anatomic region with implications for ablation of atrial fibrillation. *Eur Heart J.* (2008) 29:356–62. doi: 10.1093/eurheartj/ehm606
26. Ho SY, Sanchez-Quintana D. The importance of atrial structure and fibers. *Clin Anat.* (2009) 22:52–63. doi: 10.1002/ca.20634
27. Chauvin M, Shah DC, Haissaguerre M, Marcellin L, Brechenmacher C. The anatomic basis of connections between the coronary sinus musculature and the left atrium in humans. *Circulation.* (2000) 101:647–52. doi: 10.1161/01.CIR.101.6.647
28. Jais P, Matsuo S, Knecht S, Weerasooriya R, Hocini M, Sacher F, et al. A deductive mapping strategy for atrial tachycardia following atrial fibrillation ablation: importance of localized reentry. *J Cardiovasc Electrophysiol.* (2009) 20:480–91. doi: 10.1111/j.1540-8167.2008.01373.x

Conflict of Interest: JC serves as a consultant for Biosense Webster, Johnson & Johnson.

The remaining authors declare that the research was conducted in the absence of any commercial or financial relationships that could be construed as a potential conflict of interest.

frontiers | Frontiers in Cardiovascular Medicine

ORIGINAL RESEARCH
published: 28 April 2022
doi: 10.3389/fcvm.2022.804424

Zero Fluoroscopy Arrhythmias Catheter Ablation: A Trend Toward More Frequent Practice in a High-Volume Center

Federica Troisi[1]*, *Pietro Guida*[1], *Federico Quadrini*[1], *Antonio Di Monaco*[1,2], *Nicola Vitulano*[1], *Rosa Caruso*[1], *Rocco Orfino*[1], *Giacomo Cecere*[1], *Matteo Anselmino*[3] and *Massimo Grimaldi*[1]

[1] Cardiology Department, Regional General Hospital "F. Miulli", Bari, Italy, [2] Department of Clinical and Experimental Medicine, University of Foggia, Foggia, Italy, [3] Division of Cardiology, Department of Medical Sciences, "Città della Salute e della Scienza di Torino" Hospital, University of Turin, Turin, Italy

OPEN ACCESS

Edited by:
Antonio Sorgente,
EpiCURA, Belgium

Reviewed by:
Giannis G. Baltogiannis,
Vrije University Brussel, Belgium
Changsheng Ma,
Capital Medical University, China
Luigi Di Biase,
Albert Einstein College of Medicine, United States

***Correspondence:**
Federica Troisi
federica.troisi@libero.it

Specialty section:
This article was submitted to Cardiac Rhythmology, a section of the journal Frontiers in Cardiovascular Medicine

Received: 29 October 2021
Accepted: 14 March 2022
Published: 28 April 2022

Citation:
Troisi F, Guida P, Quadrini F, Di Monaco A, Vitulano N, Caruso R, Orfino R, Cecere G, Anselmino M and Grimaldi M (2022) Zero Fluoroscopy Arrhythmias Catheter Ablation: A Trend Toward More Frequent Practice in a High-Volume Center. Front. Cardiovasc. Med. 9:804424. doi: 10.3389/fcvm.2022.804424

Background: Awareness of radiation exposure risks associated to interventional cardiology procedures is growing. The availability of new technologies in electrophysiology laboratories has reduced fluoroscopy usage during arrhythmias ablations. The aim of this study was to describe procedures with and without X-Rays and to assess feasibility, safety, and short-term efficacy of zero fluoroscopy intervention in a high-volume center oriented to keep exposure to ionizing radiation as low as reasonably achievable.

Methods: Cardiac catheter ablations performed in our hospital since January 2017 to June 2021.

Results: A total of 1,853 procedures were performed with 1,957 arrhythmias treated. Rate of fluoroless procedures was 15.4% (285 interventions) with an increasing trend from 8.5% in 2017 to 22.9% of first semester 2021. The most frequent arrhythmia treated was atrial fibrillation (646; 3.6% fluoroless) followed by atrioventricular nodal reentrant tachycardia (644; 16.9% fluoroless), atrial flutter (215; 8.8% fluoroless), ventricular tachycardia (178; 17.4% fluoroless), premature ventricular contraction (162; 48.1% fluoroless), and accessory pathways (112; 31.3% fluoroless). Although characteristics of patients and operative details were heterogeneous among treated arrhythmias, use of fluoroscopy did not influence procedure duration. Moreover, feasibility and efficacy were 100% in fluoroless ablations while the rate of major complications was very low and no different with or without fluoroscopy (0.45 vs. 0.35%).

Conclusion: Limiting the use of X-Rays is necessary, especially when the available technologies allow a zero-use approach. A lower radiation exposure may be reached, reducing fluoroscopy usage whenever possible during cardiac ablation procedures with high safety, full feasibility, and efficacy.

Keywords: arrhythmia, catheter ablation, efficacy, feasibility, fluoroscopy, safety, zero-fluoroscopy

INTRODUCTION

In the last 15 years, the awareness of the harmfulness of radiation used in interventional cardiology and to guide percutaneous procedure has increased. In the electrophysiological field, the development of technologies has reduced progressively fluoroscopy guidance for catheter placement during arrhythmia ablations. This all began with the birth of electroanatomical mapping systems, that allow visualization of catheters used during ablation without radiation. These systems are based on three-dimensional reconstructions of cardiac chamber and on visualization of catheters that navigate inside. Progressively over the years, new technological advances in three-dimensional (3D) electroanatomical mapping (EAM) have been introduced both as diagnostic algorithms and as structural characteristics of the catheters (1, 2). It became possible in this way to reduce fluoroscopy time until zeroing, because new algorithms facilitate the recognition of the mechanisms of arrhythmias and the localization of their site of origin. On the other hand, structural improvements of the catheters increase safety of navigation and ablation without scope (3–5).

The American College of Cardiology recommends that all catheterization laboratories adopt the principle of "ALARA:" radiation doses to be used are "As Low as Reasonably Achievable" (6). This suggestion derived from knowledge of the biological effects of radiations both on medical staff and on patients; from the interaction with organisms, X-Rays create hydroxyl radicals that can damage the DNA of cells with pro-carcinogenic effects.

In our electrophysiology laboratory, we have progressively implemented measures to reduce the use of X-Rays during procedures. For 10 years we have been carrying out zero fluoroscopy ablation procedures, at the beginning mainly on supraventricular or ventricular ablations on the right heart, then progressively other, more complex, and procedures. Our hospital today is a high-volume procedure center, with considerable experience in zero X-Rays ablations.

According to recent data from a European multicenter registry, ∼7% of procedures are conducted without any use of fluoroscopy while procedural settings (i.e., 3D-mapping system) and higher case volumes (7) are associated with a reduced usage of fluoroscopy. Data from high-volume electrophysiology laboratories that have progressively implemented measures to reduce the use of X-Rays during procedures are lacking. The aim of this study was: (1) to describe the contemporary use of fluoroscopy in an interventional electrophysiology laboratory; (2) to assess the proportion of procedures conducted without any use of fluoroscopy during catheter ablation of different arrhythmias; and (3) to evaluate feasibility, safety, and short-term efficacy of zero fluoroscopy intervention in real life.

Abbreviations: 3D, three-dimensional; AF, atrial fibrillation; AFL, atrial flutter; AP, accessory pathways; AVNRT, atrioventricular nodal reentrant tachycardia; EAM, electroanatomical mapping; PFO, patent foramen ovale; PVC, premature ventricular contraction; VT, ventricular tachycardia.

METHODS

We conducted a retrospective analysis based on the Cardiac Interventional Registry implemented at our hospital (approval number 5690 by the Ethical Review Authority of the Azienda Universitaria Ospedaliera Consorziale - Policlinico, Bari), considering catheter ablations performed in our laboratory with and without fluoroscopy since January 2017 to June 2021. For each performed procedure, we classified the ablation according to arrhythmia/arrhythmias treated: atrioventricular nodal reentrant tachycardia (AVNRT), accessory pathways (AP), atrial fibrillation (AF), atrial flutter (ALF), premature ventricular contraction (PVC), and ventricular tachycardia (VT).

All procedures were performed with the CARTO3 mapping system (Biosense Webster, Irvine, California, USA) as the main imaging modality to cardiac chambers' navigation and catheter ablation. The CARTO3 system is based on electromagnetic technology: it uses low electromagnetic fields to identify the position of the catheter. Nine coils positioned under the patient bed generate three different electromagnetic fields, allowing the creation of a strong magnetic field less sensitive to distortion potentially created by proximity to fluoroscopy. Navistar sensor-based catheters contain three magnetic sensors in the distal part of the tip that allow the exact location within the magnetic field to be created.

The choice to perform intervention with or without X-Rays was made subjectively by the operator before starting the procedure. Only in AF was the decision not to use X-Rays made during the procedure, based on the possibility of passing with the catheters in the left atrium through the patent foramen ovale (PFO), thus avoiding the phase of the transeptal puncture.

Fluoroscopy Procedures

From 2017, most procedures were performed with the integrated use of X-Rays and EAM, which reduces time of fluoroscopy compared to that of the ablative procedures used a few years ago. During fluoroscopy, ablation patients are in conscious sedation; we use a maximum of two femoral accesses for procedure. Ablation were carried out as previously described (8, 9).

Fluoroless Procedures

No additional pre-procedure radiologic imaging was performed. The procedural workflow included the following steps: common right femoral vein puncture performed echo-guided to avoid casual puncture of artery or superficial femoralvein, insertion of diagnostic multi-electrode catheter sensor based (Decanav, Biosense Webster, Irvine, California, USA) or an ablation catheter, a 3.5 mm externally irrigated radiofrequencies with contact force sensor (Thermocool Smarttouch; Biosense Webster, Irvine, California, USA); compensation for respiratory movements; and advancement of the catheter both using tactile feedback and creating a calibration matrix of the inferior vena cava by sweeping the catheter tip whilst advancing it up to the initial appearance of atrial electrograms. In this way we identify the junction between the inferior vena cava, the right atrium, and the superior vein cava and mark them with a snapshot of the catheter. Then we create 3D geometric contours of the right atrial

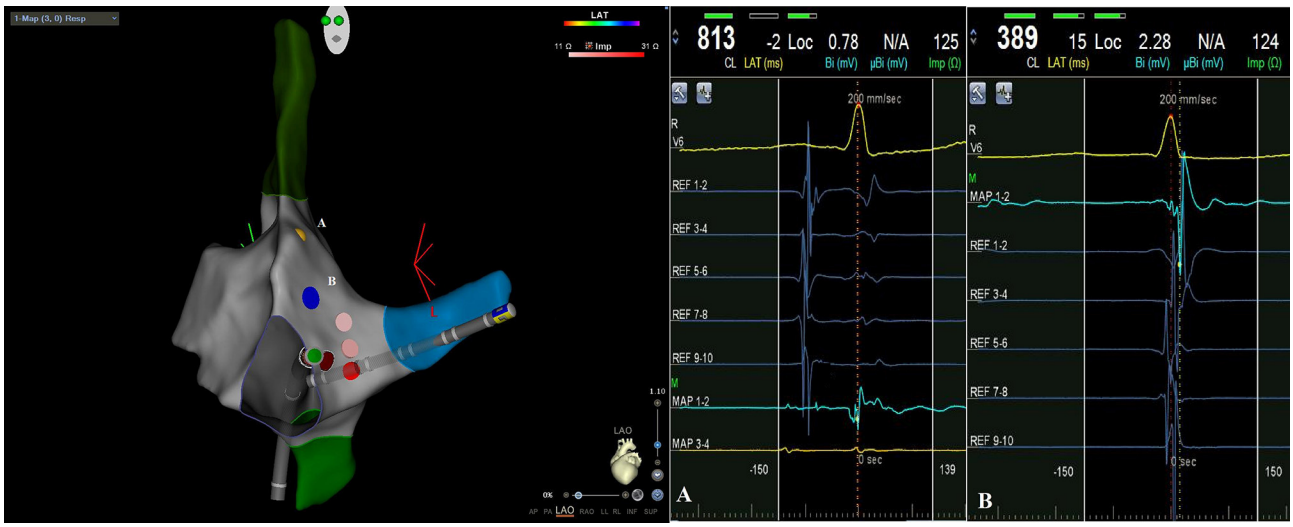

FIGURE 1 | CARTO3 left anterior oblique (LAO) image of atrioventricular nodal reentrant tachycardia ablation: during radiofrequency applications catheter remains below tagged His potential [yellow point A on EAM, intracavitary signal **(A)**] and fast way potential [blue point B on EAM, intracavitary signal **(B)**].

with fast anatomical mapping software with the aim of defining endocardial boundaries, tagging the area where a His bundle deflection was recorded, reproducing in detail the tricuspid annulus, and reconstructing the coronary sinus up to its distal portion. Finally, we advance the other diagnostic catheters, if needed, using the previously reconstructed venous and atrial geometry. The same technique is used for arterial access in case of a retrograde approach for left PVC, AP, or VT ablation.

AVNRT Fluoroless Ablation

When we arrive with catheters in the right atrium we identify and tag His potential; then we locate decapolar catheter in the coronary sinus. After inducing tachycardia by electrophysiological study, we carefully map slow pathway potential with ablation catheter, identifying and tagging the fast pathway potential. Then, always remaining below the tagged fast pathway potential, we start radiofrequency applications (**Figure 1**). Acute success was non-inducibility of tachycardia and evidence of a jump during programmed atrial stimulation with only one re-entry.

AP Fluoroless Ablation

For the left-sided accessory pathway, we used a transaortic retrograde approach. We map the accessory pathway with ablation catheter, having as anatomical reference a decapolar catheter positioned in the coronary sinus. We look for Kent's potential or, in any case, for the point of greatest fusion between the atrial and ventricular potential in sinus rhythm for manifest AP, during continuous ventricular pacing for occult accessory pathways. Acute success was non-inducibility of tachycardia and for manifest AP elimination of antegrade accessory pathway conduction.

AF Fluoroless Ablation

In our center we have used for several year a "near zero X-Rays" approach for transeptal puncture, which is the step that needs greater fluoroscopy during AF ablation procedure; this strategy was illustrated in a previous paper (10). In these procedures we did not use X-Rays at all because, during mapping of fossa ovalis it was found PFO, so we could go through to the left atrium without transeptal puncture. Once in the left atrium with the ablation catheter and the diagnostic catheter, we proceeded with the electroanatomical map guided by EAM and with the subsequent ablation procedure (pulmonary vein isolation and other ablative targets). Acute success was pulmonary veins isolation validation and non-inducibility of AF.

AFL Fluoroless Ablation

When catheters arrive in the right atrium, first of all we verify the location of the circuit with entrainment on vena cava tricuspid isthmus. If it is a typical AFL, we are already at the right place and we go to ablation. If not, we start mapping atrial arrhythmia using both electrophysiological potentials and activation map provided by EAM. Validation of bidirectional block with pacing stimulation and non-inducibility of tachycardia during electrophysiological tests was considered as acute success.

PVC and VT Fluoroless Ablation

Depending on the origin of PVC/VT diagnosed by the electrocardiogram, we use a venous or arterial approach. Once arrived with the catheters in the heart chamber of interest, we start mapping PVC/VT with activation and simultaneously substrate map processed with EAM. Complete elimination of PVC or non-inducible VT during ventricular stimulation was acute success of cardiac ablation.

Statistical Analyses

Data are summarized as the mean ± standard deviation for continuous variables or frequency and percentage for categorical variables. Characteristics of patients treated with and without fluoroscopy were compared by using Student's *t*-test or chi-squared test (respectively for continuous and categorical data) while Fisher's exact test was applied for the rate of major complications. *P*-value < 0.05 was considered to be statistically significant. All analyses were performed using STATA version 16 (StataCorp, College Station, Texas).

RESULTS

During the study period, 1,853 procedures were performed (364 in the year 2017, 434 in 2018, 444 in 2019, 362 in 2020, and 249 during the first 6 months of 2021) for a total of 1,957 arrhythmias treated (some patients were treated for more arrhythmias during their procedure). **Table 1** shows characteristics of patients treated with and without fluoroscopy. A fluoroless procedure, in comparison to the standard one, was more common in younger and female subjects. With the exception of diabetes mellitus and vascular disease, the prevalence of other comorbidities was lower in patients treated with a fluoroless intervention than those with fluoroscopy (**Table 1**). The proportion of fluoroless procedures involving a treatment of PVC or AP was greater than those performed with fluoroscopy, while AF and AFL were much more frequent with a standard approach. The relative frequency of AVNRT and VT within both groups was not different by study group (**Table 1**). The most frequently treated arrhythmia was AF (646; 33.0% of total arrhythmias) followed by AVNRT (644; 32.9%), AFL (215; 11.0%), VT (178; 9.1%), PVC (162; 8.3%), and AP (112; 5.7%). Right-sided AP, PVC, and VT were respectively 42.0, 58.0, and 23.6% of arrhythmias treated. Among procedures performed, 285 (15.4%) were fluoroless. **Figure 2** displays the growth of procedures' proportion with a fluoroless approach over the study period (from 8.5 to 22.9% on yearly basis).

Table 2 shows characteristics of patients according to arrhythmias treated. Younger subjects more frequently underwent a fluoroless approach in all types of arrhythmias, with the exception of AF ablations for which this possibility was related to anatomic features (PFO). Women were more frequently treated with a fluoroless intervention for AP, PVC, and VT (**Table 2**). Procedure duration is found to substantially overlap between procedures with and without fluoroscopy, given that differences may be due to a greater or lesser presence of right or left forms of arrhythmias. A longer procedure duration was found in ANVRT fluoroless procedures and in PVC or VT fluoroscopy interventions (**Table 2**). **Figure 3** shows fluoroscopy time and dose area product with regard to standard procedures (panel A and B). Fluoroscopy time was different among procedures: ∼8 min in ALF, 6 in AF or VT, and 4 for AVNRT and PVC (**Figure 3A**). The mean of dose area product was higher in VT, AFL, and AF with lower values in PVC, AP, and AVNRT (**Figure 3B**).

TABLE 1 | Characteristics of patients treated with and without fluoroscopy.

	Floroscopy	Fluoroless	
	***N* = 1,568**	***N* = 285**	***p***
Age (years)	57 ± 14	42 ± 19	<0.001
Males	62.1%	46.0%	<0.001
Hypertension	40.4%	18.6%	<0.001
Diabetes mellitus	5.1%	4.2%	0.524
Chronic obstructive pulmonary disease	5.0%	1.4%	0.007
Severe renal dysfunction	3.3%	1.1%	0.042
Vascular disease	6.6%	4.9%	0.274
Previous myocardial infarction	6.4%	2.5%	0.009
History of heart failure	18.3%	13.0%	0.030
Arrhythmias treated			
AF	39.7%	8.1%	<0.001
AFL	12.5%	6.7%	0.005
AP	4.9%	12.3%	0.005
AVNRT	34.1%	38.2%	0.178
PVC	5.4%	27.4%	<0.001
VT	9.4%	10.9%	0.429

Mean ± Standard Deviation or percentage.

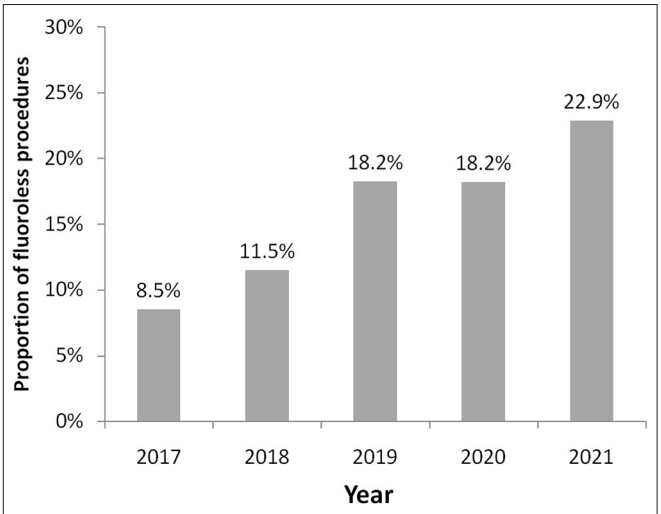

FIGURE 2 | Proportions of fluoroless procedures by calendar year. Trend of fluoroless procedures.

Feasibility, Safety, and Short-Term Efficacy

All procedures were successful in both groups. Fluoroless feasibility was 100% without any conversion to standard procedure for non-AF-ablations. There were eight (0.4% of interventions performed) major complications: two femoral artery dissections (one in AVNRT; one in VT), three pericardial effusions without cardiac tamponade (one in AF; one in PVC; one in VT), and three with cardiac tamponade (one in ALF; one in PVC; one in VT). All complications were observed in the standard procedures with fluoroscopy, with the exception of the pericardial effusion without cardiac tamponade onset during

TABLE 2 | Patients' characteristics by arrhythmias treated.

	N	Age (years)	Men/women	Procedure duration (min)
AF				
Overall	646	59 ± 11	447 (69.2%)/199 (30.8%)	141 ± 50
Fluoroless	23 (3.6%)	57 ± 15	14 (60.9%)/9 (39.1%)	138 ± 30
Floroscopy	623 (96.4%)	59 ± 10	433 (69.5%)/190 (30.5%)	141 ± 51
		$p = 0.360$	$p = 0.379$	$p = 0.808$
AFL				
Overall	215	61 ± 12	159 (74.0%)/56 (26.0%)	125 ± 58
Fluoroless	19 (8.8%)	51 ± 11	14 (73.7%)/5 (26.3%)	133 ± 49
Floroscopy	196 (91.2%)	62 ± 12	145 (74.0%)/51 (26.0%)	124 ± 59
		$p < 0.001$	$p = 0.978$	$p = 0.496$
AP				
Overall	112	31 ± 17	76 (67.9%)/36 (32.1%)	98 ± 43
Fluoroless	35 (31.3%)	20 ± 11	19 (54.3%)/16 (45.7%)	93 ± 39
Floroscopy	77 (68.8%)	36 ± 17	57 (74.0%)/20 (26.0%)	100 ± 45
		$p < 0.001$	$p = 0.038$	$p = 0.487$
AVNRT				
Overall	644	50 ± 16	248 (38.5%)/396 (61.5%)	71 ± 34
Fluoroless	109 (16.9%)	38 ± 17	34 (31.2%)/75 (68.8%)	83 ± 37
Floroscopy	535 (83.1%)	53 ± 15	214 (40.0%)/321 (60.0%)	69 ± 33
		$p < 0.001$	$p = 0.085$	$p < 0.001$
PVC				
Overall	162	51 ± 16	93 (57.4%)/69 (42.6%)	130 ± 64
Fluoroless	78 (48.1%)	47 ± 15	34 (43.6%)/44 (56.4%)	106 ± 40
Floroscopy	84 (51.9%)	55 ± 16	59 (70.2%)/25 (29.8%)	152 ± 75
		$p < 0.001$	$p = 0.001$	$p < 0.001$
VT				
Overall	178	64 ± 16	156 (87.6%)/22 (12.4%)	180 ± 80
Fluoroless	31 (17.4%)	53 ± 19	22 (71.0%)/9 (29.0%)	122 ± 44
Floroscopy	147 (82.6%)	66 ± 14	134 (91.2%)/13 (8.8%)	193 ± 80
		$p < 0.001$	$p = 0.002$	$p < 0.001$

Mean ± Standard Deviation and number (percentage) of patients.

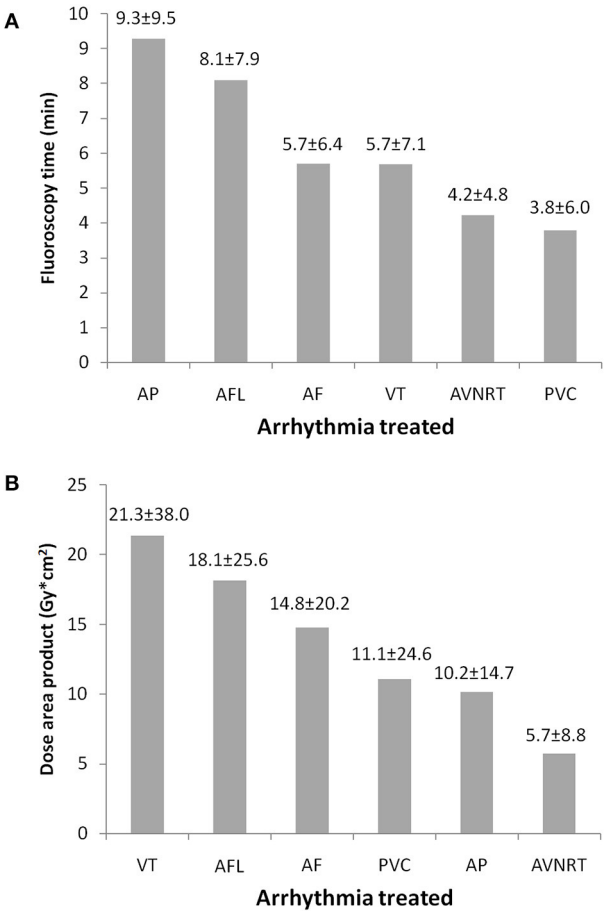

FIGURE 3 | Fluoroscopy time **(A)** and dose area product **(B)** by arrhythmias treated in procedures with fluoroscopy use. Fluoroscopy time and dose area product. AF, atrial fibrillation; AFL, atrial flutter; AP, accessory pathways; AVNRT, atrioventricular nodal reentrant tachycardia; PVC, premature ventricular contraction; VT, ventricular tachycardia.

a PVC fluoroless intervention. The rate of major complications between procedures with and without fluoroscopy was not different (0.45 vs. 0.35%; $p = 0.999$).

DISCUSSION

In our study we analyzed the experience of a high-volume electrophysiology center, where integration of X-Rays with EAM system has allowed a gradual reduction of the fluoroscopy exposure times. At the same time the growth of technical skill and the awareness of radiation damage have led to a progressive increase of ablative procedures without using fluoroscopy at all. This latter approach in our experience has proved effective, safe, and feasible to ablate almost all types of arrhythmias, as already demonstrated in previous papers (11, 12). This is a large study involving a very heterogeneous set of recent procedures performed with the conventional fluoroscopic ablations or by using the zero fluoroscopic approach. The novelty of our register compared to others is exactly the relevant number of interventions and the heterogeneity of the cases. We have shown that a single center strongly oriented to reduce fluoroscopy to zero can perform ablation procedures with fluoroless method in definitely all the possible arrhythmias to be treated.

The idea of performing fluoroless ablations initially took hold in the field of interventional electrophysiology of the pediatric age: performing ablation of reentry supraventricular tachyarrhythmias without X-Ray in children appeared immediately as an interesting opportunity (13). Simultaneously, several studies began to show that, even in adults, a non-fluoroscopic approach was possible and safe for catheter ablation of supraventricular arrhythmias (14, 15). There has also been described isolated experiences of fluoroless ablation for ventricular and more complex arrhythmias (16–18). In some cases of complex procedures, however, it is currently not technically possible to do fluoroless ablations. In fact, in patients with cardiac implantable electronic devices, it is necessary to

use fluoroscopy to visualize the catheters present in the heart chambers, while the operator moves ablation catheters. We lastly need X-Rays also in complex procedures like electrical storm ablations with cardiopulmonary support (19). In recent years, data from some hospitals have been published to highlight their volume of activity and their skill in performing ablations without fluoroscopy in various arrhythmias (20–22). In our experience we point out that the ablative procedure with the integration of X-Rays and EAM leads to a reduction in the average time of fluoroscopy compared to the past, as already known (23). The use of contact force-sensing catheters has improved the information that EAM provides during ablation, further reducing the need for fluoroscopy (24). Intracardiac echocardiography enhances direct visualization of catheter against the tissue, giving a better sense of contact. In our electrophysiology laboratory we have used contact-force sensor catheters since 2017, so we have been able to limit the use of intracardiac echocardiography in our routine. This ultrasound technique, which has a significant economic cost, is reserved for ablations of ventricular ectopic beats from papillary muscles or other challenging procedures. Transesophageal echocardiography is also a useful tool, particularly for safe transeptal puncture, but it requires general anesthesia. We performed procedures in conscious sedation, so unfortunately, we could not use it at all.

We noted that, to go fluoroless, it is important to have anatomical reference points on the electroanatomic map to work by continuously integrating electrophysiological potentials with the anatomical and structure information that EAM provides.

The advent of new technologies has led us to progressively increase fluoroless procedures over the years, so for most of the arrhythmias, we observed a trend of a progressive increase in the percentage of procedures without scope, that for AVNRT reaches almost 40% of the total ablations. For AF we have not recorded an increase in procedures, since in this arrhythmia to perform fluoroless ablation depends on the possibility of being able to pass through the PFO into the left atrium. However, the use of the technique we previously described for transseptal puncture has allowed us over the years to make this procedure a "near-zero fluoroscopy ablation" (10). In 2020, the volume of activity of our center has been slightly reduced due to the coronavirus pandemic and, in particular, urgent and non-deferrable ablative procedures were favored. For this reason, there was no substantial increase in the percentage of procedures without fluoroscopy, which remained stable compared to the year 2019. In the first 6 months of 2021, with the gradual resumption of the normal rhythm of work, the growth trend of procedures without X-Rays clearly regained.

However, in our data overall from 2017 to today, the percentage of fluoroless procedures is 15% of all ablations carried out; that is considerably higher than the percentage that emerged from the European multicenter registry of interventional electrophysiology (7). In particular, the progressive and important increase of this percentage over the years from 9 to 23% means that a center with a high volume of ablations, strongly oriented toward zero X-Rays, can carry out a quarter of its procedures with this approach.

There are ablations of some arrhythmias (such as AVNRT or AFL or AP) for which the use of the EAM system is a plus, although the costs of the procedure. There are several operators who have alternated over the study years in our electrophysiology laboratory. Among these operators, four were mid-career with more than 5 years of experience in electrophysiology and a volume of 20–40 procedures per month, while one is a mentor with more than 20 years of experience in electrophysiology and more than 40 procedures per month.

In our laboratory, regardless of which operator carrying out the procedure, the criteria used from time to time to decide on a fluoroless ablation were essentially the evaluation of the age and sex of the patients; that is in line with evidence already demonstrated (25). In general, we prefer to avoid the use of X-Rays in younger people in general and in women, particularly if of childbearing age. It has already been proven that the risks of cancer incidence and mortality decreased with aging and is always higher for female patients at the same age of intervention (26).

Ionizing radiations are carcinogenic and teratogenic both for patients and for medical staff. Biological effects of X-Rays are classified as stochastic (carcinogenic and genetic effect) and deterministic. Stochastic effects have a "linear non-threshold" model: any small amount of radiation leads to an increase in cancer risk without any threshold, and the probability increases linearly with increasing radiation dose. For deterministic effects (e.g., skin injuries, cataracts, etc.), there is a "threshold of dose:" below this value, the effect is not produced, and the severity increases with the dose (27). We calculated on the basis of the mean fluoroscopy times observed in our procedures with X-rays that the total number of fluoroless ablations since 2017 has allowed to save patients and the healthcare team from exposure of an average of 5 h of fluoroscopy for year; that means avoidance dose area product of 650 Gy^*m^2 per year. This potentially achieves a total saving of 25 h of scope and 2,955 Gy^*m^2 of dose area product over the years of interest. There are moreover physical damages for the operators, mainly of an orthopedic and neurosurgical nature, which derive from the prolonged use of protective lead apparel. Obviously, procedures without fluoroscopy do not require the use of these devices, preventing their orthopedic and ergonomic consequences (28).

All procedures that started fluoroless have been successful. Only in AF ablations were the usage of X-Rays dependent on the possibility of going through PFO. During this procedure we do not use routinely intracardiac echocardiography, therefore we cannot always avoid the use of X-Rays if there is PFO. The rate of major complications was very low (0.4%), compared to the complication rate described in literature (29, 30), without differences between ablation with and without fluoroscopy; this means that the latter approach does not increase procedural risks. We observe, furthermore, substantial equality in duration of procedure between fluoroless or traditional ablations, like in other experiences (22, 31).

The acute success of zero X-Rays arrhythmia ablation that we reported requires a long-term outcome assessment in terms of recurrences of arrhythmia and complications. In a recent study, 266 patients who underwent ablation without the use

of fluoroscopy were followed-up over a period of 6 years. The acute success was 100% and the chronic success was 90.8% with a new post-ablation arrhythmia that occurred in 7.7% of the sample (32). In another study comparing long-term outcomes of near-zero radiation ablation of paroxysmal supraventricular tachycardia with fluoroscopy-guided approach, cardiac ablation guided by EAM systems provided better results compared with conventional fluoroscopic ablation (33). According to our data, based on a large number of various arrhythmias treated, the complete elimination of fluoroscopy during catheter ablation does not reduce patient safety with an acute success comparable to conventional procedures. Further studies are needed in order to assess long-term outcomes and compare them among approaches.

Today in an electrophysiology laboratory, operators face a choice in procedures that could require an EAM: save the patient from X-Rays at the expense of an increase in the cost of the procedure. It has been proven very well that spending money today can mean saving money tomorrow in terms of gain in health and saving care costs (26). Conversely there are other procedures in which EAM is used in any case, such as PVC, VT, or AF ablation. In the latter cases, the goal is to take full advantage of the mapping system that is already being used and to go fluoroless. In these procedures using or not using X-Rays is a matter of habit and training. It is, however, recommended to start with right-sided ablations and then proceed with more complex procedures. Specific training programs are needed to instruct new operators on the development of these skills (34, 35).

STUDY LIMITATIONS

This was a retrospective single center register subjected to inherent limitations. The study was not a randomized clinical trial and reported data without a matching procedure to pair patients. The decision for a fluoroless ablation was made subjectively by operators. We did not make a formal evaluation of the learning curve of the various operators of the center, because some of them had already used zero X-Rays approach before 2017. For AF procedures, feasibility depends on PFO presence and difficulties to go through without an intra-procedural echocardiography guide. The large sample size was a point of strength for conclusions regarding safety and short-term efficacy. The absence of mid- or long-term clinical follow-up was the main limitation of our research. Specifically designed comparative studies could better investigate differences between procedural techniques.

CONCLUSION

An electrophysiology center with a high volume of procedures at the present time should be strongly oriented to a fluoroless approach, limiting the use of X-Rays only to ablations in which it is still really indispensable. We firmly believe that the continuous improvement of available technologies will give in the future the possibility to invert the current proportion between procedures with and without fluoroscopy, making those with X-rays a minority of all electrophysiological activity.

DATA AVAILABILITY STATEMENT

The original contributions presented in the study are included in the article/supplementary materials, further inquiries can be directed to the corresponding author/s.

ETHICS STATEMENT

The studies involving human participants were reviewed and approved by Azienda Universitaria Ospedaliera Consorziale - Policlinico, Bari, Italy. The patients/participants provided their written informed consent to participate in this study.

AUTHOR CONTRIBUTIONS

FT and MG contributed to conception and design of the study. FT and PG performed the statistical analysis. FT wrote the first draft of the manuscript. All authors contributed to manuscript revision, read, and approved the submitted version.

ACKNOWLEDGMENTS

The authors wish to thank Dr. Giovanna Barbara Serena Perrotta and Dr. Alberto Martinelli for their excellent technical assistance.

REFERENCES

1. Compagnucci P, Volpato G, Falanga U, Cipolletta L, Conti M, Grifoni G, et al. Recent advances in three-dimensional electroanatomical mapping guidance for the ablation of complex atrial and ventricular arrhythmias. *J Interv Card Electrophysiol.* (2021) 61:37–43. doi: 10.1007/s10840-020-00781-3
2. Gaita F, Guerra PG, Battaglia A, Anselmino M. The dream of near-zero X-rays ablation comes true. *Eur Heart J.* (2016) 37:2749–55. doi: 10.1093/eurheartj/ehw223
3. Macle L, Frame D, Gache LM, Monir G, Pollak SJ, Boo LM. Atrial fibrillation ablation with a spring sensor-irrigated contact force-sensing catheter compared with other ablation catheters: systematic literature review and meta-analysis. *BMJ Open.* (2019) 9:e023775. doi: 10.1136/bmjopen-2018-023775
4. Natale A, Reddy VY, Monir G, Wilber DJ, Lindsay BD, McElderry HT, et al. Paroxysmal AF catheter ablation with a contact force sensing catheter: results of the prospective, multicenter SMART-AF trial. *J Am Coll Cardiol.* (2014) 64:647–56. doi: 10.1016/j.jacc.2014.04.072
5. Cauti FM, Rossi P, La Greca C, Piro A, Di Belardino N, Battaglia A, et al. Minimal fluoroscopy approach for right-sided supraventricular tachycardia ablation with a novel ablation technology: insights from the multicenter CHARISMA clinical registry. *J Cardiovasc Electrophysiol.* (2021) 32:1296–304. doi: 10.1111/jce.15023
6. Hussey P, Wu I, Johnston T. 2018 ACC/HRS/NASCI/SCAI/SCCT expert consensus document on optimal use of ionizing radiation in cardiovascular imaging: best practices for safety and effectiveness-a review for the cardiac anesthesiologist. *J CardiothoracVascAnesth.* (2019) 33:2902–8. doi: 10.1053/j.jvca.2019.01.006

7. Kosiuk J, Fiedler L, Ernst S, Duncker D, Pavlović N, Guarguagli S, et al. Fluoroscopy usage in contemporary interventional electrophysiology: insights from a European registry. *Clin Cardiol.* (2021) 44:36–42. doi: 10.1002/clc.23411
8. Cronin EM, Bogun FM, Maury P, Peichl P, Chen M, Namboodiri N, et al. HRS/EHRA/APHRS/LAHRS expert consensus statement on catheter ablation of ventricular arrhythmias. *Europace.* (2019) 21:1143–4. doi: 10.1093/europace/euz132
9. Calkins H, Hindricks G, Cappato R, Kim YH, Saad EB, Aguinaga L, et al. 2017 HRS/EHRA/ECAS/APHRS/SOLAECE expert consensus statement on catheter and surgicalablation of atrialfibrillation. *Heart Rhythm.* (2017) 14:e275–444. doi: 10.1016/j.hrthm.2017.05.012
10. Troisi F, Quadrini F, Di Monaco A, Vitulano N, Caruso R, Guida P, et al. Electroanatomic guidance versus conventional fluoroscopy during transseptal puncture for atrial fibrillation ablation. *J Cardiovasc Electrophysiol.* (2020) 31:2607–13. doi: 10.1111/jce.14683
11. Anselmino M, Sillano D, Casolati D, Ferraris F, Scaglione M, Gaita F, et al. New electrophysiology era: zero fluoroscopy. *J Cardiovasc Med.* (2013) 14:221–7. doi: 10.2459/JCM.0b013e3283536555
12. Mascia G, Giaccardi M. A new era in zero X-ray ablation. *ArrhythmElectrophysiol Rev.* (2020) 9:121–7. doi: 10.15420/aer.2020.02
13. Drago F, Silvetti MS, Di Pino A, Grutter G, Bevilacqua M, Leibovich S. Exclusion of fluoroscopy during ablation treatment of right accessory pathway in children. *J Cardiovasc Electrophysiol.* (2002) 13:778–82. doi: 10.1046/j.1540-8167.2002.00778.x
14. Chen G, Wang Y, Proietti R, Wang X, Ouyang F, Ma CS, et al. Zero-fluoroscopy approach for ablation of supraventricular tachycardia using the Ensite NavX system: a multicenter experience. *BMC Cardiovasc Disord.* (2020) 20:48. doi: 10.1186/s12872-020-01344-0
15. Fadhle A, Hu M, Wang Y. The safety and efficacy of zero-fluoroscopy ablation versus conventional ablation in patients with supraventricular tachycardia. *Kardiol Pol.* (2020) 78:552–8. doi: 10.33963/KP.15293
16. Lamberti F, Di Clemente F, Remoli R, Bellini C, De Santis A, Mercurio M, et al. Catheter ablation of idiopathic ventricular tachycardia without the use of fluoroscopy. *Int J Cardiol.* (2015) 190:338–43. doi: 10.1016/j.ijcard.2015.04.146
17. Rivera S, Vecchio N, Ricapito P, Ayala-Paredes F. Non-fluoroscopic catheter ablation of arrhythmias with origin at the summit of the left ventricle. *J Interv Card Electrophysiol.* (2019) 56:279–90. doi: 10.1007/s10840-019-00522-1
18. Sadek MM, Ramirez FD, Nery PB, Golian M, Redpath CJ, Nair GM, et al. Completely non-fluoroscopic catheter ablation of left atrial arrhythmias and ventricular tachycardia. *J Cardiovasc Electrophysiol.* (2019) 30:78–88. doi: 10.1111/jce.13735
19. Di Monaco A, Quadrini F, Troisi F, Vitulano N, Caruso R, Duni N, et al. Cardiopulmonary support in patients undergoing catheter ablation of poorly tolerated ventricular arrhythmias and electrical storm. *J Cardiovasc Electrophysiol.* (2019) 30:1281–6. doi: 10.1111/jce.13995
20. Sánchez JM, Yanics MA, Wilson P, Doshi A, Kurian T, Pieper S. Fluoroless catheter ablation in adults: a single center experience. *J Interv Card Electrophysiol.* (2016) 45:199–207. doi: 10.1007/s10840-015-0088-z
21. Razminia M, Willoughby MC, Demo H, Keshmiri H, Wang T, D'Silva OJ, et al. Fluoroless catheter ablation of cardiac arrhythmias: a 5-year experience. *Pacing Clin Electrophysiol.* (2017) 40:425–33. doi: 10.1111/pace.13038
22. Santoro A, Di Clemente F, Baiocchi C, Zacà V, Bianchi C, Bellini C, et al. From near-zero to zero fluoroscopycatheterablationprocedures. *J Cardiovasc Electrophysiol.* (2019) 30:2397–404. doi: 10.1111/jce.14121
23. Sporton SC, Earley MJ, Nathan AW, Schilling RJ. Electroanatomic versus fluoroscopic mapping for catheter ablation procedures: a prospective randomized study. *J Cardiovasc Electrophysiol.* (2004) 15:310–5. doi: 10.1111/j.1540-8167.2004.03356.x
24. Lee G, Hunter RJ, Lovell MJ, Finlay M, Ullah W, Baker V, et al. Use of a contact force-sensing ablation catheter with advanced catheter location significantly reduces fluoroscopy time and radiation dose in catheter ablation of atrial fibrillation. *Europace.* (2016) 18:211–8. doi: 10.1093/europace/euv186
25. Pani A, Giuseppina B, Bonanno C, Grazia Bongiorni M, Bottoni N, Brambilla R, et al. Predictors of zero X-ray ablation for supraventricular tachycardias in a nationwide multicenter experience. *Circ Arrhythm Electrophysiol.* (2018) 11:e005592. doi: 10.1161/CIRCEP.117.005592
26. Casella M, Dello Russo A, Pelargonio G, Del Greco M, Zingarini G, Piacenti M, et al. Near zerO fluoroscopic exPosure duringc atlete ablAtion of supRavenTricular arrhYthmias: the NO-PARTY multicentre randomized trial. *Europace.* (2016) 18:1565–72. doi: 10.1093/europace/euv344
27. Sarkozy A, De Potter T, Heidbuchel H, Ernst S, Kosiuk J, Vano E, et al. Occupational radiation exposure in the electrophysiology laboratory with a focus on personnel with reproductive potential and during pregnancy: a European Heart Rhythm Association (EHRA) consensus document endorsed by the Heart Rhythm Society (HRS). *Europace.* (2017) 19:1909–22. doi: 10.1093/europace/eux252
28. Klein LW, Miller DL, Balter S, Laskey W, Naito N, Haines D, et al. Occupational health hazards in the interventional laboratory: time for a safer environment. *Catheter Cardiovasc Interv.* (2018) 250:538–44. doi: 10.1148/radiol.2502082558
29. Bohnen M, Stevenson WG, Tedrow UB, Michaud GF, John RM, Epstein LM, et al. Incidence and predictors of major complications from contemporary catheter ablation to treat cardiac arrhythmias. *Heart Rhythm.* (2011) 8:1661–6. doi: 10.1016/j.hrthm.2011.05.017
30. Cappato R, Calkins H, Chen SA, Davies W, Iesaka Y, Kalman J, et al. Updated worldwide survey on the methods, efficacy, and safety of catheter ablation for human atrial fibrillation. *Circ Arrhythm Electrophysiol.* (2010) 3:32–8. doi: 10.1161/CIRCEP.109.859116
31. Razminia M, Manankil MF, Eryazici PL, Arrieta-Garcia C, Wang T, D'Silva OJ, et al. Nonfluoroscopic catheter ablation of cardiac arrhythmias in adults: feasibility, safety, and efficacy. *J Cardiovasc Electrophysiol.* (2012) 23:1078–86. doi: 10.1111/j.1540-8167.2012.02344.x
32. Giaccardi M, Mascia G, Paoletti Perini A, Giomi A, Cartei S, Milli M. Long-term outcomes after "Zero X-ray" arrhythmiaablation. *J Interv Card Electrophysiol.* (2019) 54:43–8. doi: 10.1007/s10840-018-0390-7
33. Bergonti M, Dello Russo A, Sicuso R, Ribatti V, Compagnucci P, Catto V, et al. Long-term outcomes of near-zero radiation ablation of paroxysmal supraventricular tachycardia: a comparison with fluoroscopy-guided approach. *JACC Clin Electrophysiol.* (2021) 7:1108–17. doi: 10.1016/j.jacep.2021.02.017
34. Anselmino M, Ballatore A, Giaccardi M, Agresta A, Chieffo E, Floris R, et al. X-ray management in electrophysiology: a survey of the Italian Association of Arrhythmology and Cardiac Pacing (AIAC). *J Cardiovasc Med.* (2021) 22:751–8. doi: 10.2459/JCM.0000000000001210
35. Giaccardi M, Anselmino M, Del Greco M, Mascia G, Paoletti Perini A, Mascia P, et al. Radiation awareness in an Italian multispecialist sample assessed with a web-based survey. *Acta Cardiol.* (2021) 76:307–11. doi: 10.1080/00015385.2020.1733303

Conflict of Interest: MG has an agreement with Biosense Webster regarding the development of new technologies not related to this article.

The remaining authors declare that the research was conducted in the absence of any commercial or financial relationships that could be construed as a potential conflict of interest.

Publisher's Note: All claims expressed in this article are solely those of the authors and do not necessarily represent those of their affiliated organizations, or those of the publisher, the editors and the reviewers. Any product that may be evaluated in this article, or claim that may be made by its manufacturer, is not guaranteed or endorsed by the publisher.

Advantages of publishing in Frontiers

OPEN ACCESS
Articles are free to read for greatest visibility and readership

FAST PUBLICATION
Around 90 days from submission to decision

HIGH QUALITY PEER-REVIEW
Rigorous, collaborative, and constructive peer-review

TRANSPARENT PEER-REVIEW
Editors and reviewers acknowledged by name on published articles

Frontiers
Avenue du Tribunal-Fédéral 34
1005 Lausanne | Switzerland

Visit us: www.frontiersin.org
Contact us: frontiersin.org/about/contact

REPRODUCIBILITY OF RESEARCH
Support open data and methods to enhance research reproducibility

DIGITAL PUBLISHING
Articles designed for optimal readership across devices

FOLLOW US
@frontiersin

IMPACT METRICS
Advanced article metrics track visibility across digital media

EXTENSIVE PROMOTION
Marketing and promotion of impactful research

LOOP RESEARCH NETWORK
Our network increases your article's readership